



Durham E-Theses

Synthesis and Reactions of Viton® Model Compounds

LANCASHIRE, MARCUS,JOHN

How to cite:

LANCASHIRE, MARCUS,JOHN (2019) *Synthesis and Reactions of Viton® Model Compounds*, Durham theses, Durham University. Available at Durham E-Theses Online:
<http://etheses.dur.ac.uk/13388/>

Use policy

The full-text may be used and/or reproduced, and given to third parties in any format or medium, without prior permission or charge, for personal research or study, educational, or not-for-profit purposes provided that:

- a full bibliographic reference is made to the original source
- a [link](#) is made to the metadata record in Durham E-Theses
- the full-text is not changed in any way

The full-text must not be sold in any format or medium without the formal permission of the copyright holders.

Please consult the [full Durham E-Theses policy](#) for further details.

A thesis entitled

Synthesis and Reactions of Viton[®] Model Compounds

by

Marcus Lancashire

(Grey College)

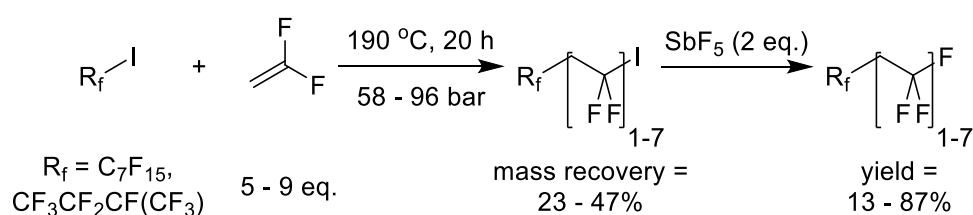
A candidate for the degree of Doctor of Philosophy

Department of Chemistry, Durham University

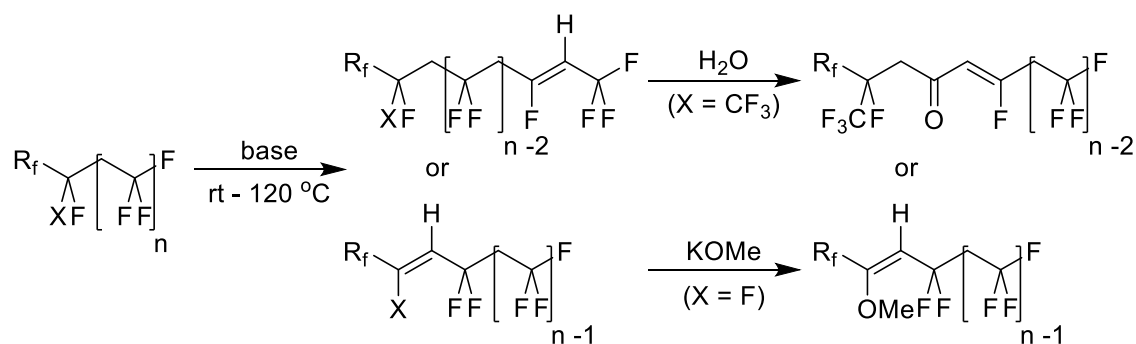
2019

Abstract

Viton® gaskets and O-ring seals are common components of engines and other industrial systems due to their high thermal and chemical resistances. However, degradation of Viton® seals has been observed when they are exposed to oils containing basic or nucleophilic petroleum additives. These processes are difficult to follow by standard analytical techniques due to Viton® being a high molecular weight polymer. In this project, a series of compounds that model the structural features of Viton® elastomers were synthesised by reaction of perfluoroalkyl iodides with vinylidene fluoride and subsequent capping with SbF₅.



These Viton® model compounds were subsequently reacted with a range of bases and nucleophiles and the products characterised by NMR spectroscopy and mass spectrometry. The analysis confirmed that exposure of -CH₂CF₂- containing Viton® model compounds to basic species (pK_a > 10) under relatively mild conditions (temperature ≤ 120 °C, atmospheric pressure) causes dehydrofluorination, synthesising alkenes that can subsequently react with certain nucleophiles such as KOMe and water.



These results indicate that Viton® elastomers are vulnerable to dehydrofluorination on exposure to basic petroleum additives, and to subsequent nucleophilic attack that can lead to unwanted crosslinking of the polymer chains and degradation of seals.

Acknowledgements

The first and most important acknowledgement must go to my supervisor Professor Graham Sandford, both for his high quality supervision and the support he has provided over the past 4 years (5 including 4th year and 8 including his role as my academic advisor). Your kindness, encouragement and, particularly recently, patience has been truly astounding and has kept me going throughout the completion of this PhD.

I would also like to thank Afton Chemical® for funding and for the additional support they've provided. In particular, Dr Ralph Lumby and Dr Marshall Baker who have helped to structure and guide this project and have ensured the results are put to good use.

This project would not have been possible without the work of the analytical and support staff at Durham, and I would like to thank all of those that have helped throughout this PhD including, but not limited to, Alan, Juan and Catherine in NMR, Dima in crystallography, Malcolm and Aaron in the glassblowing workshop and Paul, Neil and Omer in the mechanical and electrical workshops. I would like to give special thanks to Dr Li Li for her support when using the high pressure lab and autoclaves, Dr Dave Parker and Mr Peter Stokes for the specialised mass spectrometry techniques they developed for my compounds, and Mrs Annette Passmoor for keeping the department going through her efficient running of the stores and requisitions departments.

I have been fortunate to be part of one of the most welcoming and friendly research groups I could ever hope to join, and I would like to thank all of the PhD students in the Sandford Group I have known for the supportive and constructive working environment they have provided. In particular, Tony (for getting me started and not subsequently killing me), Etienne (for top quality translations), Darren (for being the biggest geezer), Josh (for the music), Alex (for ensuring my waste streams were purified), Neshat (for winning the group some prizes), Ben (for being famous and having a good grasp of the English language) and Dan (for continuing parts of this research). I would like to give special thanks to Dr Craig Fisher, as he had to bear with me both in the lab and at Grey. However, by pooling our shared interests I hope we have created a strong bond of friendship. I would also like to thank all 4th year, placement and summer project students that have been members of the lab (Alex M., Anne, Bobbi, Rob, Sophie, Lawrence, Zahide and Kiera) with the exceptions of Ellis and Jonny, who's entertaining but regular distractions have almost certainly delayed production of this thesis.

Since I started my undergraduate degree at Durham in 2011, the staff and students at Grey College have been a constant source of encouragement and support, and I would like to thank the College and its members for all they have done for me over the past 8 years. In particular, I would like to acknowledge the hard work and dedication of the MCR executive committees of the past 3 years for all they have done for the postgraduate community at Grey. Specifically, the MCR presidents (Stuart Flegg, Matthew Kirk and Lily Hulatt) as well as Craig (again), Sarah, Renju, Hannah, Maciej, Abi, Ana, Katie, Ross, Vincent, Cami, Martin, Helen, Jeff, Dan, Hannah, Rachael, Rhiannon, Ellen, Beth and Teng. I would also like to thank Dr Peter Swift, the Vice Master at Grey College, for all his assistance and for everything we worked on together, as well as Nicola and Bryan for 5 years of high quality college food.

There are many other friends I haven't been able to mention yet so I would like to thank all of them as well for their support (John, Max, Jack, Stephen, Jenny, Suzie, Richard, James, Matt, Matt, Monica, Dom, Jay, Wasit, Darren, Rom, John, Dan, Ciara, Maria, Dahui, Iman, Ryan, Laura, Sophie, David and Estelle to name a few). I would also like to thank my family, particularly my parents Lavinia and Steve, who have always been there when I needed them and have got me through the tough times during this PhD.

Lastly, I would like to thank my amazing girlfriend Alisha Brehaut for all her love and kindness. I can never thank you enough for all that you have done for me but know that you make my life better with every second you are in it and I could never have got through this without you.

Memorandum

The work described in this thesis was carried out at Durham University between October 2015 and December 2018. This thesis is the work of the author, except where acknowledged by reference, and has not been submitted for any other degree. The copyright of this thesis rests with the author. No quotation from it should be published without the author's prior written consent and information derived from it should be acknowledged.

This work has been presented, in part, at:

1. 22nd International Symposium on Fluorine Chemistry 22-27 July 2018, Oxford, *poster presentation*.
2. Postgraduate Gala Symposium, 21st June 2018, Durham, *oral presentation, 2nd place Prize for Oral Presentation*
3. RSC Fluorine Subject Group Postgraduate Meeting, 18-19 September 2017, Leicester, *poster presentation*.
4. Postgraduate Gala Symposium, 15th June 2017, Durham, *poster presentation*.

Nomenclature and Abbreviations

Ac	Acyl
Ar	Generic aromatic group
AIBN	Azobisisobutyronitrile
Bisphenol AF	4,4'-(Hexafluoroisopropylidene)diphenol
ⁱ Bu	iso-Butyl
ⁿ Bu	n-Butyl
^s Bu	sec-Butyl
^t Bu	Tertiary butyl
CFC	Chlorofluorocarbons
Chemraz®	Perfluoroelastomer
COSY	Correlation spectroscopy
CSM	Cure sight monomer
DAST	Diethylaminosulfur trifluoride
DBU	1,8-Diazabicyclo[5.4.0]undec-7-ene
DCM	Dichloromethane
Deoxo-fluor®	Bis(2-methoxyethyl)aminosulfur trifluoride
eq	Equivalent
Fluorinert™ FC-72	Mixture of perfluorohexane isomers
FTIR	Fourier-transform infrared spectroscopy
GC-MS	Gas chromatography–mass spectrometry
h	Hours
<i>hν</i>	Irradiation with UV or visible light
HCFC	Hydrochlorofluorocarbons
HFC	Hydrofluorocarbons
HFO	Hydrofluoroolefins
HFP	Hexafluoropropylene
HMBC	Heteronuclear multiple-bond correlation spectroscopy

HSQC	Heteronuclear single-quantum correlation spectroscopy
ICI	Imperial Chemical Industries
IR	Infrared
Kalrez®	Perfluoroelastomer
LDA	Lithium diisopropylamide
LHMDS	Lithium bis(trimethylsilyl)amide
LPG	Liquified petroleum gas
MSC	Maleic anhydride-styrene copolymers
NMR	Nuclear magnetic resonance
Ph	Phenyl
PMA	Poly(methyl acrylate)
PMVE	Perfluoromethyl vinyl ether
ppm	Parts per million
ⁱ Pr	iso-Propyl
ⁿ Pr	n-Propyl
PTFE	Polytetrafluoroethylene
R _f	Perfluoroalkyl group
rt	Room temperature
SBR	Styrene-butadiene co-polymer
TAIC	Triallyl- <i>iso</i> -cyanurate
TBAF	Tetrabutylammonium fluoride
TFE	Tetrafluoroethylene
T _g	Glass transition temperature
Thexyl	2,3-dimethylbutyl
THF	Tetrahydrofuran
UV	Ultraviolet
VDF	Vinylidene fluoride
XtalFluor-E®	(Diethylamino)difluorosulfonium tetrafluoroborate
XtalFluor-M®	Difluoro(morpholino)sulfonium tetrafluoroborate

Table of Contents

Abstract	ii
Acknowledgements.....	iii
Memorandum.....	v
Nomenclature and Abbreviations.....	vi
1. Synthesis and Properties of Viton® and Model Compounds of Viton®	1
1.1 Introduction – Petroleum, Petroleum Additives and Viton® Seals	1
1.2 Organofluorine Chemistry – Properties of Highly Fluorinated Systems	6
1.2.1 Properties of Highly Fluorinated Systems	6
1.3 Fluoroelastomers – Viton®	8
1.3.1 Synthesis of Viton® Monomers.....	9
1.3.2 Polymerisation Reactions – Synthesis of Viton® Elastomers.....	12
1.3.3 Crosslinking Reactions – Curing of Viton® Elastomers.....	15
1.3.4 Properties of Viton® Elastomers	19
1.3.5 Model Compounds of Viton® Elastomers.....	21
1.4 Perfluoroalkyl Iodides.....	22
1.4.1 Synthesis of Perfluoroalkyl Iodides	22
1.4.2 Reactivity of Perfluoroalkyl Iodides	24
1.4.3 Synthesis of Viton® Model Compounds Using Perfluoroalkyl Iodides	30
1.4.4 Reactions of Viton® Model Compounds.....	36
1.5 Conclusion	36
2. Aims and Objectives	37
3. Synthesis and Degradation of Straight Chain VDF Telomer Fluorides	40
3.1. Synthesis of Poly VDF Telomer Iodides – Reactions of Perfluorooctyl Iodide with VDF ..	40
3.2. Capping Reactions of Straight Chain VDF Telomer Iodides	54
3.2.1. Reaction of VDF Telomer Iodides with Tributyltin Hydride.....	54
3.2.2. Reaction of VDF Telomer Iodides with Antimony Pentafluoride.....	59

3.3. Reactions of Viton® Model Compounds with Petroleum Additive Systems	63
3.3.1. Reactions of Straight Chain Telomer Fluorides with Amines	63
3.3.2. Reactions of Straight Chain Telomer Fluorides with Anionic Bases.....	72
3.3.3. Reactions of Dehydrofluorinated Telomer Fluorides with Sulfur Nucleophiles	80
3.4 Conclusion	81
4. Synthesis and Degradation of Branched VDF Telomer Fluorides	84
4.1. Synthesis of HFP/VDF Telomer Iodides – Reactions of Perfluorooctyl Iodide with HFP ..	85
4.2. Synthesis of Branched VDF Telomer Iodides	88
4.2.1. Reaction of Perfluoro-2-iodobutane with 5 eq. of VDF	88
4.2.2. Reaction of Perfluoro-2-iodobutane with Excess VDF	94
4.3. Reactions of Branched VDF Telomer Iodides with SbF ₅	101
4.3.1. Comparison of CF ₃ CF ₂ CF(CF ₃)(CH ₂ CF ₂) ₁₋₄ F to Viton® Polymers by Solid State ¹⁹ F NMR Spectroscopy	107
4.4. Reactions of CF ₃ CF ₂ CF(CF ₃)(CH ₂ CF ₂) ₂₋₅ F with Bases.....	108
4.4.1. Reactions of CF ₃ CF ₂ CF(CF ₃)(CH ₂ CF ₂) ₂₋₅ F with Amine Bases.....	108
4.4.2. Reaction of CF ₃ CF ₂ CF(CF ₃)(CH ₂ CF ₂) ₂₋₅ F with Anionic Bases.....	110
4.4.3. Reactions of CF ₃ CF ₂ CF(CF ₃)(CH ₂ CF ₂) ₂₋₇ F with Bases Using Increasingly Forcing Conditions	110
4.5 Conclusion	120
5. Synthesis of Discrete RCF(CF ₃)R Compounds.....	121
5.1. Introduction – Me ₃ SiCF ₃ and DAST.....	122
5.1.1. Trifluoromethylation – The Ruppert – Prakash Reagent.....	123
5.1.2. Deoxofluorination Reactions – DAST	125
5.2. Reactions of Aldehydes and Ketones with Me ₃ SiCF ₃	128
5.2.1. Reactions of Dicarboxyl Compounds with Me ₃ SiCF ₃	132
5.3. Reactions of RCOH(CF ₃)R Compounds with DAST.....	133
5.4. Conclusion	144
6. Conclusion.....	146

7. Experimental.....	150
8. References	189
Appendix 1: Crystallographic data for compound 102a.....	i

1. Synthesis and Properties of Viton[®] and Model Compounds of Viton[®]

1.1. Introduction – Petroleum, Petroleum Additives and Viton[®] Seals

Petroleum (crude oil) is the most widely traded commodity in the world; approximately 100 million barrels (1 barrel = 42 US gallons, \approx 159 l) are consumed per day, 19 million of which are in the USA¹. Petroleum is a fossil fuel, derived from the organic material of prehistoric organisms that have been subject to anaerobic decomposition under high temperature and pressure². The key components of petroleum are alkanes (paraffins), cycloalkanes (naphthenes), aromatics and asphaltics (high molecular weight hydrocarbons that are insoluble in *n*-heptane)³ (Table 1) and the composition of particular batches of petroleum depend on where it is extracted⁴.

Table 1: Principle chemical components of petroleum³

Hydrocarbon	Average	Range
Alkanes (paraffins)	30%	15 – 60%
Cycloalkanes (naphthenes)	49%	30 – 60%
Aromatics	15%	3 – 30%
Asphaltics	6%	remainder

Petroleum is refined by separating the hydrocarbon mixture according to their boiling points using fractional distillation⁴, and of these fractions, approximately 85% are used as liquid fuels, such as petrol, diesel and kerosene. The remaining fractions are used as lubricants, feedstocks for the chemical and pharmaceutical industries, gaseous fuels and as asphalt^{3,5}. In addition, sulfur that is removed from crude oil is refined into oleum for the production of hydrogen sulfide and sulfuric acid⁶ (Table 2).

Hydrocracking involves cracking hydrocarbons under a high pressure of hydrogen gas, using a mixed catalyst system consisting of platinum or palladium on a zeolite support. The zeolite component catalyses the cracking reactions, producing a mixture of lower molecular weight hydrocarbons and alkenes. The platinum or palladium catalyst facilitates hydrogenation of the synthesised alkenes, as well as any aromatic compounds that were present, forming a mixture of intermediate molecular weight hydrocarbons (typically in the kerosene and diesel fractions)⁷ (Fig. 2).

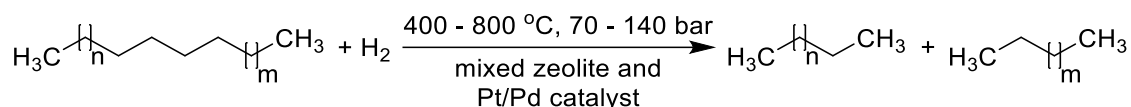


Figure 2: Typical hydrocracking reaction⁷

In order to improve the performance of petroleum products, a variety of additive compounds are included to change product properties. Most finished oils for automotive engines, gear boxes and other moving components contain between 1 and 5% additives by weight, although this can be up to 10% for certain applications (lubricants)⁸ (The oil additive industry is dominated by several large companies, including Afton Chemical[®]). Additives provide a wide range of functionality, both to improve the quality of the oils and to protect the engines and other industrial components the oils come into contact with, and some of these applications are detailed in Table 3.

Table 3: Typical oil additives and their functions⁸

Additive	Function	Typical Compounds
Corrosion Inhibitors	Inhibit degradation of metallic components through rust and copper corrosion	Metal alkyl sulfonates and phosphonates (detergents), triazoles, thiadiazoles
Antioxidants	Inhibit oxidation of oil compounds	Amines and phenols
Metal Deactivators	Complex and deactivate metal ions in oils, especially copper	Benzotriazoles, polyamines
Bases	Neutralise acids formed by the reactions of oils with air and combustion gases, prevent the formation of sulfates	Hydroxides, amines, detergents
Viscosity Modifiers	Increase the oils viscosity at high temperature without decreasing low temperature fluidity	Plastics (PMA, SBR, MSC)
Pour Point Depressants	Decrease the lowest temperature at which the oil will pour (the pour point)	PMA, MSC, long chain alkylbenzenes
Friction Modifiers	Reduce the contact between solid surfaces, limiting friction and wear	Amphiphilic compounds (glycerol mono oleates, alkyl phosphonates, organo-molybdenum species)
Extreme Pressure Agents	Reduce the contact between surfaces, even at high pressures	Polysulfides, dithiocarbamates, thiadiazoles
Antiwear Agents	Form a film on metal surfaces (tribofilms), preventing contact and wear	Zinc dithiophosphonates, polyphosphates
Dispersants	Prevents coagulations of solid contaminants by keeping them suspended in the oil	Polyamines or alcohols connected to long chain poly- <i>iso</i> -butylenes
Anti-foam Agents	Inhibits the formation of air bubbles and foam in the oil	Silicones

Gasoline containing a range of additives is used in mechanical devices such as combustion engines, gear boxes and other mechanisms. One of the key components in engines and other industrial systems are gaskets, such as O-rings, which are used to seal the joints between

adjoining surfaces by deforming under stress to occupy any irregularities and prevent leakage. Viton® is a fluoroelastomer that is commonly used to manufacture gaskets for engines and industrial components that come into contact with oils and the additives they contain. Viton® seals are used in these environments because of their high chemical and thermal resistance, combined with their improved elasticity compared to other fluorinated polymers such as PTFE⁹. These properties also make Viton® useful in the manufacture of chemical resistant gloves and hoses (Fig. 3).



Figure 3: Two example products made from Viton®; chemical resistant gloves and O-rings

Viton® is a copolymer of several fluorinated alkenes, specifically vinylidene fluoride (VDF), hexafluoropropylene (HFP) and tetrafluoroethylene (TFE), with some specialist varieties also containing perfluoromethyl vinyl ether (PMVE) and ethylene¹⁰. The key components of the structure of a typical Viton® elastomer are shown in Fig. 4.

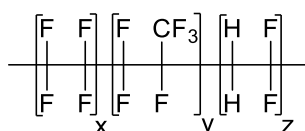


Figure 4: Structural elements found in Viton®, derived from TFE, HFP and VDF respectively¹⁰

However, degradation of Viton® seals has been observed by industry upon long term exposure to oils containing petroleum additives¹¹. Unfortunately, understanding the mechanisms by which Viton® seals are degraded is challenging due to the difficulties in examining high molecular weight polymers by standard analytical techniques, such as NMR spectroscopy and mass spectrometry¹².

In order to better understand the degradation of Viton® seals, properties of highly fluorinated systems, specifically fluoroelastomers, will be discussed. The synthesis of Viton® and its constituent monomers will be described, including details of the different classes of Viton®

elastomer and how they are crosslinked to produce finished polymers. In addition, the properties of the various Viton® elastomers will be detailed, investigating how they differ and specific applications of each.

1.2. Organofluorine Chemistry – Properties of Highly Fluorinated Systems

The global fluorochemicals industry (not including life science products) achieved sales of \$20 billion in 2017, encompassing a wide variety of different compounds such as refrigerants and fluoropolymers¹³. All fluorine used industrially is extracted from fluorspar (CaF₂), which is converted to anhydrous HF by reaction with sulfuric acid. Anhydrous HF is the starting material for the synthesis of all relevant organofluorine compounds, either directly or via intermediate species (F₂, KF and amine/ HF mixtures)¹⁴ and, of these compounds, 42% are highly fluorinated fluorocarbons such as chlorofluorocarbons (CFC), hydrochlorofluorocarbons (HCFC) and hydrofluorocarbons (HFC)¹⁵. Historically, CFCs were widely used as refrigerants; however, their use has been phased out due to their ability to damage the ozone layer¹⁶. They were replaced by HFCs, and more recently by hydrofluoroolefins (HFO), as HFCs are greenhouse gases¹⁷. CFCs and HCFCs are also important intermediates for the synthesis of polyfluorinated alkenes, which are the starting materials for fluoropolymers as described later in this review¹⁸⁻²¹, and fluoropolymer production accounts for approximately 20% of the fluorocarbon industry¹⁵. The properties of highly fluorinated compounds are principally linked to the many C – F bonds present in these systems, and these properties are described below.

1.2.1. Properties of Highly Fluorinated Systems

The properties of fluorine atoms are significantly different to those of all other elements, and some of these are detailed in Table 4.

Table 4: Properties of various period 2 elements and the halogens²²

Element (Symbol)	Hydrogen (H)	Carbon (C)	Nitrogen (N)	Oxygen (O)	Fluorine (F)	Chlorine (Cl)	Bromine (Br)
Van der Waals Radii / Å	1.20	1.70	1.55	1.52	1.47	1.75	1.85
1 st Ionisation Energy / kJ mol ⁻¹	1310	1090	1410	1320	1690	1250	1140
C – X Bond Energy / kJ mol ⁻¹	413	347	305	358	485	327	285
Pauling Electronegativity	2.20	2.55	3.04	3.44	3.98	3.16	2.96

Fluorine is the most electronegative element²³ due to its high nuclear charge compared to its size, and also has a high first ionization energy²². Fluorine's high nuclear charge means that its electrons are tightly bound to its nucleus, and so a large amount of energy is required to remove one of its outer shell electrons. Therefore, fluorine has a low van der Waals radius (between the radii of oxygen and hydrogen)²², and this is useful in medicinal compounds where fluorine atoms can replace hydrogen in order to improve the lipophilicity and lifetime of a drug with limited steric disruption²⁴. The high electronegativity of fluorine leads to the high strength of C – F bonds and the weak van der Waals interactions between polyfluorinated molecules, and these properties are detailed below.

1.2.1.1. High C – F Bond Strength

The carbon – fluorine bond is the strongest single covalent bond to carbon (485 kJ mol⁻¹, cf. C – H, 413 kJ mol⁻¹)²². The large difference in electronegativity between carbon and fluorine gives C – F bonds a significant ionic component, where most of the electron density resides on the fluorine atom and, when combined with the good orbital overlap between carbon and fluorine, this explains the high bond strength. Consequently, fluorine is a relatively poor leaving group from sp³ carbon compared to other halogens, contributing to the increased chemical stability of polyfluorinated molecules²³. The high bond strength also explains the high thermal stability of some polyfluorinated systems.

1.2.1.2. Weak Van der Waals Interactions

Individual C – F bonds are highly polar and can cause large dipole moments in molecules²³. However, in polyfluorinated species such as fluoroelastomers, the influence on polarity is different. Fluorine atoms have low polarisability and are surrounded by a tightly bound cloud of electron density which, in polyfluorinated species, creates a ‘shell’ of electrons that shields the carbon backbone. This impedes the formation of temporary dipoles, reducing van der Waals interactions between polyfluorinated molecules²⁵. The weak intermolecular interactions of perfluorinated polymers such as PTFE, combined with their high thermal and chemical stability, makes them useful as components in dry lubricants²⁰.

Polyfluorinated molecules do not interact strongly with other compounds, such as water and organic solvents and, indeed, perfluorinated liquids form a three layer system with organic solvents and water²⁵. Thus, fluoroelastomers have a high resistance to a variety of solvents, making them useful for the manufacture of chemical resistant gloves and seals⁹.

However, these properties also make processing and recycling fluoroelastomers and other fluorinated polymers very difficult, limited to grinding of the fluoroelastomer into fine particles for incorporation into new components²⁶ and the total destruction of the polymer to recover the HF²⁷.

1.3. Fluoroelastomers – Viton®

Fluoroelastomers are synthetic rubbers that have principally C – F bonds along the polymer backbone instead of C – H bonds. They are characterised by having high thermal and chemical stability combined with rubber-like elasticity⁹ and are synthesised from fluorinated alkene monomers such as vinylidene fluoride (VDF, **1**), tetrafluoroethylene (TFE, **2**), hexafluoropropylene (HFP, **3**) and perfluoromethyl vinyl ether (PMVE, **4**)¹⁰ (Fig. 5). Many varieties are commercially available and include Viton®, as well as perfluoroelastomers such as Kalrez^{®28} and Chemraz^{®29}.

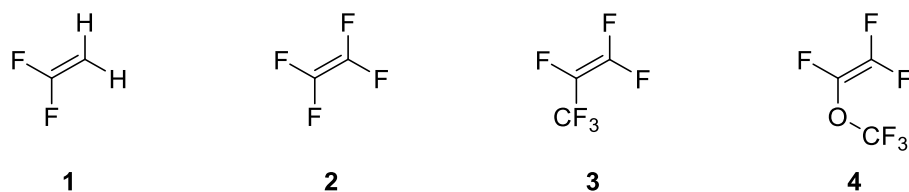


Figure 5: Monomers used in the synthesis of Viton®. From left to right: vinylidene fluoride (VDF), tetrafluoroethylene (TFE), hexafluoropropylene (HFP) and perfluoromethyl vinyl ether (PMVE)

Viton® is a family of elastomers synthesised from a variety of fluorinated and non-fluorinated monomers (Fig. 6). The most commonly used Viton® elastomers are A, B and F, and the peroxide cured equivalents, GAL-S, GBL-S and GF-S. For applications that require low temperature flexibility, PMVE containing Viton® elastomers (GLT-S, GBLT-S and GFLT-S) are used, and Viton® ETP-S (Viton® Extreme) shows significantly higher base resistance than the other elastomeric forms³⁰.

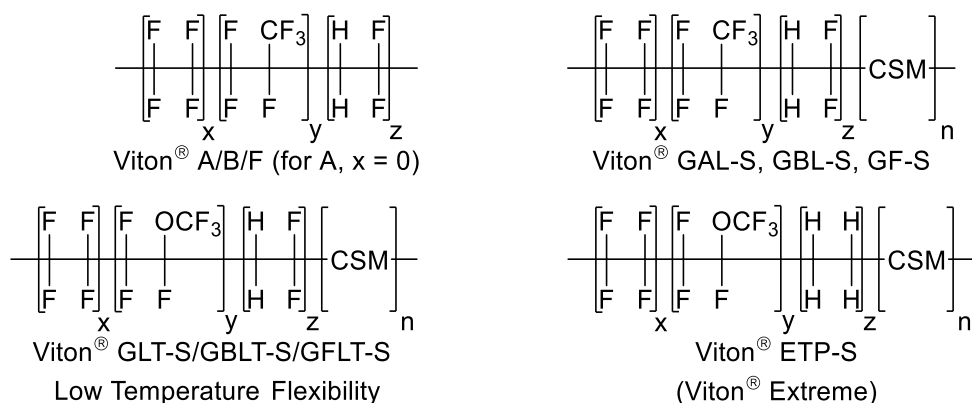


Figure 6: Structural elements found in the Viton® elastomers; CSM = cure site monomer

For peroxide cured Viton® elastomers, cure site monomers (CSM) are also present which contain C–Br bonds. These are required to produce radicals along the polymer backbone, necessary for the curing process¹⁰. The synthesis of each of the key fluorinated alkene monomers present in Viton® fluoroelastomers will be discussed in detail, and this will be followed by an examination of the polymerisation and curing reactions that are used to produce the different Viton® elastomers.

1.3.1. Synthesis of Viton® Monomers

The fluorinated monomers used in Viton® are VDF, HFP, TFE and PMVE. TFE is made industrially from HF and chloroform (5)¹⁸ (Fig. 7) but can also be synthesised in the laboratory by the reverse polymerisation (pyrolysis) of PTFE at low pressure (below 670 Pa) and high temperature (650 – 700 °C)³¹.

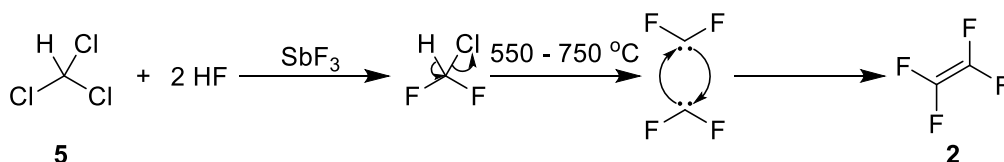


Figure 7: Synthesis of TFE from HCCl_3 using HF and SbF_3 ¹⁸

The original synthesis of HFP, reported by Henne and Woalkes¹⁹, begins with 1,2,3-trichloropropane (**6**) which is converted to HFP over seven steps using HF, Cl_2 and two different antimony fluorides (Fig. 8).

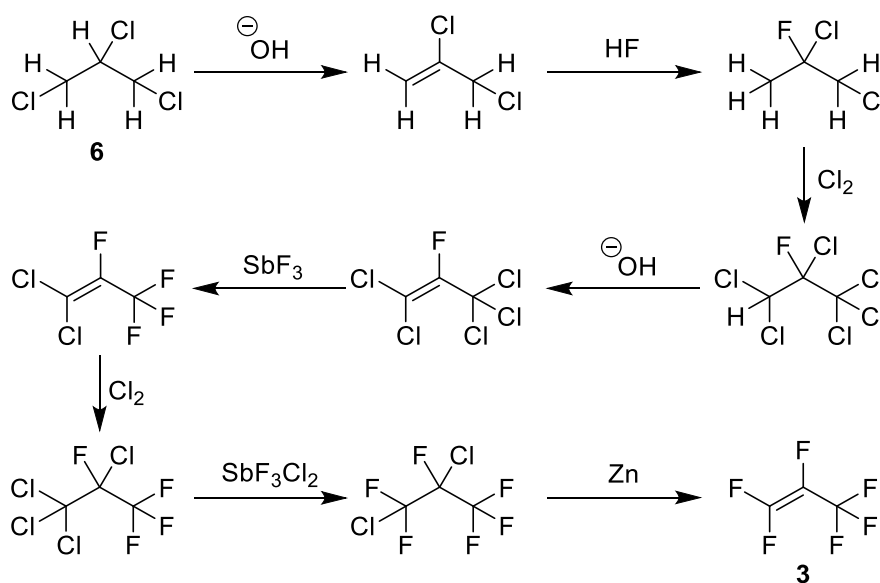


Figure 8: Synthesis of HFP from 1,2,3-trichloropropane¹⁹

HFP is now produced industrially by the more recently developed thermal cracking of TFE³²⁻³⁴ (Fig. 9).

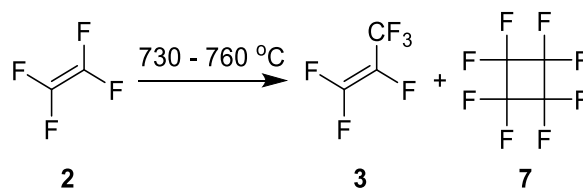


Figure 9: Synthesis of HFP by thermal cracking of TFE with octafluorocyclobutane produced as a side product³²⁻³⁴

There are two possible mechanisms for the conversion of TFE to HFP. The first, proposed by Atkinson and Atkinson, suggests that TFE first dimerises to form octafluorocyclobutane (**7**), which decomposes to HFP and difluorocarbene^{35,36} (Fig. 10).

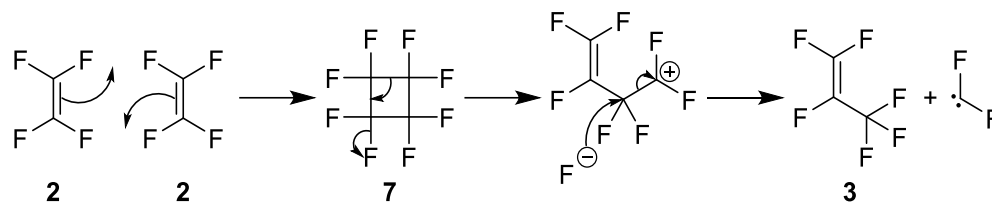


Figure 10: Mechanism for the synthesis of HFP via octafluorocyclobutane^{35,36}

The second mechanism, proposed by Kushina *et al.*, suggests that TFE undergoes alkene-carbene isomerisation to form trifluoromethylfluorocarbene, which reacts with difluorocarbene to form HFP (Fig. 11). This mechanism is supported by adding halocarbene traps to the reaction mixture, such as HCl and cyclopentadiene³⁷.

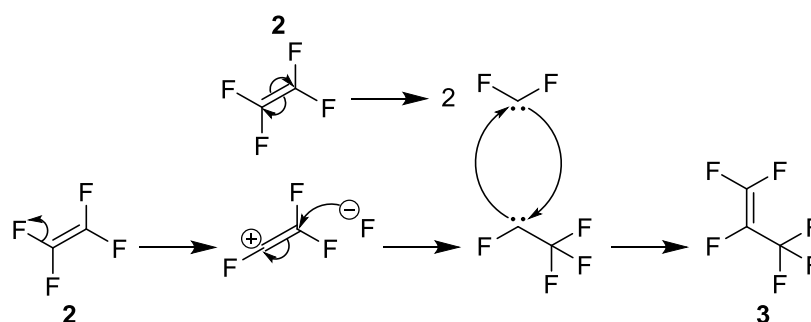


Figure 11: Mechanism for the synthesis of HFP via trifluoromethylfluorocarbene³⁷

VDF is synthesised industrially from acetylene (**8**), using HF and Cl₂^{20,21} (Fig. 12).

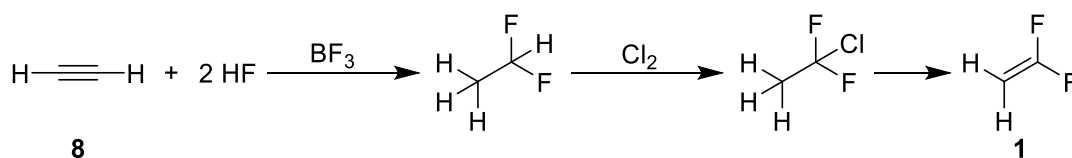


Figure 12: Synthesis of VDF from acetylene using HF and Cl₂^{20,21}

PMVE is synthesised by the reaction of hexafluoropropylene oxide (**9**) with carbonyl fluoride (**10**), producing an acid fluoride that is converted to the carboxylic acid salt and decarboxylated to yield PMVE³⁸ (Fig. 13).

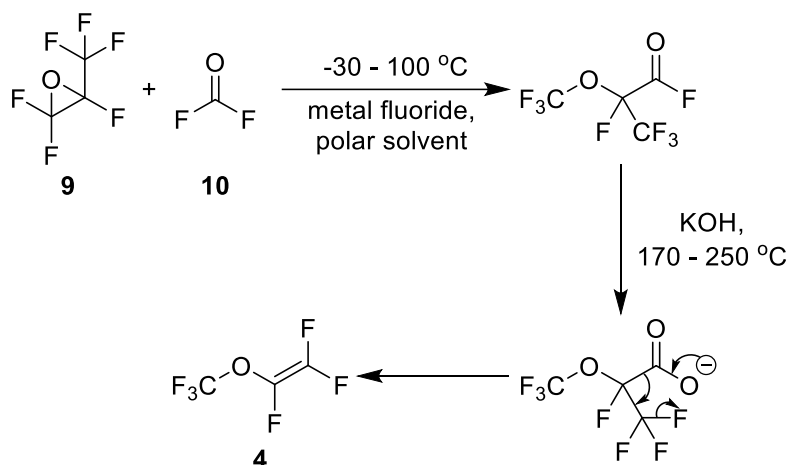


Figure 13: Synthesis of PMVE from hexafluoropropylene oxide³⁸

More recently, PMVE was also synthesised by reaction of chlorotrifluoroethylene (11) with trifluoromethoxy salts, made *in situ* from 10 and an HF/amine mixture³⁹ (Fig. 14).

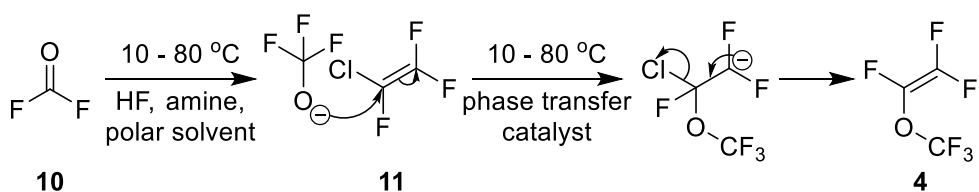


Figure 14: Synthesis of PMVE from chlorotrifluoroethylene³⁹

Several fluorinated monomers are reacted together to synthesise Viton[®], with the addition of cure site monomers and/or ethylene depending on the Viton[®] elastomer being synthesised. Such polymerisation reactions are discussed below.

1.3.2. Polymerisation Reactions – Synthesis of Viton[®] Elastomers

The monomers that are required for a particular Viton[®] elastomer react together via a free radical polymerisation mechanism⁴⁰ (Fig. 15).

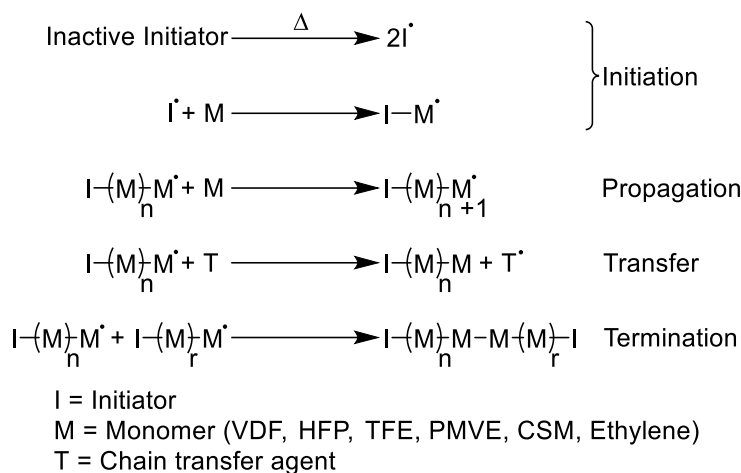


Figure 15: Synthesis of Viton® by free radical polymerisation⁴⁰

Polymerisation reactions typically take place in an aqueous emulsion at 50 – 130 °C at 10–70 bar pressure. The most common initiators for the reaction are inorganic peroxides, such as ammonium persulfate ((NH₄)₂S₂O₈), although organic peroxides are sometimes used if the reaction is carried out at low temperature^{41,42}. Fluorocarbon acid salts are used as emulsifying agents while dimethyl malonate and dimethyl ether are used as chain transfer agents⁴⁰.

The monomers are mixed together and undergo random free radical polymerisation. However, the polarities and steric bulk of the alkenes and radicals affect the regio and stereochemistry of the Viton® elastomer formed. VDF homopolymerisation is selective for head to tail addition due to the polarity difference between the CH₂ and CF₂ groups of the molecule. The electrophilic CF₂ radicals of the growing polymer chains react with the less electron deficient CH₂ group of the monomer, and this selectivity is also observed in poly VDF segments of Viton®⁴³ (Fig. 16).

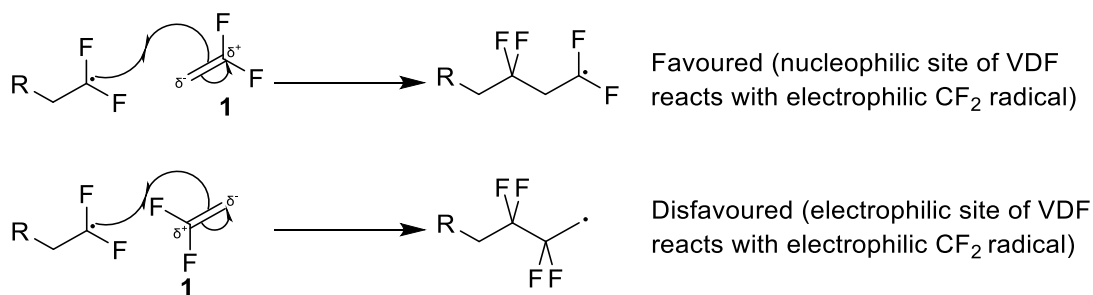


Figure 16: Reactions of a CF₂ radical with VDF. Head to tail addition is favoured⁴³

HFP and PMVE do not homopolymerise except under highly forcing conditions, due to the steric clashes that would occur between bulky CF_3/OCF_3 side chains and the CF_2 groups. Therefore, adjacent HFP/PMVE units are rare in Viton^{®44} (Fig. 17).

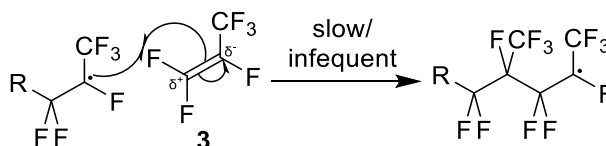


Figure 17: Reactions of a $\text{CF}(\text{CF}_3)$ radical with HFP. HFP does not homopolymerise and the same is true of PMVE⁴⁴

Reactions of HFP and PMVE with the CF_2 radicals of growing polymer chains are selective for attack at the CF_2 group of the monomer, avoiding steric clashes with the CF_3/OCF_3 groups⁴⁵ (Fig. 18).

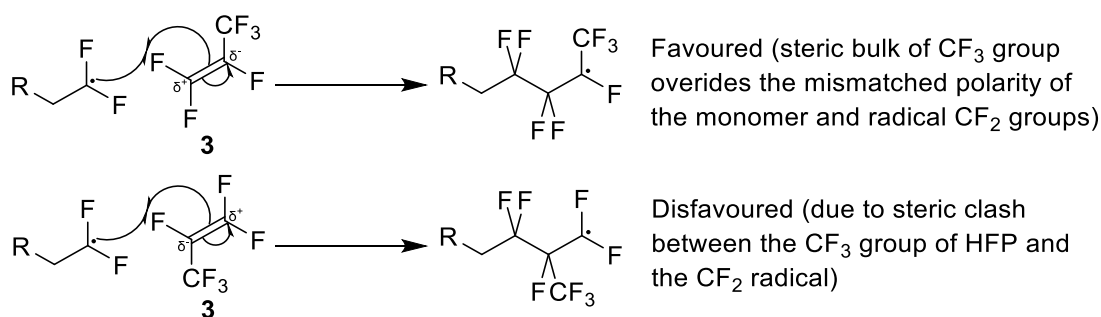


Figure 18: Reactions of a CF_2 radical with HFP. Head to tail addition is favoured (PMVE reacts in a similar fashion)⁴⁵

Reactions of VDF with $\text{CF}(\text{CF}_3)/\text{CF}(\text{OCF}_3)$ radicals of the growing polymer chains are selective for attack at the CH_2 group of VDF, as these reactions are favoured by both polarity (the electron deficient radical reacts with the less electron deficient CH_2 group of VDF) and sterics (the reaction avoids steric clashes between the $\text{CF}(\text{CF}_3)/\text{CF}(\text{OCF}_3)$ and the CF_2 group of VDF)⁴⁵ (Fig. 19).

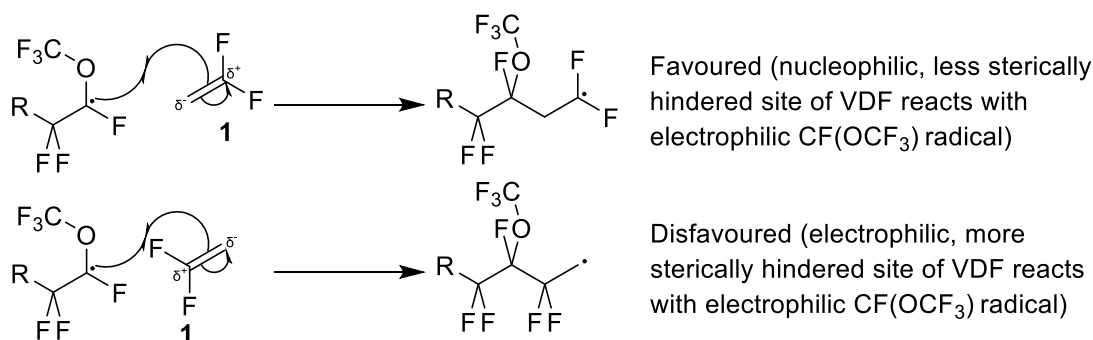


Figure 19: Reactions of $\text{CF}(\text{OCF}_3)$ radicals with VDF. Head to tail addition is favoured (the same selectivity would be observed for $\text{CF}(\text{CF}_3)$ radicals)

After synthesis of the Viton® polymer chains, crosslinking (or curing) gives the polymer a three-dimensional structure, which improves mechanical properties.

1.3.3. Crosslinking Reactions – Curing of Viton® Elastomers

Viton® was traditionally crosslinked using diamines but this cure process is slow and the resulting polymers suffer from loss of elasticity (scorching)⁴⁰. Consequently, two methods have been developed recently for crosslinking Viton®.

1.3.3.1. Crosslinking of Viton® with Bisphenol AF

Bisphenol AF (**12**) crosslinking is used in the synthesis of Viton® A, B and F, the most commonly used Viton® elastomers, and is suggested to proceed by the sequential elimination-substitution mechanism⁴⁶ described in Fig. 20.

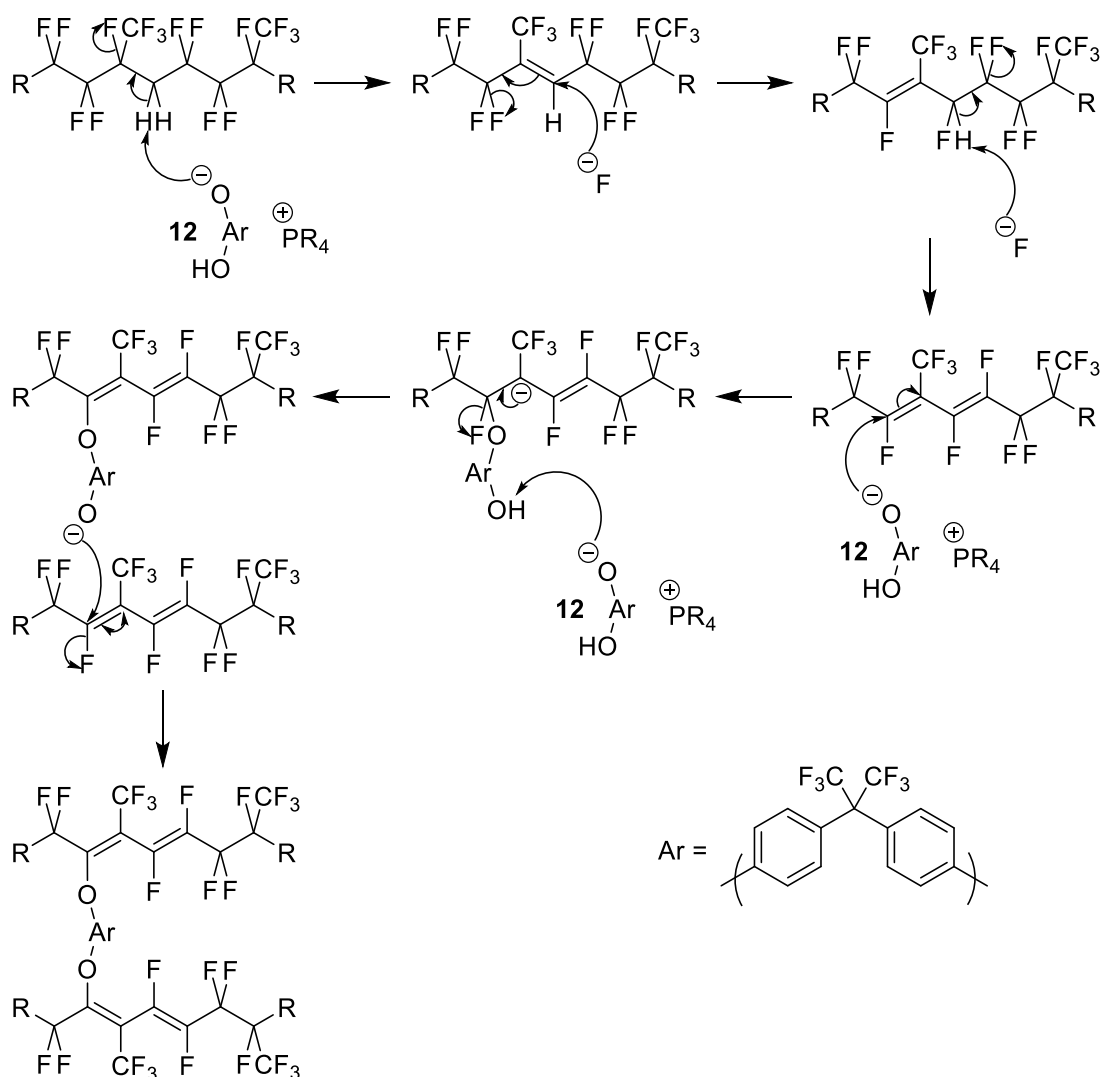


Figure 20: Mechanism for crosslinking of Viton® with bisphenol AF⁴⁶

In addition to the reagents shown, MgO and/or Ca(OH)₂ are added to sequester any HF and other volatile species produced during the reaction. Compared to Viton® crosslinked with diamines, bisphenol AF cured Viton® elastomers show improved heat and water resistance and the cure time is also shorter, leading to improved seal quality. However, the cured polymer is susceptible to reaction with high temperature water and steam at the cure site, displacing the bisphenol AF and breaking the crosslinks³⁰ (Fig. 21).

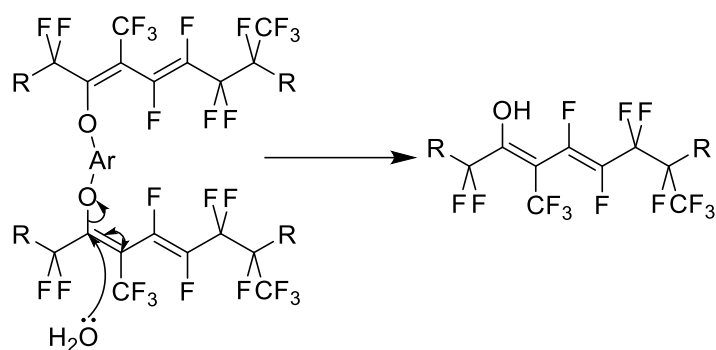


Figure 21: Breaking of bisphenol AF crosslinks in Viton® with water³⁰

Bisphenol AF crosslinking is also not suitable for Viton® elastomers that contain PMVE, as the deprotonated bisphenol AF can act as a base, eliminating HOCF₃ from the polymer and causing backbone degradation⁴⁷ (Fig. 22). The HOCF₃ decomposes further to CO₂ and HF, volatile species that disrupt the curing process and contribute to poor crosslinking.

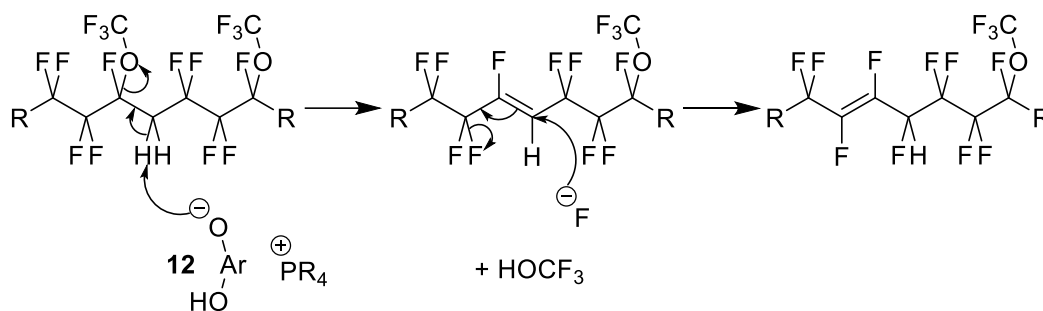


Figure 22: Reaction of deprotonated bisphenol AF with Viton® that contains PMVE⁴⁷

1.3.3.2. Crosslinking of Viton® with Peroxides

Peroxide crosslinking methods are used for synthesis of specialised Viton® elastomers (GAL-S, GBL-S, GF-S, GLT-S, GBLT-S, GFLT-S and ETP-S) and are facilitated by the incorporation of cure site monomers (CSM e.g. **13**, **14** and **15**) which contain bromine atoms, that are added to the polymer backbone⁴⁸ (Fig. 23).

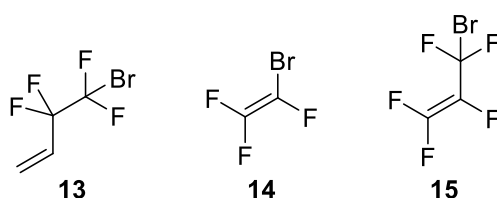


Figure 23: Typical CSM used in Viton® elastomers that undergo peroxide cures⁴⁸

The initiator is typically di-*tert*-butyl peroxide (**16**), which decomposes to methyl radicals and acetone and, in these cases, triallyl-*iso*-cyanurate (TAIC, **17**) is used as the crosslinking agent⁴⁸.

The methyl radicals abstract bromine from the cure site monomers to generate a radical along the polymer backbone, and react with the vinyl groups of **17**, forming more stable secondary carbon radicals. The radical derived from **17** can subsequently abstract bromine or react with additional molecules of **17** to form a polymer, a common side reaction during the peroxide curing process^{40,46} (Fig. 24).

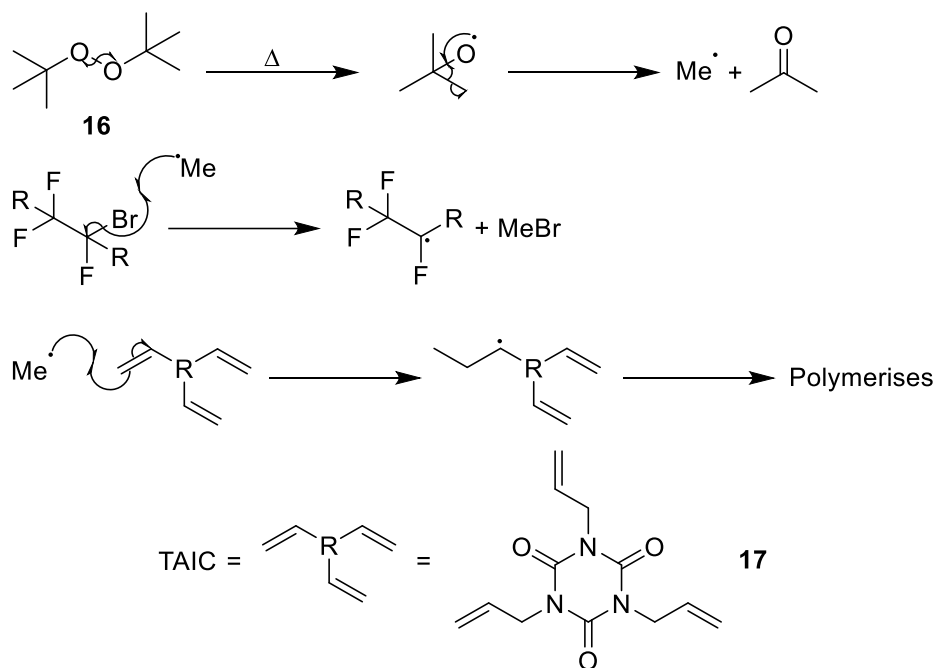


Figure 24: Initiation reactions for curing of Viton® with TAIC. The homopolymerisation of TAIC also occurs^{40,46}

Polymer backbone radicals react with the vinyl group of **17**, before abstracting a further bromine atom from a cure site monomer (Fig. 25). This reaction can occur up to three times for each molecule of **17**, crosslinking the Viton® polymer chains^{40,46}.

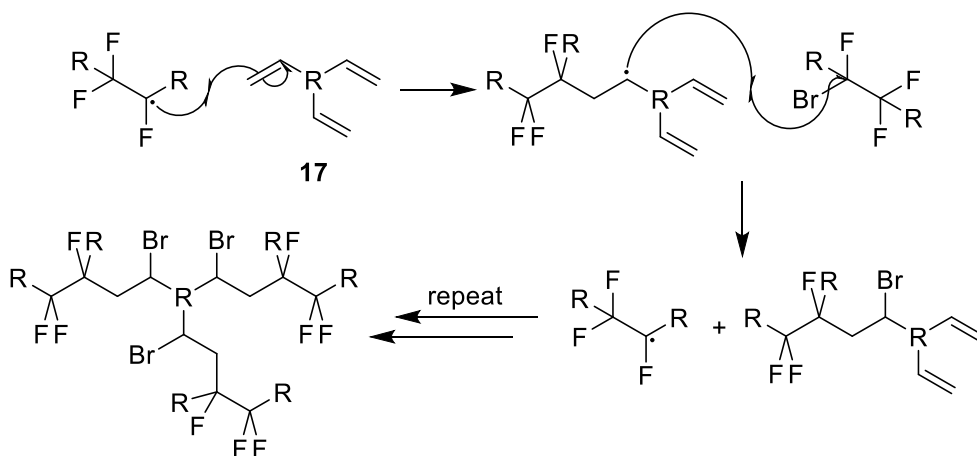


Figure 25: Propagation and termination reactions for the crosslinking of Viton® with TAIC^{40,46}

The peroxide crosslinking method is most commonly used for synthesis of Viton® elastomers containing PMVE (GLT-S, GBLT-S, GFLT-S and ETP-S); however, it is also used in the synthesis of Viton® GAL-S, GBL-S and GF-S despite these elastomers being suitable for crosslinking with Bisphenol AF (**12**). The peroxide crosslinking process has several advantages over crosslinking with **12**, such as improved resistance of the final polymer to mineral acids and high temperature water or steam. The crosslinking bond between the polymer backbone and TAIC (**17**) is a C – C bond and, therefore, is not vulnerable to attack by nucleophiles. Peroxide crosslinking is also faster which reduces the number of moulding defects and the extent of mould fouling³⁰.

The composition and structure of the synthesised Viton® elastomer determines the finished polymer’s properties and the applications for which the elastomer is suitable. These properties and applications are detailed below.

1.3.4. Properties of Viton® Elastomers

Viton® elastomers possess many desirable properties when compared to other polymers, and these properties differ between the specific classes of Viton® elastomer^{10,49}. The monomer composition, curing method and fluorine content all affect the finished polymer’s properties, as detailed in Table 5.

Table 5: Composition and properties of the Viton® elastomers^{10,49}

Viton® Elastomer	Monomers Used	Fluorine Content	Glass Transition Temperature (Tg) / °C	Curing Method
A	HFP, VDF	66%	-17	Bisphenol
B	HFP, VDF, TFE	68%	-13	Bisphenol
F	HFP, VDF, TFE	70%	-8	Bisphenol
GAL-S	HFP, VDF, TFE, CSM	66%	-19	Peroxide
GBL-S	HFP, VDF, TFE, CSM	67%	-15	Peroxide
GF-S	HFP, VDF, TFE, CSM	70%	-6	Peroxide
GLT-S	PMVE, VDF, TFE, CSM	64%	-30	Peroxide
GBLT-S	PMVE, VDF, TFE, CSM	65%	-26	Peroxide
GFLT-S	PMVE, VDF, TFE, CSM	67%	-24	Peroxide
ETP-S	PMVE, TFE, Ethylene, CSM	66%	-12	Peroxide

1.3.4.1. High and Low Temperature Properties of Viton® Elastomers

All Viton® elastomers are resistant to high temperatures, due to the strong C – F bonds along the polymer backbone²³; Viton® remains elastic indefinitely at temperatures of 204 °C and below, and can be used at temperatures of up to 316 °C for short periods of time⁴⁹.

The low temperature flexibility of fluorinated polymers is defined by the molecular structure of the polymer backbone. For example, the backbone CF₂ groups of PTFE are staggered and form rigid, spiralled, rod like structures⁵⁰; by comparison, the backbone of Viton® contains both CH₂ groups and side groups (CF₃ or OCF₃), which improve flexibility. This accounts for the lower glass transition temperature (T_g, the temperature at which the polymer becomes rigid and loses flexibility) of Viton® elastomers when compared with PTFE (115 °C). T_g's of different Viton® elastomers are affected by both monomer composition and the fluorine content of the polymer (Table 5). Viton® elastomers that contain PMVE have significantly lower T_g's than the equivalent HFP containing species due to the additional backbone flexibility provided by the oxygen spacer in the PMVE monomer. In addition, Viton® elastomers with the highest fluorine contents (F, GF-S and GFLT-S) have higher T_g's when compared to similar elastomers due to the increased TFE content in these species^{10,49}.

1.3.4.2. Chemical Resistance of Viton® Elastomers

Whilst Viton® elastomers show strong resistance to aliphatic and aromatic hydrocarbon solvents, most Viton® elastomers swell significantly in contact with oxygenated solvents, with the exception of highly fluorinated elastomers (F, GF-S, GFLT-S and ETP-S), which are resistant to swelling in the presence of both alcohols and ethers^{49,51}. However, only Viton® ETP-S does not swell significantly when exposed to low molecular weight carbonyl compounds, such as acetone⁴⁷.

All Viton® elastomers show moderate resistance to acids and water/steam. However, peroxide cured elastomers are significantly more resistant to these species due to the lack of bisphenol AF crosslinking bonds, which are susceptible to attack by nucleophiles. Therefore, peroxide cured Viton® elastomers are recommended for hoses used in vehicles that use biodiesel, since biodiesel can break down to produce fatty acids³⁰.

Most Viton® seals have poor resistance to both organic and inorganic bases, particularly bisphenol AF cured Viton® elastomers which are susceptible to attack by bases at the crosslinking sites. Peroxide cured Viton® elastomers are more resistant to bases but are still

vulnerable to dehydrofluorination. This causes unwanted crosslinking or swelling of the polymer, leading to seal degradation⁴⁰. Only Viton® ETP-S (Viton® Extreme) is resistant to bases, due to the lack of VDF in the polymer structure¹⁰.

1.3.5. Model Compounds of Viton® Elastomers

Understanding the exact mechanisms by which Viton® seals are degraded would help inform decisions about the composition of additive systems and the choice of seals for particular applications. However, the degradation of Viton® is difficult to analyse; for example, a recent article examined the reaction of uncured Viton® A with KOH by ¹H and ¹⁹F NMR spectroscopy and FTIR spectroscopy¹². The results provided significant insight into the degradation of Viton® by hydroxide, but interpretation of the results is made difficult due to the overlapping signals in the NMR and IR spectra.

As an alternative to directly examining the degradation of Viton®, low molecular weight model compounds can, in principle, be synthesised that contain the core structural features of the Viton® elastomers, such as the one shown in Fig. 26. Representative model compounds can be reacted with species mimicking petroleum additives, and the products of these reactions can be examined by solution phase ¹H, ¹⁹F and ¹³C NMR spectroscopy and mass spectrometry to obtain detailed structural information about the degradation products.

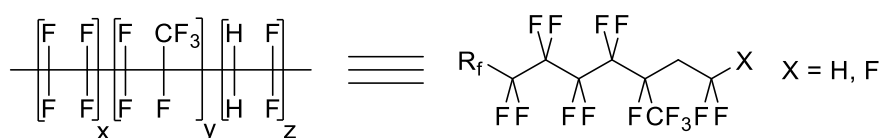


Figure 26: An example small molecule that contains the structural features present in Viton® A, B and F

The Viton® model compounds described in this thesis were synthesised by reacting perfluoroalkyl iodides with the fluorinated monomers used in the synthesis of Viton® (VDF, HFP and PMVE), producing polyfluorinated telomer iodides^{43,44}.

Consequently, the chemistry of perfluoroalkyl iodides will be discussed in detail here as background information, beginning with their synthesis from readily available fluorinated building blocks. This will be followed by a discussion of some of the reactions of perfluoroalkyl iodides with unsaturated molecules, including their reactions with the monomer gases of Viton.

1.4. Perfluoroalkyl Iodides

1.4.1. Synthesis of Perfluoroalkyl Iodides

Perfluoroalkyl iodides are synthesised using readily available fluorinated starting materials, such as TFE and HFP, and halogenating agents. For example, pentafluoroethyl iodide (**18**), the starting material for the synthesis of straight chain perfluoroalkyl iodides that contain an even number of carbon atoms, is synthesised by initial reaction of TFE with iodine, forming 1,2-diiodotetrafluoroethane, followed by reaction with IF_5 (Fig. 27).

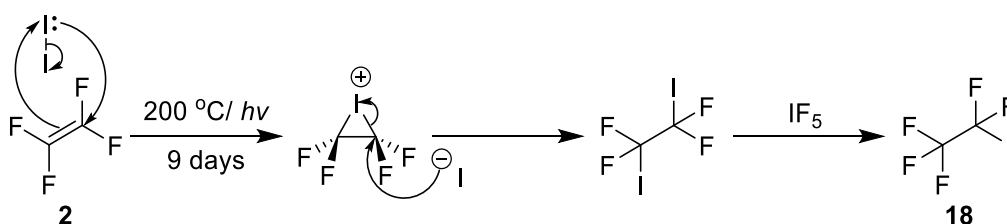


Figure 27: Synthesis of pentafluoroethyl iodide from TFE⁵²

Once synthesised, **18** can be reacted with TFE to produce higher molecular weight perfluoroalkyl iodide telomers by a radical chain mechanism⁵² (Fig. 28).

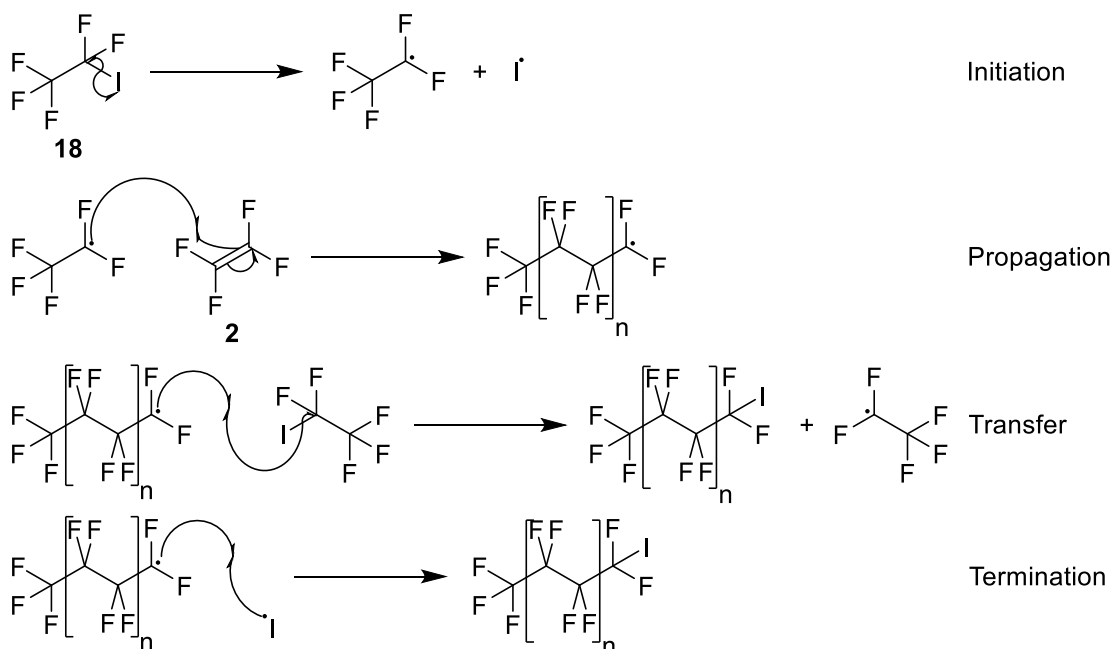


Figure 28: Synthesis of perfluoroalkyl iodides containing an even number of carbon atoms from pentafluoroethyl iodide and TFE⁵²

Straight chain perfluoroalkyl iodides containing an odd number of carbon atoms are synthesised by reacting commercially available CF₃I (**19**) with TFE in a radical process as described above⁵³ (Fig. 29).

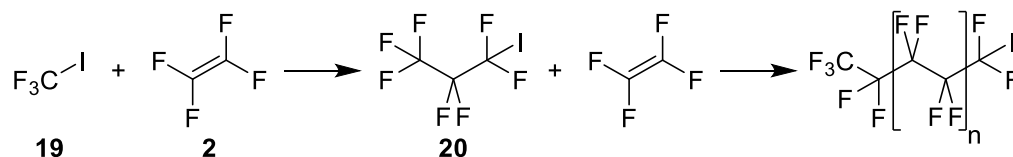


Figure 29: Synthesis of perfluoroalkyl iodides containing an odd number of carbon atoms from CF₃I and TFE⁵²

Branched perfluoroalkyl iodides are derived from perfluoro-*iso*-propyl iodide (**21**), which is synthesised by reacting HFP with ICl and HF, using BF₃ as a catalyst⁵⁴ (Fig. 30).

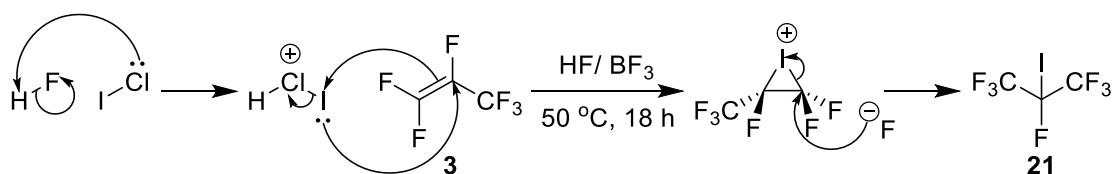


Figure 30: Synthesis of 2-iodoperfluoropropane from HFP⁵⁴

Telomerisation of **21** with TFE produces terminally branched perfluoroalkyl iodides⁵⁵ (Fig. 31).

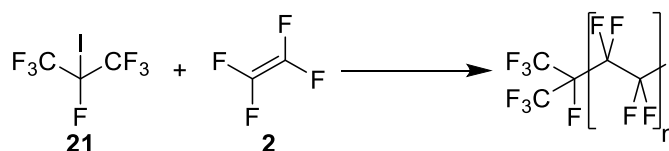


Figure 31: Synthesis of terminally branched perfluoroalkyl iodides from 2-iodoperfluoropropane and TFE⁵⁵

To introduce branches at positions in the middle of the carbon backbone, HFP is reacted with straight chain perfluoroalkyl iodides to produce terminally branched species which can be further reacted with TFE⁵⁶ (Fig. 32).

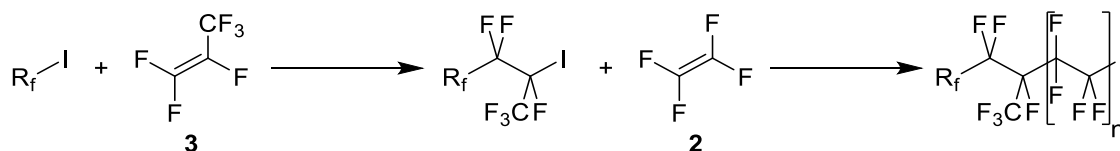


Figure 32: Synthesis of branched perfluoroalkyl iodides from R_f-I, HFP and TFE⁵⁶

1.4.2. Reactivity of Perfluoroalkyl Iodides

Perfluoroalkyl iodides give electrophilic perfluoroalkyl radicals by homolytic cleavage of the C – I bond, achieved by heating or irradiation with UV light⁵⁷ (Fig. 33).

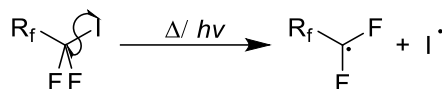


Figure 33: Homolytic cleavage of the C – I bond in a perfluoroalkyl iodide⁵⁷

In reactions that are sensitive to heat or UV radiation, radical initiators are used to promote the reactivity of perfluoroalkyl iodides. One of the most commonly used initiators is AIBN (**22**); however, a by-product of reactions involving **22** is tetramethylsuccinonitrile (**25**), which is highly toxic. As a result, other radical initiators are increasingly being used instead^{52,58} (**23**, **24**) (Fig. 34).

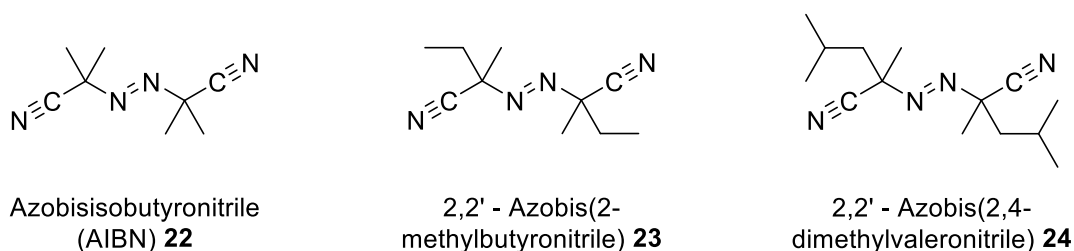


Figure 34: Initiators for reactions involving perfluoroalkyl iodides

Perfluoroalkyl iodides react readily with unsaturated compounds in a radical chain process^{57,59} (Fig. 35 – 37)

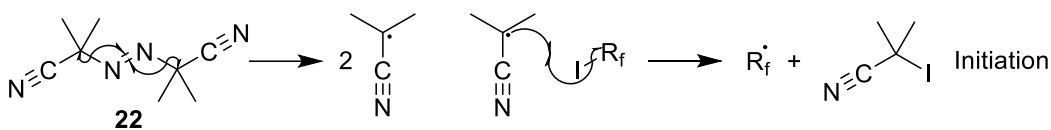


Figure 35: Initiation step of the radical chain reaction of a perfluoroalkyl iodide with an alkene, using AIBN as an initiator^{57,59}

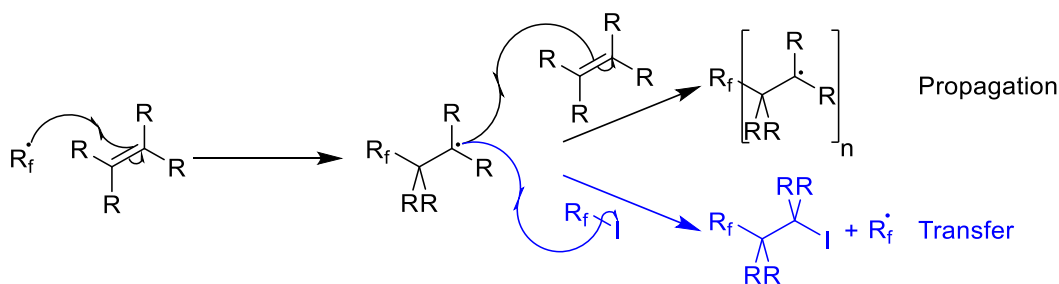


Figure 36: Propagation and transfer steps of the radical chain reaction of a perfluoroalkyl iodide with an alkene

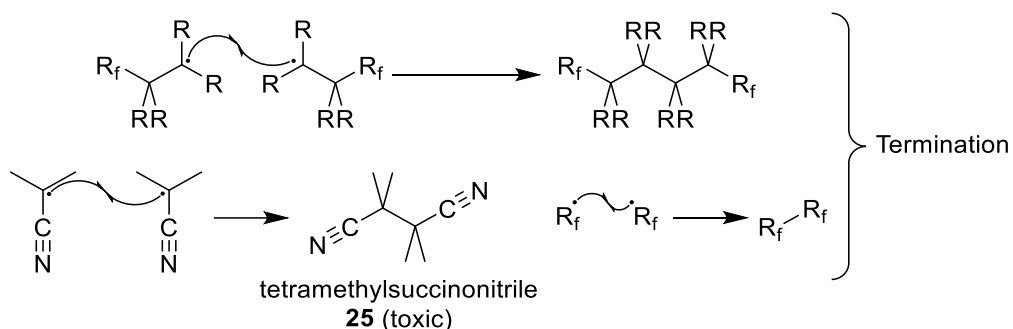


Figure 37: Termination processes of the radical chain reaction of a perfluoroalkyl iodide with an alkene

The reactions of perfluoroalkyl iodides with alkynes are analogous and produce the corresponding vinyl iodides⁶⁰. All of these reactions are exothermic, as the π bond of the alkene or alkyne is broken and replaced by a stronger σ bond to the perfluoroalkyl group. As a consequence, reactions of perfluoroalkyl iodides must be carefully controlled to avoid thermal runaway, often by using limited quantities of the initiator (1 – 2%)⁵².

Perfluoroalkyl radicals are electrophilic and as such react selectively with the most nucleophilic groups of alkenes as described in the examples below. However, the electrophilicity of perfluoroalkyl radicals depends on their structure. Fluorine atoms directly bonded to the carbon bearing the radical stabilise the singly occupied molecular orbital by resonance donation of electron density. This resonance effect partially counteracts the inductive electron withdrawing effects of the fluorine atoms, reducing the electron deficiency of straight chain perfluoroalkyl radicals. By comparison, terminally branched perfluoroalkyl radicals are more electron deficient, and those with perfluoroalkyl branches are more electrophilic than those with CF_3 branches, as longer chain perfluoroalkyl groups are more electron withdrawing than shorter chain groups (Fig. 38 and 39)⁵⁷.

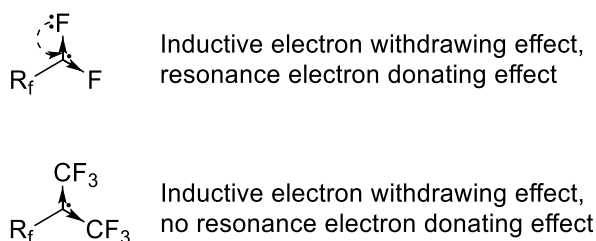


Figure 38: Explanation of the difference in electrophilicity of straight chain and branched perfluoroalkyl radicals⁵⁷

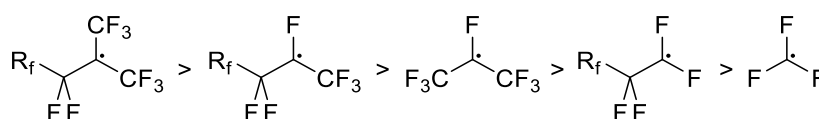


Figure 39: Scale of electrophilicity of perfluoroalkyl radicals⁵⁷

In order to better understand the reactivity of perfluoroalkyl iodides, several examples of reactions with unsaturated compounds are detailed below.

1.4.2.1. Reactions of Perfluoroalkyl Iodides with Styrene Derivatives

The reactions of several perfluoroalkyl iodides with a range of styrene derivatives have been investigated (Fig. 40, Table 6) which demonstrate the importance of polarity and steric effects on the rates of addition of perfluoroalkyl radicals to alkenes^{57,60–62}.

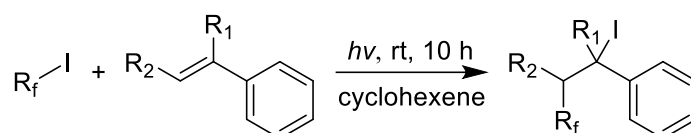


Figure 40: Reaction of perfluoroalkyl iodides with styrene derivatives^{57,60–62}

Table 6: Rate constants for the reactions of perfluoroalkyl iodides with styrene derivatives^{57,60–62}

Alkene	Rate constant for addition of R_f^\bullet to the alkene (k_{add}) / $10^6 \text{ M}^{-1} \text{ s}^{-1}$					
	CF_3^\bullet	$\text{CF}_3\text{CF}_2^\bullet$	$\text{CF}_3\text{CF}_2\text{CF}_2^\bullet$	$n\text{-C}_7\text{F}_{15}^\bullet$	$(\text{CF}_3)_2\text{CF}^\bullet$	$(\text{CF}_3)_3\text{C}^\bullet$
styrene 26	53	79	43	46	120	363
pentafluorostyrene 27	26	23	13	-	81	16
α -methylstyrene 28	87	94	78	89	-	589
β -methylstyrene 29	17	7	3.8	3.7	1.9	2.5

As Table 6 above shows, styrene (**26**), a nucleophilic alkene, reacted readily with all the perfluoroalkyl iodides and the rates of reaction depended on the electrophilicity of the attacking radical. $\text{CF}_3\text{CF}_2^\bullet$ reacted more quickly with **26** than CF_3^\bullet , due to the increased electrophilicity of perfluoroalkyl radicals compared with trifluoromethyl radicals⁶². By contrast, longer chain radicals ($\text{CF}_3\text{CF}_2\text{CF}_2^\bullet$, $n\text{-C}_7\text{F}_{15}^\bullet$) reacted more slowly because of the decreased electrophilicity of the β R_f groups on the attacking radicals, compared to the β fluorine atom on $\text{CF}_3\text{CF}_2^\bullet$ ($R_f - \text{CF}_2\text{CF}_2^\bullet$ is less electrophilic than $\text{F} - \text{CF}_2\text{CF}_2^\bullet$)⁶¹. However, branched radicals ($(\text{CF}_3)_2\text{CF}^\bullet$, $(\text{CF}_3)_3\text{C}^\bullet$) reacted significantly more quickly than any of the straight chain systems, consistent with the increased electrophilicity of branched perfluoroalkyl radicals⁵⁷.

Pentafluorostyrene (**27**) reacts more slowly with all the perfluoroalkyl radicals than **26**^{61,62}, which is consistent with **27** being a more electrophilic alkene. In particular, $(\text{CF}_3)_3\text{C}^\bullet$ reacted at a similar rate to the straight chain perfluoroalkyl radicals despite reacting significantly faster with **26**. This suggests that steric factors have more influence on the rate of reaction than the

polarity difference between the alkene and the radical⁵⁷. By contrast, α -methylstyrene (**28**) reacts faster with all perfluoroalkyl radicals than **26**, as it is a significantly more nucleophilic^{61,62}.

1.4.2.2. Reactions of Perfluoroalkyl Iodides with Terminal Aliphatic Dienes

The reactions of perfluoroalkyl iodides with terminal aliphatic dienes generally give two products arising from mono and di-addition of the perfluoroalkyl iodide, in amounts depending on the number of equivalents of perfluoroalkyl iodide (Fig. 41)⁶³⁻⁶⁶.

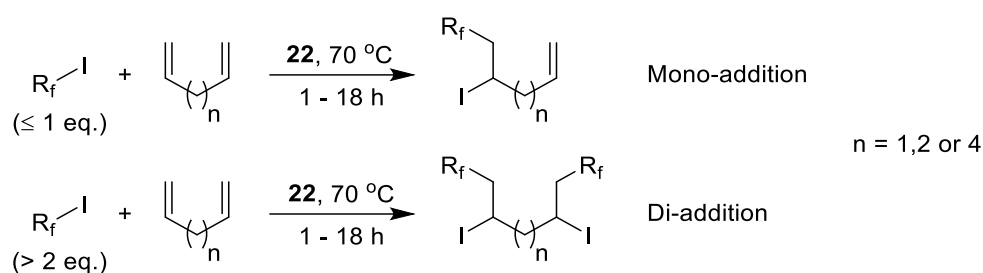


Figure 41: Reactions of terminal aliphatic dienes with perfluoroalkyl iodides⁶³⁻⁶⁶

As an example, the conditions and product ratios for the reactions of perfluoro-*n*-butyl iodide ($\text{CF}_3\text{CF}_2\text{CF}_2\text{CF}_2\text{I}$) with a range of terminal aliphatic dienes are detailed in Table 7^{63,66}.

Table 7: Conditions and products for the reactions of terminal aliphatic dienes with $\text{CF}_3\text{CF}_2\text{CF}_2\text{CF}_2\text{I}$ at 70 °C^{63,66}

Diene	Equivalents of R_fI	Time / h	22 / %	Yield / %	Conversion to products / %	
					Mono addition	Di addition
1,4-pentadiene 30	0.25	16	2	86	74	12
	0.506	16	4	77	70.8	6.1
	4.0	8	1	76	22.1	53.5
1,5-hexadiene 31	0.21	16	1	90	74.4	15.7
	0.25	21	1	76	64.8	11.6
	2.5	2	4	98	15	83
1,7-octadiene 32	0.25	18	1	90	72	10
	0.5	16	1	56	48.5	7.6
	2.0	18	1	97	21	76
	2.1	9	1.5	95	38.2	56.8

The data in Table 7 shows that increasing the relative amount of perfluoro-*n*-butyl iodide increased the amount of di-addition product formed compared to mono-addition product. In addition, when an excess of perfluoro-*n*-butyl iodide was used, increasing the reaction time increased the relative amount di-addition product. Yields are reduced because side reactions such as H-abstraction consume some of the initiator^{63,66}.

However, reactions of 1,6-heptadiene (**33**) with perfluoroalkyl iodides yielded a third cyclisation product which is favoured due to the entropic benefit of the intramolecular reaction and the low ring strain of the five membered ring product (Fig. 42). The mechanism for the formation of all three products is given in Fig. 43^{64,65}.

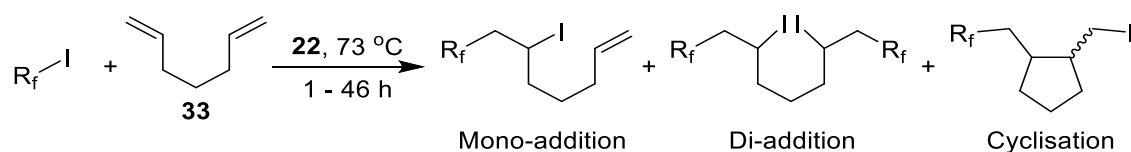


Figure 42: Products from the reaction of 1,6-heptadiene with a perfluoroalkyl iodide^{64,65}

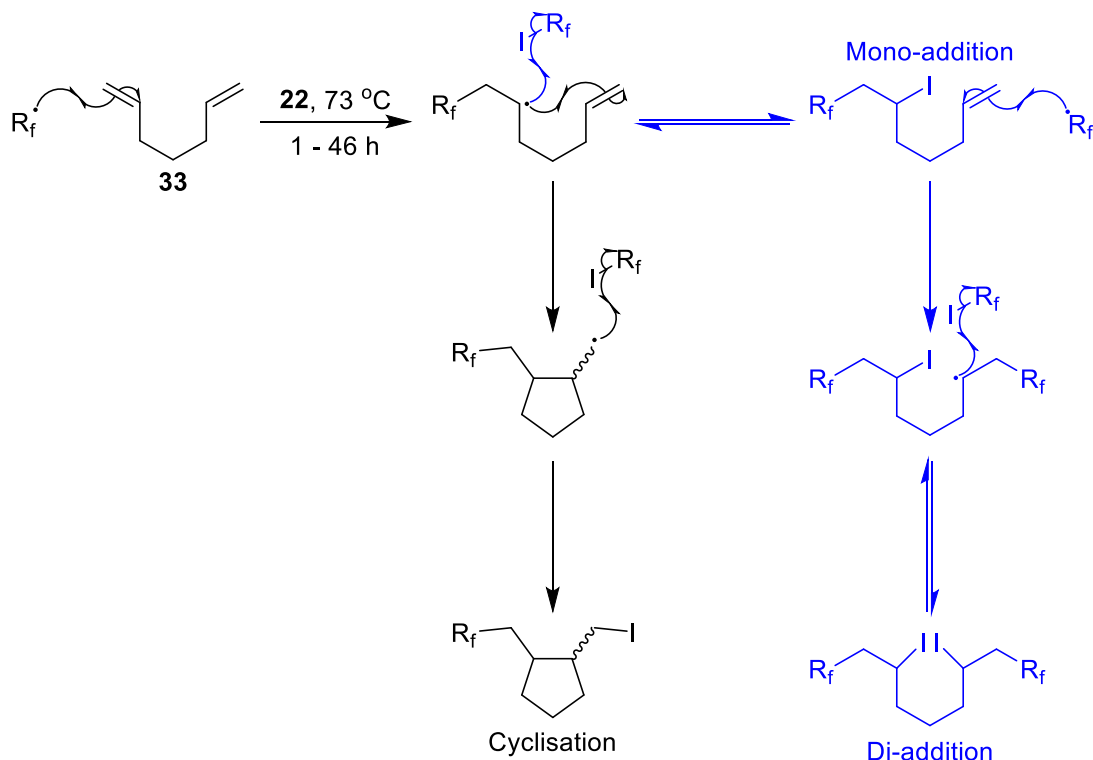


Figure 43: Mechanism for the formation of all three products from the reaction of 1,6-heptadiene with perfluoroalkyl iodides^{64,65}

As an example, reactions of **33** with two equivalents of perfluoro-*n*-propyl iodide were monitored over time, with AIBN (**22**) as initiator (Table 8).

Table 8: Product ratios of the reaction of 1,6-heptadiene with perfluoro-*n*-propyl iodide^{64,65}

Time / h	Conversion to product / %				Ratio of cyclic products: non-cyclic products
	Mono addition	Di addition	<i>Trans</i> cyclic	<i>Cis</i> cyclic	
1	43.2	2.3	9.3	45.2	1.20:1
4	29.3	4.0	10.0	56.8	2.00:1
7	24.9	3.6	12.0	59.5	2.50:1
12	15.8	2.1	14.5	67.6	4.58:1
24.5	8.6	4.0	17.3	67.3	6.70:1
46	2.9	1.3	16.8	76.1	31.0:1

The ratio of cyclic to non-cyclic products increased with time, suggesting that the formation of the mono-addition product is reversible, but the cyclisation step is irreversible^{64,65} (Fig. 44).

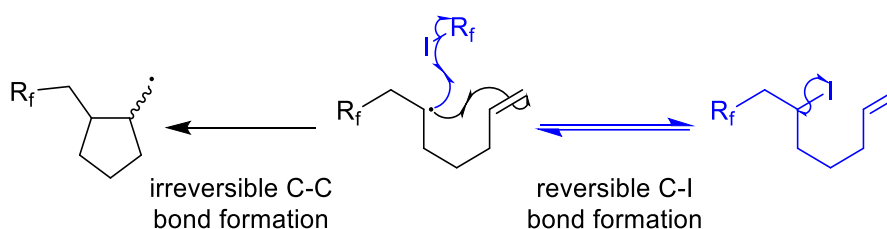


Figure 44: Reversible and irreversible reaction of the radical intermediate^{64,65}

1.4.2.3. Reactions of Perfluoroalkyl Iodides with Aromatic Systems

Reactions of perfluoroalkyl iodides with aromatic compounds give perfluoroalkyl aromatic species by single electron oxidation mechanisms, such as UV light and TiO₂ catalysed reactions between an excess of a benzene derivative and perfluorohexyl iodide⁶⁷ (Fig. 45).

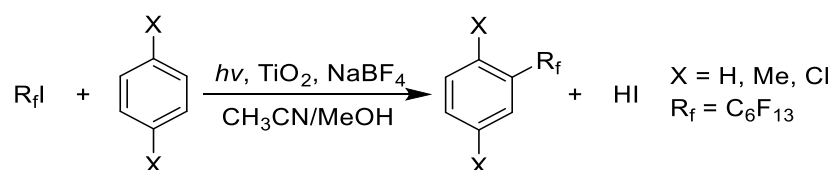


Figure 45: Reactions of substituted benzenes with perfluorohexyl iodide, using TiO₂ as redox catalyst⁶⁷

Solid TiO₂ was irradiated with UV light to produce free electrons and ‘holes’ (oxidised TiO₂), and these free electrons reduce the perfluorohexyl iodide at the metal oxide surface to produce perfluorohexyl radicals. The perfluorohexyl radicals subsequently react with the benzene derivative to produce an aryl radical, which is oxidised by the holes on the TiO₂ surface to form the corresponding cation. Elimination of a proton from the cation gives the final product⁶⁷ (Fig. 46).

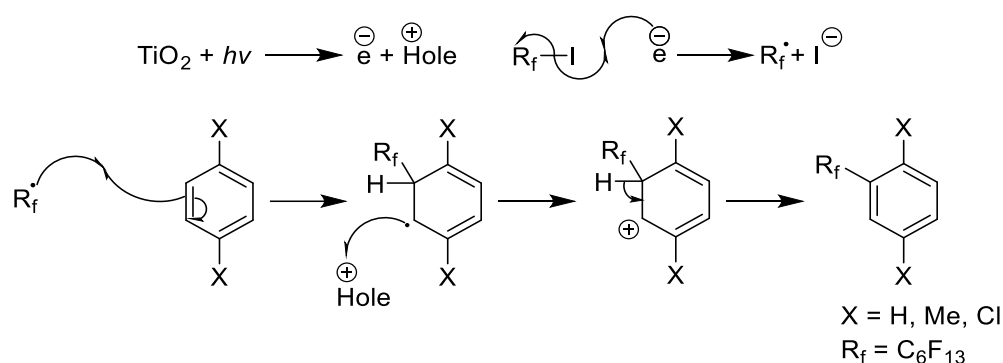


Figure 46: Mechanism for the reaction of substituted benzenes with perfluorohexyl iodide⁶⁷

1.4.3. Synthesis of Viton® Model Compounds Using Perfluoroalkyl Iodides

Perfluoroalkyl iodides react with the alkene monomer gases used in the synthesis of Viton® to produce a range of telomer iodides, that may undergo further transformation as detailed below.

1.4.3.1. Telomerisation Reactions of Perfluoroalkyl Iodides and Viton® Monomers

Reactions of perfluoroalkyl iodides with the monomers used in the synthesis of Viton® elastomers have been investigated previously by Ameduri *et al.*^{43–45,68}. In particular, the reactions of perfluoroalkyl iodides with VDF then HFP have been explored.

1.4.3.1.1. Reactions of Perfluoroalkyl Iodides with VDF

Perfluoroalkyl iodides were reacted with VDF to produce a series of VDF telomer iodides ($R_f - (VDF)_n - I$) (Fig. 47)⁴³. The reactions proceeded by a radical chain mechanism similar to that for the reaction of CF_3CF_2I with TFE that was described previously for the synthesis of perfluoroalkyl iodides, and the results of these reactions are given in Table 9.

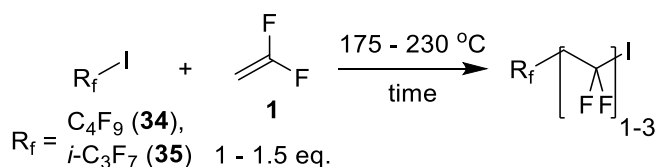


Figure 47: Reactions of perfluoroalkyl iodides with VDF⁴³

Table 9: Results from the reactions of perfluoroalkyl iodides with VDF for 15 h⁴³

Perfluoroalkyl iodide	Eq. VDF	Temp. / °C	Ratio of products ($R_f - (VDF)_n - I$) by GC-MS / %			Conversion / %
			n = 1	n = 2	n ≥ 3	
34	1.43	175	62.7	35.2	2.2	85.0
34	1.16	202	67.5	28.0	4.5	94.5
34	1.00	210	64.3	28.2	7.5	93.2
34	1.25	220	66.0	28.2	5.8	93.5
34	1.19	230	60.5	33.0	6.5	95.5
34	1.11	200	64.1	33.1	2.8	92.8
35^a	1.22	220	66.0	28.2	5.8	96.8
35	1.20	230	60.5	33.0	6.5	97.5
35^b	1.00	200	64.1	33.1	2.8	93.2

a. Reaction time, 75 h

b. Reaction time, 4 h

The reactions were carried out in an autoclave for 15 hours, using 1 – 1.43 equivalents of VDF compared to the perfluoroalkyl iodide. The product mixtures consisted principally of the mono-addition ($R_f - (VDF)_1 - I$, 60 – 68%) and di-addition ($R_f - (VDF)_2 - I$, 28 – 35%) products, with small amounts of higher molecular weight telomers (< 8%) also synthesised. Conversions of over 90% were observed for the reactions that were carried out above 200 °C, but product composition depended principally on the amount of VDF used in each reaction⁴³.

Addition of VDF to the perfluoroalkyl iodide (synthesising $R_f - \text{VDF} - \text{I}$) was almost 100% selective for attack of the perfluoroalkyl radical at the CH_2 site of VDF, due to the different polarities of the two groups as described above. However, the second addition of VDF (synthesising $R_f - (\text{VDF})_2 - \text{I}$), was only 93% selective for attack at CH_2 and, therefore, a small amount of the reverse isomer ($R_f\text{CH}_2\text{CF}_2\text{CF}_2\text{CH}_2\text{I}$) was also produced⁴³ (Fig. 48).

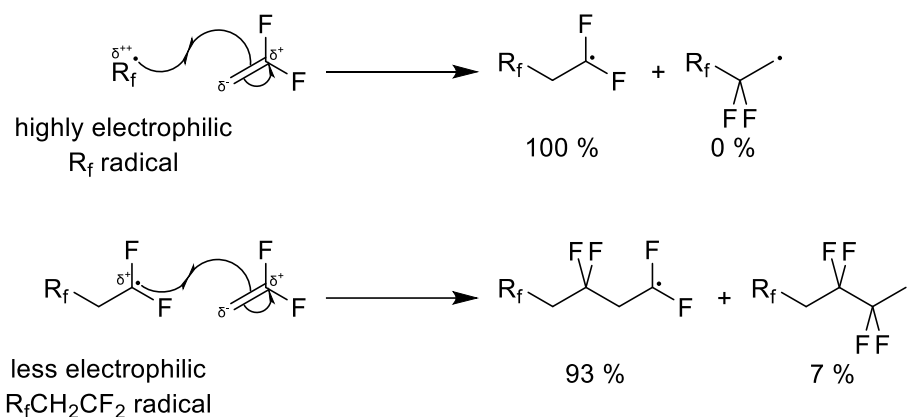


Figure 48: Selectivity of the reactions of R_f^\bullet and $R_f\text{CH}_2\text{CF}_2^\bullet$ with VDF⁴³

The $R_f\text{CH}_2\text{CF}_2$ radical is less electrophilic than the perfluoroalkyl radical, therefore, the second (and subsequent) additions of VDF were less selective for attack at the more nucleophilic CH_2 group of VDF⁴³.

1.4.3.1.2. Reactions of Perfluoroalkyl Iodides with HFP

Reactions of perfluoroalkyl iodides with HFP followed a similar procedure to those of perfluoroalkyl iodides with VDF. The reactions were carried out in an autoclave with 0.56 – 1.43 eq. of HFP. However, due to the lower reactivity of HFP compared to VDF, the reactions were all run for 75 hours. In addition, temperatures above 230 °C were required for high conversion ($\geq 75\%$)⁴⁴ (Fig. 49). The results of these reactions are detailed in Table 10.

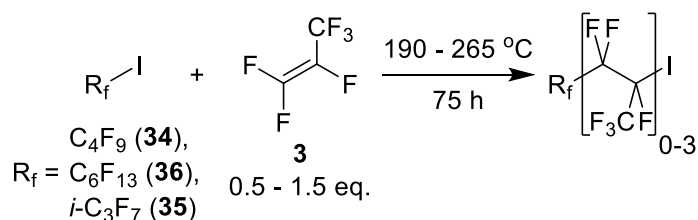


Figure 49: Reactions of perfluoroalkyl iodides with HFP⁴⁴

Table 10: Results from the reactions of perfluoroalkyl iodides with HFP⁴⁴

Perfluoroalkyl iodide	Eq. HFP	Temp. / °C	Ratio of products (R _f – (HFP) _n – I) by GC-MS / %			Conversion / %
			n = 1	n = 2	n ≥ 3	
34	1.43	190	87.5	12.5	0	45
34	1.43	205	87.0	13.0	0	50
34	0.56	220	90.5	9.5	0	62
34	0.91	230	78.5	19.5	2.0	73
34	0.91	240	84.6	12.8	2.6	83
34	0.91	250	83.6	13.6	2.8	90
34	1.00	255	87.0	10.7	2.3	93
36	1.00	240	71.1	21.6	7.3	75
36	0.91	248	78.0	17.6	4.4	83
36	1.11	265	76.0	20.0	4.0	92
36	1.25	256	70.0	29.4	0.6	94
35	0.77	230	90.0	10.0	0	30
35	1.00	250	91.2	8.8	0	36
35	1.00	100.0	60.5	0	0	11

The reactions were selective for attack of the perfluoroalkyl radical at the CF₂ group of HFP, due to competing polarity and steric effects described previously, and the selectivity improved with increasing temperature (90% at 200 °C, 99% at 255 °C) (Fig. 50). However, reactions with perfluoro-*iso*-propyl iodide were almost 100% selective for attack at the CF₂ group of HFP at all temperatures, and conversions for these reactions were low (< 40%), due to the increased steric bulk of the perfluoro-*iso*-propyl radical⁴⁴.

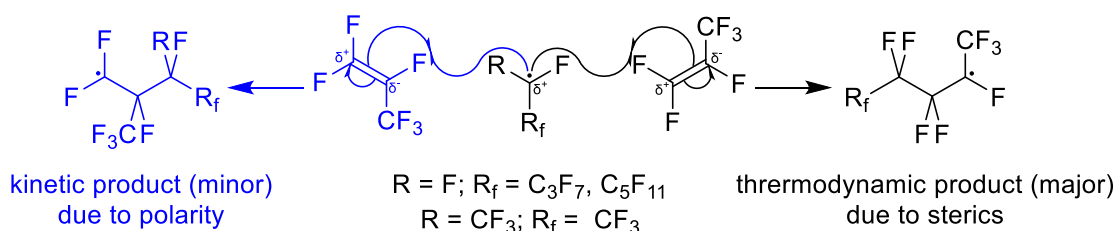


Figure 50: Products and selectivity of the reactions of HFP with perfluoroalkyl iodides⁴⁴

All of the reactions produced principally the mono-addition product ($R_f - (\text{HFP})_1 - \text{I}$, 70 – 100%), with small amounts of the di-addition product ($R_f - (\text{HFP})_2 - \text{I}$, 0 – 30%) also observed, consistent with the fact that HFP does not homopolymerise.

1.4.3.2. Reactions of Polyfluorinated Telomer Iodides

Polyfluorinated telomer iodides can be ‘capped’ by transforming them to other compounds that do not contain iodine, and there are several different methods for effecting these transformations.

1.4.3.2.1. Coupling of Two Telomer Iodides

Capping of polyfluorinated telomer iodides has been achieved by the coupling of two telomer iodides using UV radiation and mercury as an initiator⁵⁵ (Fig. 51).

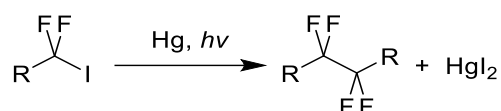


Figure 51: Coupling reaction of telomer iodides using mercury and UV radiation⁵⁵

However, an alternative method for the coupling of polyfluorinated telomer iodides is reaction with zinc and acetic anhydride in DCM⁶⁹ (Fig. 52).

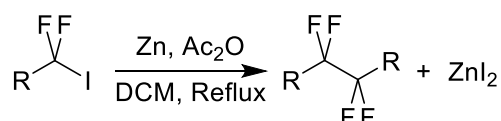


Figure 52: Coupling reaction of telomer iodides using zinc and acetic anhydride⁶⁹

1.4.3.2.2. Replacing the Iodine Atom with Hydrogen or Fluorine

Substitution of iodine for hydrogen in VDF telomer iodides has been carried out using tributyl tin hydride, a source of hydrogen radicals, producing VDF telomer hydrides in good yields^{43–45} (Fig. 53).



Figure 53: Reaction of VDF telomer iodides with Bu_3SnH

For perfluoroalkyl iodides and HFP telomer iodides, strong aqueous base can also be used for this transformation. However, for VDF telomer iodides, elimination of H – I was the predominant reaction, yielding the corresponding alkene⁵⁵ (Fig. 54).

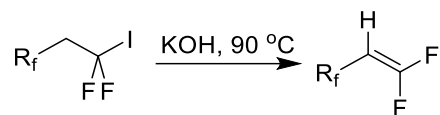


Figure 54: Elimination of H – I from VDF telomer iodides by strong aqueous base

Telomer iodides have also been capped by substitution of iodine for fluorine, using a wide variety of reagents. These substitution reactions have been carried out using BrF_3 , ClF_3 and CoF_3/F_2 ⁵³, but these reagents are highly toxic, corrosive and/or explosive. SbF_3Cl_2 has also been used as a fluoride source⁵⁵, but this required *in-situ* synthesis of the reagent from SbF_3 and chlorine gas. An alternative reagent for this reaction is antimony pentafluoride (SbF_5), which is relatively shelf stable^{69,70} (Fig. 55).

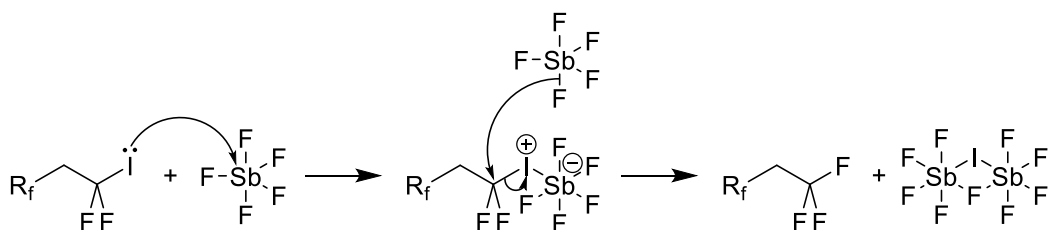


Figure 55: Reaction of telomer iodides with antimony pentafluoride

1.4.4. Reactions of Viton® Model Compounds

Despite research into the synthesis of Viton® model compounds, subsequent reactions of these systems have not been investigated to any great extent. Only one example of dehydrofluorination of a Viton® model compounds, and subsequent reaction with 2-phenylethylamine (**40**), has been reported⁴⁵ (Fig. 56).

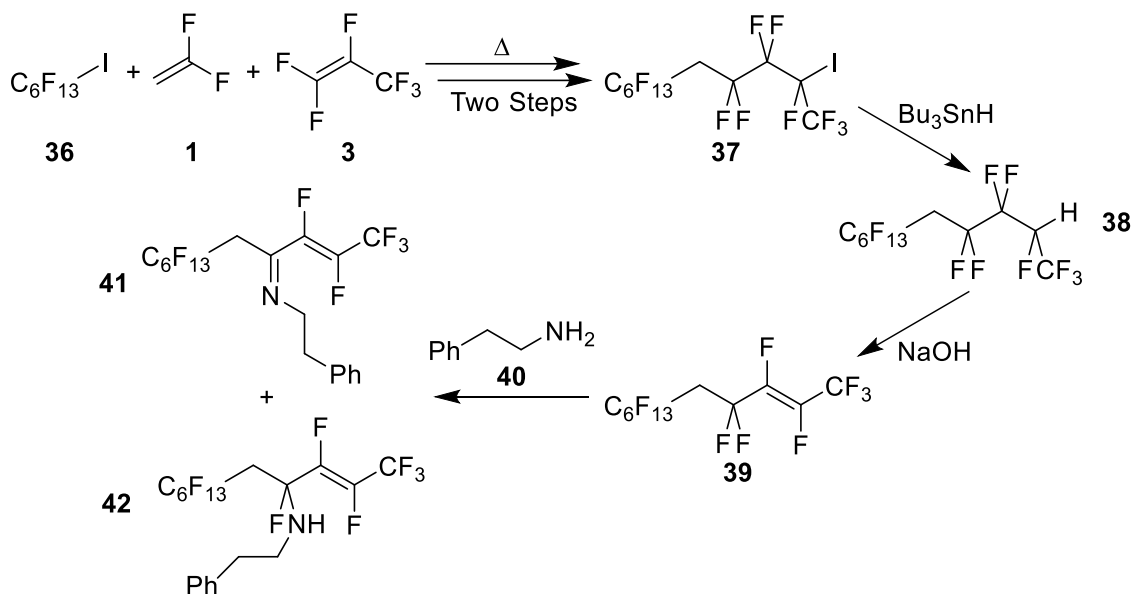


Figure 56: Synthesis, dehydrofluorination and reaction of a Viton® model compound with 2- phenylethylamine

1.5. Conclusion

Petroleum additives provide a wide range of additional functionality to petroleum products, improving oil performance and the lifetime of engines and industrial components. Engines often contain gaskets and O-rings made from Viton® elastomers, which are synthesised from fluorinated alkene monomers (VDF, HFP, TFE, PMVE) by free radical polymerisation. Viton® seals have a wide range of desirable properties, such as high chemical and heat resistance. However, degradation of Viton® O – rings and seals has been observed in the presence of petroleum additives. Viton® elastomers are synthesised by free radical polymerisation of a variety of fluorinated olefins monomers, including VDF, HFP, TFE and PMVE. These monomers are also used in the synthesis of perfluoroalkyl iodides, an important source of perfluoroalkyl radicals for organic synthesis, by reaction with I₂ and CF₃I. Examining the degradation of Viton® elastomers is difficult due to it being a high molecular weight polymer that cannot be analysed by standard solution phase and small molecule spectroscopic techniques.

2. Aims and Objectives

The degradation of Viton® seals and O-rings by petroleum additives is difficult to analyse due to Viton® elastomers being high molecular weight polymers. In this project, model compounds of Viton® elastomers will be synthesised; in particular models of structures (a) – (e) that are found in Viton® A, B, F, GAL-S, GBL-S and GF-S (Fig. 57).

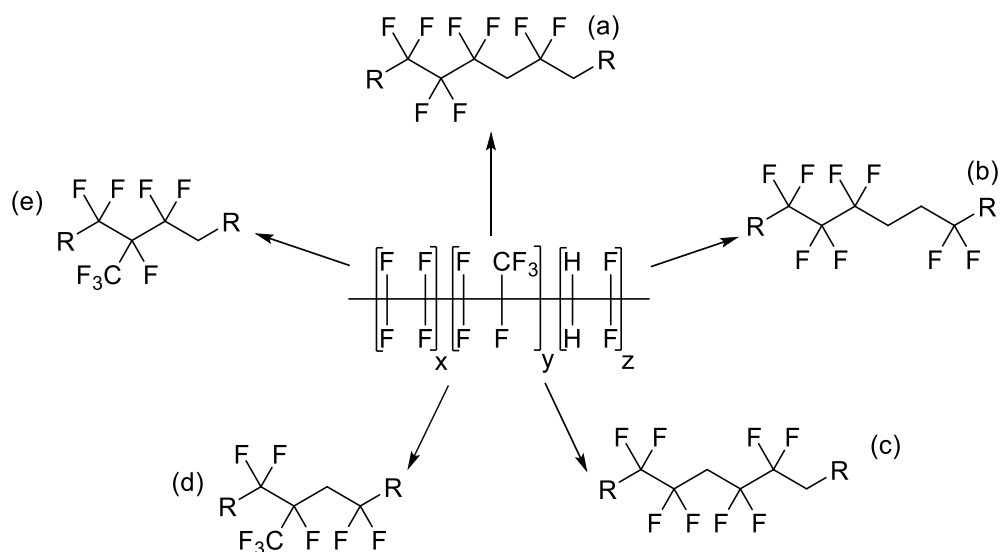


Figure 57: Key structural features of Viton®

Chemistry of these model systems will be explored, and products characterised by NMR spectroscopy and mass spectrometry. This will provide detailed structural information about the degradation of Viton® seals and O – rings that can be used to inform additive design and choice of seal material for particular applications.

Viton® model compounds will be synthesised by reacting perfluoroalkyl iodides with the monomer gases used in the production of Viton® elastomers, in particular VDF and HFP, producing polyfluorinated telomer iodides. Further reaction with ‘capping’ agents, substituting the iodine atom for hydrogen or fluorine is the strategy to synthesise model compounds that contain the key structural features of Viton® A, B, F, GAL-S, GBL-S and GF-S (Fig. 58).

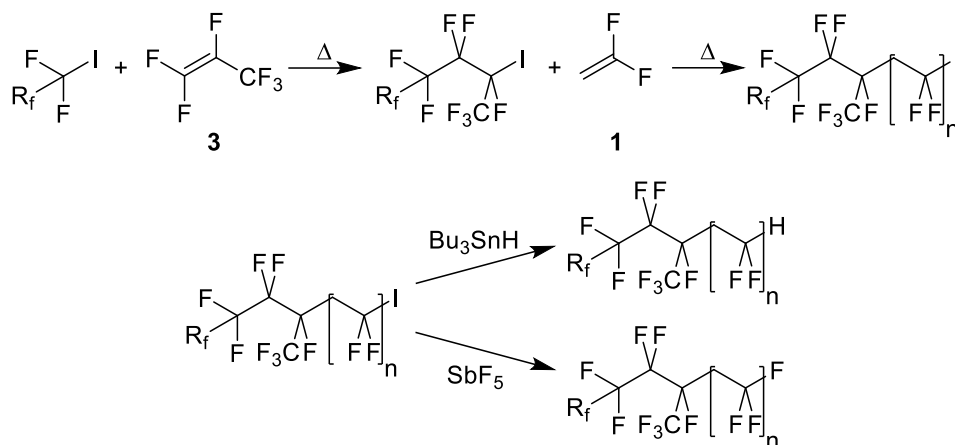


Figure 58: Synthesis of Viton® model compounds using perfluoroalkyl iodides, Viton® monomer gases and capping reagents

Due to the use of gaseous reagents and the high temperatures required for the telomerisation reactions, they will be contained in a Hastelloy autoclave and carried out in the High Pressure Laboratory, a purpose built facility unique to Durham University (Fig. 59).



Figure 59: The High Pressure Laboratory at Durham University

Once synthesised, Viton® model compounds will be reacted with a range of molecules that are representative of petroleum additives, as well as species that would form through the general wear of engines, such as iron oxides. Of particular interest are those additives that contain basic or nucleophilic groups, such as those in Fig. 60 (**43**, **44**), as these are known to cause degradation of Viton® seals^{69,70}.

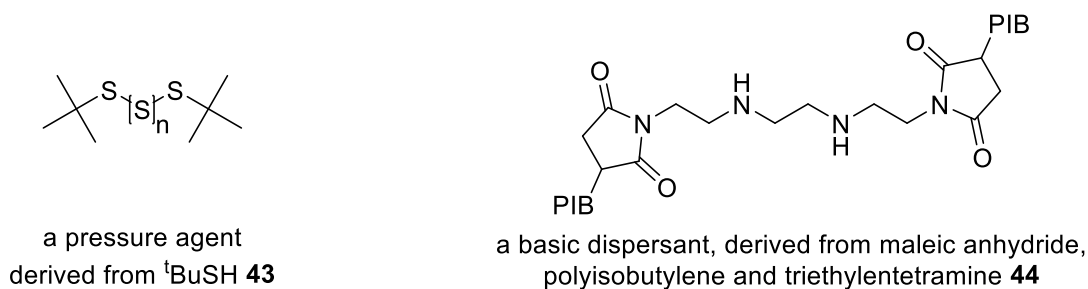


Figure 60: Examples of additives that could cause degradation of Viton® seals

Consequently, in order to mimic seal degradation, Viton® model compounds will be reacted with a range of bases that have different pK_a 's, as well as with a variety of sulfur-based nucleophiles and iron oxides (Fig. 61). The products of these reactions will be characterised by ¹H, ¹⁹F and ¹³C NMR spectroscopy and mass spectrometry and this will reveal detailed structural information about the degradation of Viton® seals in the presence of petroleum additives.

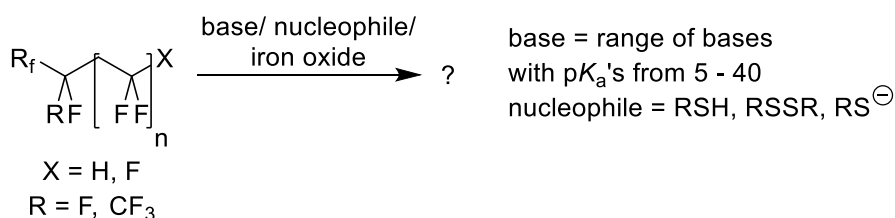


Figure 61: Reactions of Viton® model compounds with bases and nucleophiles

3. Synthesis and Degradation of Straight Chain VDF Telomer Fluorides

Following the strategy outlined above, the first model compounds that were targeted were structures (a) – (c) (Fig. 62), models of the poly VDF and TFE segments found in Viton® A, B, F, GAL-S, GBL-S, GF-S, GLT-S, GBLT-S and GFLT-S.

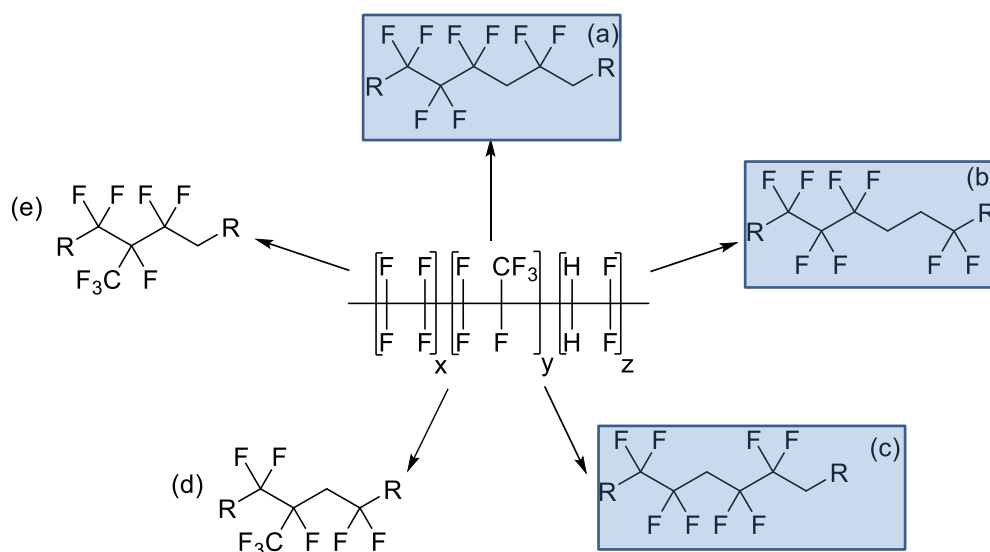


Figure 62: Structural features of Viton®

3.1. Synthesis of Poly VDF Telomer Iodides – Reactions of Perfluorooctyl Iodide with VDF

The first step of the synthesis of Viton® model compounds (a) – (c) were reactions of perfluoroalkyl iodides with VDF. Perfluorooctyl iodide (C₈F₁₇I, **45**) was chosen as the starting material because it is a good model of the poly TFE segments found in Viton® elastomers and products of the free radical reaction would not be too volatile due to its high molecular weight. Due to the use of gaseous reagents, these reactions were carried out in an autoclave in Durham University's High-Pressure Lab and were repeated multiple times in order to synthesise sufficient VDF telomer iodides for use in future reactions. In addition, a number of reactions failed due to mechanical problems encountered when using the autoclave, such as blockages, leaks and damage to bursting disks. Of the successful reactions, two are detailed below.

The first successful synthesis was the reaction of **45** with 1.5 equivalents of VDF based on a literature procedure⁴³. The autoclave was charged with degassed **45**, followed by addition of 1.5 equivalents of VDF by vacuum transfer. The autoclave was secured in a rocking furnace and heated to 190 °C for 20 hours. After cooling, the autoclave was opened, releasing any unreacted VDF, and a brown solid was collected. The reaction was worked up by washing with sodium thiosulfate solution, removing iodine contamination from the organic products. After workup, the final mixture was 13.14 g of a yellow solid, a 57% mass recovery. However, 22% of this mixture was unreacted starting material, giving an overall conversion of 78% and a product mass recovery of 45% (Fig. 63).

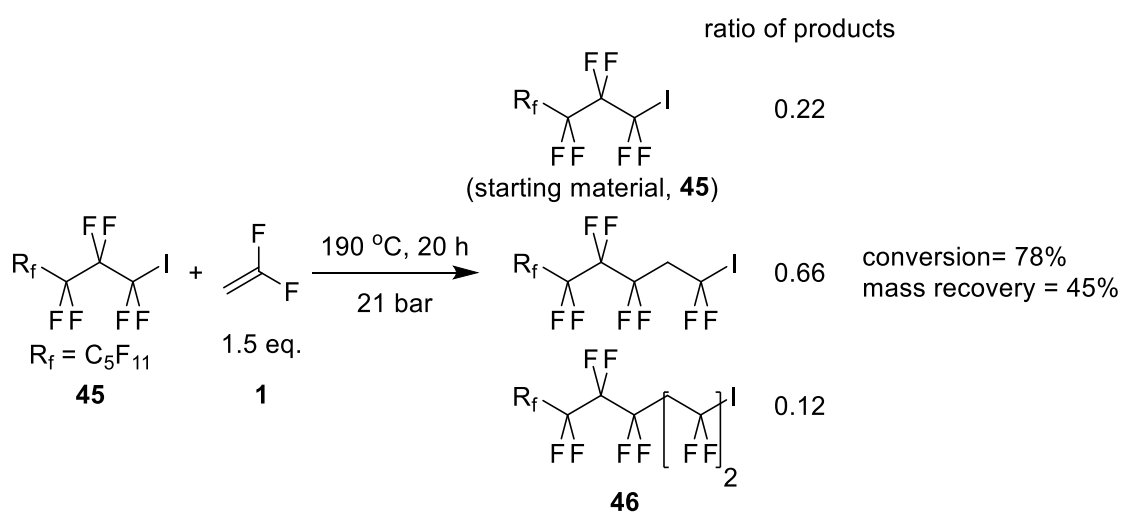


Figure 63: Radical chain reaction of $\text{C}_8\text{F}_{17}\text{I}$ with VDF (1.5 eq.) to synthesise $\text{C}_8\text{F}_{17}(\text{CH}_2\text{CF}_2)_{0-2}\text{I}$

Initial analysis of the product mixture (**46**) was performed using GC-MS to establish the extent of telomerisation and product distribution (Fig. 64).

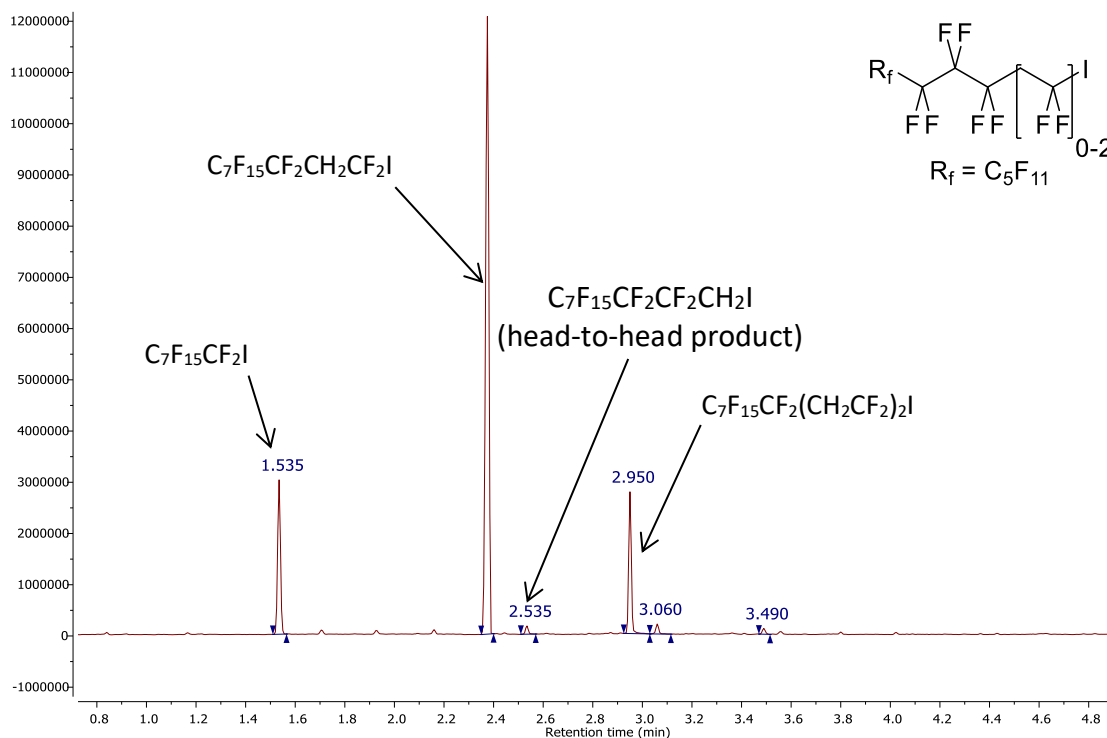


Figure 64: Gas chromatogram of the product mixture, $C_8F_{17}(CH_2CF_2)_{0-2}I$

The gas chromatogram indicated that three major components were present in the product mixture; the starting material ($C_8F_{17}I$), 2H,2H 1-iodoperfluorodecane ($C_8F_{17}CH_2CF_2I$, $n = 1$) and 2H,2H,4H,4H 1-iodoperfluorododecane ($C_8F_{17}(CH_2CF_2)_2I$, $n = 2$). For the two telomer iodides that had been synthesised, a second very minor peak is seen at slightly higher retention time to the main peak. These are attributed to the head-to-head addition of VDF to give $C_8F_{17}CF_2CH_2I$ and $C_8F_{17}CH_2CF_2CF_2CH_2I$, minor side products of this reaction that are models of structure (c) derived from the head-to-head addition of VDF.

The mass spectrum of $C_8F_{17}CH_2CF_2I$ is shown in Fig. 65, and several fragmentations indicative of head-to-tail species are observed.

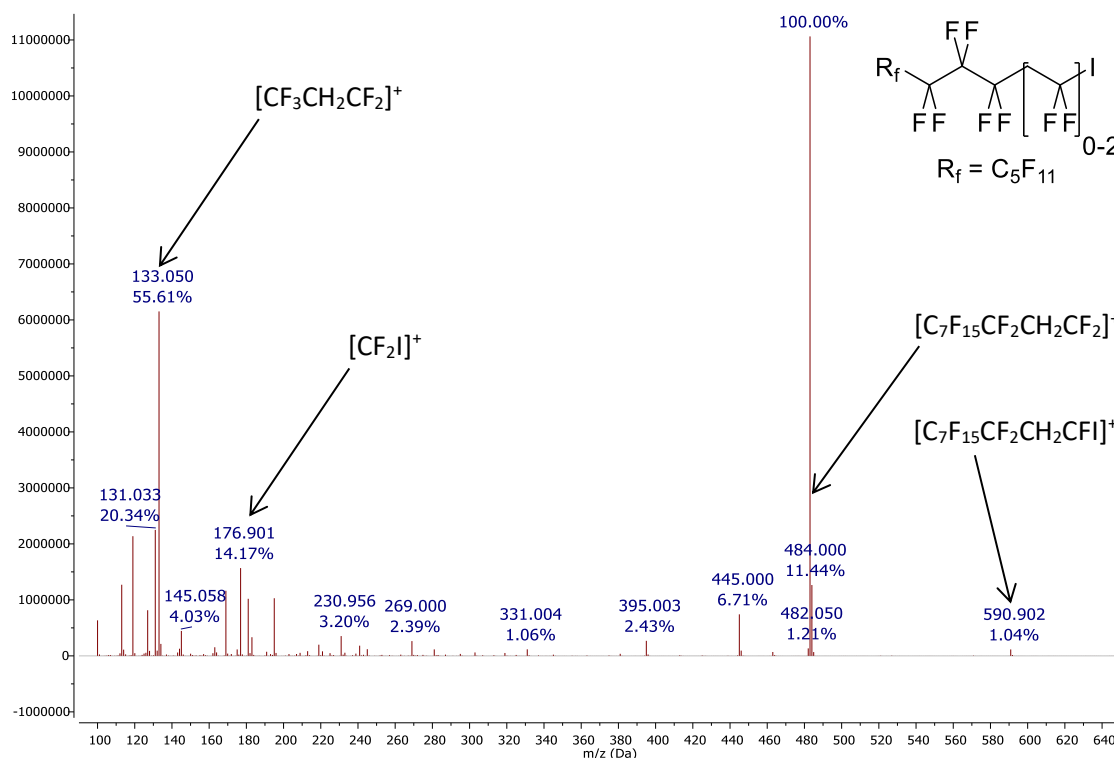


Figure 65: Mass spectrum of $C_8F_{17}CH_2CF_2I$

The peak for the molecular ion ($m/z = 609.9$) is not observed in the mass spectrum of $C_8F_{17}CH_2CF_2I$. However, the highest molecular weight peak was a fragment with $m/z = 590.9$, which corresponds to $[M - F]^+$, and the peak with the highest intensity was a fragment with $m/z = 483.0$, corresponding to $[M - I]^+$. Interestingly, the molecular ion peak is observed in the mass spectrum of the head-to-head product ($C_8F_{17}CF_2CH_2I$), whereas the $[M - F]^+$ and $[M - I]^+$ peaks are not observed. This observation can be explained by the structures of the two carbocations which are present in the gas phase (Fig. 66 and 67).

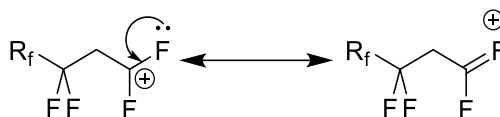


Figure 66: Resonance stabilisation of the $[M - I]^+$ fragment formed from the head-to-tail product ($C_8F_{17}R_fCH_2CF_2I$)

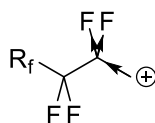


Figure 67: Inductive destabilisation of the $[M - I]^+$ fragment (not observed) formed from the head-to-head product ($C_8F_{17}R_fCF_2CH_2I$)

The $R_f\text{CH}_2\text{CF}_2^+$ fragment (formed from $\text{C}_8\text{F}_{17}\text{R}_f\text{CH}_2\text{CF}_2\text{I}$, the head-to-tail product), can be stabilised by p-p resonance of a fluorine lone pair into the empty p orbital of the carbocation. By contrast, the unobserved $R_f\text{CF}_2\text{CH}_2^+$ fragment (formed from $\text{C}_8\text{F}_{17}\text{R}_f\text{CF}_2\text{CH}_2\text{I}$, the head-to-head product), an already unstable primary carbocation, is further destabilised by the withdrawing inductive effect of the neighbouring CF_2 group.

The ^1H and ^{13}C NMR spectra of the product mixture could only be partially assigned, due to the splitting of the resonances by the fluorine atoms and the overlapping signals of related products. Therefore, the NMR spectra of the product mixture were compared to those of the starting material and, in addition to information derived from correlation spectroscopy (COSY, HSQC and HMBC), data about key functional groups could be deduced.

The ^{13}C NMR spectra of **46** ($\text{C}_8\text{F}_{17}(\text{CH}_2\text{CF}_2)_{0-2}\text{I}$) and the starting material are detailed in Fig. 68.

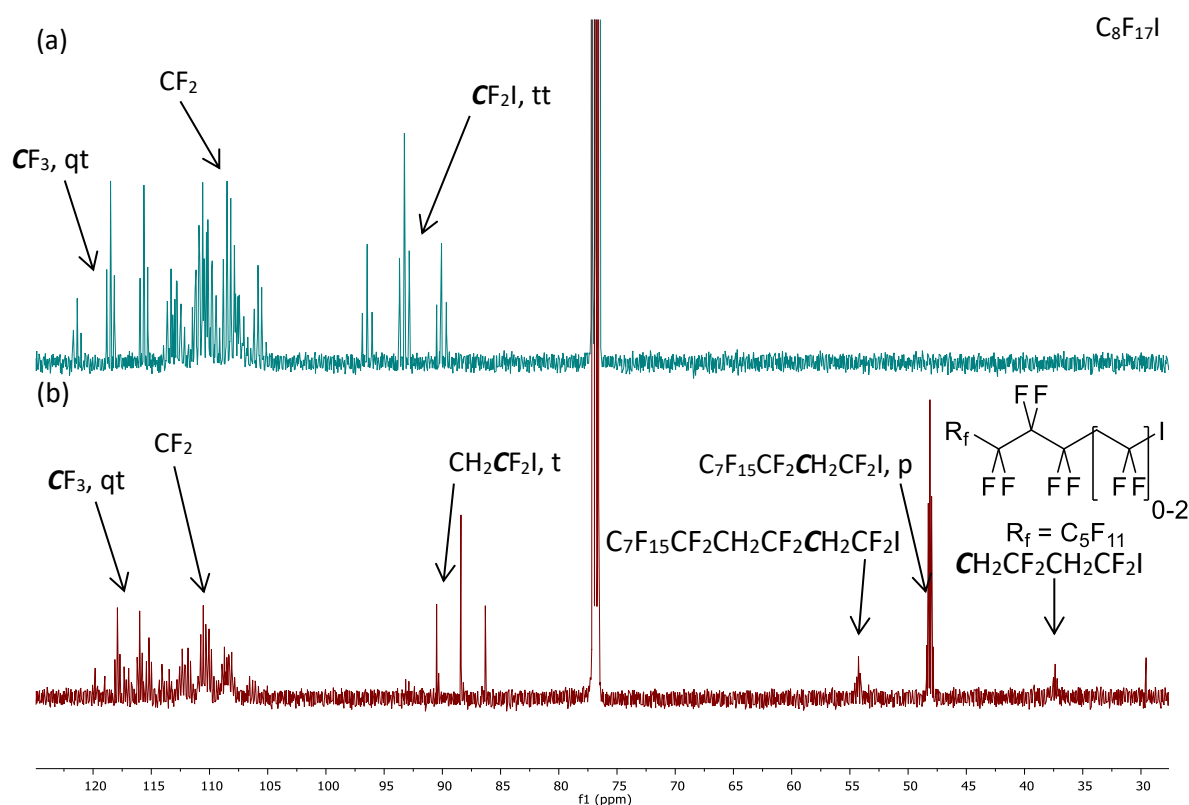


Figure 68: ^{13}C NMR spectra of $\text{C}_8\text{F}_{17}\text{I}$ (a) and $\text{C}_8\text{F}_{17}(\text{CH}_2\text{CF}_2)_{0-2}\text{I}$ (b)

The region between 105 and 113 ppm is difficult to interpret in both spectra, due to the overlapping CF_2 signals. However, there are several signals that can be distinguished, for example, both spectra have a quartet of triplets at ≈ 117 ppm ($^1J_{\text{CF}} = 288.7$ Hz, $^2J_{\text{CF}} = 33.7$ Hz) due to the terminal CF_3 group present in both molecules. In addition, there is a clear triplet of triplets at 93.26 ppm ($^1J_{\text{CF}} = 321.1$ Hz, $^2J_{\text{CF}} = 41.9$ Hz) in the spectrum of $\text{C}_8\text{F}_{17}\text{I}$ (a), the resonance

from the CF_2I carbon. However, in the spectrum of $\text{C}_8\text{F}_{17}(\text{CH}_2\text{CF}_2)_{0-2}\text{I}$ (b), there is instead a triplet at 88.73 ppm ($^1J_{\text{CF}} = 315.3$ Hz). This resonance is due to the $\text{CH}_2\text{CF}_2\text{I}$ carbons of the product mixture and is a triplet only due to the absence of the two bond C – F coupling. The presence of this signal confirms that the major product of this reaction is $\text{C}_8\text{F}_{17}\text{CH}_2\text{CF}_2\text{I}$ and this is further proven by the pentet at 48.45 ppm ($^2J_{\text{CF}} = 21.3$). This resonance appears as a pentet due to four C – F two bond couplings from the adjacent CF_2 groups in the $\text{CF}_2\text{CH}_2\text{CF}_2\text{I}$ fragment of $\text{C}_8\text{F}_{17}\text{CH}_2\text{CF}_2\text{I}$, confirming the structure of the major product.

Having assigned the ^{13}C NMR resonances of the major product, there are two additional resonances in the ^{13}C NMR spectrum, at 37.79 and 54.52 ppm that need to be assigned. In addition, the proton spectrum has several resonances that need to be accounted for (Fig. 69).

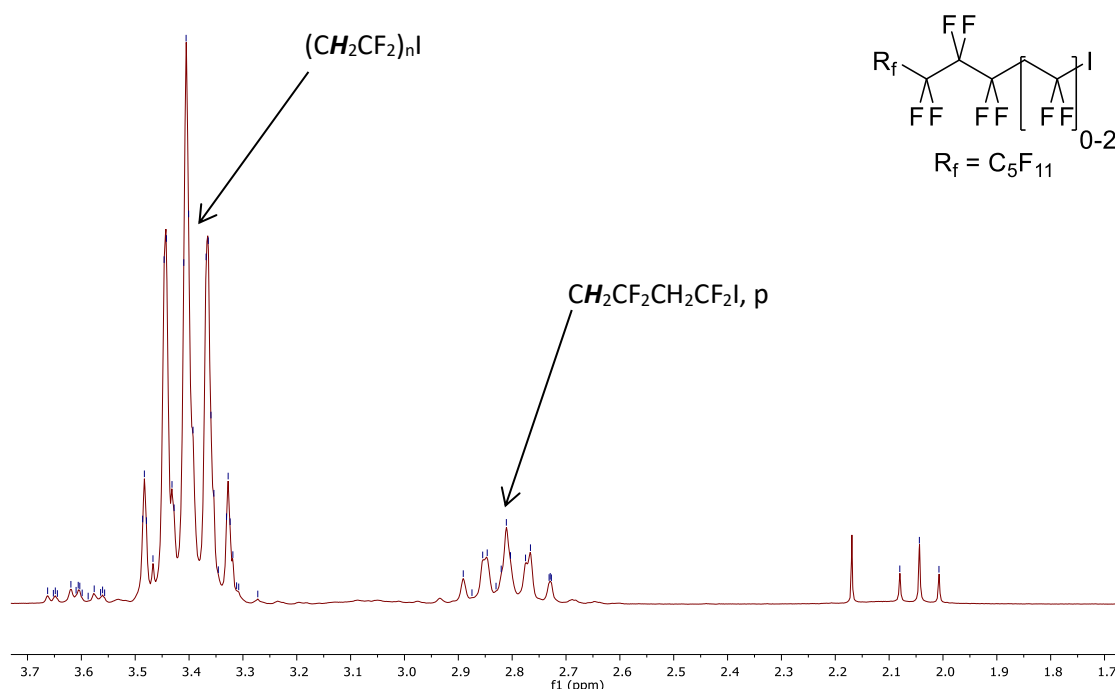
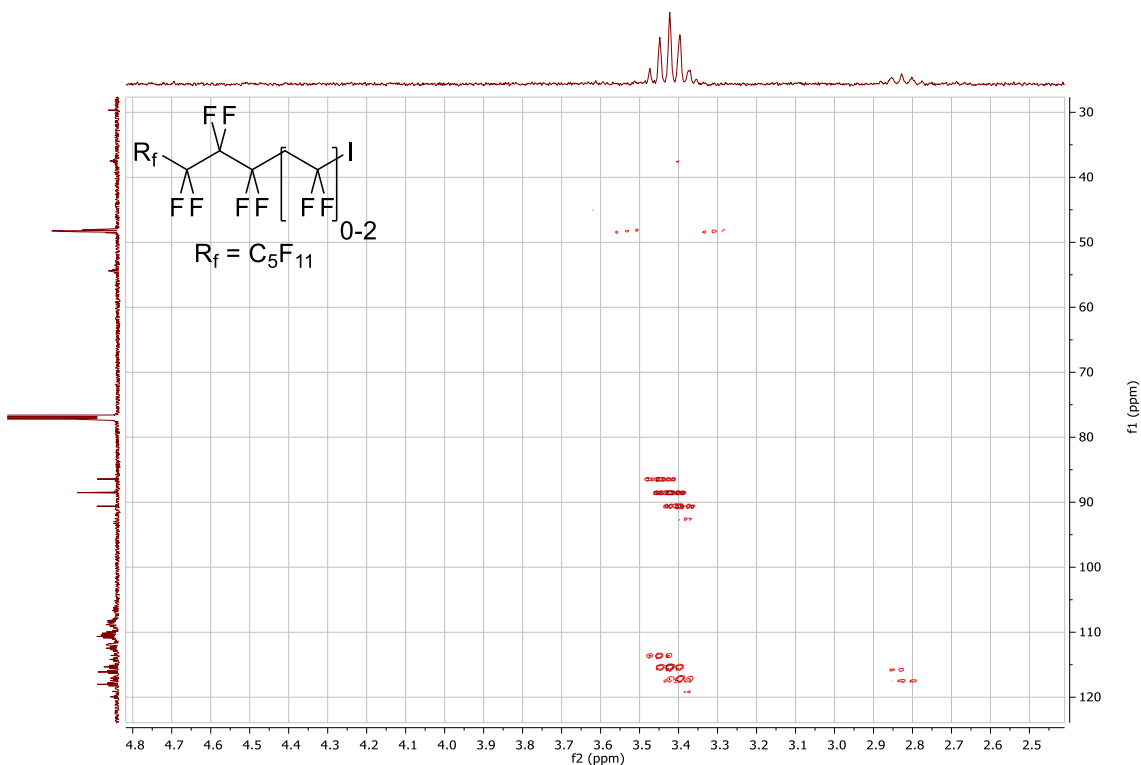
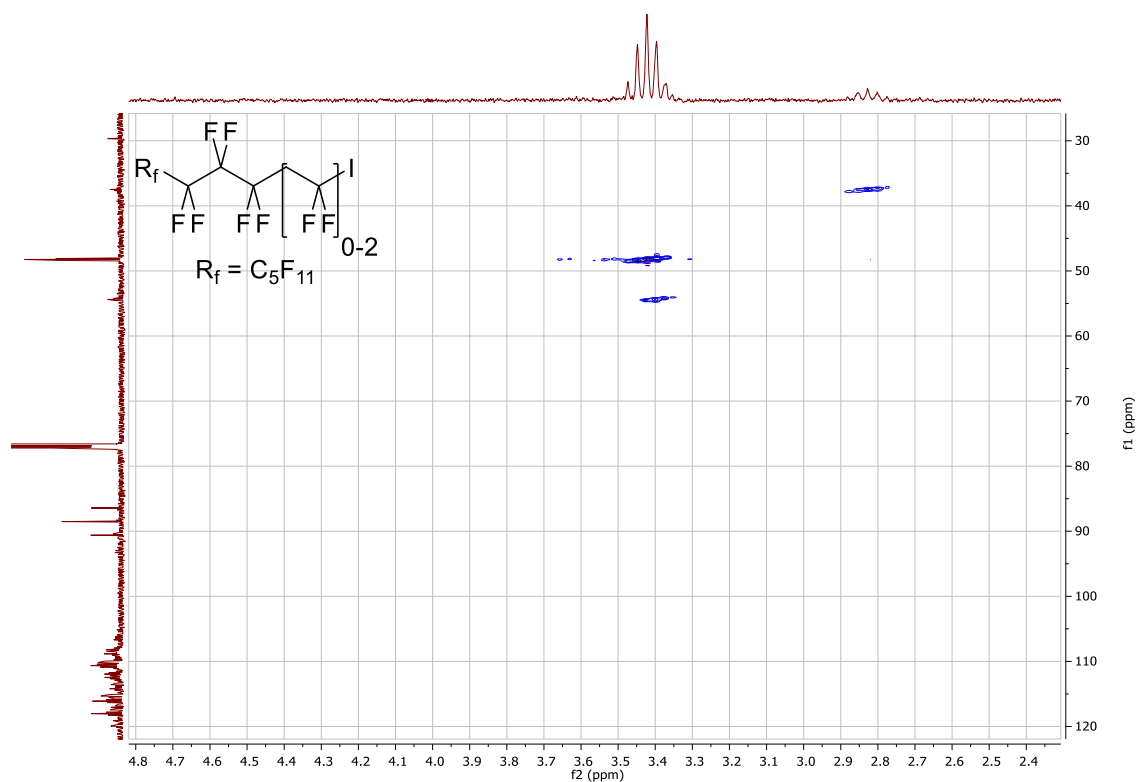


Figure 69: ^1H NMR spectrum of $\text{C}_8\text{F}_{17}(\text{CH}_2\text{CF}_2)_{0-2}\text{I}$

The resonance at 3.42 ppm (pentet, $^3J_{\text{HF}} = 15.6$ Hz) corresponds to CH_2 protons of the major product ($\text{C}_8\text{F}_{17}\text{CH}_2\text{CF}_2\text{I}$), but there is an additional large resonance at 2.83 ppm (pentet, $^3J_{\text{HF}} = 16.1$ Hz) and a further, smaller peak overlapping with the peak at 3.42 ppm. To assign these peaks, and the additional resonances in the ^{13}C NMR spectrum, correlation spectroscopy was used (Fig. 70 and 71).



From the HSQC spectrum, there is a one bond correlation between the 1H NMR signal at 2.83 ppm and the ^{13}C NMR signal at 37.79 ppm, and a second one bond correlation between the 1H NMR signal at 3.39 ppm (overlapping with the main signal at 3.42 ppm) and the ^{13}C

NMR signal at 54.52 ppm. These resonances arise from the $C_8F_{17}CH_2CF_2CH_2CF_2I$ groups of the di-addition product ($n = 2$). In the HMBC spectrum, the only two bond correlation to the 1H NMR signal at 2.83 ppm is to the CF_2 carbons of the perfluorooctyl chain, suggesting that this resonance arises from the CH_2 protons furthest from the iodine ($C_8F_{17}CH_2CF_2CH_2CF_2I$). There are two bond correlations of the 1H NMR signal at 3.42 ppm to both the CF_2I carbon and the CF_2 carbons of the perfluorooctyl chain as expected. However, the signal overlapping with the 1H NMR signal at 3.42 ppm additionally shows a three bond correlation to the CH_2 carbon at 37.79 ppm, suggesting that this resonance is from the CH_2CF_2I protons of $C_8F_{17}CH_2CF_2CH_2CF_2I$.

Overall, the key resonances from the ^{13}C , 1H and ^{19}F NMR spectra of the starting material ($C_8F_{17}I$) and major products ($C_8F_{17}CH_2CF_2I$ and $C_8F_{17}(CH_2CF_2)_2I$, **46**) are detailed in Table 11.

Table 11: List of key resonances from the major components of the product mixture from the reaction of $C_8F_{17}I$ with VDF (1.5 eq.), $C_8F_{17}(CH_2CF_2)_{0-2}I$ (chemical shifts in ppm, coupling constants in Hz)

Compound	Fragment	1H	^{19}F	^{13}C
$C_8F_{17}I$	CF_2I	N.A.	-59.25 – -59.42, m	93.26, tt, $^1J_{CF} =$ 321.1, $^2J_{CF} = 41.9$
	CF_3CF_2	N.A.	-81.45, tt, $^3J_{FF} =$ 10.1, $^4J_{FF} = 2.4$	117.07, qt, $^1J_{CF} =$ 287.9, $^2J_{CF} = 32.9$
$C_8F_{17}CH_2CF_2I$	$CF_2CH_2CF_2I$	N.A.	-38.26 – -38.43, m	88.73, t, $^1J_{CF} = 315.3$
	$CF_2CH_2CF_2I$	3.42, p, $^3J_{HF} = 15.6$	N.A.	48.45, p, $^2J_{CF} = 21.3$
	CF_3CF_2	N.A.	-81.32 – -81.43, m	116.95, qt, $^1J_{CF} =$ 288.7, $^2J_{CF} = 33.7$
$C_8F_{17}(CH_2CF_2)_2I$	CH_2CF_2I	N.A.	-39.08, ttt, $^3J_{FH} = 15.6$, $^4J_{FF} =$ 9.4, $^5J_{FH} = 3.0$	88.73, t, $^1J_{CF} = 315.3$
	$CF_2CH_2CF_2CH_2CF_2I$	3.39, p, $^3J_{HF} = 15.1$	N.A.	54.77 – 54.36, m
	$CF_2CH_2CF_2CH_2CF_2I$	2.83, p, $^3J_{HF} = 16.1$	N.A.	37.94 – 37.42, m
	CF_3CF_2	N.A.	-81.32 – -81.43, m	116.95, qt, $^1J_{CF} =$ 288.7, $^2J_{CF} = 33.7$

In order to synthesise higher molecular weight VDF telomer iodides, the reaction between $C_8F_{17}I$ and VDF was repeated using five equivalents of VDF. Crude product was collected as a pink solid and worked up in the same fashion as the previous reaction to yield the final product mixture as 16.58 g of a white solid (mass recovery 47%) (Fig. 72).

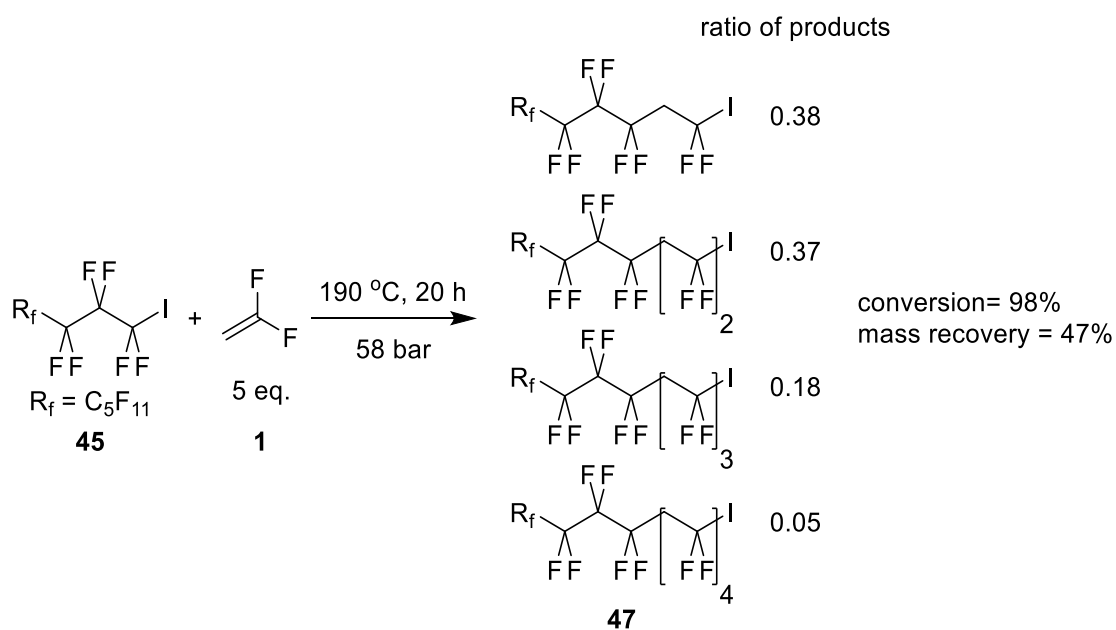


Figure 72: Reaction of $C_8F_{17}I$ with VDF (5 eq.) to synthesise $C_8F_{17}(CH_2CF_2)_{1-4}I$

Again, analysis of the product mixture (**47**) was performed using GC-MS to establish the extent of telomerisation and the product distribution (Fig. 73).

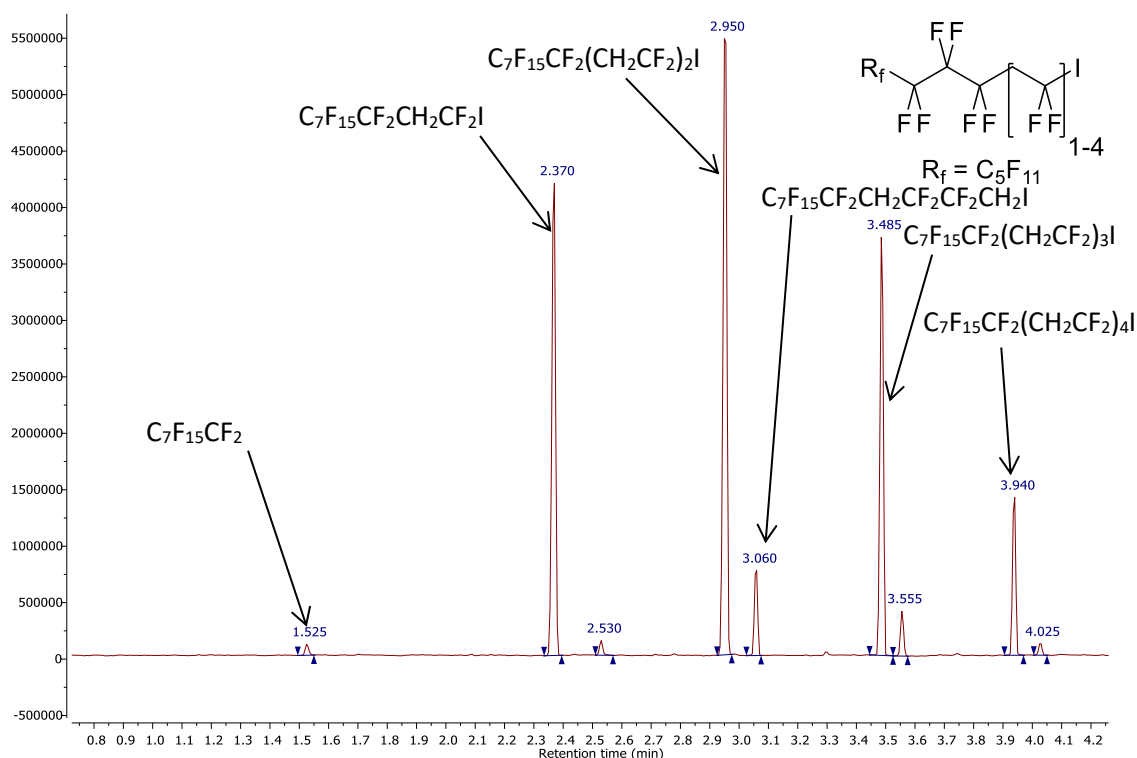


Figure 73: Gas chromatogram of $C_8F_{17}(CH_2CF_2)_{1-4}I$

As the gas chromatogram shows, conversion to products is very high as there is only a low intensity peak for the starting material ($C_8F_{17}I$, 2%) in the product mixture. The major components of the product mixture are *2H,2H* 1-iodoperfluorodecane ($C_8F_{17}CH_2CF_2I$), *2H,2H,4H,4H* 1-iodoperfluorododecane ($C_8F_{17}(CH_2CF_2)_2I$), *2H,2H,4H,4H,6H,6H* 1-iodoperfluorotetradecane ($C_8F_{17}(CH_2CF_2)_3I$) and *2H,2H,4H,4H,6H,6H,8H,8H* 1-iodoperfluorohexadecane ($C_8F_{17}(CH_2CF_2)_4I$). Additionally, each product peak has a second smaller peak at slightly higher retention time attributed to the related head-to-head products ($C_8F_{17}(CH_2CF_2)_{0-3}CF_2CH_2I$), and these are a more significant component of the product mixture than observed previously.

The NMR spectra of **47**, $C_8F_{17}(CH_2CF_2)_{1-4}I$, were more complex than those of **46**, $C_8F_{17}(CH_2CF_2)_{0-2}I$. However, by comparing the spectra obtained for both product mixtures, the signals corresponding to key functional groups can be identified.

For example, the ^{13}C NMR spectra for product mixtures 1 and 2 are shown in Fig. 74.

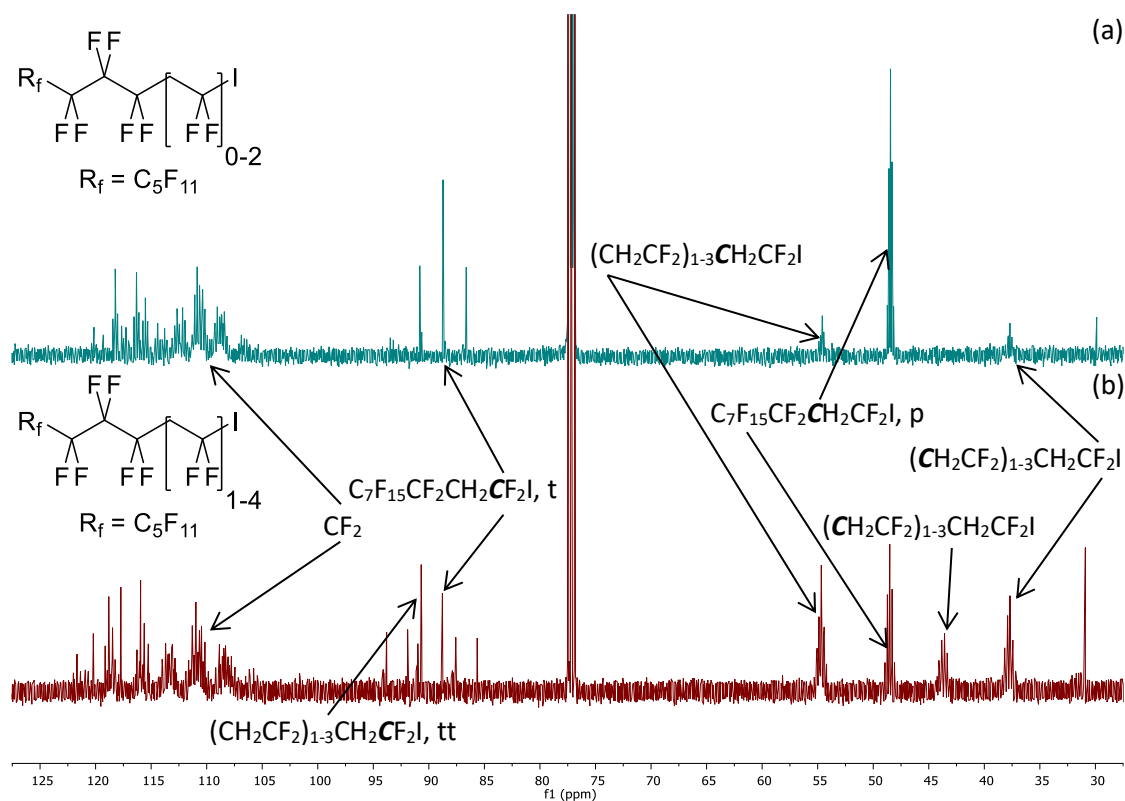


Figure 74: Comparison of the ^{13}C NMR spectrum of $\text{C}_8\text{F}_{17}(\text{CH}_2\text{CF}_2)_{0-2}\text{I}$ (a) and $\text{C}_8\text{F}_{17}(\text{CH}_2\text{CF}_2)_{1-4}\text{I}$ (b)

The ^{13}C NMR spectrum of $\text{C}_8\text{F}_{17}(\text{CH}_2\text{CF}_2)_{1-4}\text{I}$ (**47**, (b)) contains several signals that were not present in the spectrum of $\text{C}_8\text{F}_{17}(\text{CH}_2\text{CF}_2)_{0-2}\text{I}$ (**46**, (a)). For example, the multiplets at 53.83 – 53.39 and 38.42 – 36.89 ppm are of higher intensity, and there is a new multiplet at 44.37 – 42.67 ppm in spectrum (b). These are the resonances from the $\text{CF}_2\text{CH}_2\text{CF}_2$ carbons found in $\text{C}_8\text{F}_{17}(\text{CH}_2\text{CF}_2)_{3-4}\text{I}$. The region from 85 – 95 ppm, assigned to the CF_2I carbons of the products, is of particular interest (Fig. 75).

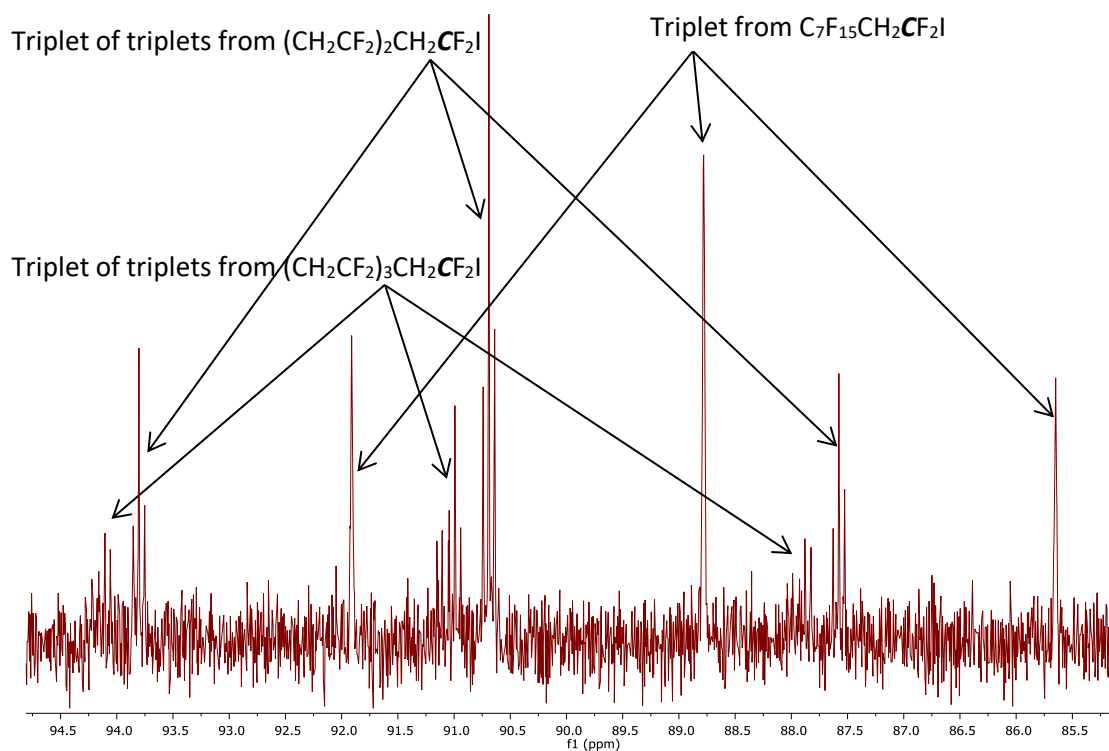


Figure 75: Expansion of the region at ≈ 90 ppm for $C_8F_{17}(CH_2CF_2)_{1-4}I$

This region contains a triplet at 88.77 ppm ($^1J_{CF} = 315.4$ Hz) assigned previously to the CF_2I signal for $C_8F_{17}CH_2CF_2I$. However, the ^{13}C NMR spectrum of $C_8F_{17}(CH_2CF_2)_{1-4}I$ also contains two additional triplets of triplets at 90.69 ($^1J_{CF} = 313.3$ Hz, $^3J_{CF} = 5.1$ Hz), and 91.02 ppm ($^1J_{CF} = 313.4$ Hz, $^3J_{CF} = 5.1$), arising from the CF_2I carbons of $C_8F_{17}(CH_2CF_2)_2I$ and $C_8F_{17}(CH_2CF_2)_3I$ respectively.

The ^{19}F NMR spectra of both product mixtures were challenging to interpret due to the many signals observed. However, by cross referencing the ^{19}F NMR spectra from both reactions, the spectra can be assigned (Fig. 76).

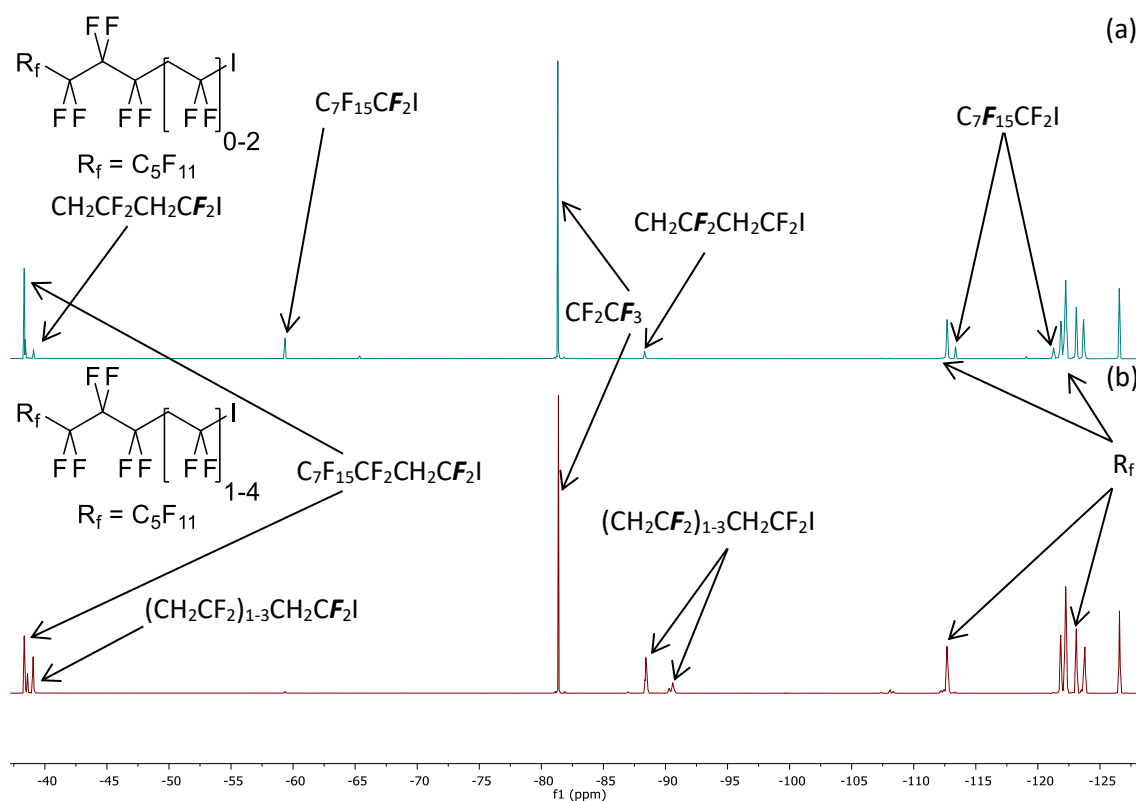


Figure 76: Comparison of the ^{19}F NMR spectra of $\text{C}_8\text{F}_{17}(\text{CH}_2\text{CF}_2)_{0-2}\text{I}$ (a) and $\text{C}_8\text{F}_{17}(\text{CH}_2\text{CF}_2)_{1-4}\text{I}$ (b)

The spectrum of $\text{C}_8\text{F}_{17}(\text{CH}_2\text{CF}_2)_{0-2}\text{I}$, (a) shows a small amount of starting material ($\text{C}_8\text{F}_{17}\text{I}$) but the spectrum of $\text{C}_8\text{F}_{17}(\text{CH}_2\text{CF}_2)_{1-4}\text{I}$, (b) does not. Therefore, the signals present in (a) but not in (b), at -59.36 ($\text{C}_7\text{F}_{15}\text{CF}_2\text{I}$), -113.36 and -121.27 ($\text{C}_7\text{F}_{15}\text{CF}_2\text{I}$) ppm, arise from $\text{C}_8\text{F}_{17}\text{I}$. Similarly, the signals at -39.08 ($\text{CH}_2\text{CF}_2\text{CH}_2\text{CF}_2\text{I}$) and -88.40 ($\text{CH}_2\text{CF}_2\text{CH}_2\text{CF}_2\text{I}$) ppm in higher intensity in spectrum (b), and those at -38.61 ($(\text{CH}_2\text{CF}_2)_{2-3}\text{CH}_2\text{CF}_2\text{I}$), and -90.58 ($(\text{CH}_2\text{CF}_2)_{2-3}\text{CH}_2\text{CF}_2\text{I}$) ppm observed only in spectrum (b) must, therefore, arise from $\text{C}_8\text{F}_{17}(\text{CH}_2\text{CF}_2)_2\text{I}$, $\text{C}_8\text{F}_{17}(\text{CH}_2\text{CF}_2)_3\text{I}$ and $\text{C}_8\text{F}_{17}(\text{CH}_2\text{CF}_2)_4\text{I}$.

The key resonances from the ^1H , ^{19}F and ^{13}C NMR spectra of **47** ($\text{C}_8\text{F}_{17}(\text{CH}_2\text{CF}_2)_{1-4}\text{I}$) are detailed in Table 12, and this data is in good agreement with that reported for related systems by Ameduri *et al*⁴³.

Table 12: List of key shifts for the major components of the product mixture from the reaction of C₈F₁₇I with VDF (5 eq.), C₈F₁₇(CH₂CF₂)₁₋₄I (chemical shifts in ppm, coupling constants in Hz)

Compound	Fragment	¹ H	¹⁹ F	¹³ C
C ₈ F ₁₇ CH ₂ CF ₂ I	CH ₂ CF ₂ I	N.A.	-38.34, tt, ³ J _{FH} = 13.7, ⁴ J _{FF} = 12.6	88.78, t, ¹ J _{CF} = 315.4
	CF ₂ CH ₂ CF ₂ I	3.51 – 3.20, m	N.A.	48.51, p, ² J _{CF} = 21.7
	CF ₃ CF ₂	N.A.	-81.38, t, ³ J _{FF} = 10.1	117.39, qt, ¹ J _{CF} = 287.7, ² J _{CF} = 32.8
C ₈ F ₁₇ (CH ₂ CF ₂) ₂ I	CH ₂ CF ₂ I	N.A.	-39.06, ttt, ³ J _{FH} = 15.7, ⁴ J _{FF} = 9.5, ⁵ J _{FH} = 3.1	90.69, tt, ¹ J _{CF} = 313.3, ³ J _{CF} = 5.1
	CF ₂ CH ₂ CF ₂ I	3.51 – 3.20, m	N.A.	53.83 – 53.39, m
	CF ₂ CH ₂ CF ₂ CH ₂ CF ₂ I	2.99 – 2.58, m	N.A.	38.42 – 36.89, m
	CF ₃ CF ₂	N.A.	-81.38, t, ³ J _{FF} = 10.1	117.39, qt, ¹ J _{CF} = 287.7, ² J _{CF} = 32.8
C ₈ F ₁₇ (CH ₂ CF ₂) ₃ I	CH ₂ CF ₂ I	N.A.	-38.51 – -38.70, m	91.02, tt, ¹ J _{CF} = 313.4, ³ J _{CF} = 5.1
	CF ₂ CH ₂ CF ₂ I	3.51 – 3.20, m	N.A.	53.83 – 53.39, m
	CF ₂ CH ₂ CF ₂ CH ₂ CF ₂ I	2.99 – 2.58, m	N.A.	38.42 – 36.89, m
	CF ₂ CH ₂ CF ₂ (CH ₂ CF ₂) ₂ I	2.99 – 2.58, m	N.A.	44.37 – 42.67, m
	CF ₃ CF ₂	N.A.	-81.38, t, ³ J _{FF} = 10.1	117.39, qt, ¹ J _{CF} = 287.7, ² J _{CF} = 32.8
C ₈ F ₁₇ (CH ₂ CF ₂) ₄ I	CH ₂ CF ₂ I	N.A.	-38.43 – -38.52, m	91.02, tt, ¹ J _{CF} = 313.4, ³ J _{CF} = 5.1
	CF ₂ CH ₂ CF ₂ I	3.51 – 3.20, m	N.A.	53.83 – 53.39, m
	CF ₂ CH ₂ CF ₂ CH ₂ CF ₂ I	2.99 – 2.58, m	N.A.	38.42 – 36.89, m
	CF ₂ CH ₂ CF ₂ (CH ₂ CF ₂) ₂₋₃ I	2.99 – 2.58, m	N.A.	44.37 – 42.67, m
	CF ₃ CF ₂	N.A.	-81.38, t, ³ J _{FF} = 10.1	117.39, qt, ¹ J _{CF} = 287.7, ² J _{CF} = 32.8

Autoclave reactions of C₈F₁₇I with VDF were repeated to synthesise more C₈F₁₇(CH₂CF₂)₁₋₄I which were used, without further purification, for the synthesis of Viton® model compounds.

3.2. Capping Reactions of Straight Chain VDF Telomer Iodides

The mixtures of VDF Telomer Iodides (**47**, $C_8F_{17}(CH_2CF_2)_{1-4}I$) are intermediates in the synthesis of Viton® model compounds. However, the C – I bonds in the telomer iodides are reactive centres that are not present in Viton®, therefore, the iodine atom must be substituted by either H or F in order to synthesise Viton® model compounds.

Two methods were investigated to achieve these ‘capping’ reactions; substitution of iodine by hydrogen using tributyltin hydride and substitution by fluorine using antimony pentafluoride.

3.2.1. Reaction of VDF Telomer Iodides with Tributyltin Hydride

The first method for capping telomer iodides that was investigated, based on previous literature^{43,45}, was the substitution of iodine for hydrogen using tributyltin hydride (Bu_3SnH) (Fig. 77). In order to avoid decomposition of the Bu_3SnH , all reactions were carried out under an inert atmosphere. The telomer iodide mixture (**47**) was dissolved in DCM and Bu_3SnH was added. The reaction mixture was stirred for 24 hours and the contents worked up. This synthesis was repeated three times and 100% conversion was achieved on each occasion.

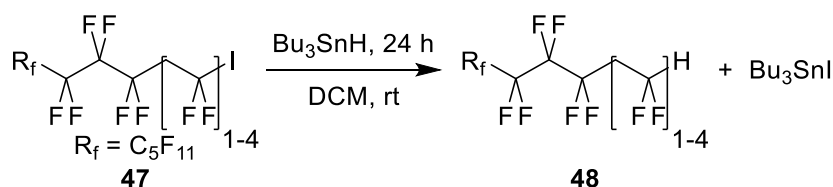


Figure 77: Reaction of $C_8F_{17}(CH_2CF_2)_{1-4}I$ with Bu_3SnH to synthesise $C_8F_{17}(CH_2CF_2)_{1-4}H$

Table 13: Conditions for the synthesis of $C_8F_{17}(CH_2CF_2)_{1-4}H$ using Bu_3SnH

Reaction attempt	Work up method	Moles of Tin residues in the product mixture / %	Yield of telomer hydrides based on purity / %
1	A	35	-
	B	10	-
	C	3	10
2	C	15	-
	D	4	15
3	D	11	30

The major issue encountered with these reactions was the separation of residual tin species from the product mixtures ($C_8F_{17}(CH_2CF_2)_{1-4}H$, **48**) as shown in Table 13. This is a well-established problem in free radical chemistry, and methods for attempting to extracting residual tin species from organic products have been reviewed⁷¹. However, unlike in many free radical reactions, where Bu_3SnH is used in low concentrations as a radical initiator, the syntheses described above used stoichiometric concentrations of Bu_3SnH , making the removal of tin residues even more challenging. In the first work up method that was attempted (A), the crude product mixture was stirred with aqueous KF for 30 minutes to convert any Bu_3SnI that had formed to insoluble Bu_3SnF . However, after filtration and removal of solvent there was still a significant quantity of tin species (35%, Table 13, entry 1 A) in the product mixture.

In an attempt to improve purity of the $C_8F_{17}(CH_2CF_2)_{1-4}H$ (**48**) mixture, the crude product was stirred for 5 hours with aqueous KF and filtered through celite (workup B). This reduced the quantity of tin residues (10%, Table 13, entry 1 B) but did not eliminate them completely. In order to convert any residual tributyltin hydride to tributyltin iodide, the crude product was reacted with iodine, followed by sodium thiosulfate to remove excess I_2 . This mixture was then filtered through a column containing a 9:1 silica:KF mixture (solvent = hexane) (workup C) which successfully removed most of the remaining tin residues from the product mixture although traces remained (3%, Table 13, entry 1 C). Conversion to $C_8F_{17}(CH_2CF_2)_{1-4}H$ was observed by 1H NMR spectroscopy (Fig. 78 and 79).

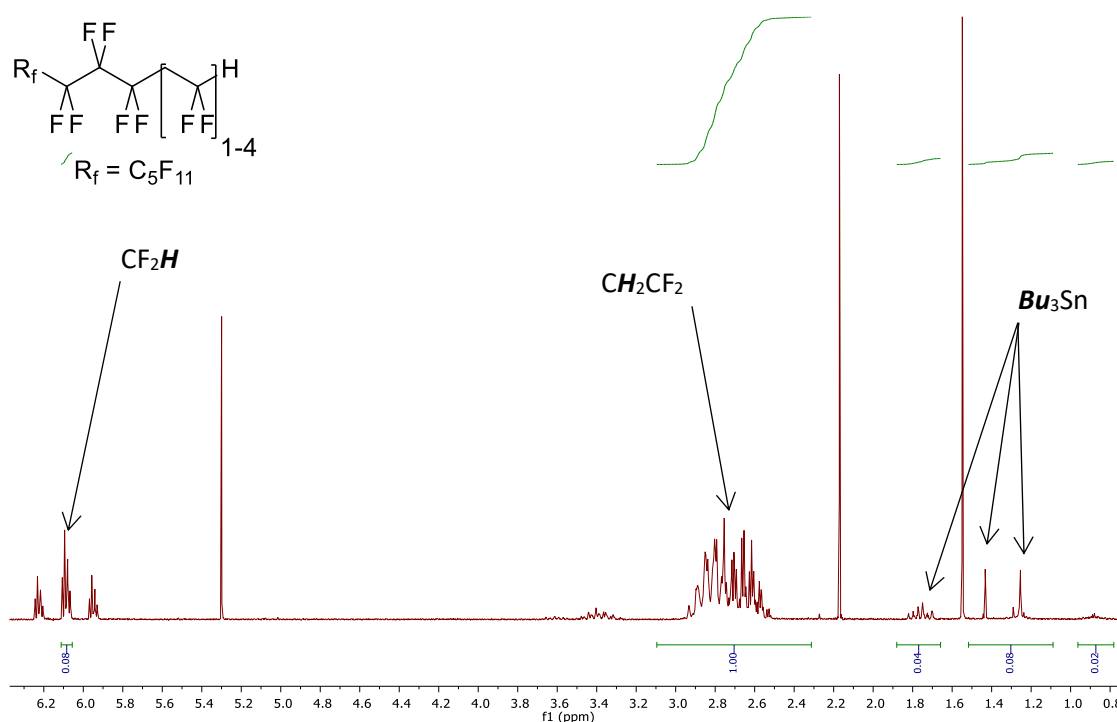


Figure 78: 1H NMR of $C_8F_{17}(CH_2CF_2)_{1-4}H$, that contains Bu_3Sn impurities (3%, Table 13, entry 1 C)

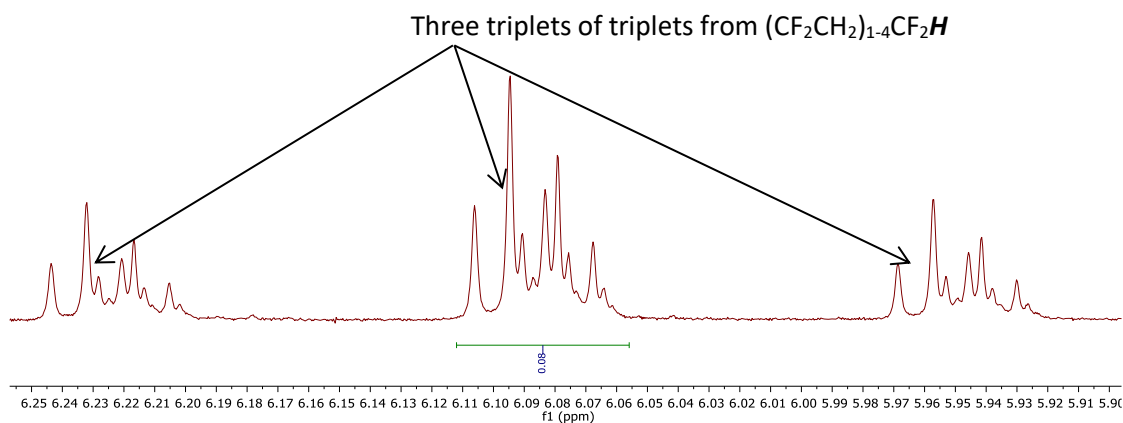


Figure 79: Expansion of the region between 6.25 and 5.90 ppm in the ^1H NMR of $\text{C}_8\text{F}_{17}(\text{CH}_2\text{CF}_2)_{1-4}\text{H}$

The ^1H NMR spectrum of $\text{C}_8\text{F}_{17}(\text{CH}_2\text{CF}_2)_{1-4}\text{H}$ contains three triplets of triplets at shifts of 6.09 ppm ($^2J_{\text{HF}} = 55.0$ Hz, $^3J_{\text{HH}} = 4.6$ Hz), 6.08 ppm ($^2J_{\text{HF}} = 55.0$ Hz, $^3J_{\text{HH}} = 4.6$ Hz) and 6.07 ppm (tt, $^2J_{\text{HF}} = 55.1$ Hz, $^3J_{\text{HH}} = 4.5$ Hz), the resonances from the $(\text{CF}_2\text{CH}_2)_{1-4}\text{CF}_2\text{H}$ protons of the product mixture. Conversion to $\text{C}_8\text{F}_{17}(\text{CH}_2\text{CF}_2)_{1-4}\text{H}$ was confirmed by comparing the ^{19}F NMR spectrum of the product mixture to that of the starting material (**47**) (Fig. 80).

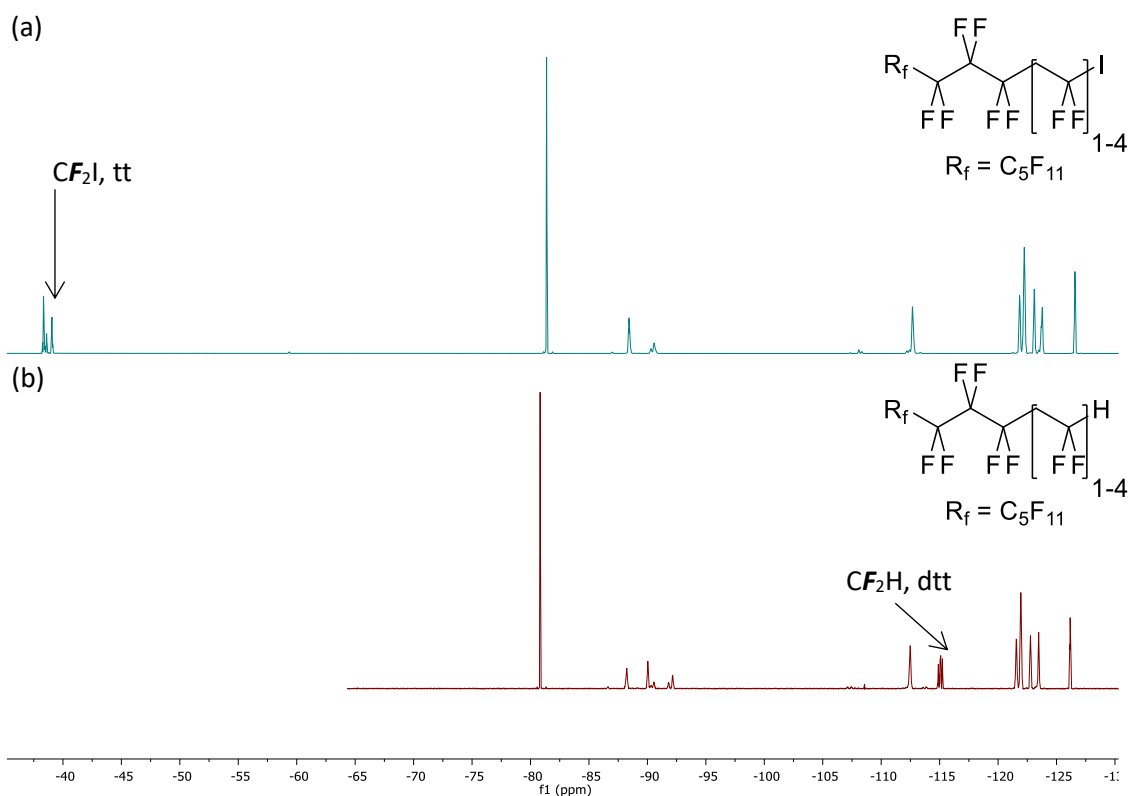


Figure 80: Comparison of the ^{19}F NMR spectra of $\text{C}_8\text{F}_{17}(\text{CH}_2\text{CF}_2)_{1-4}\text{I}$ (a) and $\text{C}_8\text{F}_{17}(\text{CH}_2\text{CF}_2)_{1-4}\text{H}$ (b)

The resonances of the CF_2I fluorines (tt between -40.13 – -41.02 ppm) have been replaced by new CF_2H resonances (dtt between -114.34 – -115.59 ppm) as expected.

The second reaction (Table 13, entry 2) was worked up using method C. The crude product was stirred with iodine followed by sodium thiosulfate, before being filtered through a column containing a 9:1 silica:KF mixture (solvent = hexane) as described above. After this process was carried out, significant tin residues remained (15%, Table 13, entry 2 C) and, in order to remove the remaining impurities, an organic-fluorous separation was attempted (workup D). $C_8F_{17}(CH_2CF_2)_{1-4}H$ is a polyfluorinated compound and, thus, preferentially dissolves in highly fluorinated solvents instead of organic solvents. Therefore, it was believed that the desired product mixture could be extracted from the tin residues by performing a fluorous extraction. The crude product was added to perfluorohexane and extracted three times using hexane. The fluorous phase was separated and the solvent removed *in vacuo* to recover the product mixture containing 4% tin residues (Table 13, entry 2 D, Fig. 81).

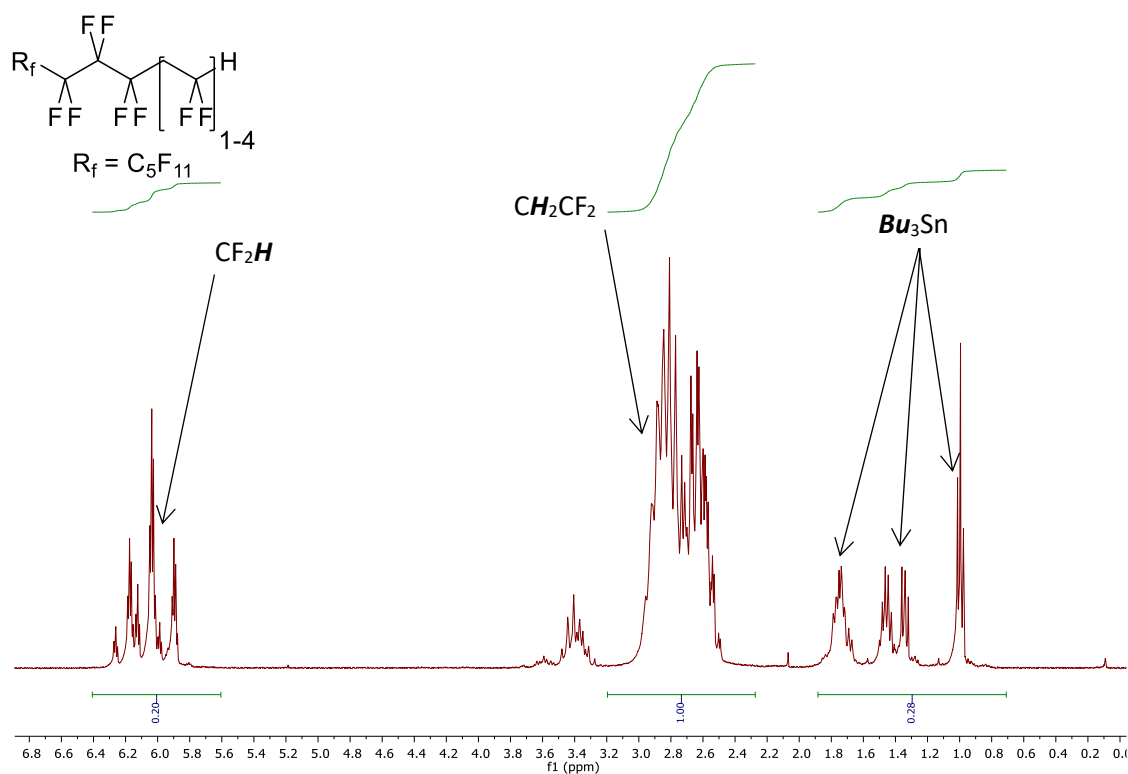


Figure 81: 1H NMR of $C_8F_{17}(CH_2CF_2)_{1-4}H$, that contains Bu_3Sn impurities (4% by, Table 13, entry 2 D)

Analysis on the $C_8F_{17}(CH_2CF_2)_{1-4}H$ product mixture was also performed using GC-MS (Fig. 82).

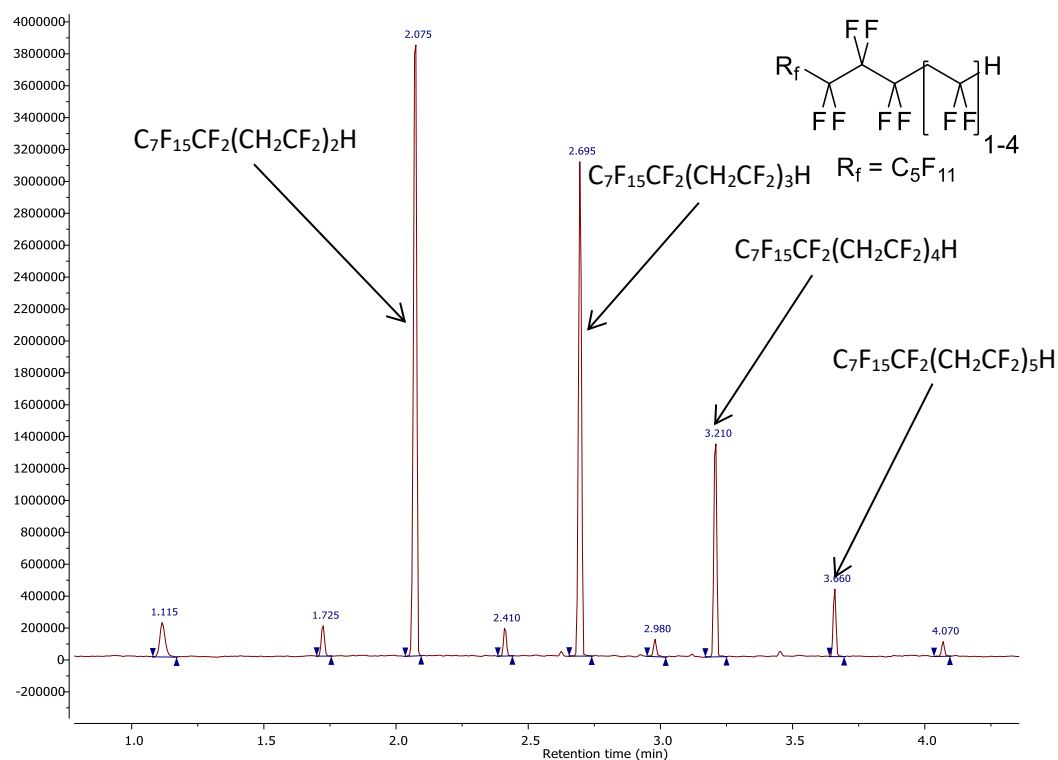


Figure 82: Gas chromatogram of $C_8F_{17}(CH_2CF_2)_{1-4}H$ (Table 13, entry 2 D)

The mono addition product ($C_8F_{17}CH_2CF_2H$) was not observed by GC-MS due to evaporation on workup of this highly volatile compound. In all cases, the molecular ion was not observed for any of the products. Instead, the highest molecular weight peak observed for $C_8F_{17}(CH_2CF_2)_2H$ was a fragment with $m/z = 529.0$, corresponding to $[M - F]^+$. For the other major products ($C_8F_{17}(CH_2CF_2)_{3-4}H$), the highest molecular weight peaks corresponded to the $[M - HF_2]^+$ fragments ($m/z = 573.0$ for $C_8F_{17}(CH_2CF_2)_3H$ and $m/z = 637.0$ for $C_8F_{17}(CH_2CF_2)_4H$).

The third reaction was worked up using method D. However, upon analysis the product still contained a significant quantity of tin residues (11%, Table 13, entry 3 D). Consequently, due to the difficulties encountered when purifying the products of the reactions of **47** with Bu_3SnH , this route to Viton[®] model compounds was abandoned in favour of capping the telomer iodides with fluorine.

3.2.2. Reaction of VDF Telomer Iodides with Antimony Pentafluoride

The second method of capping VDF telomer iodides that are investigated was the substitution of iodine for fluorine using antimony pentafluoride (SbF_5). The mixture of telomer iodides ($\text{C}_8\text{F}_{17}(\text{CH}_2\text{CF}_2)_{1-4}\text{I}$, **47**) was dissolved in a fluorinated solvent and cooled to 0°C . SbF_5 , dissolved in the same solvent, was added and the solution was stirred for a further hour. Water was added to the mixture and the solution was neutralised with NaHCO_3 . Separation and evaporation of the fluoruous solvent gave the desired product mixture (Fig. 83).

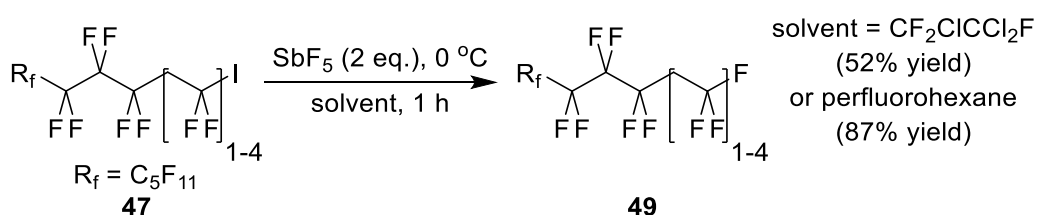


Figure 83: Reaction of $\text{C}_8\text{F}_{17}(\text{CH}_2\text{CF}_2)_{1-4}\text{I}$ with SbF_5 to synthesise $\text{C}_8\text{F}_{17}(\text{CH}_2\text{CF}_2)_{1-4}\text{F}$

The first reaction, using $\text{CCl}_2\text{FCClF}_2$ as a solvent, followed a procedure similar to conditions used previously for related systems⁷⁰ and the composition of the product mixture was determined by GC-MS (Fig. 84).

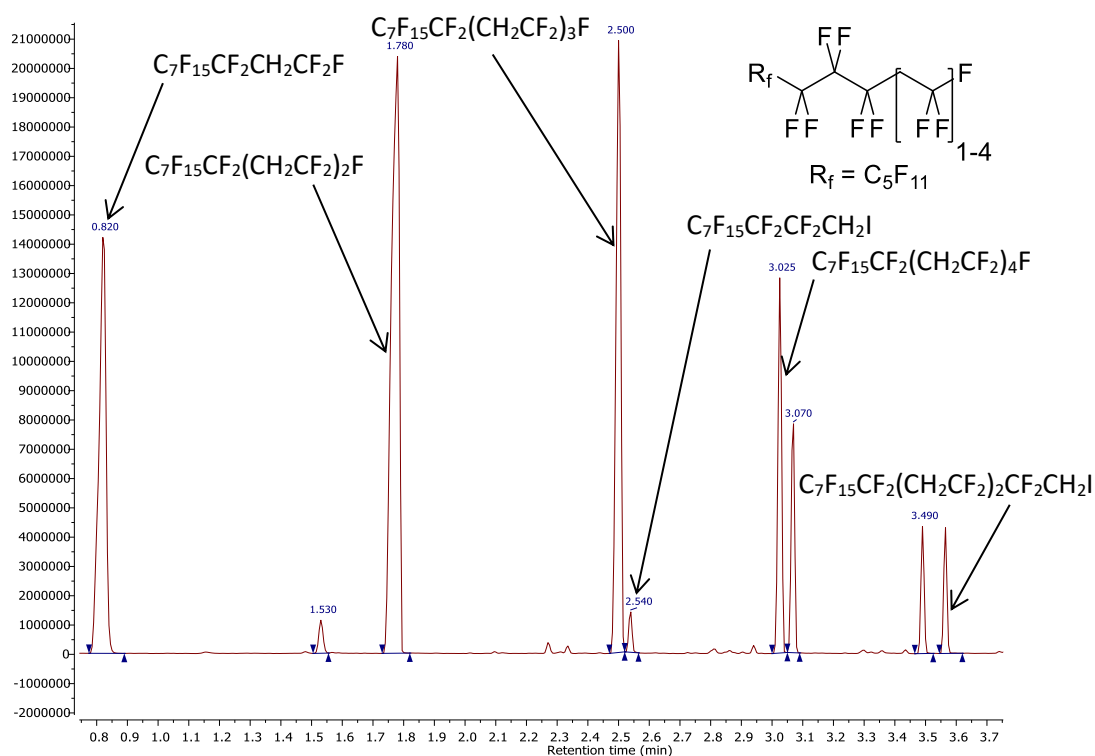


Figure 84: Gas chromatogram of the product mixture, $\text{C}_8\text{F}_{17}(\text{CH}_2\text{CF}_2)_{1-4}\text{F}$

The gas chromatogram shows that the four major components of the starting material ($C_8F_{17}(CH_2CF_2)_{1-4}I$, **47**) were all converted to the corresponding VDF telomer fluorides ($C_8F_{17}(CH_2CF_2)_{1-4}F$, **49**). In all cases, the molecular ions were not observed for these products. Instead, the highest molecular weight peak observed for $C_8F_{17}CH_2CF_2F$, $C_8F_{17}(CH_2CF_2)_2F$ and $C_8F_{17}(CH_2CF_2)_3F$ had masses of 483.0, 547.0 and 611.0 respectively, corresponding to the $[M - F]^+$ fragments. For $C_8F_{17}(CH_2CF_2)_4F$ the highest molecular weight peak was a fragment with $m/z = 655.1$, which instead corresponds to $[M - HF_2]^+$. In addition, there are several smaller peaks in the gas chromatogram that correspond to $R_fCF_2(CH_2CF_2)_{0-3}CF_2CH_2I$. These compounds are the head-to-head addition by-products from the reaction of $C_8F_{17}I$ with VDF, but unlike $C_8F_{17}(CH_2CF_2)_{1-4}I$ systems, these systems did not react with SbF_5 which is consistent with the relative stabilities of the corresponding carbocations that form during the reaction with SbF_5 . The CH_2^+ carbocation that is destabilised by the electron withdrawing effect of the neighbouring CF_2 group. By comparison, the CF_2^+ carbocation formed during the reaction of $C_8F_{17}(CH_2CF_2)_{1-4}I$ with SbF_5 , is stabilised by p-p resonance of a fluorine lone pair into the empty p orbital of the carbocation (Fig. 85).

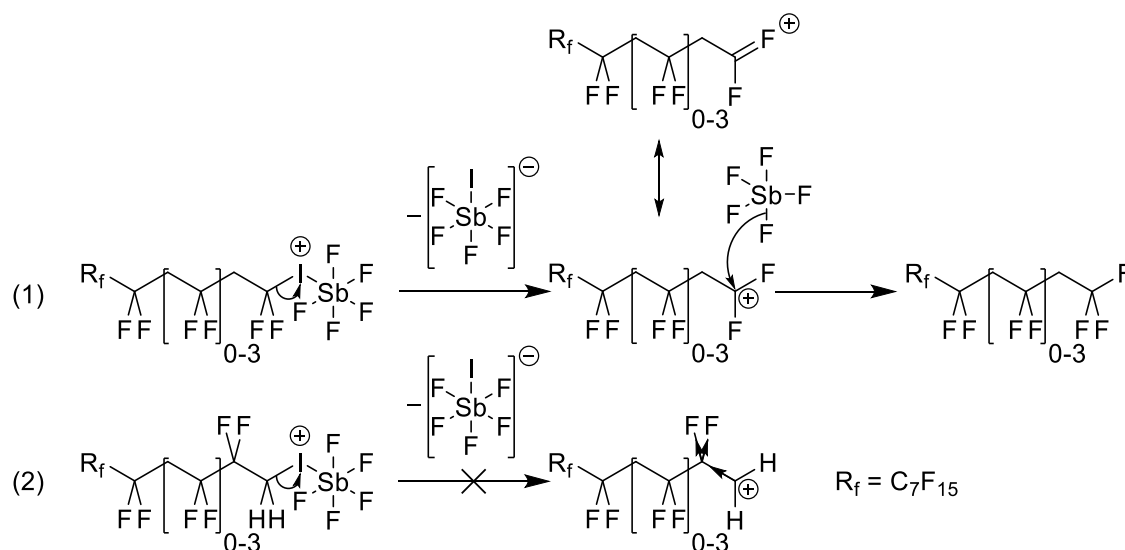


Figure 85: Relative stabilities and reactions of $C_8F_{17}(CH_2CF_2)_{0-3}CF_2CH_2I$ (**1**) and $C_8F_{17}(CH_2CF_2)_{1-4}I$ (**2**) with SbF_5

The first small scale synthesis of $C_8F_{17}(CH_2CF_2)_{1-4}F$ used CCl_2FCClF_2 as a solvent, which is an ozone depleting CFC. Therefore, the synthesis was repeated using a mixture of perfluorohexane isomers (Fluorinert™ FC-72) as the solvent on a 24 mmol scale. This reaction procedure gave the same product mixture in higher yield (87%). The ^{19}F and ^{13}C NMR spectra of the product mixture ($C_8F_{17}(CH_2CF_2)_{1-4}F$, **49**) compared with those of the starting material (**47**) confirms that the desired reaction has occurred (Fig. 86 and 87).

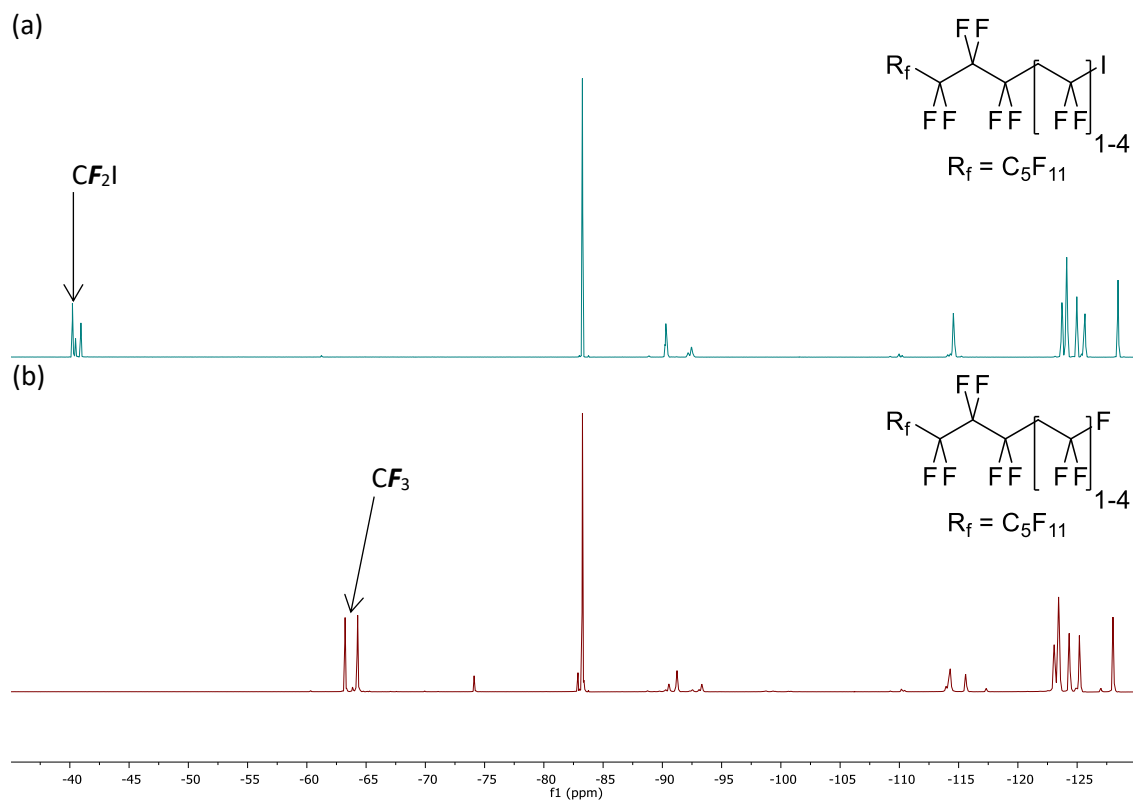


Figure 86: Comparison of the ^{19}F NMR spectra of $C_8F_{17}(CH_2CF_2)_{1-4}I$ (a) and $C_8F_{17}(CH_2CF_2)_{1-4}F$ (b)

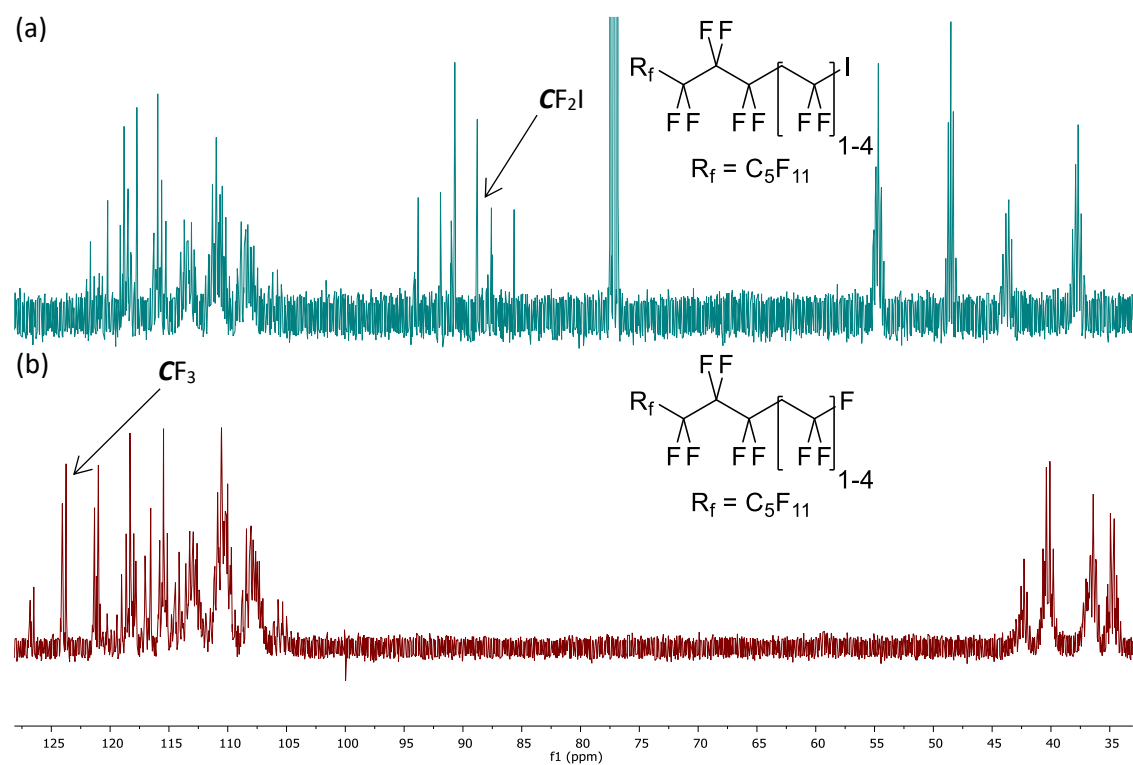


Figure 87: Comparison of the ^{13}C NMR spectra of $C_8F_{17}(CH_2CF_2)_{1-4}I$ (a) and $C_8F_{17}(CH_2CF_2)_{1-4}F$ (b)

In both the ^{19}F and ^{13}C NMR spectra, the resonances of the CF_2I groups (at $-40.13 - -41.02$ ppm and $93.88 - 85.61$ ppm respectively) have been replaced by new CF_3 resonances (at $-63.17 - -64.35$ ppm and $127.00 - 118.23$ ppm respectively) as expected. The key resonances from the ^1H , ^{19}F and ^{13}C NMR spectra of $\text{C}_8\text{F}_{17}(\text{CH}_2\text{CF}_2)_{1-4}\text{F}$ are detailed in Table 14.

Table 14: List of key shifts for the major components of the product mixture from the reaction of $\text{C}_8\text{F}_{17}\text{I}$ with VDF (5 eq.), $\text{C}_8\text{F}_{17}(\text{CH}_2\text{CF}_2)_{1-4}\text{I}$ (chemical shifts in ppm, coupling constants in Hz)

Compound	Fragment	^1H	^{19}F	^{13}C
$\text{C}_8\text{F}_{17}\text{CH}_2\text{CF}_2\text{F}$	CH_2CF_3	N.A.	-63.27 , p, $^3J_{\text{FH}} = 9.4$	122.37 , q, $^1J_{\text{CF}} = 276.5$
	$\text{CF}_2\text{CH}_2\text{CF}_3$	$3.04 - 2.43$, m	N.A.	$41.10 - 39.53$, m
	CF_3CF_2	N.A.	-83.26 , t, $^3J_{\text{FF}} = 10.3$	116.94 , qt, $^1J_{\text{CF}} = 287.2$, $^2J_{\text{CF}} = 32.9$
$\text{C}_8\text{F}_{17}(\text{CH}_2\text{CF}_2)_2\text{F}$	CH_2CF_3	N.A.	-64.34 , p, $^3J_{\text{FH}} = 9.6$	122.70 , qt, $^1J_{\text{CF}} = 275.4$, $^3J_{\text{CF}} = 6.7$
	$\text{CF}_2\text{CH}_2\text{CF}_3$	$3.04 - 2.43$, m	N.A.	$43.33 - 41.74$, m
	$\text{CF}_2\text{CH}_2\text{CF}_2\text{CH}_2\text{CF}_3$	$3.04 - 2.43$, m	N.A.	$35.64 - 34.12$, m
	CF_3CF_2	N.A.	-83.26 , t, $^3J_{\text{FF}} = 10.3$	116.94 , qt, $^1J_{\text{CF}} = 287.2$, $^2J_{\text{CF}} = 32.9$
$\text{C}_8\text{F}_{17}(\text{CH}_2\text{CF}_2)_3\text{F}$	CH_2CF_3	N.A.	-64.24 , p, $^3J_{\text{FH}} = 9.7$	122.70 , qt, $^1J_{\text{CF}} = 275.4$, $^3J_{\text{CF}} = 6.7$
	$\text{CF}_2\text{CH}_2\text{CF}_3$	$3.04 - 2.43$, m	N.A.	$43.33 - 41.74$, m
	$\text{CF}_2\text{CH}_2\text{CF}_2\text{CH}_2\text{CF}_3$	$3.04 - 2.43$, m	N.A.	$35.64 - 34.12$, m
	$\text{CF}_2\text{CH}_2\text{CF}_2(\text{CH}_2\text{CF}_2)_2\text{F}$	$3.04 - 2.43$, m	N.A.	$37.66 - 35.86$, m
	CF_3CF_2	N.A.	-83.26 , t, $^3J_{\text{FF}} = 10.3$	116.94 , qt, $^1J_{\text{CF}} = 287.2$, $^2J_{\text{CF}} = 32.9$
$\text{C}_8\text{F}_{17}(\text{CH}_2\text{CF}_2)_4\text{F}$	CH_2CF_3	N.A.	-63.89 , p, $^3J_{\text{FH}} = 9.5$	122.70 , qt, $^1J_{\text{CF}} = 275.4$, $^3J_{\text{CF}} = 6.7$
	$\text{CF}_2\text{CH}_2\text{CF}_3$	$3.04 - 2.43$, m	N.A.	$43.33 - 41.74$, m
	$\text{CF}_2\text{CH}_2\text{CF}_2\text{CH}_2\text{CF}_3$	$3.04 - 2.43$, m	N.A.	$35.64 - 34.12$, m
	$\text{CF}_2\text{CH}_2\text{CF}_2(\text{CH}_2\text{CF}_2)_{2-3}\text{F}$	$3.04 - 2.43$, m	N.A.	$37.66 - 35.86$, m
	CF_3CF_2	N.A.	-83.26 , t, $^3J_{\text{FF}} = 10.3$	116.94 , qt, $^1J_{\text{CF}} = 287.2$, $^2J_{\text{CF}} = 32.9$

The synthesised mixtures of VDF telomer fluorides ($C_8F_{17}(CH_2CF_2)_{1-4}F$, **49**), a novel class of Viton[®] model compounds, are suitable models of the poly TFE $(CF_2CF_2)_n$ and poly VDF $(CH_2CF_2)_n$ segments found in Viton[®] elastomers.

3.3. Reactions of Viton[®] Model Compounds with Petroleum Additive Systems

Having synthesised mixtures of VDF telomer fluorides ($C_8F_{17}(CH_2CF_2)_{1-4}F$, **49**), these Viton[®] model compounds were reacted with a variety of substrates which mimic petroleum additive components. Reactions were carried out in non-polar solvents (petroleum ethers, diethyl ether) where possible to best model the conditions found within engines and other mechanical systems.

3.3.1. Reactions of Straight Chain Telomer Fluorides with Amines

Reactions of straight chain Viton[®] model compounds with amines (pK_a range 5 – 14) were the first to be screened (Table 15) and, initially, were carried out at room temperature (RT). The mixture of telomer fluorides ($C_8F_{17}(CH_2CF_2)_{1-4}F$, **49**) was added to petroleum ether 40 – 60 °C, followed by the amine (2 equivalents). The reactions were stirred for two days at rt, and the products were analysed by 1H and ^{19}F NMR spectroscopy. Of the amines screened, only DBU reacted with **49**, which dehydrofluorinated to give a mixture of alkenes (**50** and **51**) (Fig. 88). In order to investigate this reactivity further, the reactions were repeated at 80 °C, using additional bases with higher pK_a 's (*N,N'*-dimethyl ethylenediamine, triethylamine and 2-*tert*-butyl-1,1,3,3-tetramethylguanidine) in petroleum ether 60 – 80 °C. The products were analysed by 1H and ^{19}F NMR spectroscopy and, again, only DBU reacted with **49**. However, the extent of dehydrofluorination significantly increases at higher temperature, as shown by the 1H NMR spectra of the starting material, **49** (a), the products after reaction with DBU at rt (b) and after reaction with DBU at 80 °C (c) (Fig. 89).

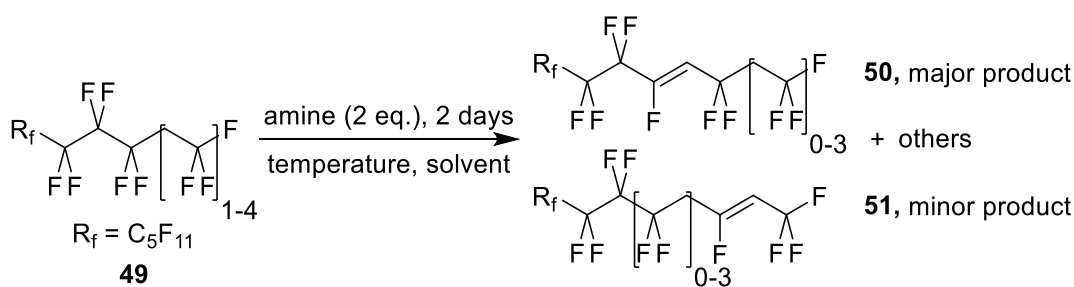


Figure 88: Reactions of $\text{C}_8\text{F}_{17}(\text{CH}_2\text{CF}_2)_{1-4}\text{F}$ with amine bases

Table 15: List of amine bases, their pK_a 's and their extent of reactivity with $\text{C}_8\text{F}_{17}(\text{CH}_2\text{CF}_2)_{1-4}\text{F}$

Base	pK_a	Conditions	Conversion / %
<i>N,N</i> -dimethyl aniline	5.15	petroleum ether 40 – 60 °C, rt, 2 days	0
<i>N,N</i> -dimethyl aniline	5.15	petroleum ether 60 – 80 °C, 80 °C, 2 days	0
pyridine	5.25	petroleum ether 40 – 60 °C, rt, 2 days	0
pyridine	5.25	petroleum ether 60 – 80 °C, 80 °C, 2 days	0
morpholine	8.36	petroleum ether 40 – 60 °C, rt, 2 days	0
morpholine	8.36	petroleum ether 60 – 80 °C, 80 °C, 2 days	0
DABCO	8.80	petroleum ether 40 – 60 °C, rt, 2 days	0
DABCO	8.80	petroleum ether 60 – 80 °C, 80 °C, 2 days	0
<i>N,N'</i> -dimethyl ethylenediamine	10.16	petroleum ether 60 – 80 °C, 80 °C, 2 days	0
triethylamine	11.01	petroleum ether 60 – 80 °C, 80 °C, 2 days	0
DBU	13.5	petroleum ether 40 – 60 °C, rt, 2 days	7
DBU	13.5	Petroleum ether 60 – 80 °C, 80 °C, 2 days	35
2- <i>tert</i> -butyl-1,1,3,3-tetramethylguanidine	13.6	Petroleum ether 60 – 80 °C, 80 °C, 2 days	0

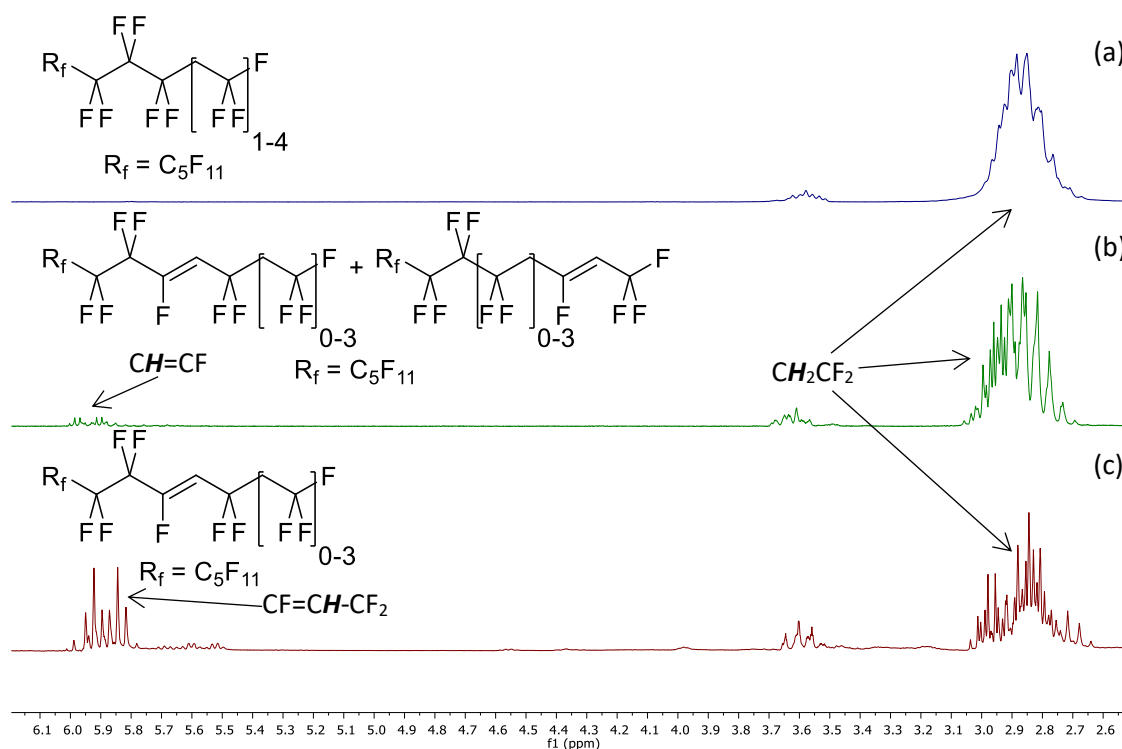


Figure 89: ^1H NMR spectra of the starting material, $\text{C}_8\text{F}_{17}(\text{CH}_2\text{CF}_2)_{1-4}\text{F}$ (a), the products after reaction with DBU at rt (b) and after reaction with DBU at $80\text{ }^\circ\text{C}$ (c)

The principal new peak observed for the dehydrofluorinated products is a doublet of triplets at 5.88 ppm ($^3J_{\text{HF}} = 31.3\text{ Hz}$, $^3J_{\text{HF}} = 10.8\text{ Hz}$). This resonance is indicative of the presence of a $\text{CF}=\text{CH}-\text{CF}_2$ group, suggesting that under these conditions, dehydrofluorination occurs adjacent to the C_7F_{15} group to synthesise $\text{C}_7\text{F}_{15}\text{CF}=\text{CHCF}_2(\text{CH}_2\text{CF}_2)_{0-3}\text{F}$ (**50**) (Fig. 90).

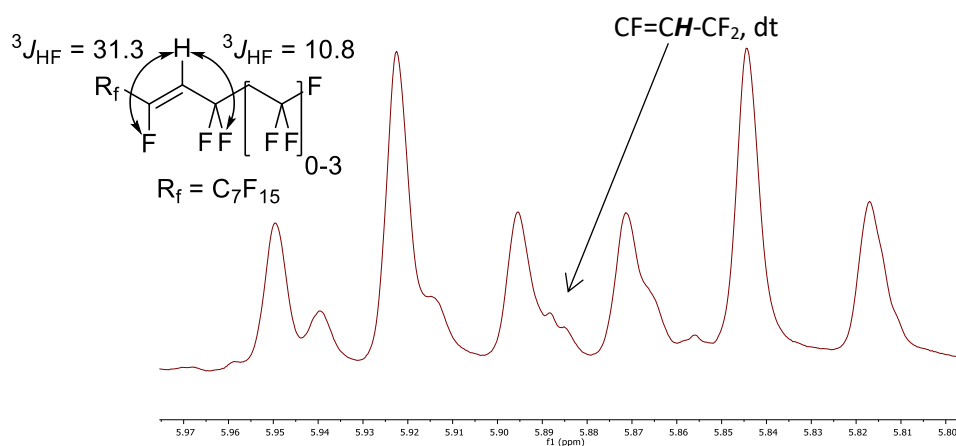


Figure 90: Expansion of the alkene region of the ^1H NMR of $\text{C}_8\text{F}_{17}(\text{CH}_2\text{CF}_2)_{1-4}\text{F}$ after reaction with DBU and the couplings observed in the major product

The structures of the principal dehydrofluorinated products were confirmed by ^{19}F NMR spectra of the starting material (a) and product (b) (Fig. 91).

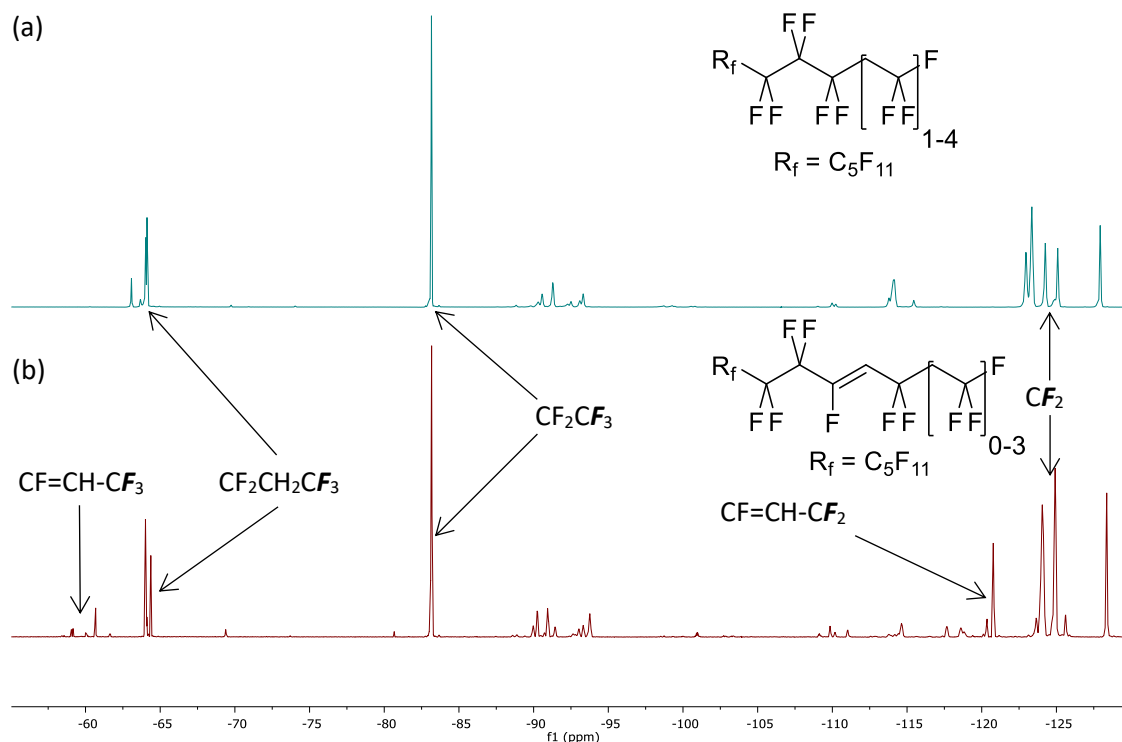


Figure 91: ^{19}F NMR of $\text{C}_8\text{F}_{17}(\text{CH}_2\text{CF}_2)_{1-4}\text{F}$ before (a) and after (b) reaction with DBU, synthesising principally $\text{C}_7\text{F}_{15}\text{CF}=\text{CHCF}_2(\text{CH}_2\text{CF}_2)_{0-3}\text{F}$

As the spectra show, there is a new peak in the ^{19}F NMR spectrum of the product mixture at -120.77 ppm, and other smaller peaks at roughly the same shift, attributed to the $\text{CF}=\text{CH}-\text{CF}_2$ and $\text{CF}=\text{CH}-\text{CF}_3$ in $\text{C}_7\text{F}_{15}\text{CF}=\text{CHCF}_2(\text{CH}_2\text{CF}_2)_{0-3}\text{F}$. There are additional minor peaks in the ^{19}F NMR spectrum of the product mixture at -58 – -62 ppm, which correspond to the resonances of the $\text{CF}=\text{CH}-\text{CF}_3$ groups present in other dehydrofluorinated products such as $\text{C}_7\text{F}_{15}(\text{CF}_2\text{CH}_2)_{0-3}\text{CF}=\text{CHCF}_3$ (51) and $\text{C}_7\text{F}_{15}\text{CF}=\text{CH}-\text{CF}=\text{CHCF}_3$ (52).

In order to further examine the products of the reactions with amines, the reaction of **49** with DBU at 80 °C was repeated on 5 g scale to obtain a sufficient amount of material to attempt purification (Fig. 92).

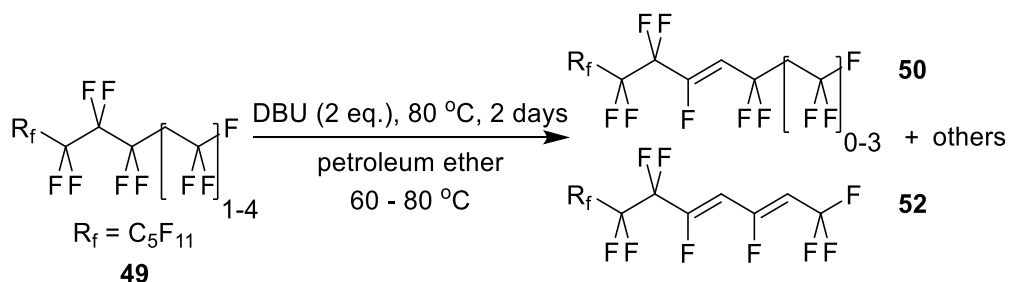


Figure 92: Reactions of $\text{C}_8\text{F}_{17}(\text{CH}_2\text{CF}_2)_{1-4}\text{F}$ with DBU (5 g scale)

The reaction yielded a viscous black oil that was purified using Kugelrohr distillation under high vacuum. Three fractions were collected, an orange oil that contained polymerised products and two clear oils that contained a mixture of products. The most volatile fraction could be analysed by GC-MS (Fig. 93).

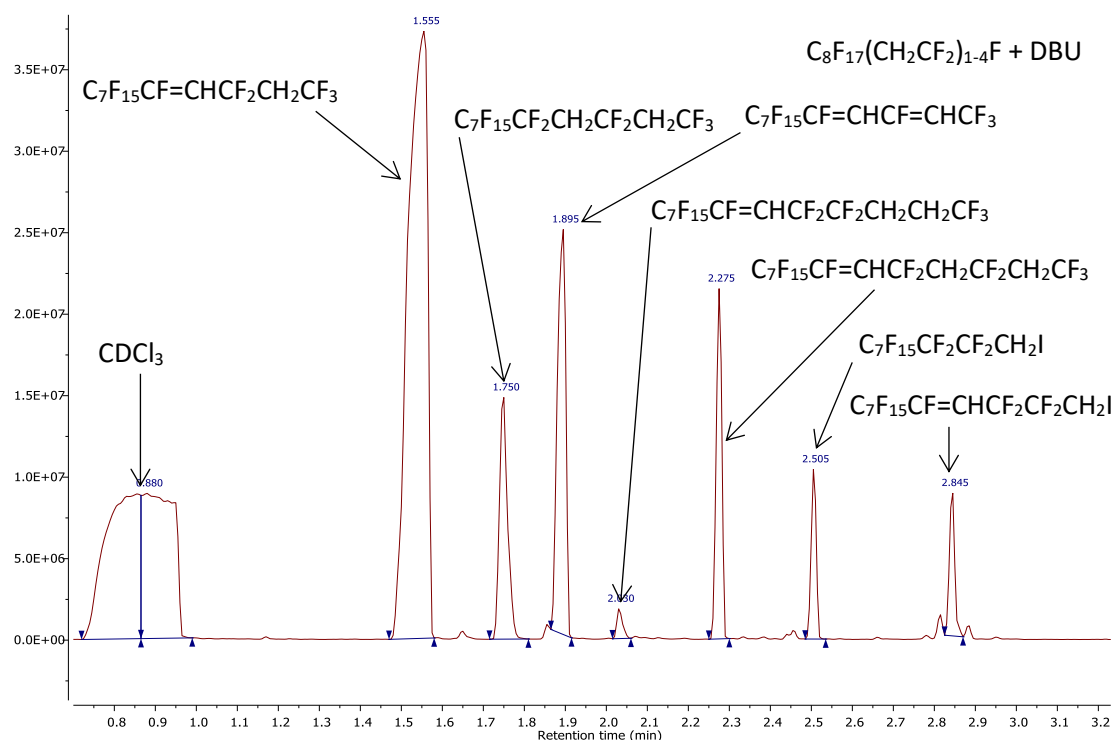


Figure 93: Gas chromatogram from the reaction of $C_8F_{17}(CH_2CF_2)_{1-3}F$ with DBU

The gas chromatogram shows that the mixture of products contains both dehydrofluorinated species and starting materials ($C_8F_{17}(CH_2CF_2)_{1-4}F$, **49**) which can all be identified. For example, the peaks at 1.555 and 2.275 are derived from the dehydrofluorination of $C_8F_{17}(CH_2CF_2)_2F$ and $C_8F_{17}(CH_2CF_2)_3F$ respectively. As an example, the mass spectrum from the peak at 1.555 is shown in Fig. 94.

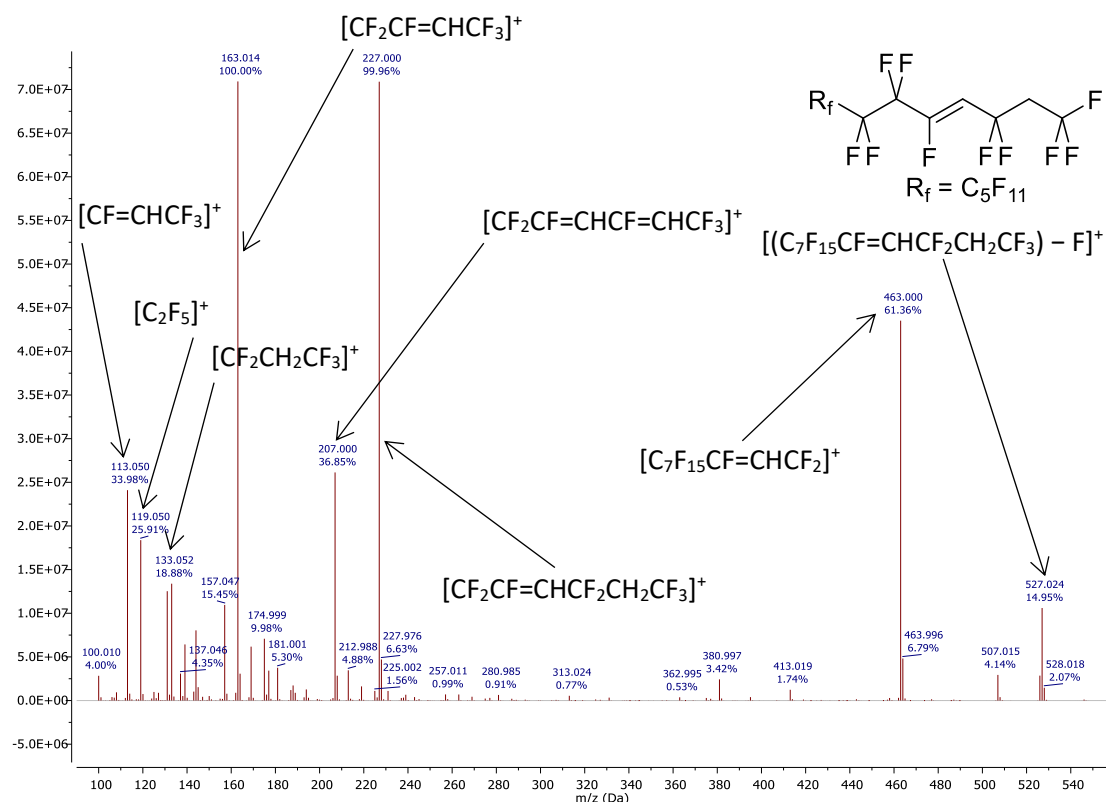


Figure 94: Mass spectrum of $C_7F_{15}CF=CHCF_2CH_2CF_3$ (retention time, 1.555)

Of particular interest are the fragments with masses of 463.0, 227.0, 207.0 and 133.1. The fragment at $m/z = 463.0$ has a structure of $[C_7F_{15}CF=CHCF_2]^+$, which suggests that dehydrofluorination occurs adjacent to the C_7F_{15} group, as was inferred previously from the doublet of triplets in the 1H NMR spectrum at 5.88 ppm. The fragments at $m/z = 227.0$ ($[CF_2CF=CHCF_2CH_2CF_3]^+$), and $m/z = 133.1$ ($[CF_2CH_2CF_3]^+$) confirm that the structure of the product is $C_7F_{15}CF=CHCF_2CH_2CF_3$, as these fragments can only be formed if dehydrofluorination had occurred adjacent to the C_7F_{15} group instead of the CF_3 group. The fragment at $m/z = 207.0$ is assigned to $[CF_2CF=CHCF=CHCF_3]^+$, which is formed by dehydrofluorination during the electron ionisation process. This fragment carbocation is stabilised by resonance with the two double bonds (Fig. 95).

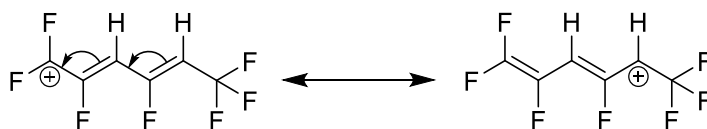


Figure 95: Resonance stabilisation of the $CF_2CF=CHCF=CHCF_3$ diene fragment

The peak at 1.750 in the gas chromatogram is unreacted $C_8F_{17}(CH_2CF_2)_2F$, and the peak at 2.505 is from $C_8F_{17}CF_2CF_2CH_2I$, one of the by-products carried through from the reaction of $C_8F_{17}I$ with VDF that did not react with SbF_5 and remains unreacted on exposure to base. Interestingly,

there is a peak in the gas chromatogram at 2.845. This peak is for $C_7F_{15}CF=CHCF_2CF_2CH_2$, formed by the dehydrofluorination of $C_8F_{17}CH_2CF_2CF_2CH_2$.

There is a small peak in the gas chromatogram at 2.030, the mass spectrum of which is given in Fig. 96.

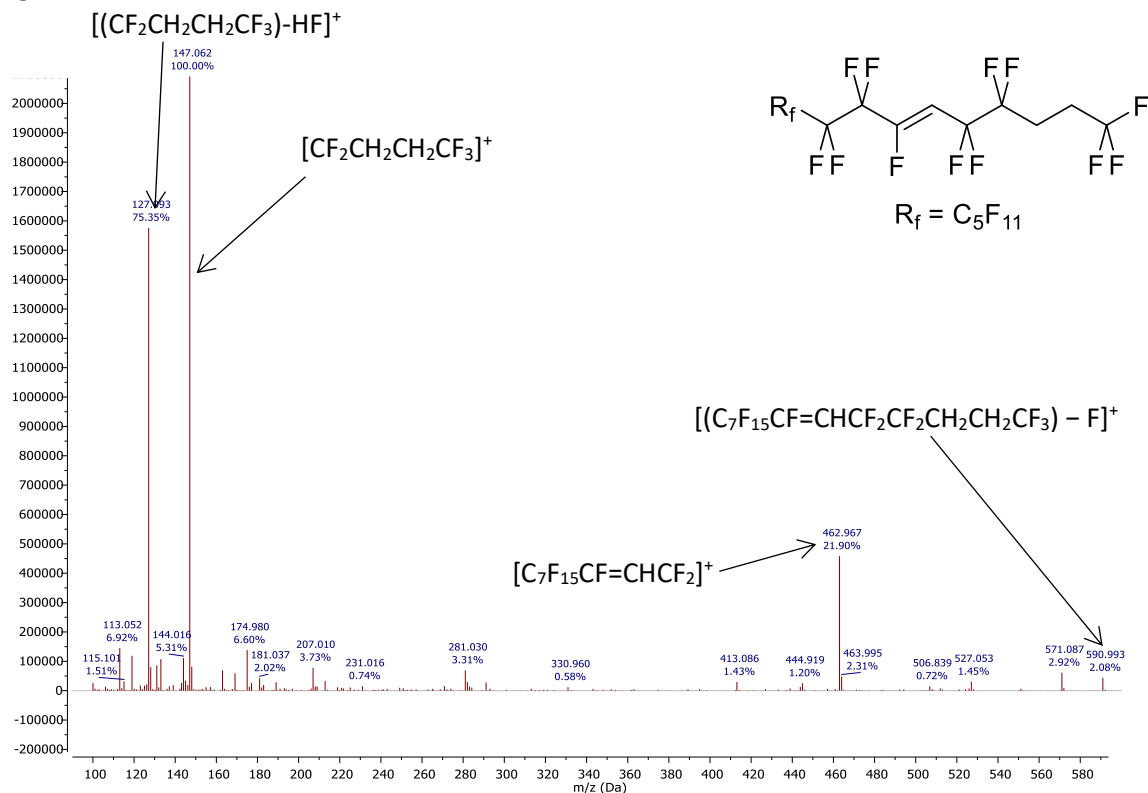


Figure 96: Mass spectrum of $C_7F_{15}CF=CHCF_2CF_2CH_2CF_3$ (retention time, 2.030)

The fragment with an m/z of 463.0 corresponds to $[C_7F_{15}CF=CHCF_2]^+$, but the peaks at $m/z = 147.1$ and 127.1 are unique to this species. The fragment at $m/z = 147.1$ has the empirical formula $[C_4F_5H_4]^+$ but it is unlikely that this fragment has the structure $[CH_2CF_2CH_2CF_3]^+$, as these types of primary carbocations are relatively unstable. Instead, this fragment suggests that this compound is an internal head-to-head addition product that leads to the fragment with the structure $[CF_2CH_2CH_2CF_3]^+$. This is confirmed by the absence of a fragment with an m/z of 133.0 ($[CF_2CH_2CF_3]^+$) which is present in several of the other products. The fragment at $m/z = 127.1$ has the structure $[CF_2CH_2CH=CF_2]^+$, and is derived from the dehydrofluorination of the above fragment ($[CF_2CH_2CH_2CF_3]^+$) during electron ionisation. The presence of this peak indicates that $C_7F_{15}CF_2CH_2CF_2CF_2CH_2CH_2CF_3$ (**54**), a compound containing structures (b) and (c), is synthesised as a minor side product in previous reactions and subsequently dehydrofluorinated adjacent to the C_7F_{15} group on exposure to DBU to form $C_7F_{15}CF=CHCF_2CF_2CH_2CH_2CF_3$ (**55**) (Fig. 97).

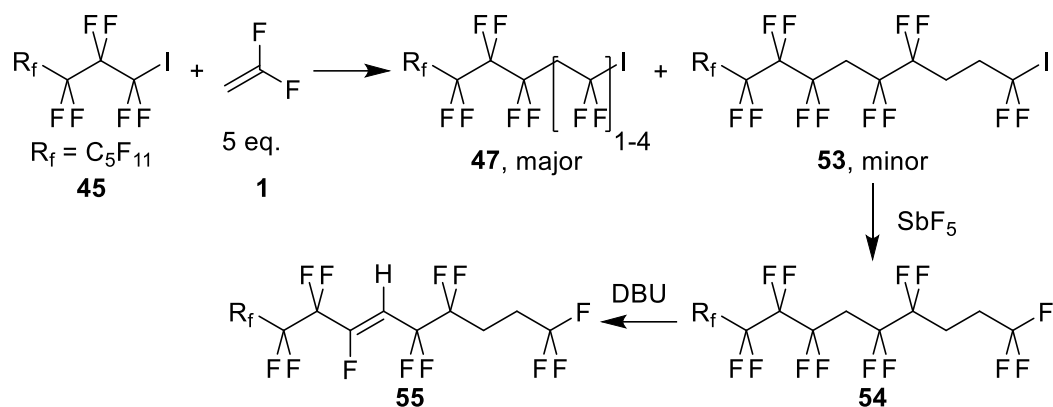


Figure 97: Synthesis of $C_7F_{15}CF_2CH_2CF_2CF_2CH_2CH_2CF_3$ and subsequent reaction with DBU

The peak in the gas chromatogram at 1.895 is of particular interest, and the mass spectrum of this peak is given in Fig. 98.

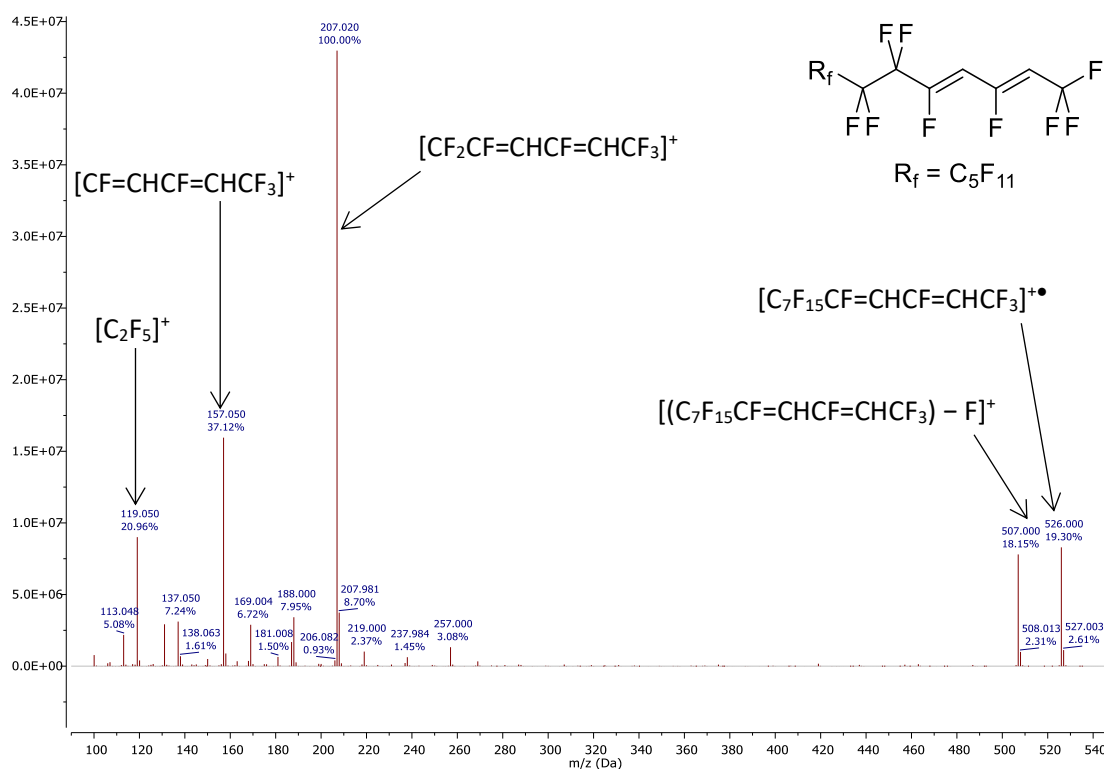


Figure 98: Mass spectrum of $C_7F_{15}CF=CHCF=CHCF_3$ (retention time, 1.895)

The compound with retention time 1.895 shows strong fragments at $m/z = 526.0$, 507.0 , 207.0 and 157.1 . The peak at $m/z = 207.0$ has the structure $[CF_2CF=CHCF=CHCF_3]^+$ as described above, and the peak at $m/z = 157.1$ is attributed to $[CF=CHCF=CHCF_3]^+$. This suggests that this product is formed by the double dehydrofluorination of $C_7F_{15}CF_2CH_2CF_2CF_2CH_2CH_2CF_3$ to give $C_7F_{15}CF=CHCF=CHCF_3$ (**52**). This is confirmed by the molecular ion peak ($m/z = 526.0$, $[R_fCF=CHCF=CHCF_3]^+$), the fragment at $m/z = 507.0$ ($[(R_fCF=CHCF=CHCF_3) - F]^+$) and by the absence of the fragments at $m/z = 227.0$ ($[CF_2CF=CHCF_2CH_2CF_3]^+$) and 133.0 ($[CF_2CH_2CF_3]^+$).

The ^1H NMR spectrum of the distilled fraction confirms the composition of the product mixture (Fig. 99 and 100).

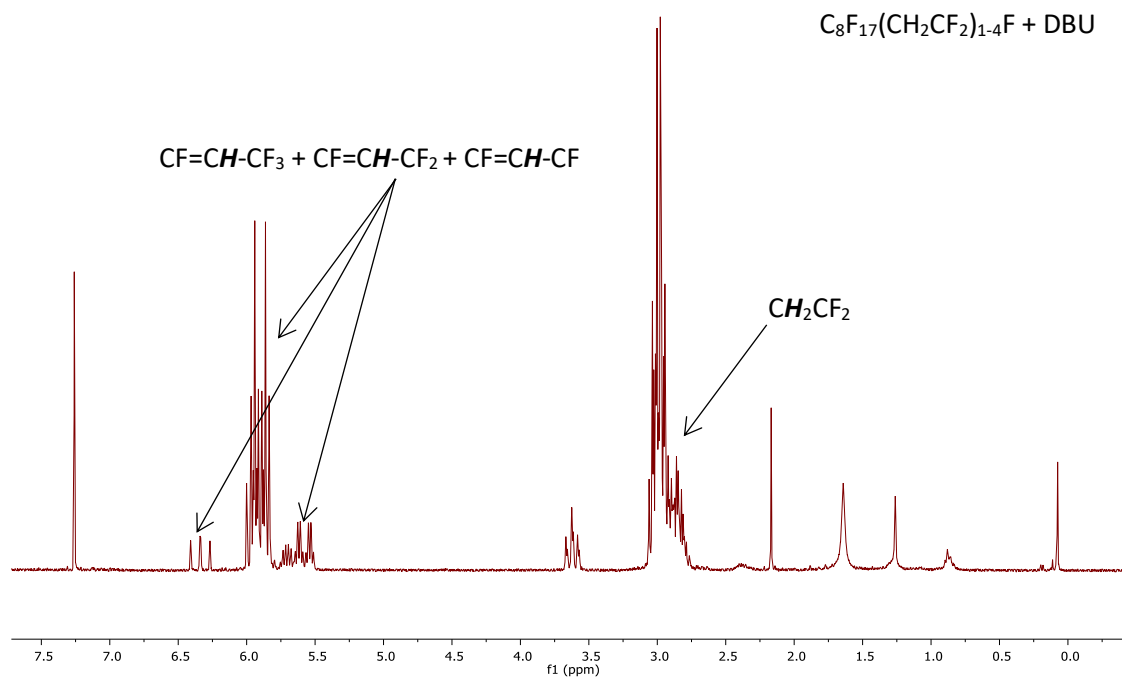


Figure 99: ^1H NMR spectrum of the product mixture from the reaction of $\text{C}_8\text{F}_{17}(\text{CH}_2\text{CF}_2)_{1-4}\text{F}$ with DBU

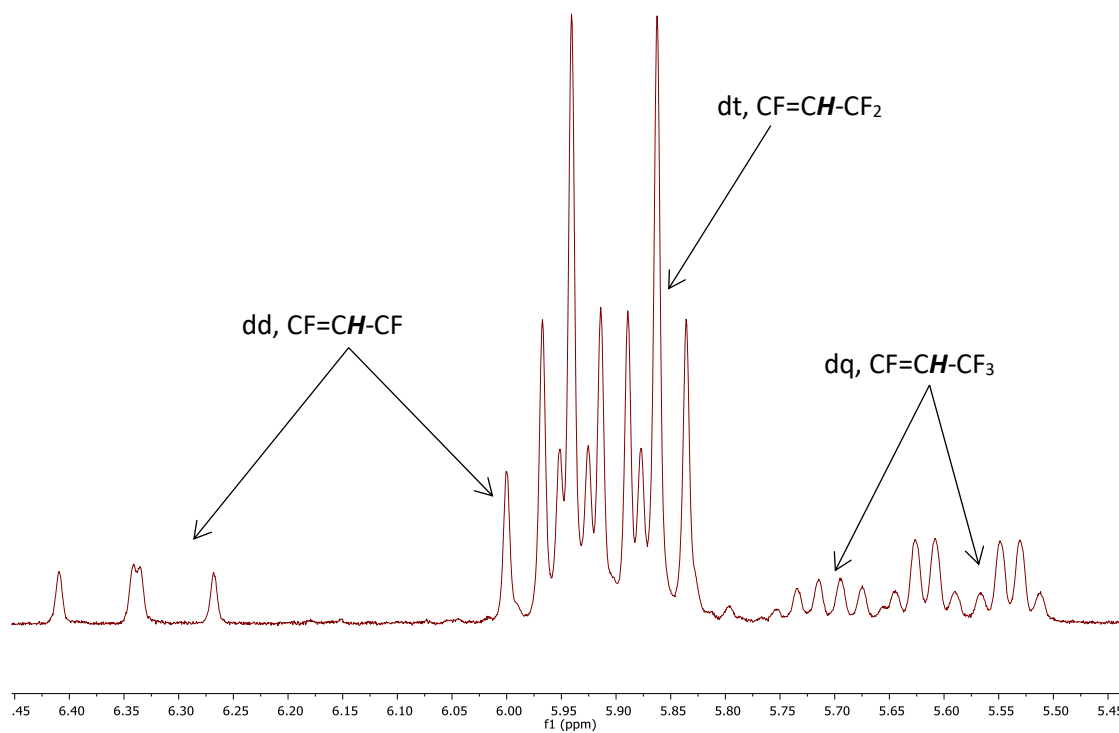


Figure 100: Expansion of the region between 5.5 and 6.5 in the ^1H NMR spectrum of the product mixture from the reaction of $\text{C}_8\text{F}_{17}(\text{CH}_2\text{CF}_2)_{1-4}\text{F}$ with DBU

The doublet of triplets at 5.90 ppm (${}^3J_{\text{HF}} = 31.3$ Hz, ${}^3J_{\text{HF}} = 10.7$ Hz) is the resonance from the alkene protons of the major products ($\text{C}_7\text{F}_{15}\text{CF}=\text{CH}(\text{CF}_2\text{CH}_2)_{1-3}\text{CF}_3$). However, there is a second resonance overlapping with the peak at 5.94 ppm which has the same integral as the peak at 5.58 ppm. These resonances are due to the alkene protons in $\text{C}_7\text{F}_{15}\text{CF}=\text{CHCF}=\text{CHCF}_3$, specifically the doublet of doublets at 5.94 ppm (${}^3J_{\text{HF}} = 29.8$ Hz, ${}^3J_{\text{HF}} = 19.5$ Hz) that arises from $\text{C}_7\text{F}_{15}\text{CF}=\text{CHCF}$, and the doublet of quartets at 5.58 ppm (${}^3J_{\text{HF}} = 31.1$ Hz, ${}^3J_{\text{HF}} = 7.3$ Hz) arises from $\text{CF}=\text{CHCF}_3$ (Fig. 101). There is a second pair of peaks at 6.34 (dd) and 5.70 ppm (dq) that are the resonances from the alkene protons in $\text{C}_7\text{F}_{15}\text{CF}_2\text{CH}_2\text{CF}=\text{CHCF}=\text{CHCF}_3$

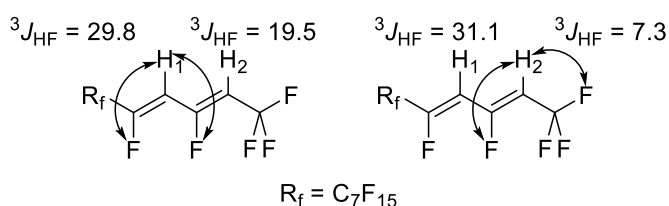


Figure 101: Observed couplings in the ${}^1\text{H}$ NMR spectrum of $\text{C}_7\text{F}_{15}\text{CF}=\text{CHCF}=\text{CHCF}_3$

In conclusion, the data from the above reactions indicates that poly VDF $(\text{CH}_2\text{CF}_2)_n$ segments of Viton[®] elastomers are vulnerable to dehydrofluorination in the presence of strong amine bases, such as DBU, that are related to common components of petroleum additive mixtures.

3.3.2. Reactions of Straight Chain Telomer Fluorides with Anionic Bases

In order to gain a better understanding of the degradation of Viton[®] model compounds by basic petroleum additives, further reactions were carried out using a range of anionic bases (Fig. 102) in a variety of different conditions and solvents. The mixture of telomer fluorides (**49**) was added to the reaction solvent, followed by the base. The reactions were stirred at the temperature and for the durations given in Table 16, and products were analysed by ${}^1\text{H}$ and ${}^{19}\text{F}$ NMR spectroscopy. The conditions and results of these reactions are detailed in Table 16.

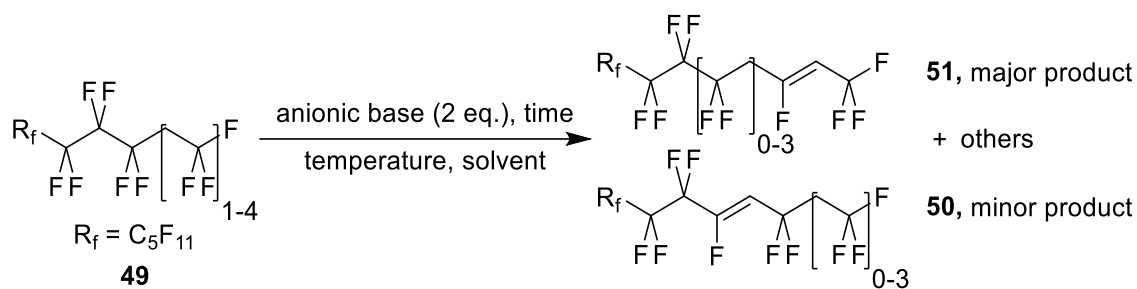


Figure 102: Reactions of $\text{C}_8\text{F}_{17}(\text{CH}_2\text{CF}_2)_{1-4}\text{F}$ with anionic bases

Table 16: List of anionic bases, their $\text{p}K_a$'s and their extent of reactivity with $\text{C}_8\text{F}_{17}(\text{CH}_2\text{CF}_2)_{1-4}\text{F}$

Base	$\text{p}K_a$	Conditions	Conversion / %
NaOEt (2 eq.)	15.5	Ether, rt, 2 days	trace
KOMe (2 eq.)	15.5	Petroleum ether 60 – 80 °C, 80 °C, 4 days	>50
KO ^t Bu (2 eq.)	17	Ether, rt, 2 days	30
KO ^t Bu (2 eq.)	17	Petroleum ether 60 – 80 °C, 80 °C, 2 days	30
NaO ^t Bu (2 eq.)	17	Petroleum ether 60 – 80 °C, 80 °C, 4 days	>50
LHMDS (2 eq.)	26	Ether, rt, 2 days	0
LDA (1 eq.)	36	THF, –78 °C, 1 day (synthesised LDA)	20
<i>n</i> -BuLi (1 eq.)	50	THF, –78 °C, 1 day	polymer
FeO	-	Petroleum ether 60 – 80 °C, 80 °C, 2 days	0

Of these bases, KOMe, KO^tBu, NaO^tBu, LDA and *n*-BuLi reacted with **49**. The reaction with *n*-BuLi produced a black polymeric tar that was insoluble in organic solvents and, therefore, could not be characterised, but the other bases gave product mixtures that could be analysed.

For example, the ^1H NMR spectra of the starting material (a) and product mixture (b) from the reaction of **49** with LDA is given in Fig. 103.

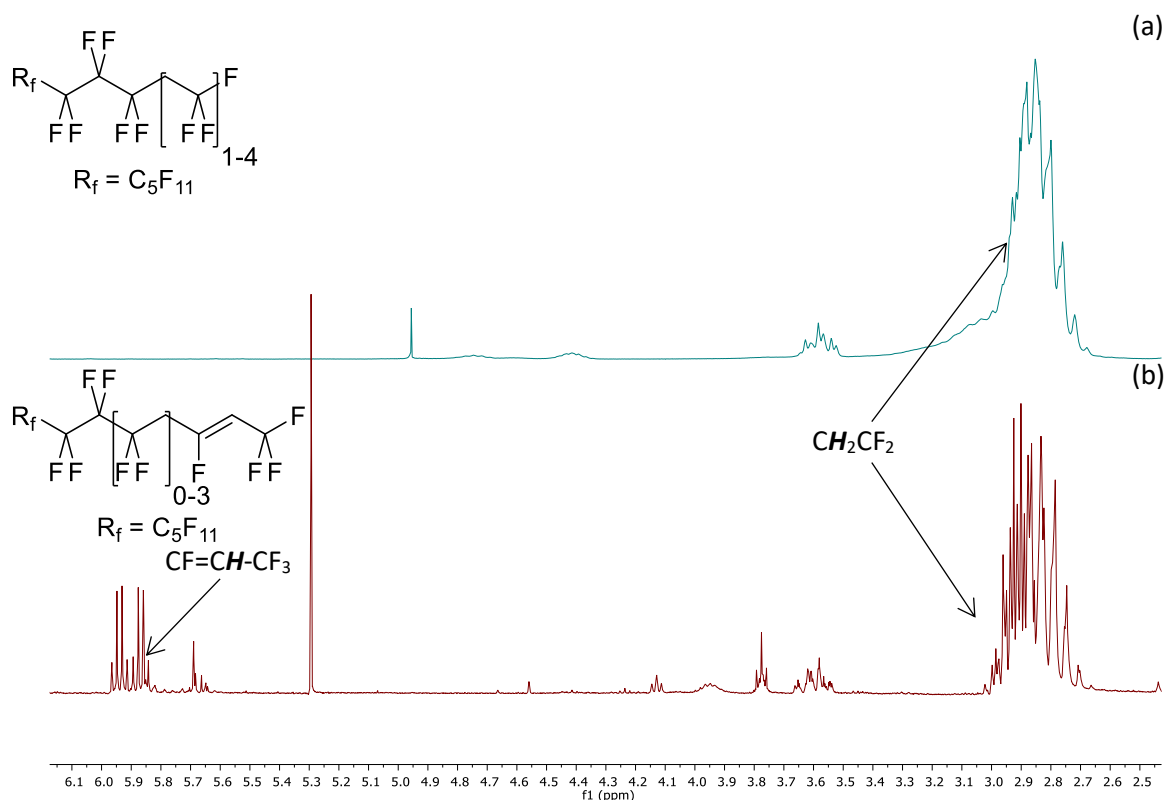


Figure 103: ^1H NMR of $\text{C}_8\text{F}_{17}(\text{CH}_2\text{CF}_2)_{1-4}\text{F}$ before (a) and after (b) reaction with LDA, synthesising principally $\text{C}_7\text{F}_{15}(\text{CF}_2\text{CH}_2)_{0-3}\text{CF}=\text{CHCF}_3$

The major dehydrofluorinated products are alkenes, but in this case, the doublet of quartet at 5.90 ppm ($^3J_{\text{HF}} = 28.8$ Hz, $^3J_{\text{HF}} = 6.9$ Hz) is indicative of a $\text{CF}=\text{CH}-\text{CF}_3$ group, suggesting that dehydrofluorination has occurred adjacent to the terminal CF_3 group to give $\text{C}_7\text{F}_{15}(\text{CF}_2\text{CH}_2)_{0-3}\text{CF}=\text{CHCF}_3$ (**51**) as the major product (Fig. 104).

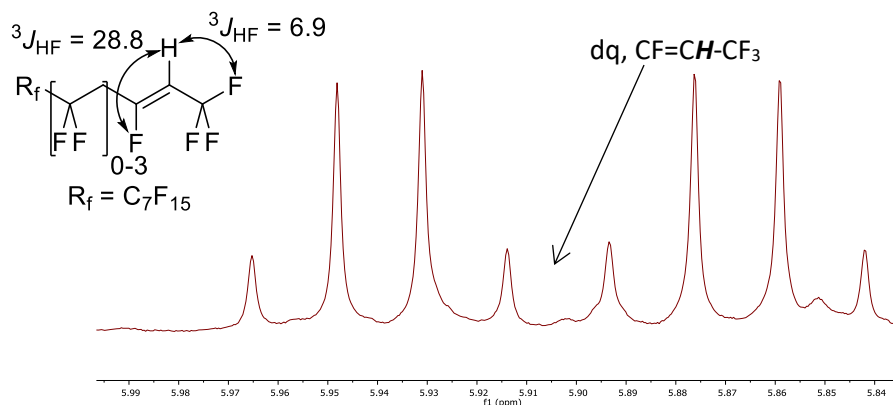


Figure 104: Expansion of the alkene region of the ^1H NMR of the product mixture from the reaction of $\text{C}_8\text{F}_{17}(\text{CH}_2\text{CF}_2)_{1-4}\text{F}$ with LDA and the couplings observed in the major product

The structures of the major products were confirmed by the ^{19}F NMR spectra of the starting material (a) and product mixture (b) (Fig. 105).

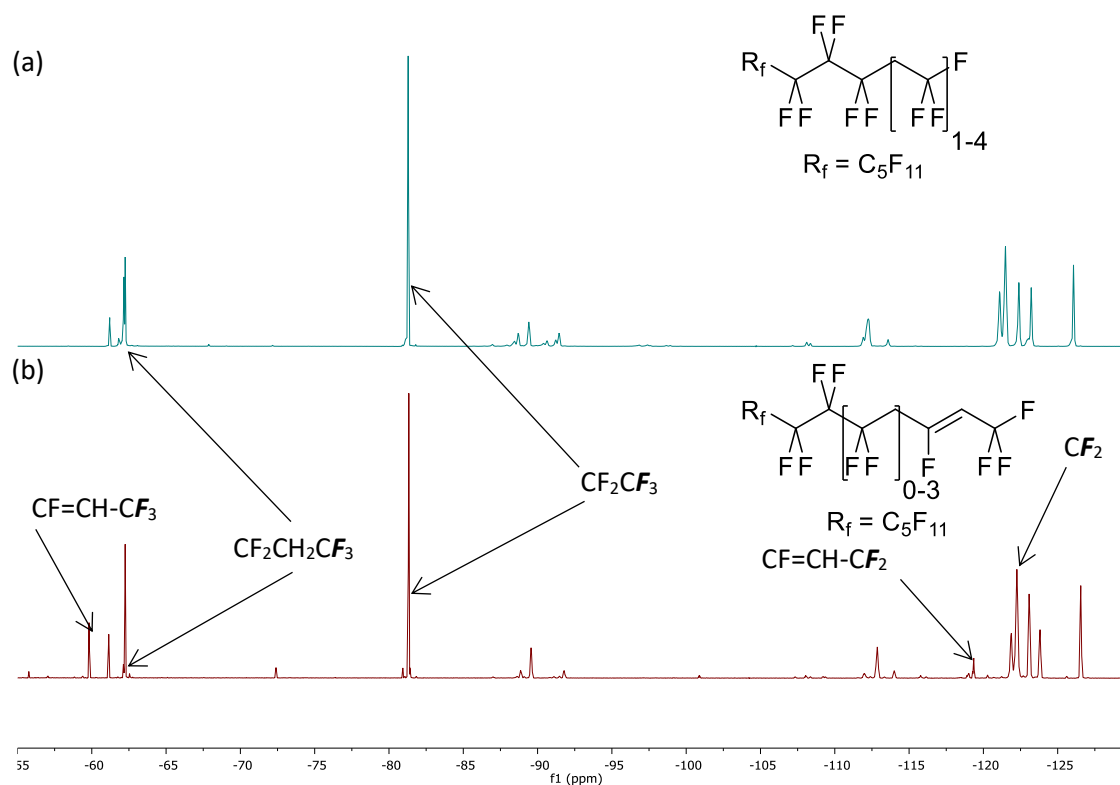


Figure 105: ^{19}F NMR of $\text{C}_8\text{F}_{17}(\text{CH}_2\text{CF}_2)_{1-4}\text{F}$ before (a) and after (b) reaction with LDA, synthesising principally $\text{C}_7\text{F}_{15}(\text{CF}_2\text{CH}_2)_{0-3}\text{CF}=\text{CHCF}_3$

The ^{19}F NMR spectrum of the product mixture shows a small peak at -119.33 ppm corresponding to $\text{CF}=\text{CH}-\text{CF}_2$ groups present in some of the dehydrofluorinated products. However, there is a larger new peak at -59.80 ppm (ddt, $^3J_{\text{FH}} = 17.5$ Hz, $^4J_{\text{FF}} = 6.9$, $^5J_{\text{FH}} = 2.0$ Hz) that is indicative of $\text{CF}=\text{CH}-\text{CF}_3$, confirming that the major products of this reaction are $\text{C}_7\text{F}_{15}(\text{CF}_2\text{CH}_2)_{0-3}\text{CF}=\text{CHCF}_3$ systems.

Reaction of **49** with KO^tBu was carried out at both rt and 80 °C, and the products of these reactions were different as observed by ¹H NMR spectroscopy (Fig. 106).

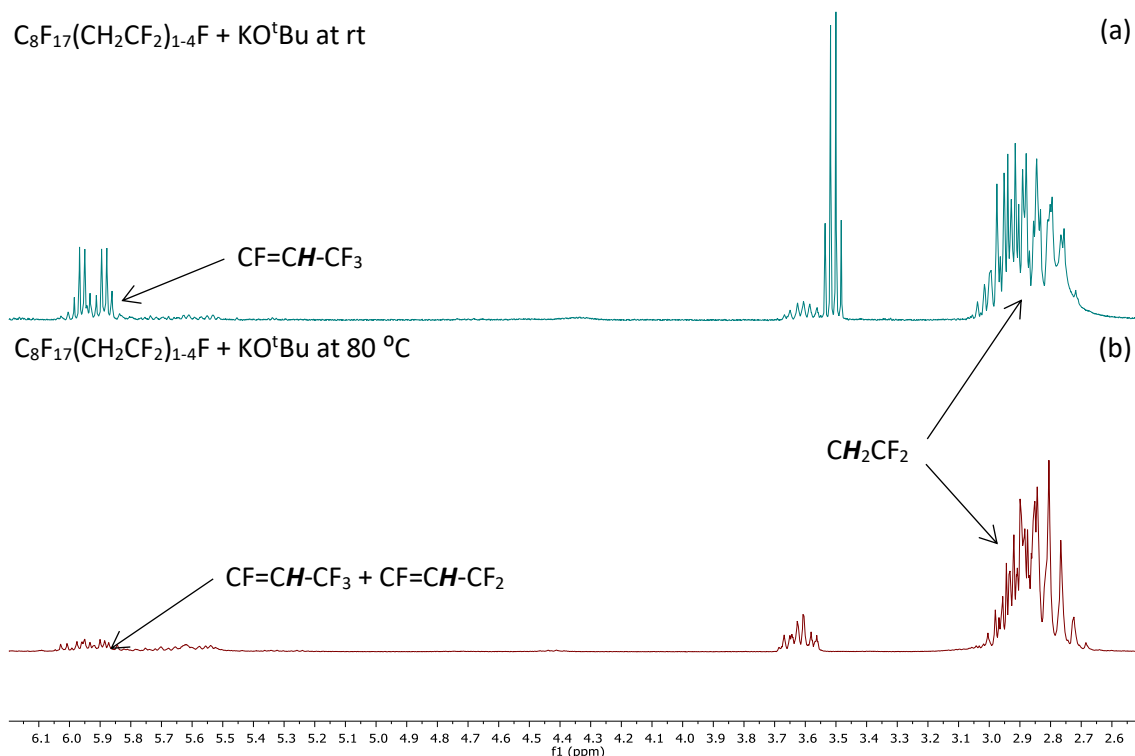


Figure 106: ¹H NMR spectra of the products from the reactions of C₈F₁₇(CH₂CF₂)₁₋₄F with KO^tBu at rt (a) and at 80 °C (b)

As the peak at 5.98 ppm (dq) in the ¹H NMR spectrum shows, the reaction with KO^tBu at rt produced primarily C₇F₁₅(CF₂CH₂)₀₋₃CF=CHCF₃ (**51**), the same product mixture that was obtained from the reaction of **49** with LDA. However, the ¹H NMR spectrum of the product mixture from reaction with KO^tBu at 80 °C has a range of peaks between 6.1 and 5.5 ppm, suggesting a mixture of C₇F₁₅(CF₂CH₂)₀₋₃CF=CHCF₃ and C₇F₁₅CF=CHCF₂(CH₂CF₂)₀₋₃F was formed. Therefore, at higher temperature, several competing dehydrofluorination processes occur.

Reactions of C₈F₁₇(CH₂CF₂)₁₋₄F with KOMe and NaO^tBu were carried out using similar conditions but with greater reaction durations (4 days) in an attempt to increase conversion (Fig. 107).

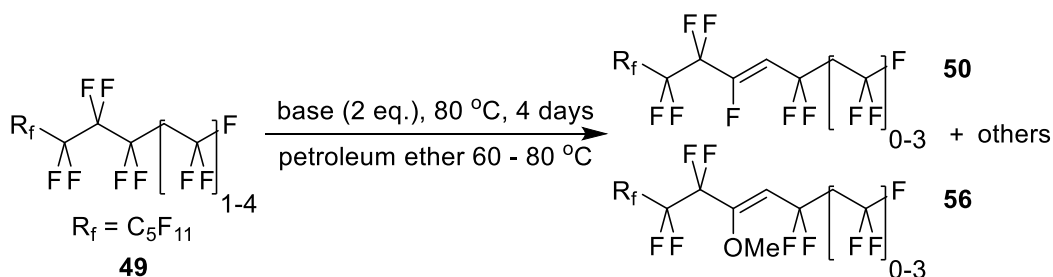


Figure 107: Reactions of C₈F₁₇(CH₂CF₂)₁₋₄F with NaO^tBu (**50**) and KOMe (**56**)

Reaction of $C_8F_{17}(CH_2CF_2)_{1-4}F$ with NaO^tBu produced a similar mixture of products to those obtained using KO^tBu , detailed in Fig. 106. However, reaction of $C_8F_{17}(CH_2CF_2)_{1-4}F$ with KOMe gave a unique mixture of products as observed by 1H and ^{19}F NMR spectroscopy (Fig. 108 and 109).

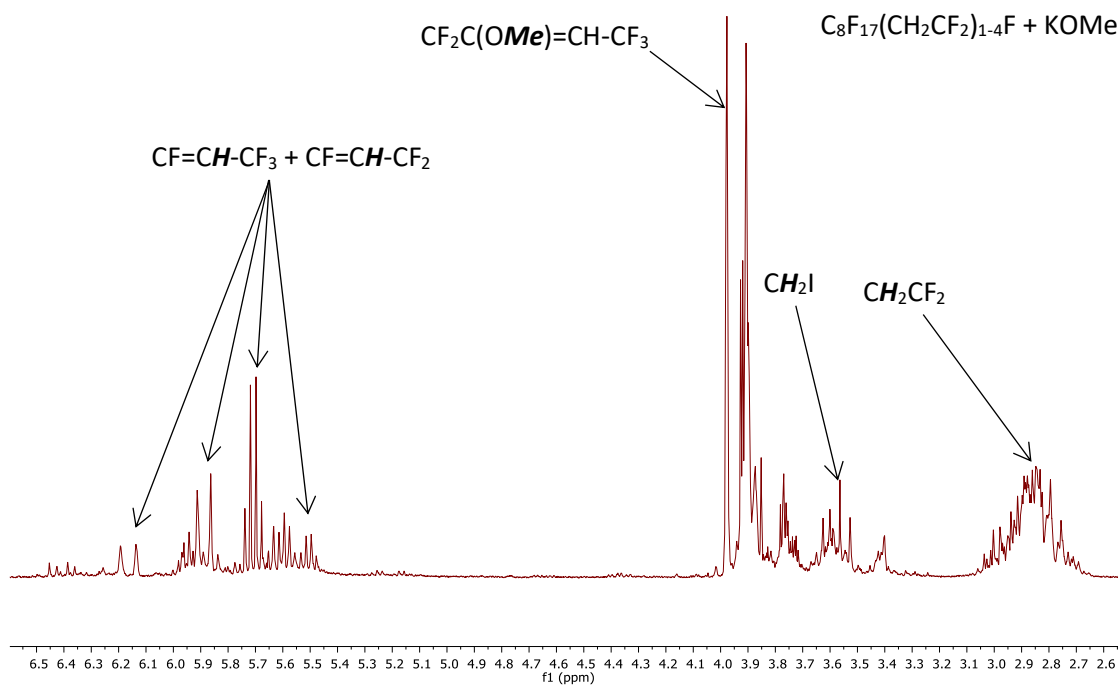


Figure 108: 1H NMR spectrum from the reaction of $C_8F_{17}(CH_2CF_2)_{1-4}F$ with KOMe

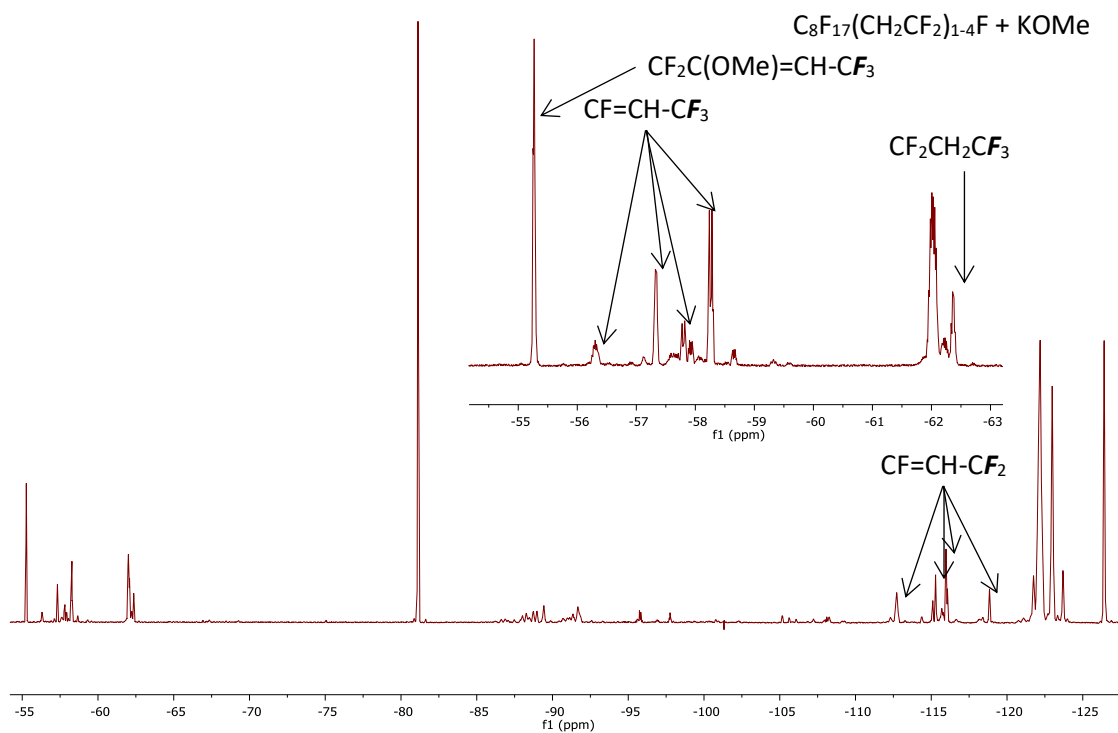


Figure 109: ^{19}F NMR spectrum from the reaction of $C_8F_{17}(CH_2CF_2)_{1-4}F$ with KOMe

As the NMR spectra show, KOMe causes significant dehydrofluorination of **49**. The NMR spectra of the product mixture contained resonances from compounds previously observed (^1H : 6.3 – 5.4 ppm, $\text{CF}=\text{CH}-\text{CF}_3 + \text{CF}=\text{CH}-\text{CF}_2$; ^{19}F : -56 – -60 ppm, $\text{CF}=\text{CH}-\text{CF}_3$, -112 – -120 ppm, $\text{CF}=\text{CH}-\text{CF}_3$). However, the spectra also contain signals that are unique to this product mixture. In the ^1H NMR spectrum, there are two singlets at 3.98 and 3.91 ppm, and in the ^{19}F NMR spectrum there is a triplet at -55.27 ppm ($^3J_{\text{HF}} = 7.5$ Hz) which suggest methoxy groups are present in $\text{CF}_2\text{C}(\text{OMe})=\text{CH}-\text{CF}_{2-3}$ type systems.

This is confirmed by GC-MS analysis of the product mixture which reveals that the product mixture contains several compounds that produce fragment patterns that can only be rationalised by the presence of methoxy groups, compounds with the structure $\text{C}_7\text{F}_{15}\text{C}(\text{OMe})=\text{CH}(\text{CF}_2\text{CH}_2)_{0-3}\text{CF}_3$ (**56**) (Fig. 110).

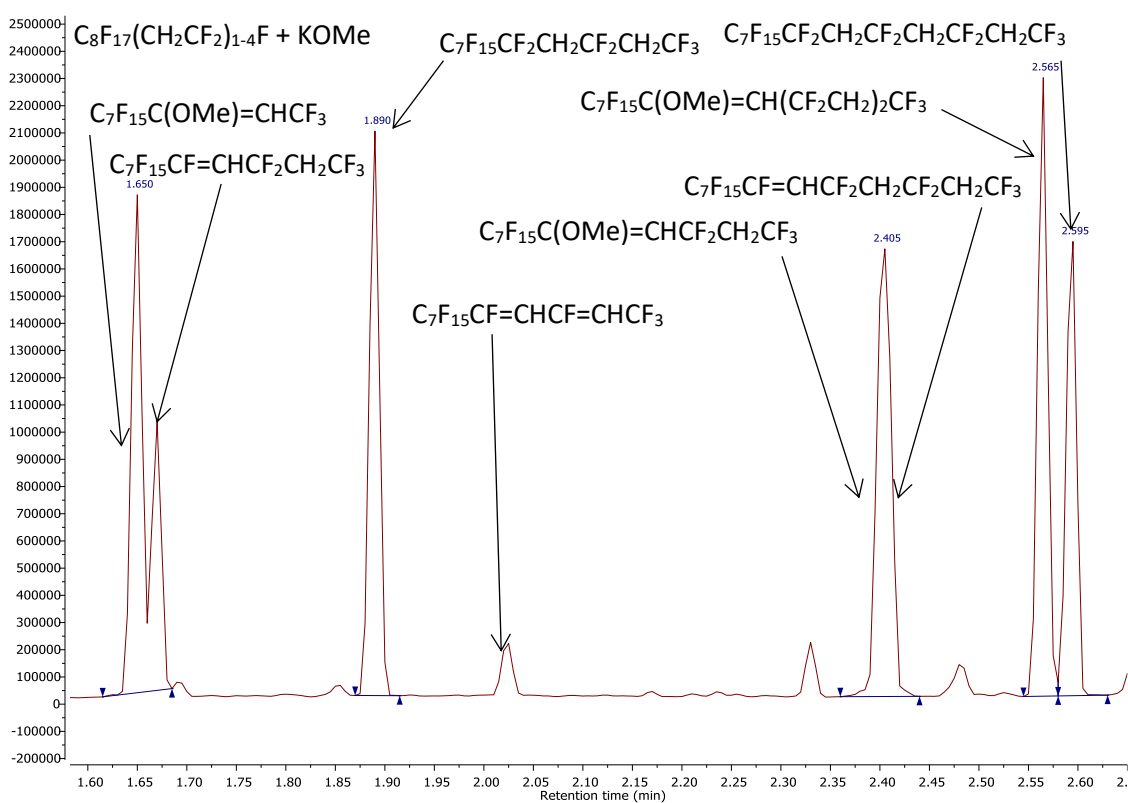


Figure 110: Gas chromatogram from the reaction of $\text{C}_8\text{F}_{17}(\text{CH}_2\text{CF}_2)_{1-4}\text{F}$ with KOMe

For example, the mass spectrum of the compound at 1.640 is detailed in Fig. 111.

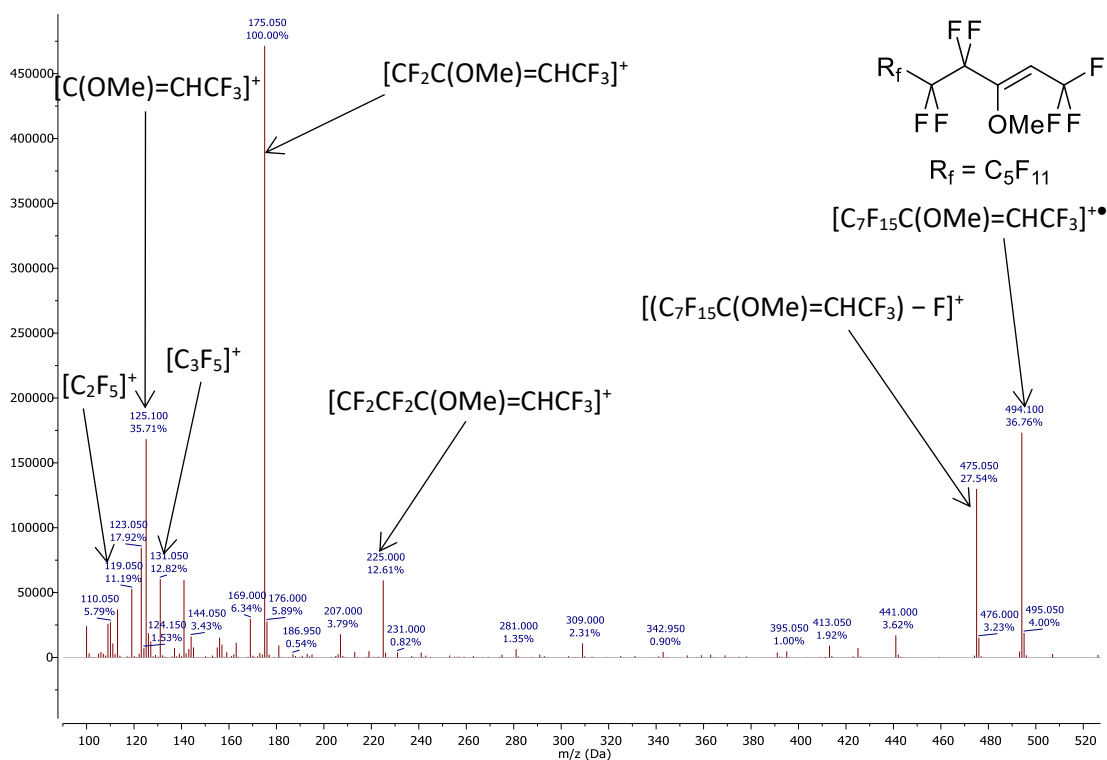


Figure 111: Mass spectrum of $C_7F_{15}C(OMe)=CHCF_3$ (retention time, 1.650)

The molecular ion peak for this compound (m/z 494.1) has the structure $[C_7F_{15}C(OMe)=CHCF_3]^+\bullet$. In addition there are several fragments that contain OMe groups, in particular at $m/z = 125.1$ ($[C(OMe)=CHCF_3]^+$), $m/z = 175.1$ ($[CF_2C(OMe)=CHCF_3]^+$) and $m/z = 225.0$ ($[CF_2CF_2C(OMe)=CHCF_3]^+$). The mechanism for the incorporation of methoxide into $C_7F_{15}CF=CHCF_3$ can be postulated as a nucleophilic addition elimination reaction (Fig. 112).

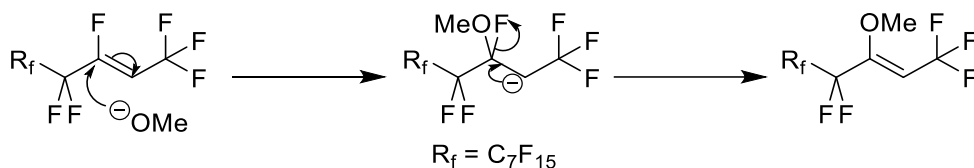


Figure 112: Mechanism for the attack of methoxide on $C_7F_{15}CF=CHCF_3$

The results from this reaction indicate that any additive present in petroleum that is sufficiently nucleophilic may react with the poly VDF segments of Viton® polymer chains that have been dehydrofluorinated by exposure to basic compounds. This could cause degradation of seals by crosslinking of the polymer chains, leading to swelling and brittleness.

3.3.3. Reactions of Dehydrofluorinated Telomer Fluorides with Sulfur Nucleophiles

In order to investigate the potential crosslinking reactions of dehydrofluorinated Viton® polymers with nucleophiles, the mixture of dehydrofluorinated telomer fluorides ($C_7F_{15}CF=CHCF_2(CH_2CF_2)_{0-3}F$ (**50**), $C_7F_{15}CF=CHCF=CHCF_3$ (**52**)) was reacted with a variety of sulfur nucleophiles (**57** – **59**), which act as models of extreme pressure agents that are part of petroleum additive mixtures (Fig. 114). The mixture of **49**, **50** and **52** was added to the reaction solvent and stirred at a given temperature for 2 days. The solvent was removed *in vacuo* and the products analysed by ^{19}F NMR spectroscopy (Fig. 113).

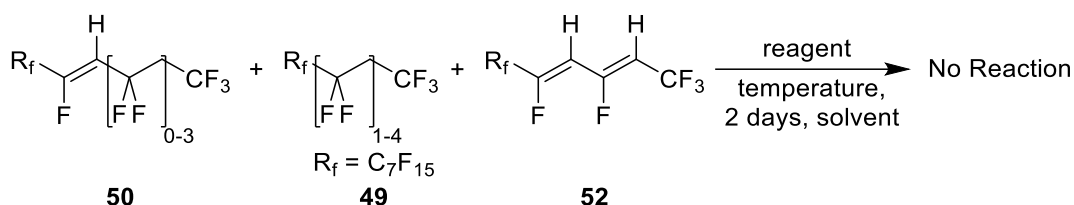


Figure 113: Reactions of $C_7F_{15}CF=CHCF_2(CH_2CF_2)_{0-3}F$ with sulfur nucleophiles

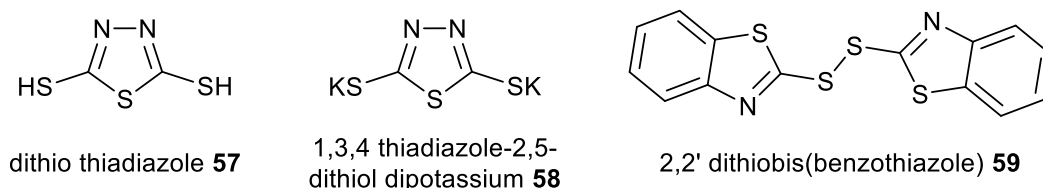


Figure 114: Reagents for the reactions of $C_7F_{15}CF=CHCF_2(CH_2CF_2)_{0-3}F$ with sulfur nucleophiles

However, reactions at room temperature and 80 °C for 2 days showed no reaction by ^{19}F NMR spectroscopy, indicating that these sulfur centred nucleophiles did not react with the deprotonated VDF telomer fluorides under these relatively mild reactions conditions in the laboratory.

3.4. Conclusion

Viton[®] model compounds, containing the poly VDF (CF_2CF_2)_n and poly TFE (CH_2CF_2)_n structural units from models (a), (b) and (c), were synthesised by a two-step strategy. Perfluorooctyl iodide (**45**) was reacted with VDF at high temperature and pressure to produce mixtures of VDF telomer iodides ($\text{C}_8\text{F}_{17}(\text{CH}_2\text{CF}_2)_{1-4}\text{I}$ (**47**)), which were subsequently reacted with SbF_5 to give the intended model telomer fluorides ($\text{C}_8\text{F}_{17}(\text{CH}_2\text{CF}_2)_{1-4}\text{F}$ (**49**)) in excellent yields (Fig. 115).

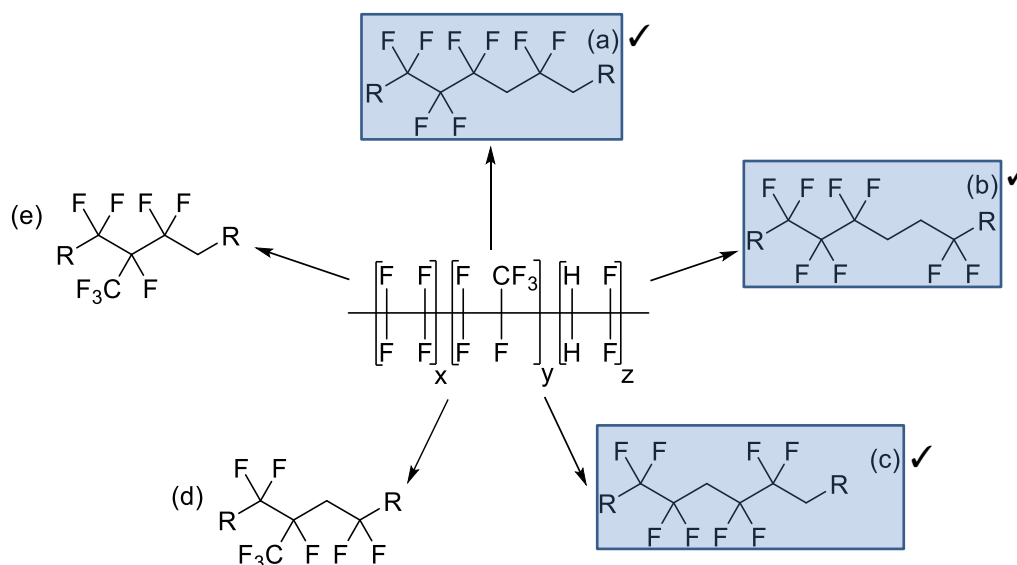


Figure 115: Structures found within Viton[®]

VDF telomer fluorides were reacted with a range of organic and ionic bases and the products of these reactions were analysed by ^1H and ^{19}F NMR spectroscopy and GC-MS. DBU, KOMe, KO^tBu , NaO^tBu , LDA and *n*-BuLi react with **49**, producing a mixture of dehydrofluorinated products. By comparing the ^1H NMR spectra from several of these reactions, an interesting trend in the composition of the products is observed (Fig. 116).

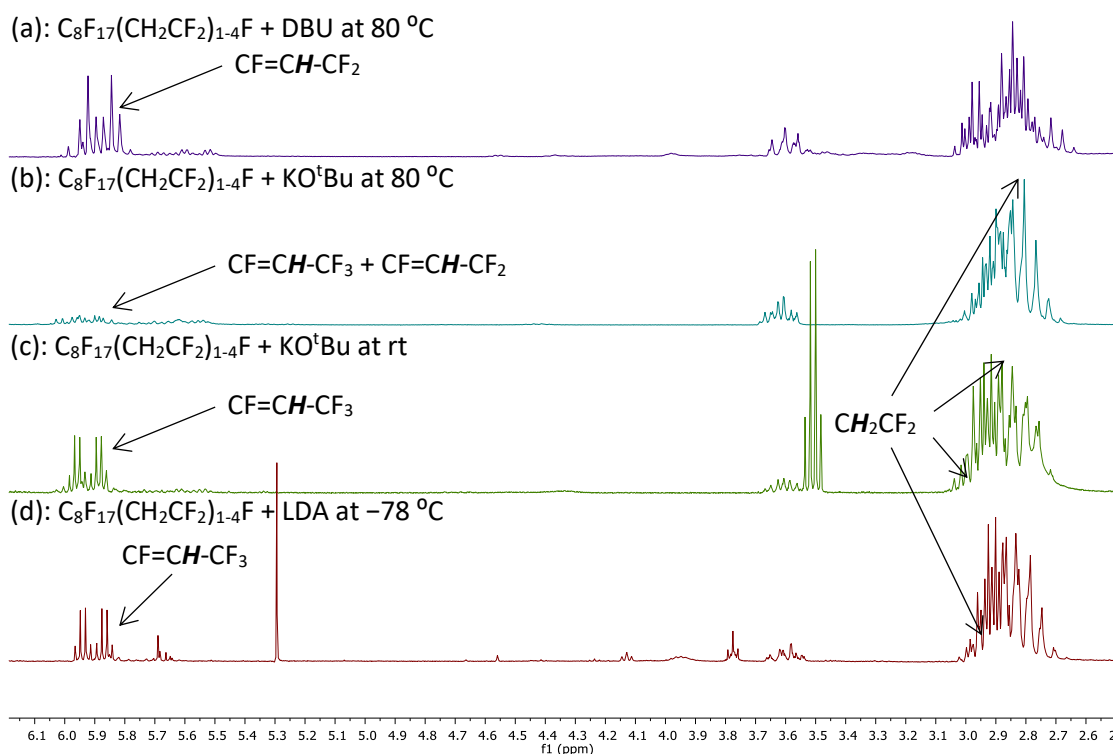


Figure 116: Comparison of ^1H NMR from the reactions of $\text{C}_8\text{F}_{17}(\text{CH}_2\text{CF}_2)_{1-4}\text{F}$ with DBU at $80\text{ }^\circ\text{C}$ (a), KO^tBu at $80\text{ }^\circ\text{C}$ (b), KO^tBu at rt (c) and LDA at $-78\text{ }^\circ\text{C}$ (d)

The reaction of **49** with LDA at $-78\text{ }^\circ\text{C}$, produced $\text{C}_7\text{F}_{15}(\text{CF}_2\text{CH}_2)_{0-3}\text{CF}=\text{CHCF}_3$ (**51**) as the only major product, synthesised by dehydrofluorination adjacent to the CF_3 group, as indicated by the resonance at 5.90 ppm (dq). By comparison, the reaction with DBU at $80\text{ }^\circ\text{C}$, produced $\text{C}_7\text{F}_{15}\text{CF}=\text{CH}(\text{CF}_2\text{CH}_2)_{0-3}\text{CF}_3$ (**50**) as the principal product, synthesised by dehydrofluorination adjacent to the C_7F_{15} group, as indicated by the resonance at 5.88 ppm (dt). However, the reactions with KO^tBu produced different product mixtures depending on the reaction temperature. At room temperature, the major product was $\text{C}_7\text{F}_{15}(\text{CF}_2\text{CH}_2)_{0-3}\text{CF}=\text{CHCF}_3$, as indicated by the resonance at 5.98 ppm (dq). However, the reaction at $80\text{ }^\circ\text{C}$ produced a mixture of $\text{C}_7\text{F}_{15}(\text{CF}_2\text{CH}_2)_{0-3}\text{CF}=\text{CHCF}_3$ and $\text{C}_7\text{F}_{15}\text{CF}=\text{CHCF}_2(\text{CH}_2\text{CF}_2)_{0-3}\text{F}$, as indicated by the overlapping resonances between 6.1 and 5.5 ppm.

These results suggest that the structures of the product(s) synthesised by base induced dehydrofluorination reactions are dependent on competing kinetic or thermodynamic control (Fig. 117). The reactions with anionic bases at low temperature gave principally the kinetic product ($\text{C}_7\text{F}_{15}(\text{CF}_2\text{CH}_2)_{0-3}\text{CF}=\text{CHCF}_3$, **51**) by attack of the base on the most sterically available proton adjacent to the terminal CF_3 group. By contrast, the reactions with organic bases (DBU) at high temperature gave principally the thermodynamic product ($\text{C}_7\text{F}_{15}\text{CF}=\text{CHCF}_2(\text{CH}_2\text{CF}_2)_{0-3}\text{F}$, **50**) by attack of the base on the most acidic proton adjacent to the C_7F_{15} and CF_2 groups.

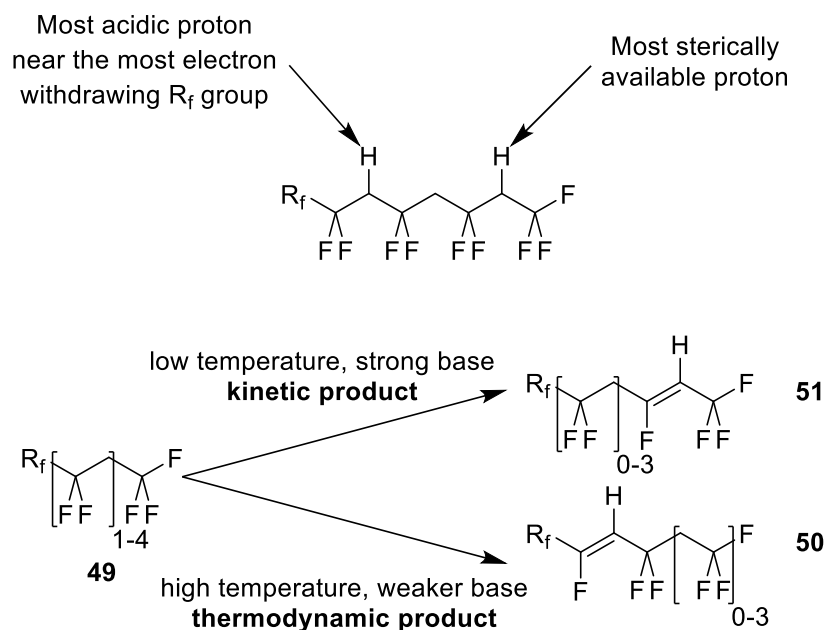


Figure 117: Origin of the different products from the reactions of C₈F₁₇(CH₂CF₂)₁₋₄F with a range of bases

Whatever the mechanism of dehydrofluorination, the reactions of Viton® model compounds with bases indicate that exposure to petroleum additives containing basic groups can cause dehydrofluorination of Viton® seals within engines and other mechanical components at the poly VDF ((CH₂CF₂)_n) segments of the elastomers. Dehydrofluorinated polymers could subsequently react with nucleophilic compounds, as shown by the reactions of **49** with KOMe that produced R_fC(OMe)=CH(CF₂CH₂)₀₋₃CF₃ (**56**) by nucleophilic attack of the methoxide ion. This could lead to further degradation of seals by the nucleophilic crosslinking of dehydrofluorinated polymer chains. The results of these reactions indicate that contact between Viton® seals and basic or nucleophilic petroleum additives should be minimised where possible, in order to prevent degradation and eventual failure of seals.

4. Synthesis and Degradation of Branched VDF Telomer Fluorides

Having previously synthesised representative models of structures (a) – (c), routes to structures (d) and (e) were investigated, since these are models of the HFP-VDF structural units found in Viton® A, B, F, GAL-S, GBL-S and GF-S (Fig. 118).

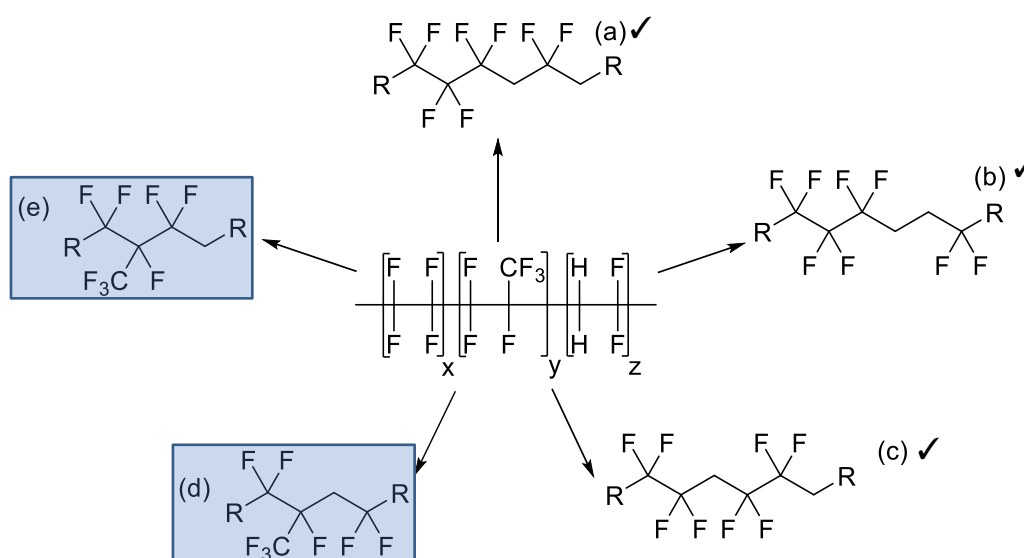


Figure 118: Structures found within Viton®

In particular, it might be expected that structure (d) is vulnerable to attack by bases due to the presence of the CF_3 group adjacent to the CH_2 ⁷⁰, and this decomposition may occur via two possible routes (Fig. 119).

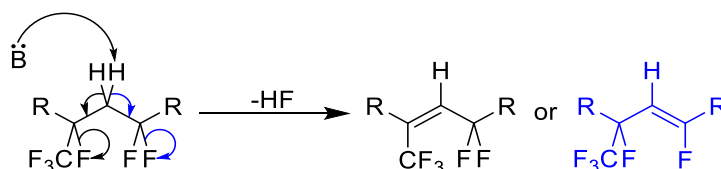


Figure 119: Degradation of structure (d) within Viton® under basic conditions

4.1. Synthesis of HFP/VDF Telomer Iodides – Reactions of Perfluorooctyl Iodide with HFP

The first method investigated for the synthesis of branched Viton® model compounds began with autoclave reactions of perfluorooctyl iodide (**45**) with HFP, based on a literature procedure⁴⁵. The autoclave was charged with the degassed **45**, followed by the addition of five equivalents of HFP by vacuum transfer. The autoclave was secured in a rocking furnace and heated to 200 °C for 100 hours. After cooling, the autoclave was opened, releasing any unreacted HFP, and a black liquid was collected (Fig. 120).

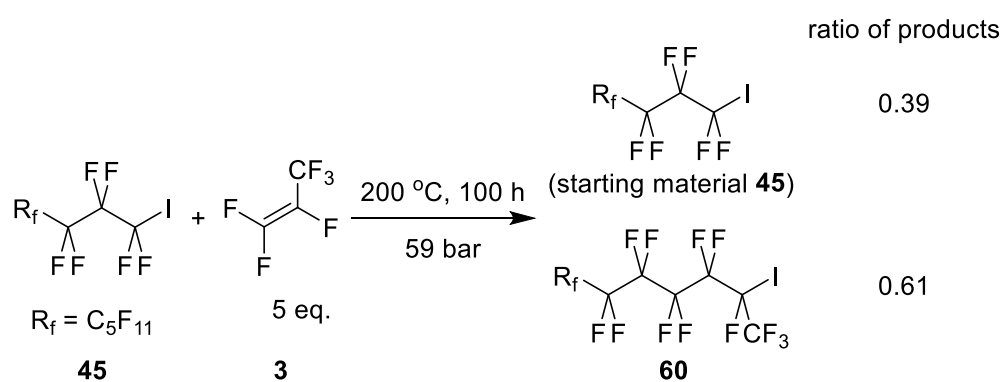


Figure 120: Reaction of perfluorooctyl iodide with HFP (5 eq.) to synthesise $\text{C}_8\text{F}_{17}(\text{CF}_2\text{CF}(\text{CF}_3))_{0-1}\text{I}$

The dark liquid product mixture was examined by ^{19}F and ^{13}C NMR spectroscopy, using perfluoro-2-iodobutane ($\text{CF}_3\text{CF}_2\text{CF}(\text{CF}_3)\text{I}$ (**61**)) as a reference (Fig. 121 and 122).

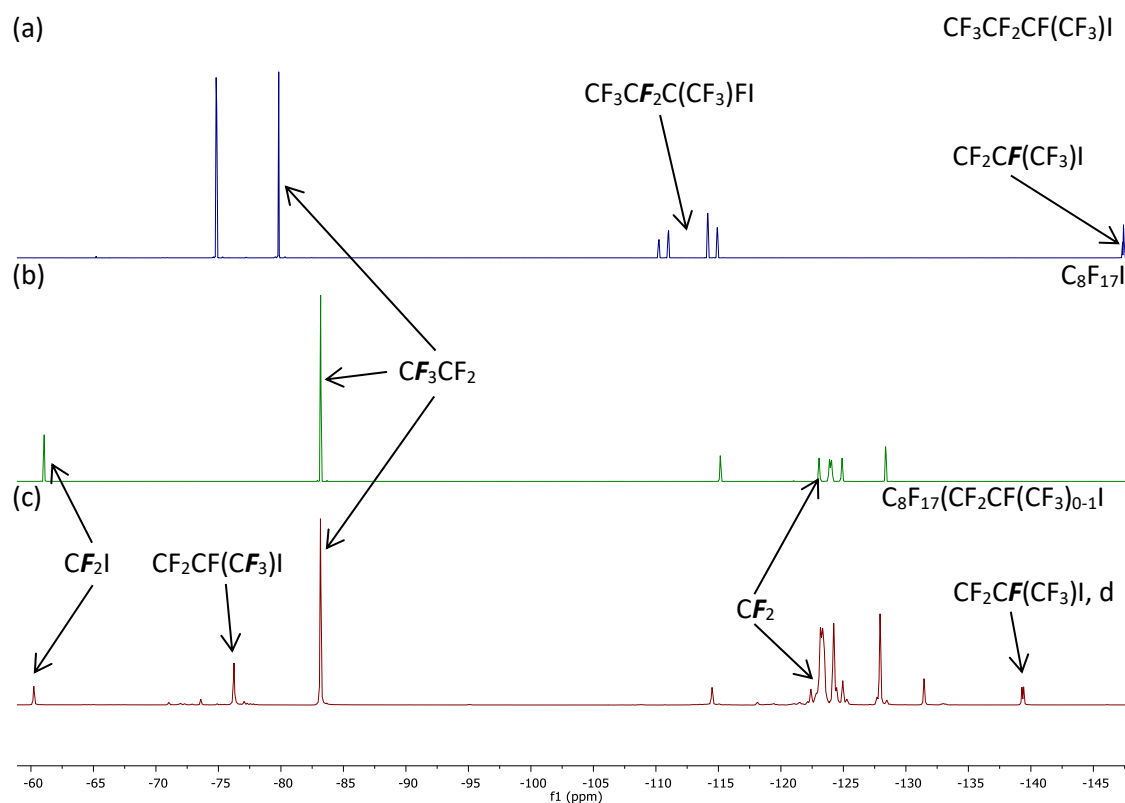


Figure 121: ^{19}F NMR spectra of $\text{CF}_3\text{CF}_2\text{CF}(\text{CF}_3)\text{I}$ (a), $\text{C}_8\text{F}_{17}\text{I}$ (b) and $\text{C}_8\text{F}_{17}(\text{CF}_2\text{CF}(\text{CF}_3))_{0-1}\text{I}$ (c)

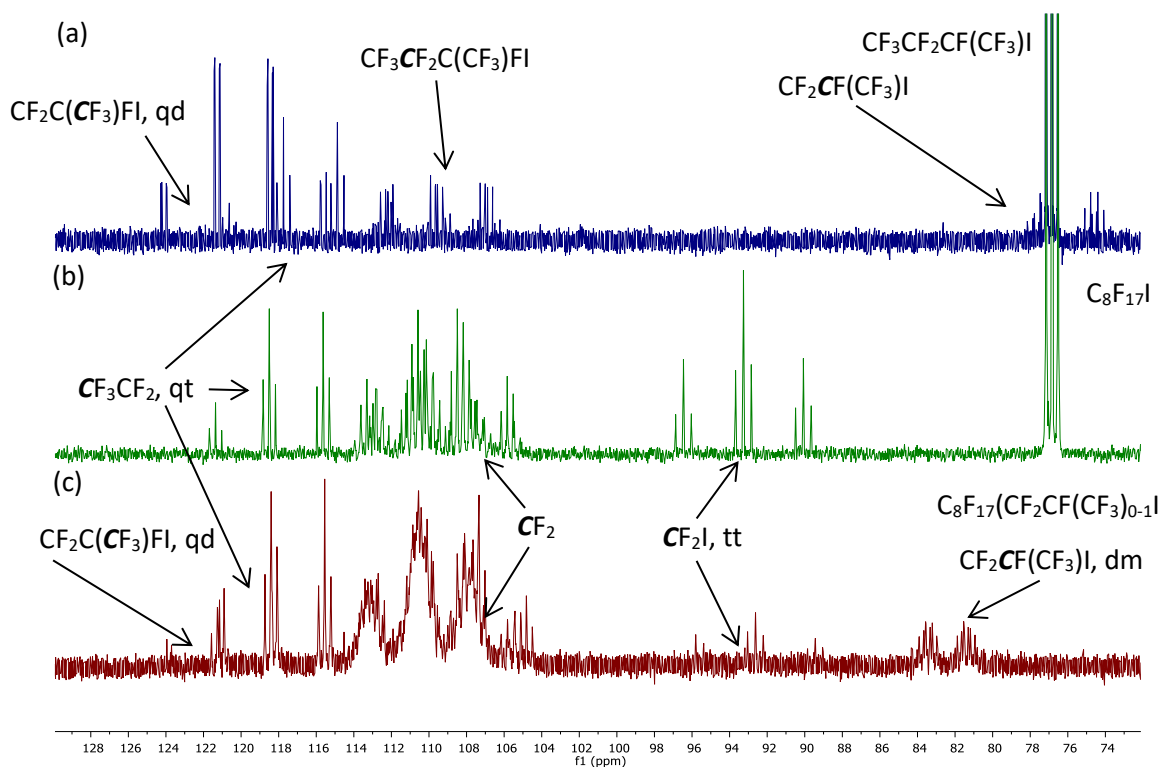


Figure 122: ^{13}C NMR spectra of $\text{CF}_3\text{CF}_2\text{CF}(\text{CF}_3)\text{I}$ (a), $\text{C}_8\text{F}_{17}\text{I}$ (b) and $\text{C}_8\text{F}_{17}(\text{CF}_2\text{CF}(\text{CF}_3))_{0-1}\text{I}$ (c)

By comparing the NMR spectra, we observe that partial conversion to the intended product ($C_8F_{17}CF_2CF(CF_3)I$ (**60**)) has occurred. For example, the peaks for the CF_2I groups in both the ^{19}F and ^{13}C NMR spectra (at -61.04 and 93.26 ppm respectively) have decreased in intensity. In their place, new peaks for $CF_2CF_2CF(CF_3)I$ groups are observed in both spectra. In particular, there are new signals for the $CF_2CF_2CF(CF_3)I$ group in the ^{19}F (-76.24 ppm) and ^{13}C (119.76 , qd, $^1J_{CF} = 282.1$ Hz, $^2J_{CF} = 25.8$ Hz) NMR spectra, and for the $CF_2CF_2CF(CF_3)I$ group in the ^{19}F (-139.35 ppm, dh, $^3J_{FF} = 28.2$ Hz) and ^{13}C (82.40 , dm, $^1J_{CF} = 205.6$ Hz) NMR spectra. There is no evidence in the NMR spectra for compounds containing $CF_2CF(CF_3)CF_2I$ groups, suggesting that head-to-tail addition of HFP to give $C_8F_{17}CF_2CF(CF_3)I$ was the only reaction. This is consistent with the conditions used, as the reaction was run at high temperature, favouring the less sterically hindered thermodynamic product over the kinetic product (Fig. 123).

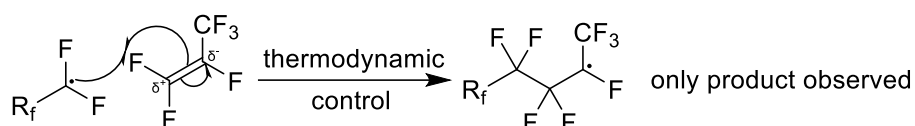


Figure 123: Product from the reaction of R_fCF_2I with HFP under thermodynamic conditions

There is also no evidence of $C_8F_{17}(CF_2CF(CF_3))_2I$ in either of the NMR spectra, suggesting that di-addition of HFP had not occurred in this reaction as expected. HFP is more electron deficient and more sterically demanding than VDF and, therefore, does not naturally homopolymerise except under very forcing conditions (730 °C).

The product mixture was filtered through celite in an attempt to extract the liquid products from the solid residue. However, the majority of the product was trapped on the celite and could not be extracted. Therefore, due to the challenges encountered when carrying out reactions using HFP, different routes to branched Viton[®] model compounds were investigated.

4.2. Synthesis of Branched VDF Telomer Iodides

As an alternative route to branched VDF telomer iodides, perfluoro-2-iodobutane ($\text{CF}_3\text{CF}_2\text{CF}(\text{CF}_3)\text{I}$ (**61**)) was reacted with VDF to synthesise $\text{CF}_3\text{CF}_2\text{CF}(\text{CF}_3)(\text{CH}_2\text{CF}_2)_n\text{I}$, and several different reaction conditions for this transformation were investigated.

4.2.1. Reaction of Perfluoro-2-iodobutane with 5 eq. of VDF

The reaction between **61** and VDF was first carried out with 5 equivalents of VDF at 190 °C for 20 hours. After cooling, the autoclave was opened, releasing any unreacted VDF, and a brown solid was extracted. The reaction was washed with $\text{Na}_2\text{S}_2\text{O}_3$ solution, yielding 6.2 g (23% mass recovery) of the product mixture ($\text{CF}_3\text{CF}_2\text{CF}(\text{CF}_3)(\text{CH}_2\text{CF}_2)_{1-4}\text{I}$ (**62**)) as a yellow oil (Fig. 124).

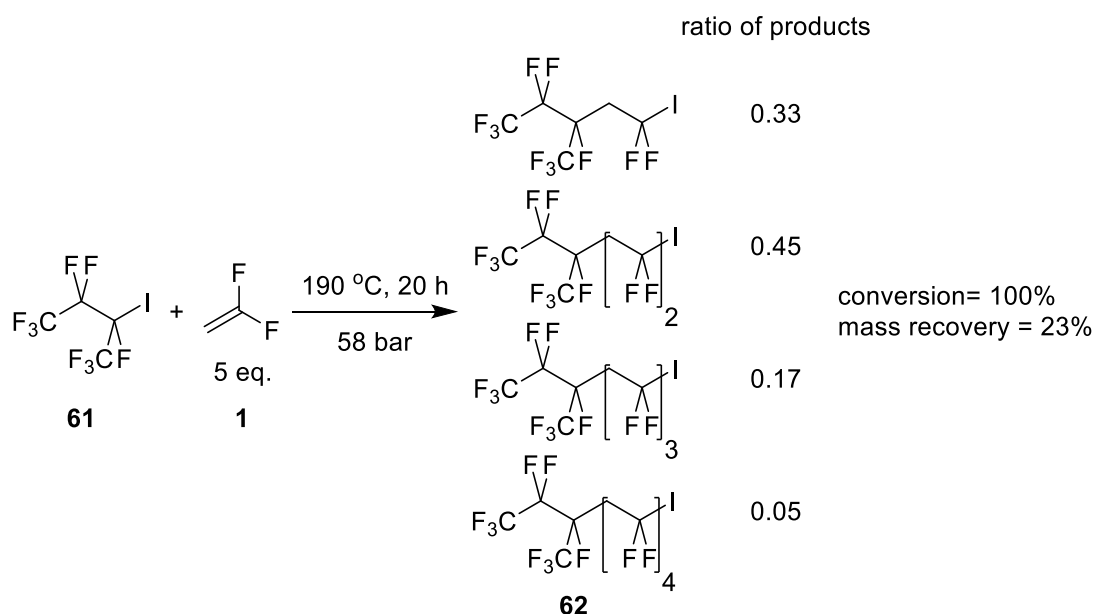


Figure 124: Reaction of perfluoro-2-iodobutane with VDF (5 eq.) to synthesise $\text{CF}_3\text{CF}_2\text{CF}(\text{CF}_3)(\text{CH}_2\text{CF}_2)_{1-4}\text{I}$

The ^{19}F NMR spectra of $\text{CF}_3\text{CF}_2\text{CF}(\text{CF}_3)(\text{CH}_2\text{CF}_2)_{1-4}\text{I}$ (**62**, (b)), compared to the starting material (**61**, (a)), are detailed in Fig. 125 and 126.

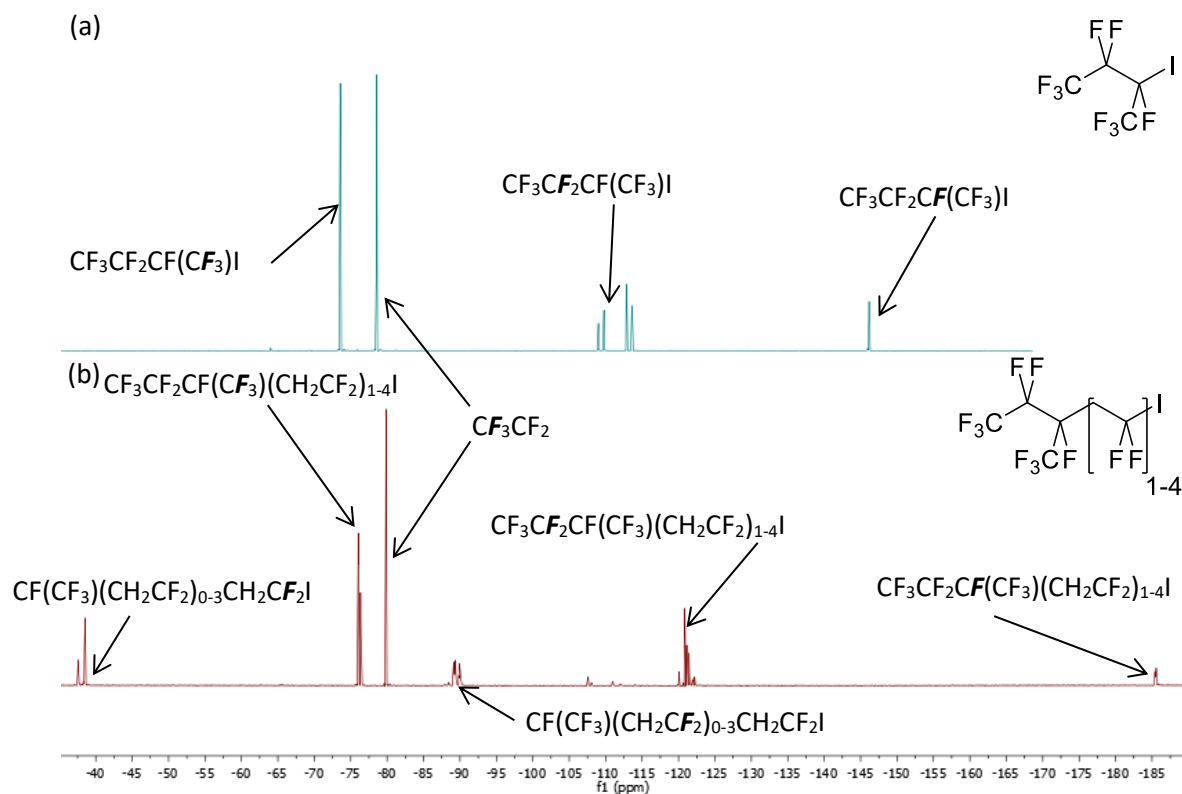


Figure 125: ^{19}F NMR spectra of $\text{CF}_3\text{CF}_2\text{CF}(\text{CF}_3)\text{I}$ (a) and $\text{CF}_3\text{CF}_2\text{CF}(\text{CF}_3)(\text{CH}_2\text{CF}_2)_{1-4}\text{I}$ (b)

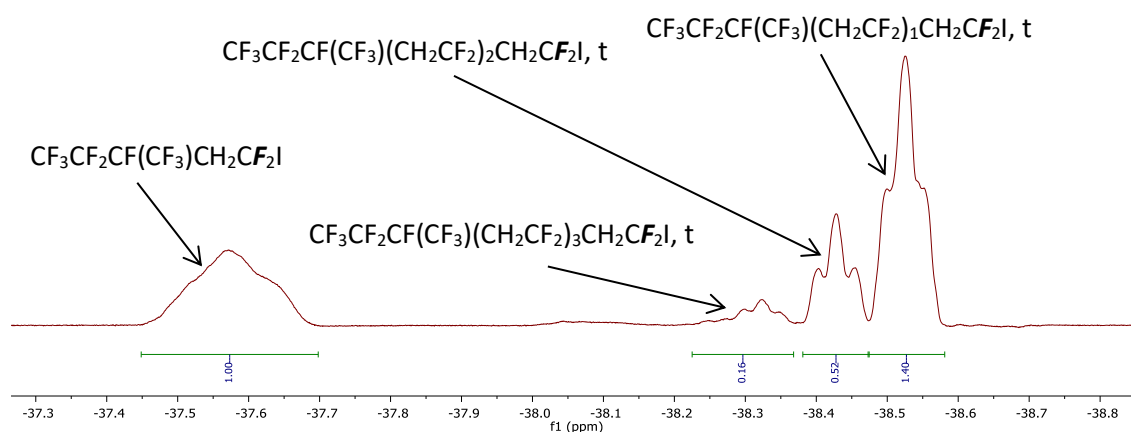


Figure 126: $\{^1\text{H}\}$ ^{19}F NMR spectrum of the CF_2I region (between -37 and -39 ppm) of $\text{CF}_3\text{CF}_2\text{CF}(\text{CF}_3)(\text{CH}_2\text{CF}_2)_{1-4}\text{I}$

The ^{19}F NMR spectrum of $\text{CF}_3\text{CF}_2\text{CF}(\text{CF}_3)(\text{CH}_2\text{CF}_2)_{1-4}\text{I}$ indicates a series of new signals between -37.4 and -38.6 ppm, which are the resonances for the $\text{CF}_3\text{CF}_2\text{CF}(\text{CF}_3)(\text{CH}_2\text{CF}_2)_{0-3}\text{CH}_2\text{CF}_2\text{I}$ fluorines of the product mixture. The individual peaks were not resolved in the standard ^{19}F NMR spectrum, but could be distinguished in the decoupled $\{^1\text{H}\}$ ^{19}F NMR spectrum, specifically a multiplet at -37.45 – -37.69 ppm ($\text{CF}_3\text{CF}_2\text{CF}(\text{CF}_3)\text{CH}_2\text{CF}_2\text{I}$), and three triplets at

-38.53 (CF₃CF₂CF(CF₃))(CH₂CF₂)₁CH₂CF₂I, ⁴J_{FF} = 10.5 Hz), -38.43 (CF₃CF₂CF(CF₃))(CH₂CF₂)₂CH₂CF₂I, ⁴J_{FF} = 9.4 Hz) and -38.32 ppm (CF₃CF₂CF(CF₃))(CH₂CF₂)₃CH₂CF₂I, ⁴J_{FF} = 9.7 Hz). There are additional new signals between -88 and -91 ppm for the CF₃CF₂CF(CF₃)(CH₂CF₂)₀₋₃CH₂CF₂I fluorines, and the CF₃CF₂CF(CF₃) signal in the starting material at -146.16 ppm has shifted to -185.48 ppm in the product mixture.

Conversion to the intended product is confirmed by comparison of the ¹³C NMR spectra of the starting material (**61**, (a)) and CF₃CF₂CF(CF₃)(CH₂CF₂)₁₋₄I, (**62**, (b)) (Fig. 127 and 128).

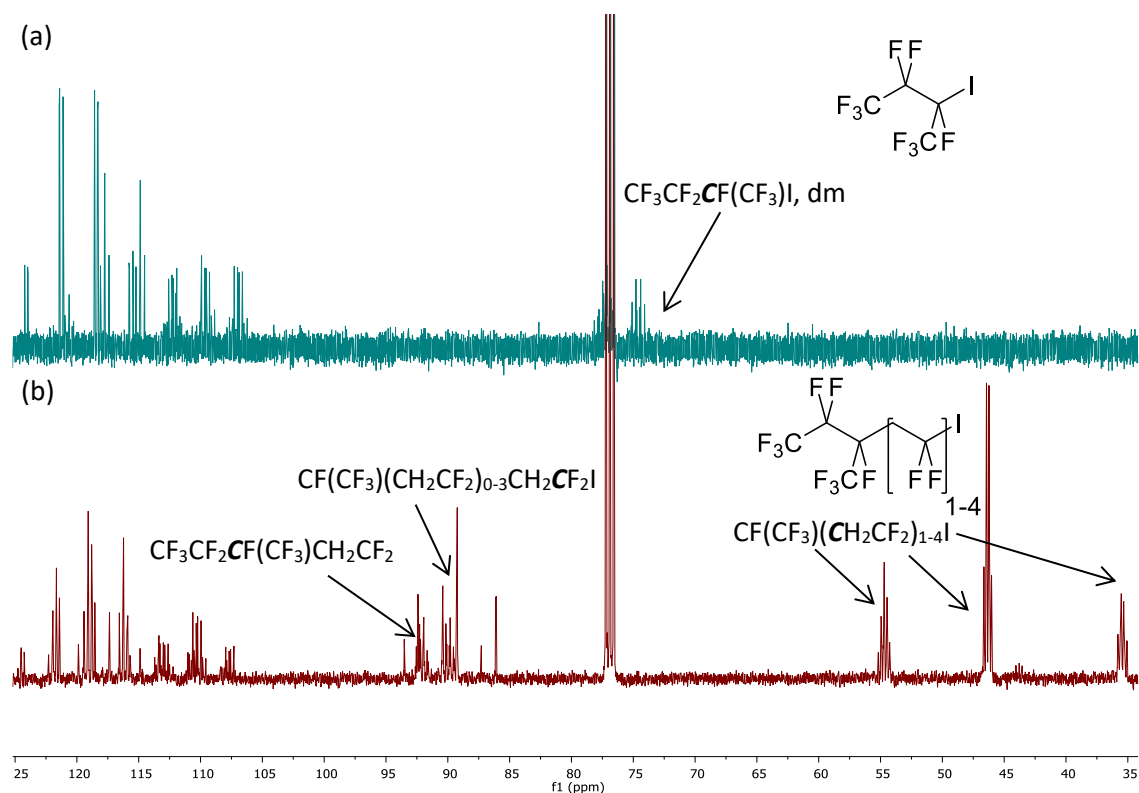


Figure 127: ¹³C NMR spectra of CF₃CF₂CF(CF₃)I (a) and CF₃CF₂CF(CF₃)(CH₂CF₂)₁₋₄I (b)

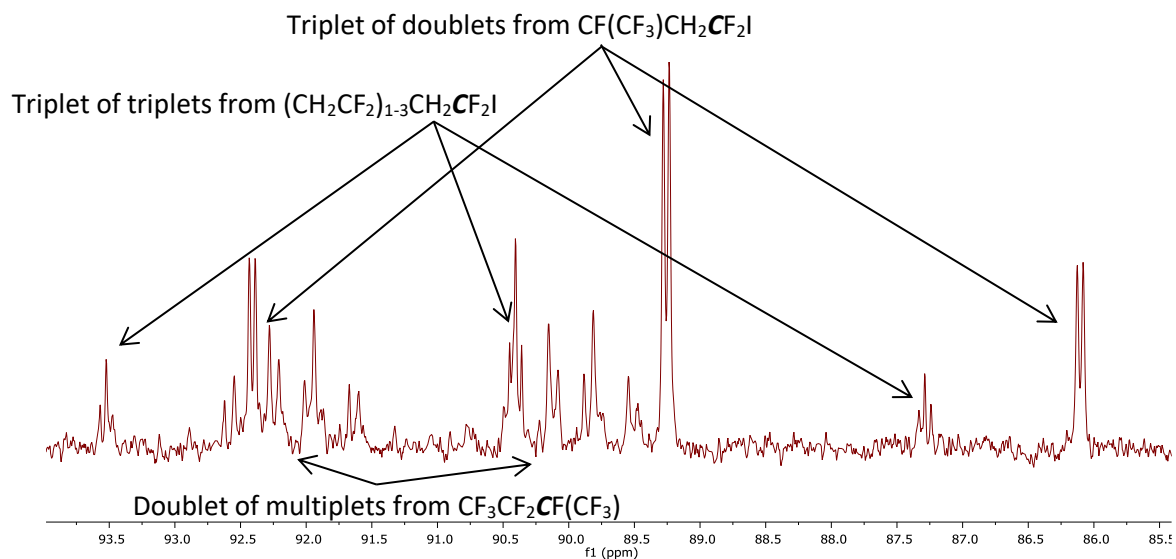


Figure 128: ^{13}C NMR spectrum of the CF_2I and $\text{CF}(\text{CF}_3)$ region (between 94 and 85 ppm) of $\text{CF}_3\text{CF}_2\text{CF}(\text{CF}_3)(\text{CH}_2\text{CF}_2)_{1-4}\text{I}$

There are new peaks in the ^{13}C NMR spectrum of $\text{CF}_3\text{CF}_2\text{CF}(\text{CF}_3)(\text{CH}_2\text{CF}_2)_{1-4}\text{I}$ between 55 and 35 ppm, which are the resonances for the $\text{CF}(\text{CF}_3)(\text{CH}_2\text{CF}_2)_{1-4}\text{I}$ carbon. There are also two new peaks for the $(\text{CF}_3\text{CF}_2\text{CF}(\text{CF}_3)(\text{CH}_2\text{CF}_2)_{0-3}\text{CH}_2\text{CF}_2\text{I})$ carbons, a triplet of doublets at 89.26 ppm, ($^1J_{\text{CF}} = 317.2$ Hz, $^3J_{\text{CF}} = 4.6$ Hz) for the mono addition product ($\text{CF}_3\text{CF}_2\text{CF}(\text{CF}_3)\text{CH}_2\text{CF}_2\text{I}$) and a triplet of triplets at 90.40 ppm ($^1J_{\text{CF}} = 313.7$ Hz, $^3J_{\text{CF}} = 4.7$ Hz) for the other $\text{CF}_3\text{CF}_2\text{CF}(\text{CF}_3)(\text{CH}_2\text{CF}_2)_{1-3}\text{CH}_2\text{CF}_2\text{I}$ products. The doublet of multiplets for the $\text{CF}_3\text{CF}_2\text{CF}(\text{CF}_3)$ carbon is also at a different shift in the product mixture (92.66 – 89.35 ppm instead of 76.80 – 74.05 ppm).

The product mixture (**62**) was further examined by GC-MS (Fig. 129).

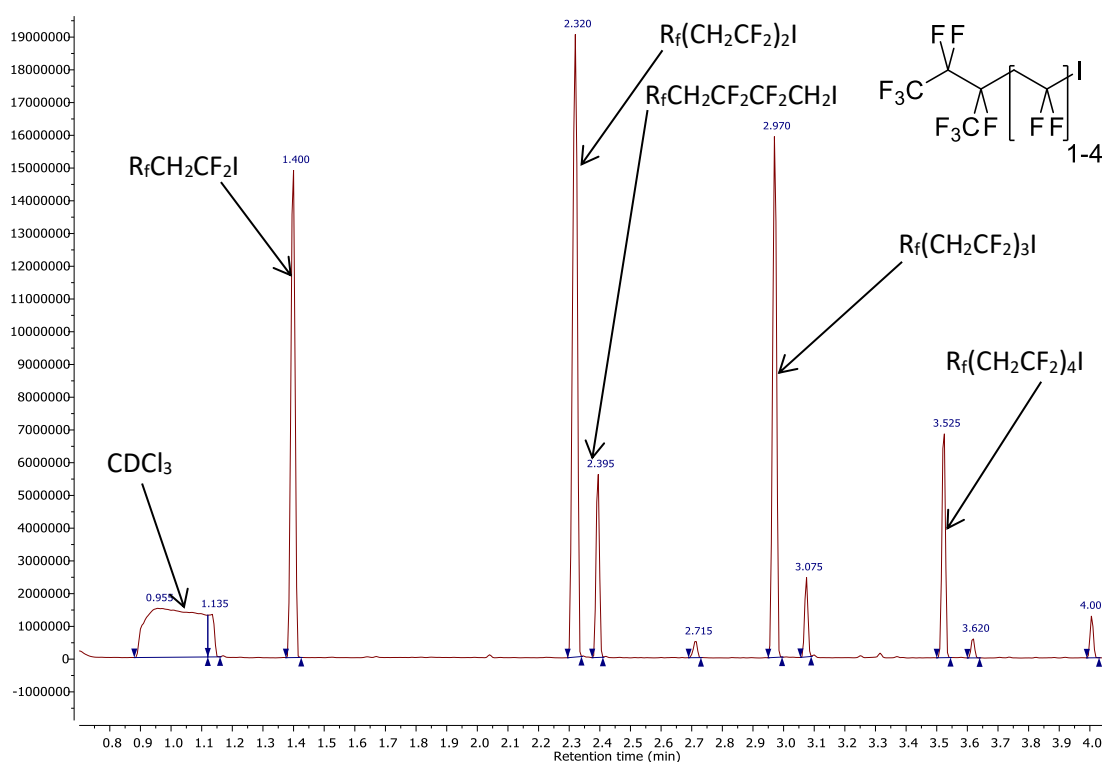


Figure 129: Gas chromatogram of the product mixture, $CF_3CF_2CF(CF_3)(CH_2CF_2)_{1-4}I$ ($R_f = CF_3CF_2CF(CF_3)$)

The gas chromatogram confirms the product composition and indicates the high volatility of these compounds, as all $CF_3CF_2CF(CF_3)(CH_2CF_2)_{1-4}I$ species have retention times of approximately half a minute less than the corresponding $C_8F_{17}(CH_2CF_2)_{1-4}I$ (**47**) species. It also shows that the mixture of $CF_3CF_2CF(CF_3)(CH_2CF_2)_{1-4}I$ contains a small amount of $CF_3CF_2CF(CF_3)(CH_2CF_2)_{0-3}CF_2CH_2I$ from head-to-head addition of VDF as expected.

The key resonances from the ^1H , ^{19}F and ^{13}C NMR spectra of $\text{CF}_3\text{CF}_2\text{CF}(\text{CF}_3)(\text{CH}_2\text{CF}_2)_{1-4}\text{I}$ (**62**) are detailed in Table 17.

Table 17: List of key shifts for the major components of the product mixture from the reaction of perfluoro-2-iodobutane with 5 eq. of VDF, $\text{CF}_3\text{CF}_2\text{CF}(\text{CF}_3)(\text{CH}_2\text{CF}_2)_{1-4}\text{I}$ (chemical shifts in ppm, coupling constants in Hz)

Compound	Fragment	^1H	^{19}F	^{13}C
$\text{CF}_3\text{CF}_2\text{CF}(\text{CF}_3)(\text{CH}_2\text{CF}_2)_n\text{I}$	$(\text{CH}_2\text{CF}_2)_{n-1}\text{CH}_2\text{CF}_2\text{I}$	3.69 – 3.43, m	N.A.	55.31 – 54.12, m
	$\text{CF}_2\text{CH}_2\text{CF}_2\text{CH}_2\text{CF}_2\text{I}$	3.12 – 2.53, m	N.A.	35.92 – 34.94, m
	$\text{CF}_2\text{CH}_2\text{CF}_2(\text{CH}_2\text{CF}_2)_{n-1}\text{I}$	3.06 – 2.66, m	N.A.	46.33, q, $^2J_{\text{CF}} = 20.8$
	$\text{CF}_3\text{CF}_2\text{CF}(\text{CF}_3)$	N.A.	-76.13 – -76.38, m; -76.47 – -76.68, m	120.11, qdd, $^1J_{\text{CF}} = 286.6$, $^2J_{\text{CF}} = 27.4$, $^3J_{\text{CF}} = 3.5$
	$\text{CF}_3\text{CF}_2\text{CF}(\text{CF}_3)$	N.A.	-185.39 – -185.89, m	92.66 – 89.35, dm, $^1J_{\text{CF}} = 213.9$
	$\text{CF}_3\text{CF}_2\text{CF}(\text{CF}_3)$	N.A.	-120.18 – -122.50, m	113.83 – 107.21, m
	CF_3CF_2	N.A.	-79.99 – -80.24, m	117.65, qt, $^1J_{\text{CF}} = 287.7$, $^2J_{\text{CF}} = 34.3$
$\text{CF}_3\text{CF}_2\text{CF}(\text{CF}_3)\text{CH}_2\text{CF}_2\text{I}$	$\text{CF}(\text{CF}_3)\text{CH}_2\text{CF}_2\text{I}$ $\{^1\text{H}\}$	N.A.	-37.45 – -37.69, m	89.26, td, $^1J_{\text{CF}} = 317.2$, $^3J_{\text{CF}} = 4.6$
$\text{CF}_3\text{CF}_2\text{CF}(\text{CF}_3)(\text{CH}_2\text{CF}_2)_2\text{I}$	$\text{CH}_2\text{CF}_2\text{CH}_2\text{CF}_2\text{I}$ $\{^1\text{H}\}$	N.A.	-38.53, t, $^4J_{\text{FF}} = 10.5$	90.40, tt, $^1J_{\text{CF}} = 313.7$, $^3J_{\text{CF}} = 4.7$
$\text{CF}_3\text{CF}_2\text{CF}(\text{CF}_3)(\text{CH}_2\text{CF}_2)_3\text{I}$	$(\text{CH}_2\text{CF}_2)_2\text{CH}_2\text{CF}_2\text{I}$ $\{^1\text{H}\}$	N.A.	-38.43, t, $^4J_{\text{FF}} = 9.4$	90.40, tt, $^1J_{\text{CF}} = 313.7$, $^3J_{\text{CF}} = 4.7$
$\text{CF}_3\text{CF}_2\text{CF}(\text{CF}_3)(\text{CH}_2\text{CF}_2)_4\text{I}$	$(\text{CH}_2\text{CF}_2)_3\text{CH}_2\text{CF}_2\text{I}$ $\{^1\text{H}\}$	N.A.	-38.32, t, $^4J_{\text{FF}} = 9.7$	90.40, tt, $^1J_{\text{CF}} = 313.7$, $^3J_{\text{CF}} = 4.7$

4.2.2. Reaction of Perfluoro-2-iodobutane with Excess VDF

The reaction of $\text{CF}_3\text{CF}_2\text{CF}(\text{CF}_3)\text{I}$ with VDF was repeated using 9 eq. of VDF in order to synthesise a higher molecular weight, less volatile mixture of $\text{CF}_3\text{CF}_2\text{CF}(\text{CF}_3)(\text{CH}_2\text{CF}_2)_n\text{I}$. These reactions followed the same procedure as used previously, and the most successful yielded 15.24 g (41% mass recovery) of $\text{CF}_3\text{CF}_2\text{CF}(\text{CF}_3)(\text{CH}_2\text{CF}_2)_{2-7}\text{I}$ (**63**) as a yellow oil, (Fig. 130).

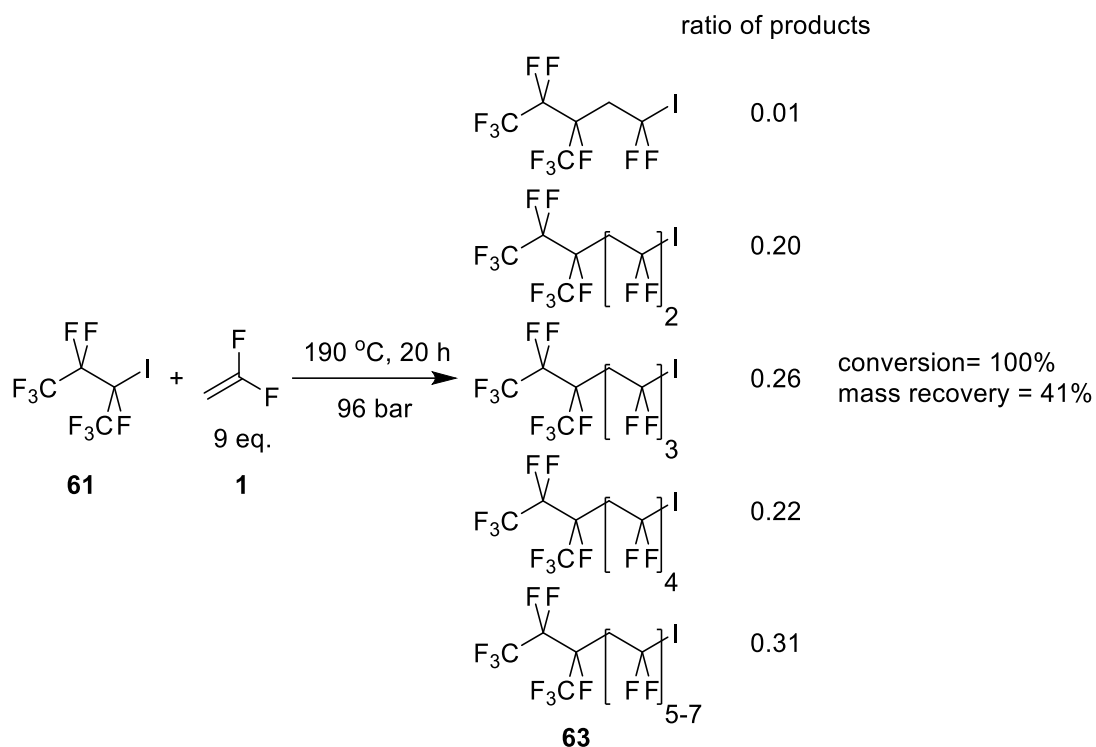


Figure 130: Reaction of perfluoro-2-iodobutane with VDF (9 eq.) to synthesise $\text{CF}_3\text{CF}_2\text{CF}(\text{CF}_3)(\text{CH}_2\text{CF}_2)_{2-7}\text{I}$

The product composition was determined by the proton decoupled $\{^1\text{H}\} ^{19}\text{F}$ NMR spectrum (Fig. 131) and confirmed by GC-MS (Fig. 132).

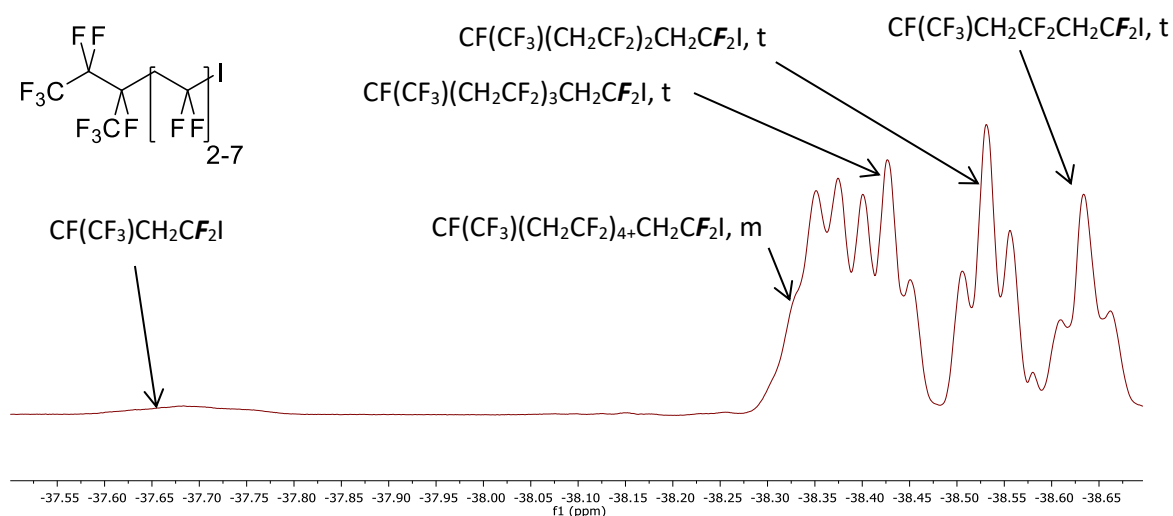


Figure 131: $\{^1\text{H}\} ^{19}\text{F}$ NMR spectrum of the CF_2I region of $\text{CF}_3\text{CF}_2\text{CF}(\text{CF}_3)(\text{CH}_2\text{CF}_2)_{2-7}\text{I}$

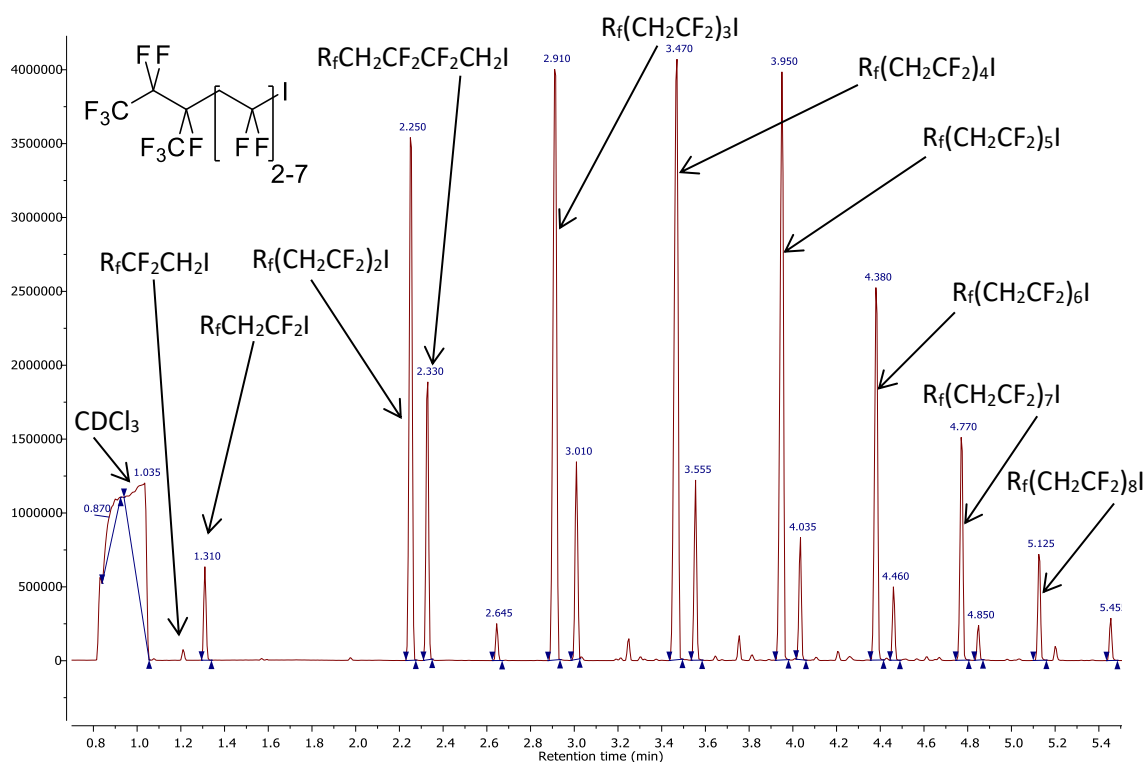


Figure 132: Gas chromatogram of the product mixture, $\text{CF}_3\text{CF}_2\text{CF}(\text{CF}_3)(\text{CH}_2\text{CF}_2)_{2-7}\text{I}$ ($R_f = \text{CF}_3\text{CF}_2\text{CF}(\text{CF}_3)$)

The gas chromatogram proves the composition of the product mixture and identifies the highest molecular weight products as principally $\text{CF}_3\text{CF}_2\text{CF}(\text{CF}_3)(\text{CH}_2\text{CF}_2)_{5-7}\text{I}$. The molecular ion peak is not observed for any of the $\text{CF}_3\text{CF}_2\text{CF}(\text{CF}_3)(\text{CH}_2\text{CF}_2)_{2-7}\text{I}$ (**63**) compounds; instead the highest molecular weight fragments observed are the $[\text{M} - \text{I}]^+$ fragments. The gas chromatogram also indicates an increase in the amount of $\text{CF}_3\text{CF}_2\text{CF}(\text{CF}_3)(\text{CH}_2\text{CF}_2)_{1-6}\text{CF}_2\text{CH}_2\text{I}$ compounds formed in this reaction, including a trace amount of $\text{CF}_3\text{CF}_2\text{CF}(\text{CF}_3)\text{CF}_2\text{CH}_2\text{I}$, a model

of structure (e). This is consistent with the established reaction mechanism⁴³; as the active CF_2^\bullet moves further from the R_f group in the higher molecular weight compounds, the electrophilicity of the radical decreases, reducing the head-to-tail preference of the reaction (Fig. 133).

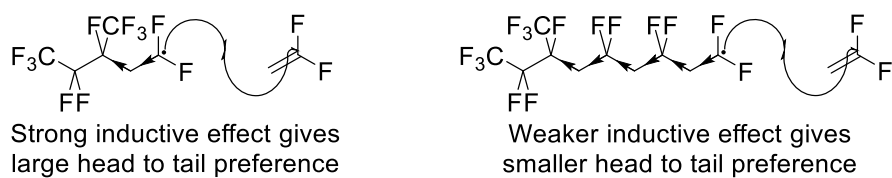


Figure 133: Explanation for the increased $\text{CF}_3\text{CF}_2\text{CF}(\text{CF}_3)(\text{CH}_2\text{CF}_2)_{1-6}\text{CF}_2\text{CH}_2\text{I}$ content of the product mixture

The key resonances from the ^1H , ^{19}F and ^{13}C NMR spectra of $\text{CF}_3\text{CF}_2\text{CF}(\text{CF}_3)(\text{CH}_2\text{CF}_2)_{2-7}\text{I}$ (**63**) are detailed in Table 18.

Table 18: List of key shifts for the major components of the product mixture from the reaction of perfluoro-2-iodobutane with 9 eq. of VDF, $\text{CF}_3\text{CF}_2\text{CF}(\text{CF}_3)(\text{CH}_2\text{CF}_2)_{2-7}\text{I}$ (chemical shifts in ppm, coupling constants in Hz)

Compound	Fragment	^1H	^{19}F	^{13}C
$\text{CF}_3\text{CF}_2\text{CF}(\text{CF}_3)(\text{CH}_2\text{CF}_2)_n\text{I}$	$(\text{CH}_2\text{CF}_2)_{n-1}\text{CH}_2\text{CF}_2\text{I}$	3.44 – 3.26, m	N.A.	53.83 – 53.39, m
	$\text{CF}_2\text{CH}_2\text{CF}_2\text{CH}_2\text{CF}_2\text{I}$	3.12 – 2.53, m	N.A.	36.89 – 38.42, m
	$\text{CF}_2\text{CH}_2\text{CF}_2(\text{CH}_2\text{CF}_2)_{n-1}\text{I}$	3.12 – 2.53, m	N.A.	44.37 – 42.67, m
	$\text{CF}_3\text{CF}_2\text{CF}(\text{CF}_3)$	N.A.	-76.36 – -76.52, m	120.11, qdd, $^1J_{\text{CF}}$ = 287.6, $^2J_{\text{CF}}$ = 27.5, $^3J_{\text{CF}}$ = 3.5
	$\text{CF}_3\text{CF}_2\text{CF}(\text{CF}_3)$	N.A.	-185.70, s	92.64 – 89.41, dm, $^1J_{\text{CF}}$ = 208.6
	$\text{CF}_3\text{CF}_2\text{CF}(\text{CF}_3)$	N.A.	-119.91 – -122.32, m	113.84 – 107.18, m
	CF_3CF_2		-79.88 – -80.05, m	117.74, qt, $^1J_{\text{CF}}$ = 287.7, $^2J_{\text{CF}}$ = 34.3
$\text{CF}_3\text{CF}_2\text{CF}(\text{CF}_3)(\text{CH}_2\text{CF}_2)_2\text{I}$	$\text{CH}_2\text{CF}_2\text{CH}_2\text{CF}_2\text{I}$ { ^1H }	N.A.	-38.63, t, $^4J_{\text{FH}}$ = 10.6	90.42, tt, $^1J_{\text{CF}}$ = 313.7, $^3J_{\text{CF}}$ = 5.1
$\text{CF}_3\text{CF}_2\text{CF}(\text{CF}_3)(\text{CH}_2\text{CF}_2)_3\text{I}$	$(\text{CH}_2\text{CF}_2)_2\text{CH}_2\text{CF}_2\text{I}$ { ^1H }	N.A.	-38.53, t, $^4J_{\text{FH}}$ = 9.6	90.76, tt, $^1J_{\text{CF}}$ = 313.7, $^3J_{\text{CF}}$ = 4.6
$\text{CF}_3\text{CF}_2\text{CF}(\text{CF}_3)(\text{CH}_2\text{CF}_2)_4\text{I}$	$(\text{CH}_2\text{CF}_2)_3\text{CH}_2\text{CF}_2\text{I}$ { ^1H }	N.A.	-38.43, t, $^4J_{\text{FH}}$ = 9.8	90.76, tt, $^1J_{\text{CF}}$ = 313.7, $^3J_{\text{CF}}$ = 4.6
$\text{CF}_3\text{CF}_2\text{CF}(\text{CF}_3)(\text{CH}_2\text{CF}_2)_{5+}\text{I}$	$(\text{CH}_2\text{CF}_2)_4+\text{CH}_2\text{CF}_2\text{I}$ { ^1H }	N.A.	-38.29 – -38.41, m	90.76, tt, $^1J_{\text{CF}}$ = 313.7, $^3J_{\text{CF}}$ = 4.6

The reactions described above were repeated several times to synthesise various mixtures of branched VDF telomer iodides.

4.2.1.1. Reaction of Perfluoro-2-iodobutane with 9 eq. of VDF at 240 °C

The reaction of $\text{CF}_3\text{CF}_2\text{CF}(\text{CF}_3)\text{I}$ with VDF was repeated at 240 °C instead of 190 °C in an attempt to synthesise a higher molecular weight mixture of $\text{CF}_3\text{CF}_2\text{CF}(\text{CF}_3)(\text{CH}_2\text{CF}_2)_n\text{I}$. The reaction yielded 21.65 g (79% mass recovery) of a brown viscous liquid (Fig. 134).

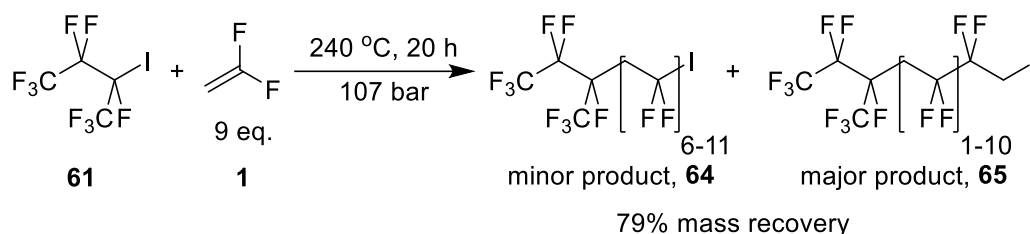


Figure 134: Reaction of perfluoro-2-iodobutane with VDF (9 eq.) at 240 °C to synthesise $\text{CF}_3\text{CF}_2\text{CF}(\text{CF}_3)(\text{CH}_2\text{CF}_2)_{1-10}\text{CF}_2\text{CH}_2\text{I}$

The product mixture had a physical appearance that was very different to those synthesised previously, and differences were also observed in ^{19}F NMR spectrum of the product, compared to previously obtained $\text{CF}_3\text{CF}_2\text{CF}(\text{CF}_3)(\text{CH}_2\text{CF}_2)_{2-5}\text{I}$ products (**66**) (Fig. 135).

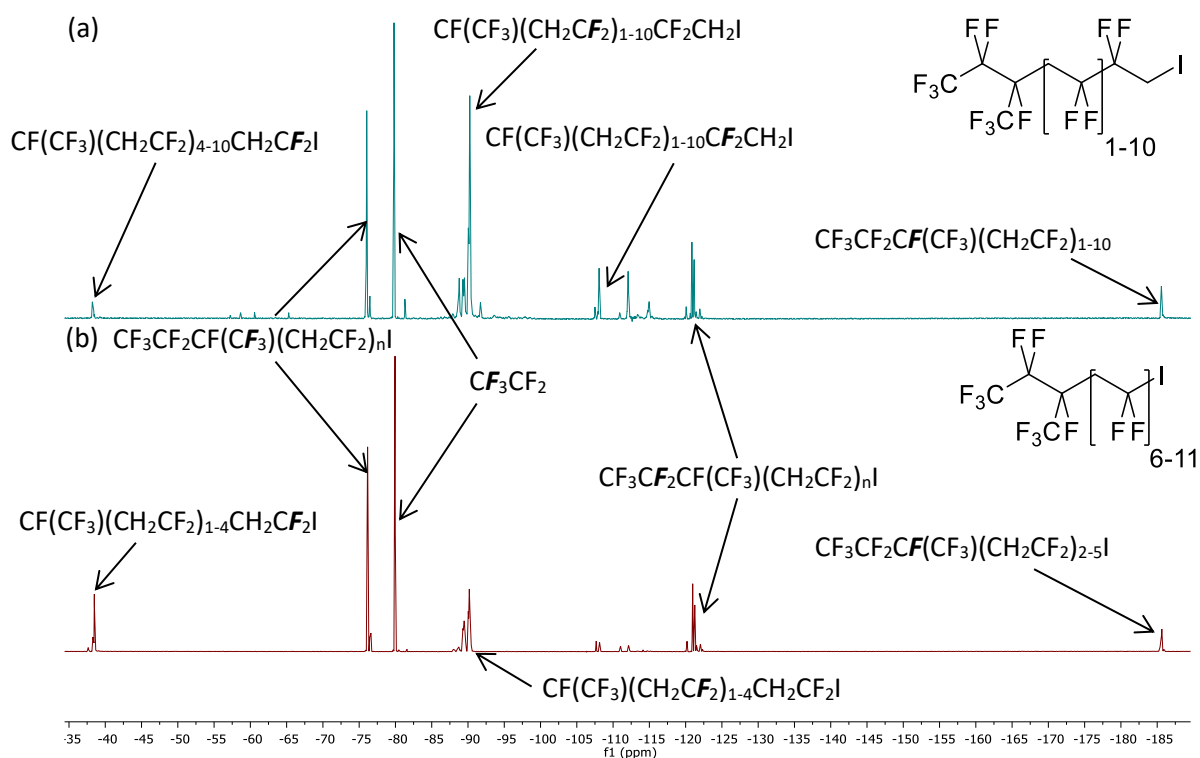


Figure 135: ^{19}F NMR spectra of the product mixture ($\text{CF}_3\text{CF}_2\text{CF}(\text{CF}_3)(\text{CH}_2\text{CF}_2)_{1-10}\text{CF}_2\text{CH}_2\text{I}$, (a)) and the product mixture from a similar reaction carried out at 190 °C ($\text{CF}_3\text{CF}_2\text{CF}(\text{CF}_3)(\text{CH}_2\text{CF}_2)_{2-5}\text{I}$, (b))

The resonances for the $\text{CF}(\text{CF}_3)(\text{CH}_2\text{CF}_2)_{5-10}\text{CH}_2\text{CF}_2\text{I}$ fluorines (between $-38.1 - -38.6$ ppm) in the ^{19}F NMR spectrum of the product mixture synthesised at 240°C are of low intensity compared to those from the spectrum of **66**. The spectrum instead has a series of peaks between -107.2 and -115.5 ppm, resonances for $\text{CF}(\text{CF}_3)(\text{CH}_2\text{CF}_2)_{1-10}\text{CF}_2\text{CH}_2\text{I}$ fluorines synthesised by terminal head-to-head addition of VDF. The composition of the product was confirmed by ^1H NMR spectroscopy (Fig. 136).

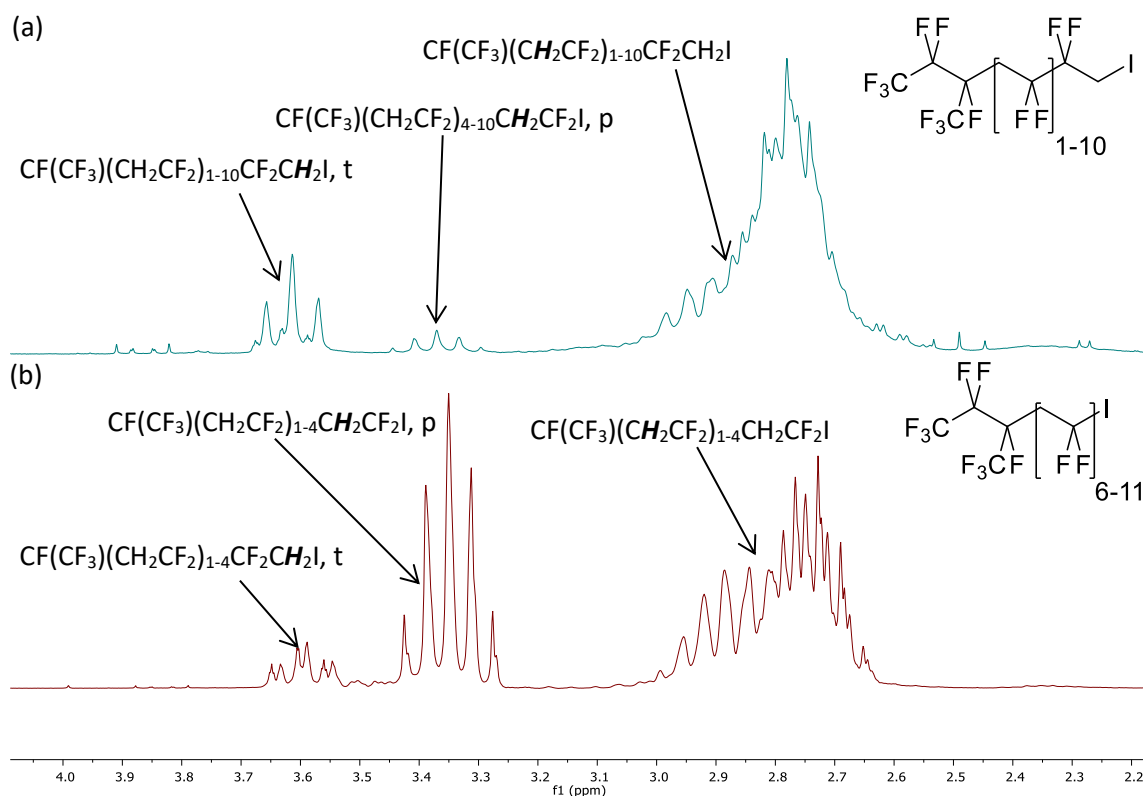


Figure 136: ^1H NMR spectra of the product mixture $\text{CF}_3\text{CF}_2\text{CF}(\text{CF}_3)(\text{CH}_2\text{CF}_2)_{1-10}\text{CF}_2\text{CH}_2\text{I}$, (a) and the product mixture from a similar reaction carried out at 190°C $\text{CF}_3\text{CF}_2\text{CF}(\text{CF}_3)(\text{CH}_2\text{CF}_2)_{2-5}\text{I}$, (b)

The intensity of the pentet at 3.37 ppm ($^3J_{\text{HF}} = 14.8$ Hz), the resonance for the $\text{CF}(\text{CF}_3)(\text{CH}_2\text{CF}_2)_{5-10}\text{CH}_2\text{CF}_2\text{I}$ protons, in the ^1H NMR spectrum of the product mixture synthesised at 240°C is significantly lower than the similar signal at 3.35 ppm in the spectrum of $\text{CF}_3\text{CF}_2\text{CF}(\text{CF}_3)(\text{CH}_2\text{CF}_2)_{1-4}\text{CH}_2\text{CF}_2\text{I}$. However, the two overlapping triplets at 3.63 ($^3J_{\text{HF}} = 17.6$ Hz) and 3.61 ppm ($^3J_{\text{HF}} = 17.5$ Hz), resonances from the $\text{CF}(\text{CF}_3)(\text{CH}_2\text{CF}_2)_{1-10}\text{CF}_2\text{CH}_2\text{I}$ protons of the terminal head-to-head addition products, were significantly more intense in this product mixture.

The exact composition of the product was determined by GC-MS (Fig. 137).

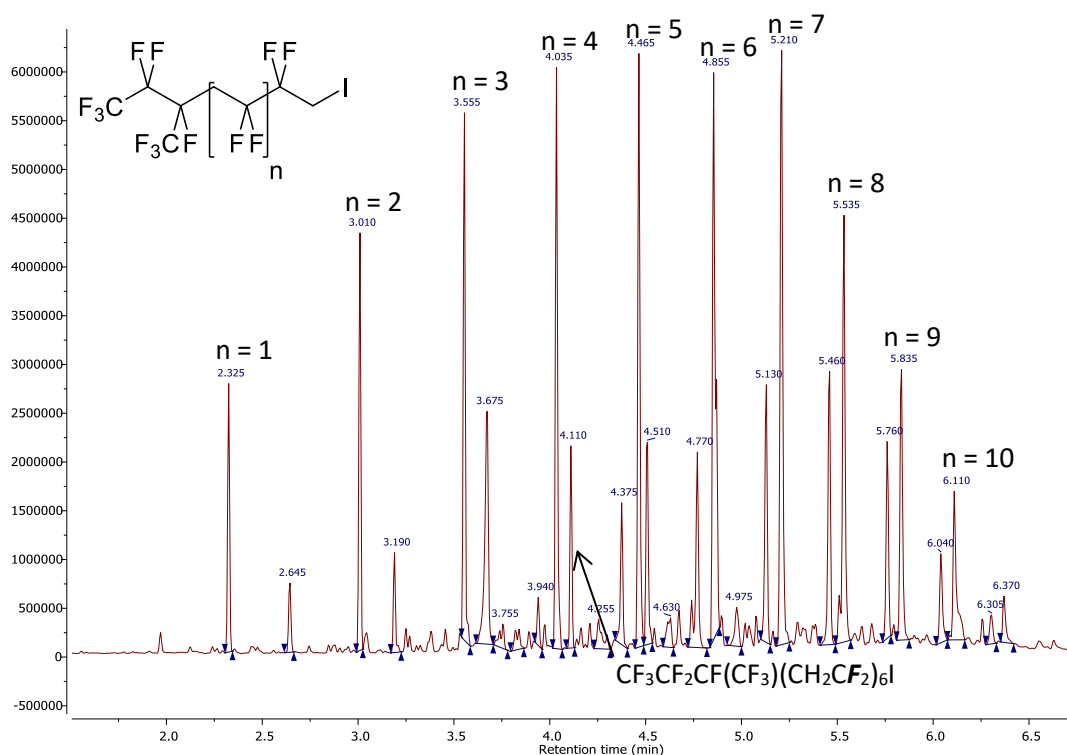


Figure 137: Gas chromatogram of the product mixture, $\text{CF}_3\text{CF}_2\text{CF}(\text{CF}_3)(\text{CH}_2\text{CF}_2)_n\text{CF}_2\text{CH}_2\text{I}$ ($n = 1 - 10$)

The GC-MS above indicates that the major components of the product mixture are the terminal head-to-head products, $\text{CF}_3\text{CF}_2\text{CF}(\text{CF}_3)(\text{CH}_2\text{CF}_2)_{1-10}\text{CF}_2\text{CH}_2\text{I}$ (**65**), confirming the data from ^{19}F and ^1H NMR spectra above. The head-to-tail products, $\text{CF}_3\text{CF}_2\text{CF}(\text{CF}_3)(\text{CH}_2\text{CF}_2)_{5-11}\text{I}$ (**64**), were also observed, but only in the case of the higher molecular weight species. These different ratios of products compared to previous reactions can be explained by the mechanism of the radical telomerisation reaction as shown in Fig. 138.

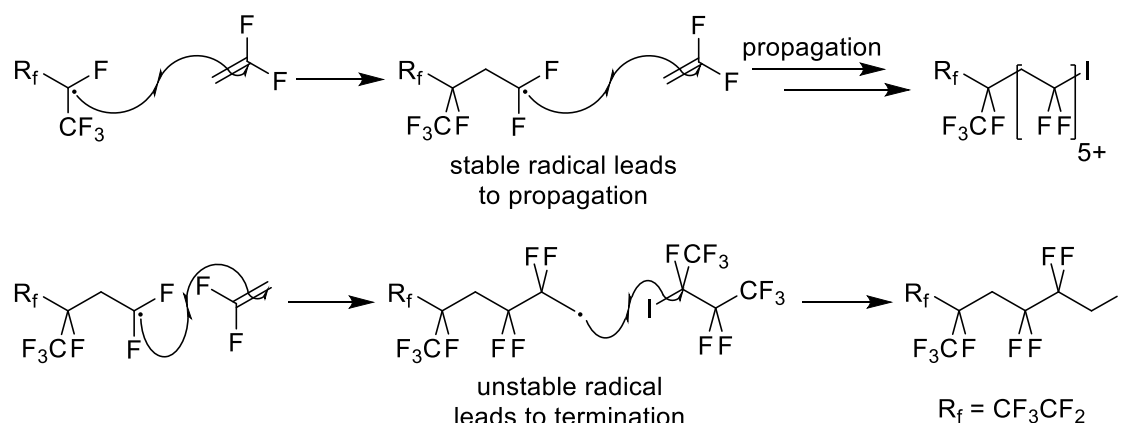


Figure 138: Mechanisms for the synthesis of $\text{CF}_3\text{CF}_2\text{CF}(\text{CF}_3)(\text{CH}_2\text{CF}_2)_{n-1}\text{CF}_2\text{CH}_2\text{I}$ and $\text{CF}_3\text{CF}_2\text{CF}(\text{CF}_3)(\text{CH}_2\text{CF}_2)_n\text{I}$

At high temperatures and with a large excess of VDF, the radical chain reaction will favour propagation, producing very high molecular weight mixtures of $\text{CF}_3\text{CF}_2\text{CF}(\text{CF}_3)(\text{CH}_2\text{CF}_2)_n\text{I}$. However, head-to-head addition of VDF during this process leads to the formation of unstable $\text{CF}_3\text{CF}_2\text{CF}(\text{CF}_3)(\text{CH}_2\text{CF}_2)_n\text{CF}_2\text{CH}_2^\bullet$ radicals that immediately undergo a termination reaction through iodine abstraction to produce $\text{CF}_3\text{CF}_2\text{CF}(\text{CF}_3)(\text{CH}_2\text{CF}_2)_n\text{CF}_2\text{CH}_2\text{I}$.

Unfortunately, $\text{CF}_3\text{CF}_2\text{CF}(\text{CF}_3)(\text{CH}_2\text{CF}_2)_n\text{CF}_2\text{CH}_2\text{I}$ does not react with SbF_5 . Therefore, this mixture could not be used to synthesise Viton[®] model compounds for use in reactions with bases.

4.3. Reactions of Branched VDF Telomer Iodides with SbF_5

In order to convert the mixtures of branched VDF telomer iodides ($\text{CF}_3\text{CF}_2\text{CF}(\text{CF}_3)(\text{CH}_2\text{CF}_2)_{1-4}\text{I}$ (**62**), $\text{CF}_3\text{CF}_2\text{CF}(\text{CF}_3)(\text{CH}_2\text{CF}_2)_{2-5}\text{I}$ (**66**) and $\text{CF}_3\text{CF}_2\text{CF}(\text{CF}_3)(\text{CH}_2\text{CF}_2)_{2-7}\text{I}$ (**63**)) into Viton[®] model compounds, they were reacted with SbF_5 at 0 °C in a fluorinated solvent for one hour. Excess SbF_5 was hydrolysed and the product was extracted to yield mixtures of branched VDF telomer fluorides (Fig. 139).

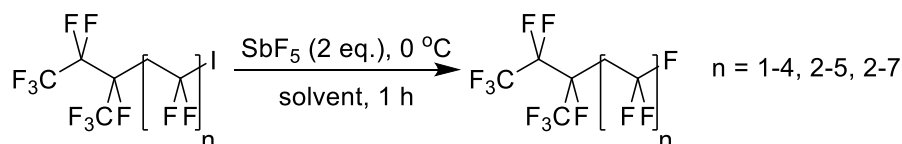


Figure 139: Reaction of $\text{CF}_3\text{CF}_2\text{CF}(\text{CF}_3)(\text{CH}_2\text{CF}_2)_n\text{I}$ with SbF_5 in fluorinated solvents to synthesise $\text{CF}_3\text{CF}_2\text{CF}(\text{CF}_3)(\text{CH}_2\text{CF}_2)_n\text{F}$

The reaction was first attempted using Fluorinert[™] FC-70 ($\text{N}(\text{C}_5\text{F}_{11})_3$) as the solvent. This fluid is high boiling (boiling point = 215 °C), therefore, it was hoped that the volatile product mixture could be extracted from the solvent by distillation. However, after the reaction was completed, only very small quantities of $\text{CF}_3\text{CF}_2\text{CF}(\text{CF}_3)(\text{CH}_2\text{CF}_2)_n\text{F}$ were successfully distilled from the solvent, not enough material for further analysis or reactions.

The above reaction was repeated in perfluoropentane, a low boiling solvent (boiling point = 29 °C) which was hoped could be removed *in vacuo* to yield the product mixture $(\text{CF}_3\text{CF}_2\text{CF}(\text{CF}_3)(\text{CH}_2\text{CF}_2)_{1-4}\text{F}$ (**67**)) (Fig. 140). However, the quantity of $\text{CF}_3\text{CF}_2\text{CF}(\text{CF}_3)(\text{CH}_2\text{CF}_2)_{1-4}\text{F}$ extracted from this reaction was still low (13% yield), and the explanation for this can be found in the GC-MS of **67** (Fig. 141).

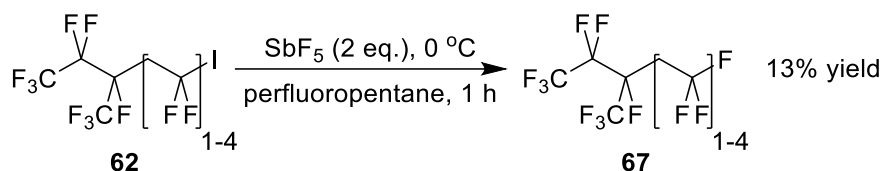


Figure 140: Reaction of $\text{CF}_3\text{CF}_2\text{CF}(\text{CF}_3)(\text{CH}_2\text{CF}_2)_{1-4}\text{I}$ with SbF_5 in perfluoropentane to synthesise $\text{CF}_3\text{CF}_2\text{CF}(\text{CF}_3)(\text{CH}_2\text{CF}_2)_{1-4}\text{F}$

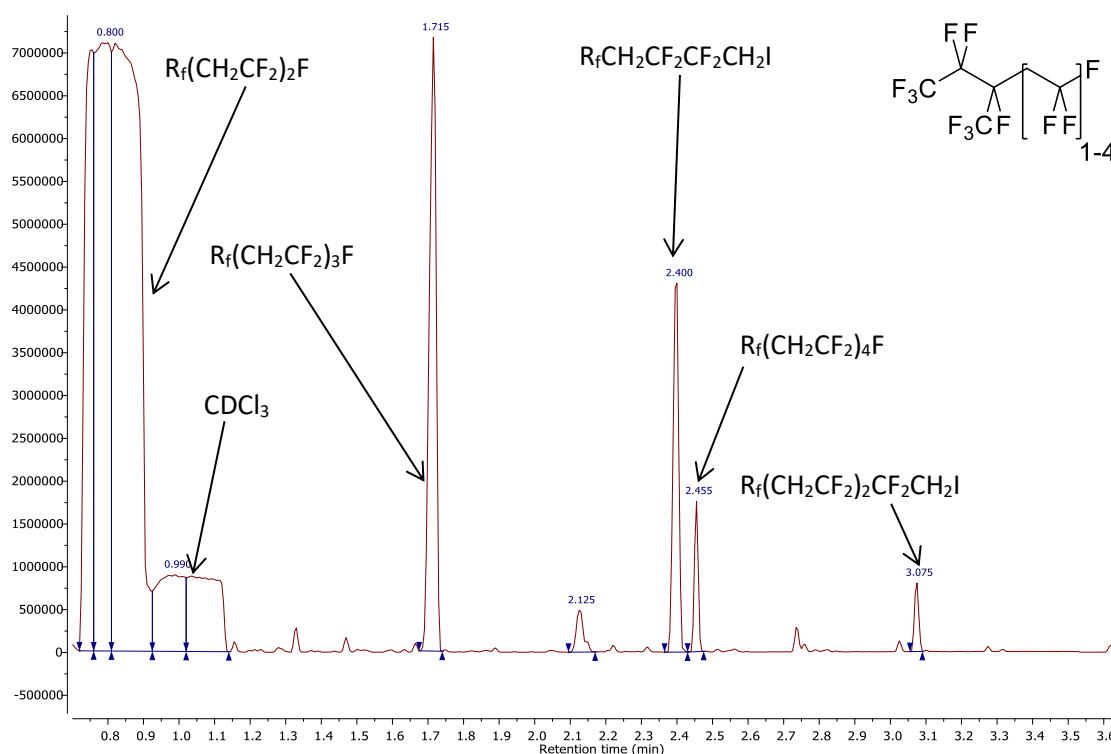


Figure 141: Gas chromatogram of the product mixture, $\text{CF}_3\text{CF}_2\text{CF}(\text{CF}_3)(\text{CH}_2\text{CF}_2)_{1-4}\text{F}$ ($R_f = \text{CF}_3\text{CF}_2\text{CF}(\text{CF}_3)$)

As the gas chromatogram indicates, the product mixture contains no $\text{CF}_3\text{CF}_2\text{CF}(\text{CF}_3)\text{CH}_2\text{CF}_2\text{F}$, and $\text{CF}_3\text{CF}_2\text{CF}(\text{CF}_3)(\text{CH}_2\text{CF}_2)_2\text{F}$ has a retention time that is less than CDCl_3 . The peaks for the unreacted terminal head-to-head addition products ($\text{CF}_3\text{CF}_2\text{CF}(\text{CF}_3)(\text{CH}_2\text{CF}_2)_n\text{CF}_2\text{CH}_2\text{I}$) are also of relatively high intensity. This suggests that the components of the product mixture are highly volatile. Consequently, higher molecular weight mixtures of branched VDF telomer iodides ($\text{CF}_3\text{CF}_2\text{CF}(\text{CF}_3)(\text{CH}_2\text{CF}_2)_{2-7}\text{I}$ (**63**) and ($\text{CF}_3\text{CF}_2\text{CF}(\text{CF}_3)(\text{CH}_2\text{CF}_2)_{2-5}\text{I}$ (**66**)) were synthesised as described previously for use in future reactions with SbF_5 .

Reactions between SbF_5 and higher molecular weight mixtures of branched VDF telomer iodides were repeated in perfluoropentane. The most successful of these reactions was with $\text{CF}_3\text{CF}_2\text{CF}(\text{CF}_3)(\text{CH}_2\text{CF}_2)_{2-7}\text{I}$ (**63**), producing the intended product mixture (**68**) in moderate yields (35 %, Fig. 142, Table 19).

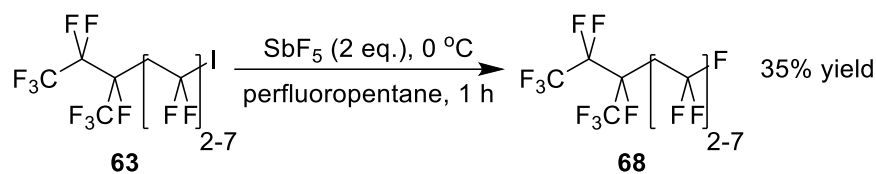


Figure 142 Reaction of $\text{CF}_3\text{CF}_2\text{CF}(\text{CF}_3)(\text{CH}_2\text{CF}_2)_{2-7}\text{I}$ with SbF_5 to synthesise $\text{CF}_3\text{CF}_2\text{CF}(\text{CF}_3)(\text{CH}_2\text{CF}_2)_{2-7}\text{F}$

Table 19: Percentage composition of the product mixture, $\text{CF}_3\text{CF}_2\text{CF}(\text{CF}_3)(\text{CH}_2\text{CF}_2)_{2-7}\text{F}$, estimated using GC-MS

Compound	Percentage Composition/ %
$\text{CF}_3\text{CF}_2\text{CF}(\text{CF}_3)(\text{CH}_2\text{CF}_2)_2\text{I}$	5
$\text{CF}_3\text{CF}_2\text{CF}(\text{CF}_3)(\text{CH}_2\text{CF}_2)_3\text{I}$	21
$\text{CF}_3\text{CF}_2\text{CF}(\text{CF}_3)(\text{CH}_2\text{CF}_2)_4\text{I}$	25
$\text{CF}_3\text{CF}_2\text{CF}(\text{CF}_3)(\text{CH}_2\text{CF}_2)_5\text{I}$	22
$\text{CF}_3\text{CF}_2\text{CF}(\text{CF}_3)(\text{CH}_2\text{CF}_2)_6\text{I}$	16
$\text{CF}_3\text{CF}_2\text{CF}(\text{CF}_3)(\text{CH}_2\text{CF}_2)_7\text{I}$	8
$\text{CF}_3\text{CF}_2\text{CF}(\text{CF}_3)(\text{CH}_2\text{CF}_2)_8\text{I}$	3

Due to the overlapping peaks in the ^{19}F NMR spectrum of $\text{CF}_3\text{CF}_2\text{CF}(\text{CF}_3)(\text{CH}_2\text{CF}_2)_{2-7}\text{F}$ (**68**), the product composition was instead estimated by GC-MS. As in the previous reaction, $\text{CF}_3\text{CF}_2\text{CF}(\text{CF}_3)\text{CH}_2\text{CF}_3$ was not isolated due to its high volatility. However, this product mixture contains a large proportion of high molecular weight telomers, explaining the improved yield.

The gas chromatogram of the product mixture is given in Fig. 143.

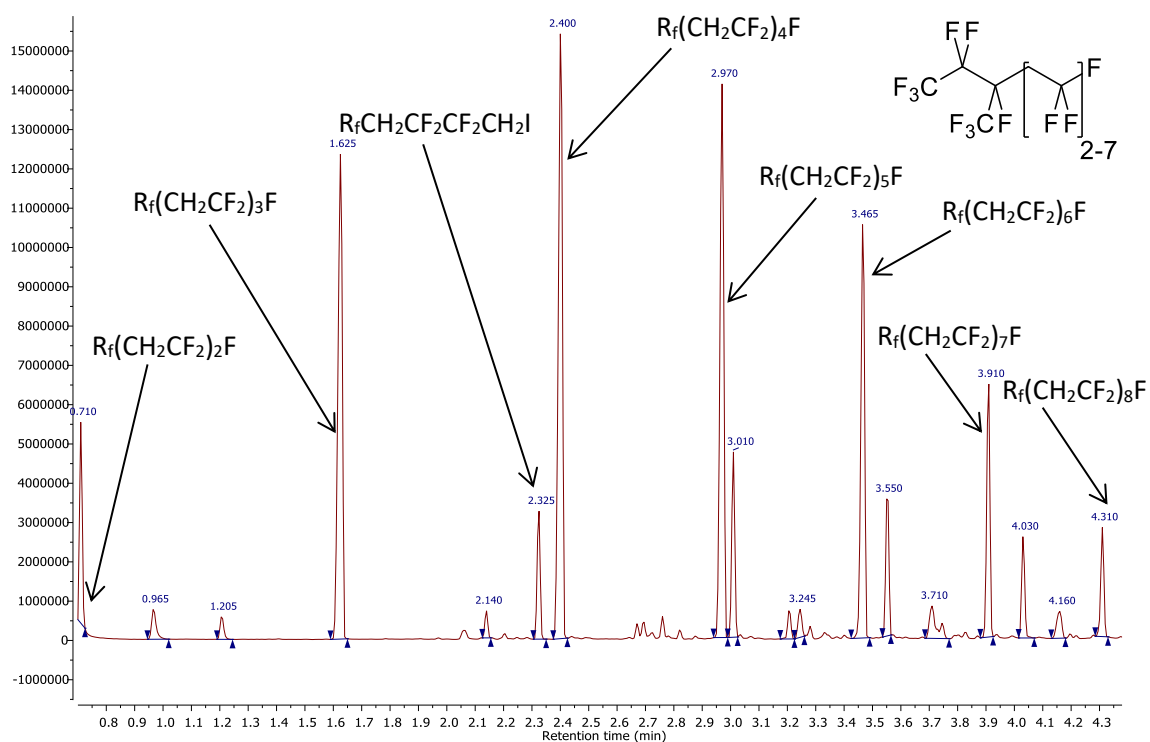


Figure 143: Gas chromatogram of the product mixture, $CF_3CF_2CF(CF_3)(CH_2CF_2)_{2-7}F$ ($R_f = CF_3CF_2CF(CF_3)$)

As indicated by the gas chromatogram, the major products of this reaction are the intended branched VDF telomer fluorides (**68**). In addition, small amounts of the terminal polyfluoriodo alkane head-to-head products that had not reacted with SbF_5 ($CF_3CF_2CF(CF_3)(CH_2CF_2)_{1-6}CF_2CH_2I$) are also present, as observed in previous reactions.

Conversion to the intended product mixture is confirmed by the ^{19}F NMR spectrum of the product compared to the starting material (Fig. 144).

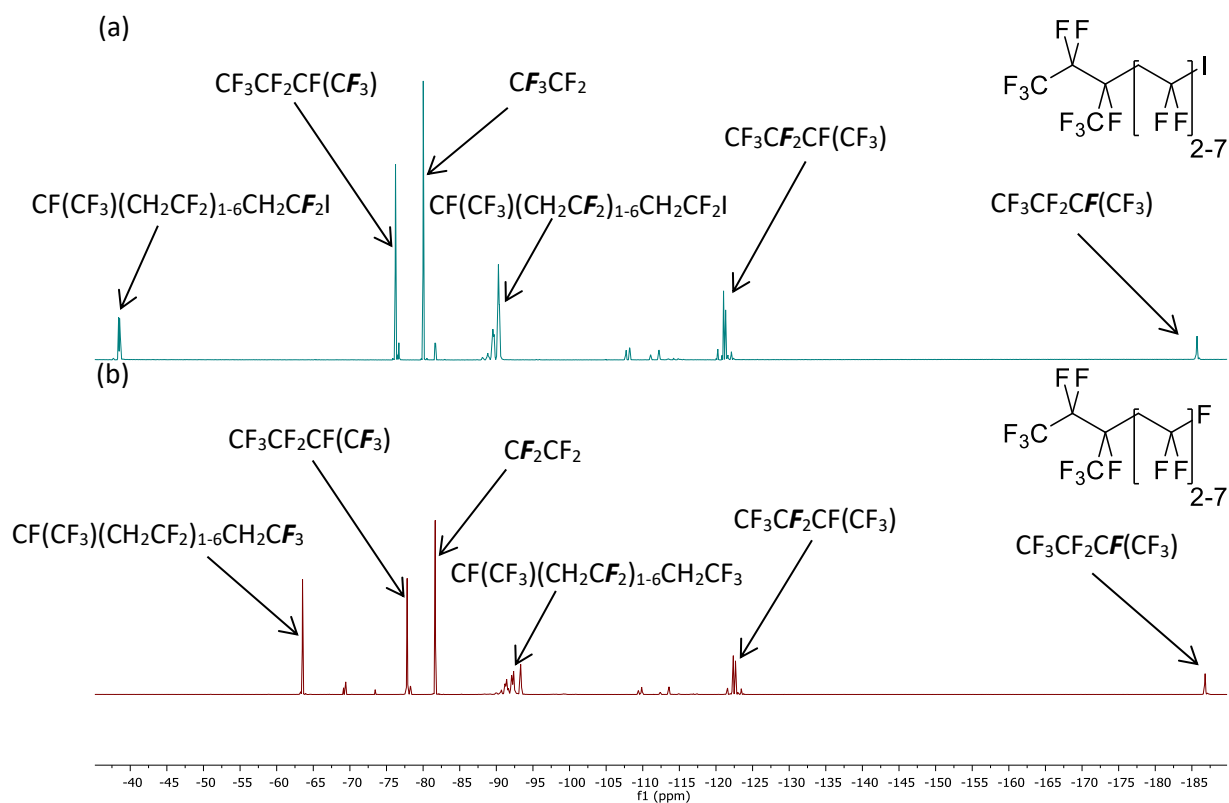


Figure 144: Comparison of the ^{19}F NMR spectra of $\text{CF}_3\text{CF}_2\text{CF}(\text{CF}_3)(\text{CH}_2\text{CF}_2)_{2-7}\text{I}$ (a) and $\text{CF}_3\text{CF}_2\text{CF}(\text{CF}_3)(\text{CH}_2\text{CF}_2)_{2-7}\text{F}$ (b)

As with the previous syntheses, the ^{19}F NMR spectra confirms conversion to $\text{CF}_3\text{CF}_2\text{CF}(\text{CF}_3)(\text{CH}_2\text{CF}_2)_{2-7}\text{F}$, due to the resonances for the CF_2I group in the starting material (between -38.2 and -38.8 ppm) being replaced by resonances for the terminal CF_3 group in the product mixture (between -63.4 and -63.6 ppm).

The key resonances from the ^1H , ^{19}F and ^{13}C NMR spectra of $\text{CF}_3\text{CF}_2\text{CF}(\text{CF}_3)(\text{CH}_2\text{CF}_2)_{2-7}\text{F}$ (**68**) are detailed in Table 20.

Table 20: List of key shifts for the major components of the product mixture from the reaction of perfluoro-2-iodobutane with 9 eq. of VDF, $\text{CF}_3\text{CF}_2\text{CF}(\text{CF}_3)(\text{CH}_2\text{CF}_2)_{2-7}\text{F}$ (chemical shifts in ppm, coupling constants in Hz)

Compound	Fragment	^1H	^{19}F	^{13}C
$\text{CF}_3\text{CF}_2\text{CF}(\text{CF}_3)(\text{CH}_2\text{CF}_2)_n\text{F}$	$(\text{CH}_2\text{CF}_2)_{n-1}\text{CH}_2\text{CF}_3$	3.02 – 2.22, m	N.A.	44.11 – 41.84, m
	$\text{CF}_2\text{CH}_2\text{CF}_2$	3.02 – 2.22, m	N.A.	40.25, h, $^2J_{\text{CF}} = 29.1$
	$\text{CF}_3\text{CF}_2\text{CF}(\text{CF}_3)\text{CH}_2\text{CF}_2$	3.02 – 2.22, m	N.A.	34.95, td, $^2J_{\text{CF}} = 25.9$, $^2J_{\text{CF}} = 20.3$
	$\text{CF}_3\text{CF}_2\text{CF}(\text{CF}_3)$	N.A.	-77.63 – -78.00, m	122.98, qd, $^1J_{\text{CF}} = 275.8$, $^2J_{\text{CF}} = 5.5$
	$\text{CF}_3\text{CF}_2\text{CF}(\text{CF}_3)$	N.A.	-186.81, s	90.86, dq, $^1J_{\text{CF}} = 210.0$, $^2J_{\text{CF}} = 30.6$
	$\text{CF}_3\text{CF}_2\text{CF}(\text{CF}_3)$	N.A.	-121.48 – -123.55, m	110.42, tqd, $^1J_{\text{CF}} = 267.3$, $^2J_{\text{CF}} = 39.3$, $^2J_{\text{CF}} = 26.1$
	$\text{CF}_3\text{CF}_2\text{CF}(\text{CF}_3)$		-81.50 – -81.80, m	121.19 – 114.11, m
	$(\text{CH}_2\text{CF}_2)_n\text{CH}_2\text{CF}_3$	N.A.	-63.42 – -63.63, m	117.86, q, $^1J_{\text{CF}} = 286.8$

The synthesised mixtures of branched VDF telomer fluorides ($\text{CF}_3\text{CF}_2\text{CF}(\text{CF}_3)(\text{CH}_2\text{CF}_2)_{2-7}\text{F}$ (**68**) and $\text{CF}_3\text{CF}_2\text{CF}(\text{CF}_3)(\text{CH}_2\text{CF}_2)_{2-5}\text{F}$ (**69**)) are suitable models of the poly VDF segments $(\text{CH}_2\text{CF}_2)_n$ and HFP-VDF structural units $(\text{CF}_2\text{CF}(\text{CF}_3)\text{CH}_2\text{CF}_2)$ found in Viton[®] elastomers (structure (d)).

4.3.1. Comparison of $\text{CF}_3\text{CF}_2\text{CF}(\text{CF}_3)(\text{CH}_2\text{CF}_2)_{2-5}\text{F}$ to Viton[®] Polymers by Solid State ^{19}F NMR Spectroscopy

Solid state ^{19}F NMR spectroscopy was carried out on a sample of polymeric Viton[®] (75 FKM 595) and the spectra was compared to that of $\text{CF}_3\text{CF}_2\text{CF}(\text{CF}_3)(\text{CH}_2\text{CF}_2)_{2-5}\text{F}$ (**69**) (Fig. 145, Table 21).

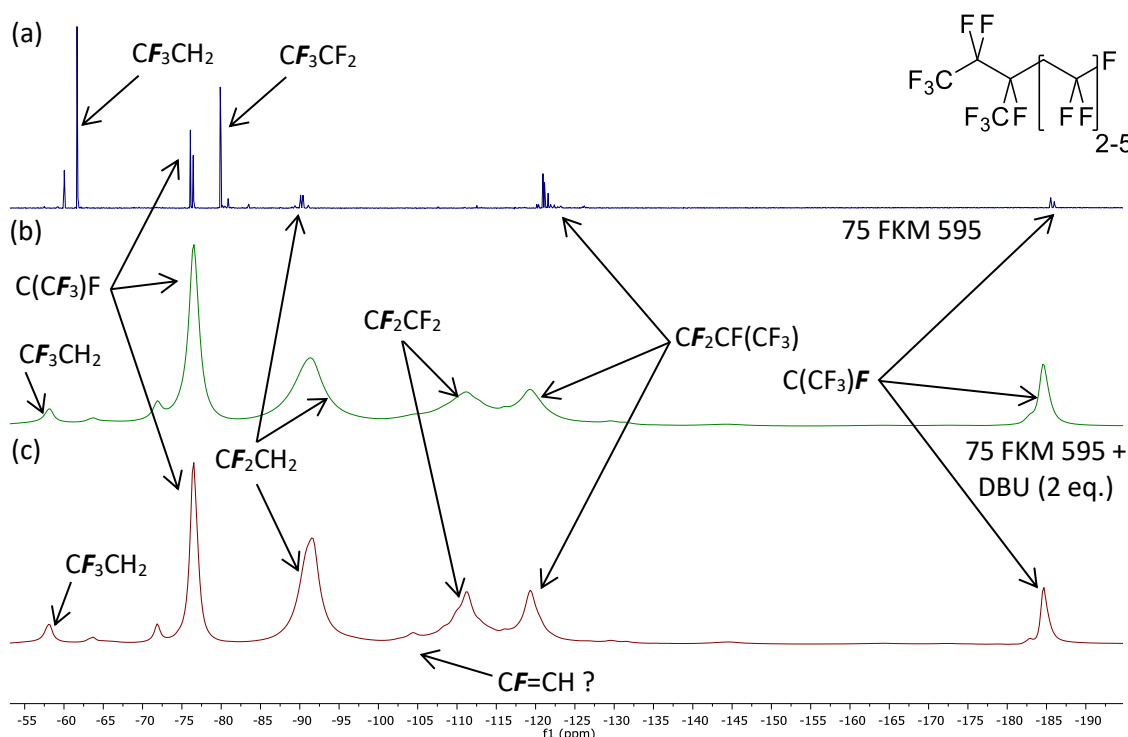


Figure 145: Comparison of the ^{19}F NMR spectra of $\text{CF}_3\text{CF}_2\text{CF}(\text{CF}_3)(\text{CH}_2\text{CF}_2)_{2-5}\text{F}$ (a), 75 FKM 595 (b), and 75 FKM 595 after reaction with DBU (2 eq.) (c)

Table 21: Resonances from the ^{19}F NMR spectra of $\text{CF}_3\text{CF}_2\text{CF}(\text{CF}_3)(\text{CH}_2\text{CF}_2)_{2-5}\text{F}$ and 75 FKM 595

Group	Shift in ^{19}F NMR spectrum of $\text{CF}_3\text{CF}_2\text{CF}(\text{CF}_3)(\text{CH}_2\text{CF}_2)_{2-5}\text{F}$ / ppm	Shift in ^{19}F NMR spectrum of 75 FKM 595/ ppm
CF_3CH_2	-59.96 – -61.89	-56.60 – -59.52
$\text{C}(\text{CF}_3)\text{F}$	-75.98 – -76.53	-73.85 – -79.90
CF_3CF_2	-79.84 – -80.03	N.A.
CF_2CH_2	-89.96 – -90.57	-86.97 – -94.98
CF_2CF_2	-113.76 – -128.33*	-106.27 – -115.30
$\text{CF}_2\text{CF}(\text{CF}_3)$	-120.08 – -122.45	-115.62 – -124.66
$\text{C}(\text{CF}_3)\text{F}$	-185.41 – -186.13	-181.22 – -187.51

*taken from the ^{19}F NMR spectrum of $\text{C}_8\text{F}_{17}(\text{CH}_2\text{CF}_2)_{1-4}\text{F}$

As the data above indicates, the synthesised mixture of model compounds contains all the key structural features found in Viton® elastomers. The only peak in the ^{19}F NMR spectrum of **69** that was not observed in that of 75 FKM 595 was the resonance for the terminal CF_3CF_2 at $-79.84 - -80.03$ ppm group, a structure not found in Viton® elastomers.

The Viton® polymer was reacted with DBU and the solid state ^{19}F NMR spectrum was recorded again as a significant colour change was observed (brown to black), indicative of surface degradation. However, there was little change in the solid-state NMR spectrum; the only new peak observed was a weak resonance at $-102.98 - -105.69$ ppm.

4.4. Reactions of $\text{CF}_3\text{CF}_2\text{CF}(\text{CF}_3)(\text{CH}_2\text{CF}_2)_{2-5}\text{F}$ with Bases

Having synthesised branched VDF telomer fluorides that model the poly VDF $(\text{CH}_2\text{CF}_2)_n$ and HFP-VDF $(\text{CF}_2\text{CF}(\text{CF}_3)\text{CH}_2\text{CF}_2)$ units found in Viton® elastomers (structures (d) and (e)), these compounds were reacted with a range of bases. Previous literature has detailed the reaction of $\text{C}_6\text{F}_{13}\text{CH}_2\text{CF}_2\text{CF}(\text{CF}_3)\text{H}$ with NaOH, which produced a mixture of dehydrofluorinated products¹² but not those of compounds containing the $\text{CF}(\text{CF}_3)\text{CH}_2$ functional group. The initial reactions investigated were those of $\text{CF}_3\text{CF}_2\text{CF}(\text{CF}_3)(\text{CH}_2\text{CF}_2)_{2-5}\text{F}$ (**69**) with bases at fixed temperatures (Fig. 146).

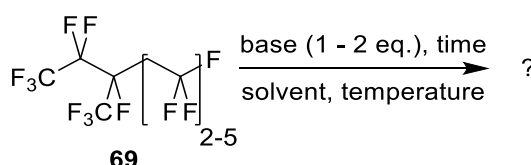


Figure 146: Reaction of $\text{CF}_3\text{CF}_2\text{CF}(\text{CF}_3)(\text{CH}_2\text{CF}_2)_{2-5}\text{F}$ with bases

4.4.1. Reactions of $\text{CF}_3\text{CF}_2\text{CF}(\text{CF}_3)(\text{CH}_2\text{CF}_2)_{2-5}\text{F}$ with Amine Bases

The first bases that were investigated were amines, as they are common components of petroleum additive mixtures. Two amine bases were initially screened; triethylamine ($\text{p}K_a = 11.01$) and DBU ($\text{p}K_a = 13.5$). DBU reacted extensively with straight chain telomers ($\text{C}_8\text{F}_{17}(\text{CH}_2\text{CF}_2)_{1-4}\text{F}$ (**49**)), but triethylamine did not. The mixture of telomer fluorides was dissolved in petroleum ether $60 - 80$ °C and two equivalents of the base were added. The reaction was heated to 80 °C for two days after which the product mixture was extracted and analysed by ^{19}F NMR spectroscopy.

The ^{19}F NMR spectra from these reactions are detailed in Fig. 147, compared to the starting material.

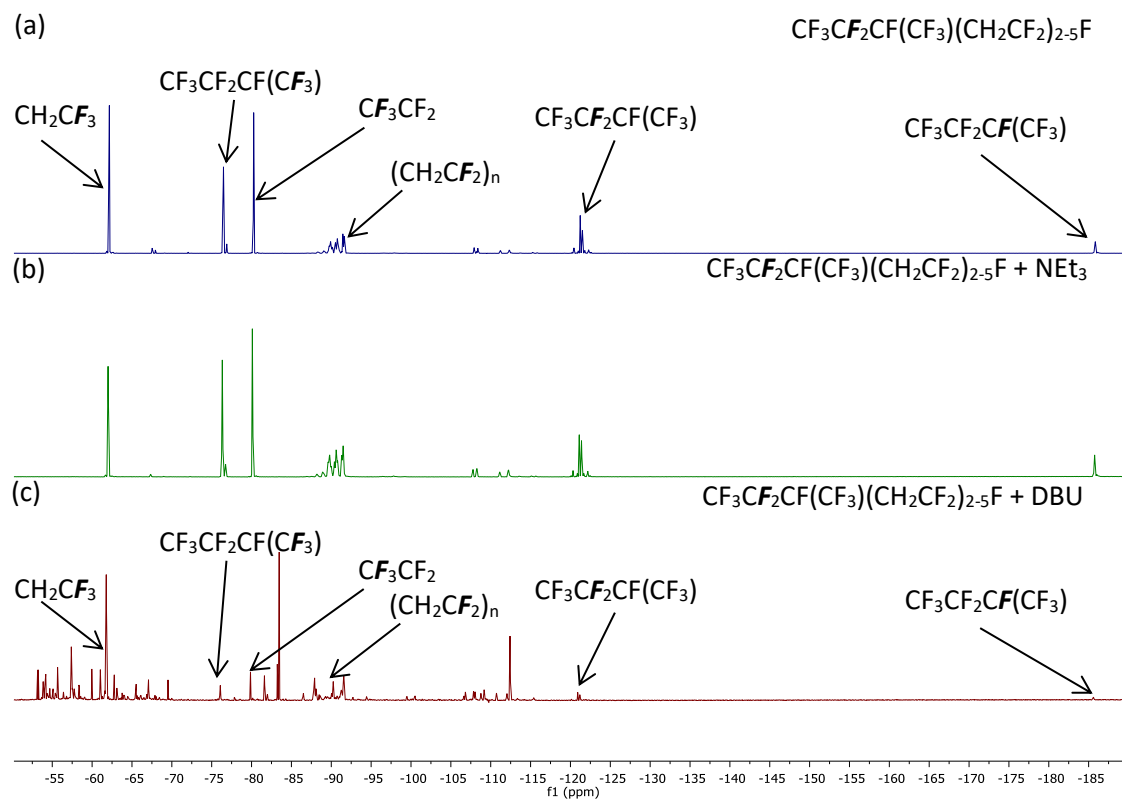


Figure 147: ^{19}F NMR spectra of $\text{CF}_3\text{CF}_2\text{CF}(\text{CF}_3)(\text{CH}_2\text{CF}_2)_{2.5}\text{F}$ (a), after reaction with NET_3 (b) and DBU (c)

Despite some minor discolouration of the reaction mixture (clear to yellow), triethylamine did not react extensively with **69**, as observed by its ^{19}F NMR spectrum (b). However, reaction with DBU caused significant degradation of **69**, forming a viscous black tar with a wide range of new peaks observed in the product mixtures ^{19}F NMR spectrum (c). Most of the peaks for the starting material are of significantly lower intensity, suggesting that a mixture of different degradation products have been formed. However, the black tar that was formed in this reaction was insoluble in standard organic solvents, making further analysis of the product mixture by GC-MS impossible. Nevertheless, it is clear that strong amine bases have a very significant deleterious effect on these systems.

4.4.2. Reaction of $\text{CF}_3\text{CF}_2\text{CF}(\text{CF}_3)(\text{CH}_2\text{CF}_2)_{2-5}\text{F}$ with Anionic Bases

The mixture of branched Viton[®] model compounds (**69**) was also reacted with a range of anionic bases; KO^tBu ($\text{pK}_a = 18$), LDA ($\text{pK}_a = 36$) and $n\text{-BuLi}$ ($\text{pK}_a = 50$), all of which reacted with the straight chain Viton[®] model compounds, $\text{C}_8\text{F}_{17}(\text{CH}_2\text{CF}_2)_{1-4}\text{F}$ as described in chapter 3. Due to the poor solubility of these bases in petroleum ether, THF was used as the reaction solvent. The mixture of telomer fluorides was reacted for one day at room temperature with one equivalent of the anionic base.

In all cases, **69** was converted to a viscous black tar on exposure to the anionic bases. However, there was no change in the extracted products by ^{19}F NMR spectroscopy so it is likely that the decomposition products of the black tar are polymeric compounds that are too insoluble in the NMR solvent (CDCl_3).

4.4.3. Reactions of $\text{CF}_3\text{CF}_2\text{CF}(\text{CF}_3)(\text{CH}_2\text{CF}_2)_{2-7}\text{F}$ with Bases Using Increasingly Forcing Conditions

In order to obtain a better understanding of the degradation of branched Viton[®] model compounds, the mixture of $\text{CF}_3\text{CF}_2\text{CF}(\text{CF}_3)(\text{CH}_2\text{CF}_2)_{2-7}\text{F}$ (**68**) was reacted with a range of bases ($\text{pK}_a = 5.15$ to 17.0) for an extended duration to mimic engine performance. $\text{CF}_3\text{CF}_2\text{CF}(\text{CF}_3)(\text{CH}_2\text{CF}_2)_{2-7}\text{F}$ was stirred with two equivalents of each base in petroleum ether $60 - 80^\circ\text{C}$. Each reaction was monitored by ^{19}F NMR spectroscopy over 7 days, and the temperature was increased by 10°C each day, starting at rt and rising to 80°C . After 7 days, the final products were extracted *in vacuo* and analysed using GC-MS, which was also used to estimate the extent of each reaction where applicable (Fig. 148, Table 22).

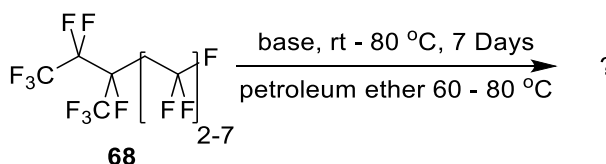


Figure 148: Reaction of $\text{CF}_3\text{CF}_2\text{CF}(\text{CF}_3)(\text{CH}_2\text{CF}_2)_{2-7}\text{F}$ with bases and the products that were observed

Table 22: List of bases, their pK_a's and their extent of reactivity with CF₃CF₂CF(CF₃)(CH₂CF₂)₂₋₇F

Base	pK _a	Decomposition / %
<i>N,N</i> -dimethyl aniline	5.15	0
pyridine	5.25	0
morpholine	8.36	0
DABCO	8.80	0
<i>N,N'</i> -dimethyl ethylenediamine	10.16	discolouration
triethylamine	11.01	discolouration
DBU	13.5	69
2- <i>tert</i> -butyl-1,1,3,3-tetramethylguanidine	13.6	65
KO ^t Bu	17	polymer

On examination, *N,N*-dimethyl aniline, pyridine, morpholine and DABCO had not reacted with **68**. *N,N'*-dimethyl ethylenediamine and triethylamine caused minor discolouration of the reaction mixture (clear to yellow), but no reaction was observed by ¹⁹F NMR spectroscopy. This is consistent with the previous reactions with linear C₈F₁₇(CH₂CF₂)₁₋₄F (**49**) and suggests that the presence of the CF(CF₃)CH₂ group in **68** did not affect the reactivity of the Viton® model compounds with these bases, under these conditions. The observed discolouration might be caused by trace amounts of decomposition products that are not observed by ¹⁹F NMR spectroscopy, or by air oxidation of the amine bases.

The reaction of KO^tBu with **68** produced a brown tar at room temperature after 10 minutes (Fig. 149). This substance could not be dissolved in any solvent, preventing examination of the product by NMR or GC-MS. The insoluble nature of this product suggests that the reaction rapidly produced a polymeric mixture. This is consistent with the high pK_a of KO^tBu and the product may have been formed by crosslinking of dehydrofluorinated Viton® model compounds.



Figure 149: Polymeric tar produced by the reaction of KO^tBu with CF₃CF₂CF(CF₃)(CH₂CF₂)₂-7F

The reactions of DBU and 2-*tert*-butyl-1,1,3,3-tetramethylguanidine with **68** caused extensive decomposition of the Viton® model compounds, as observed in the ¹⁹F NMR spectra of these reactions over time (Fig. 150 and 151).

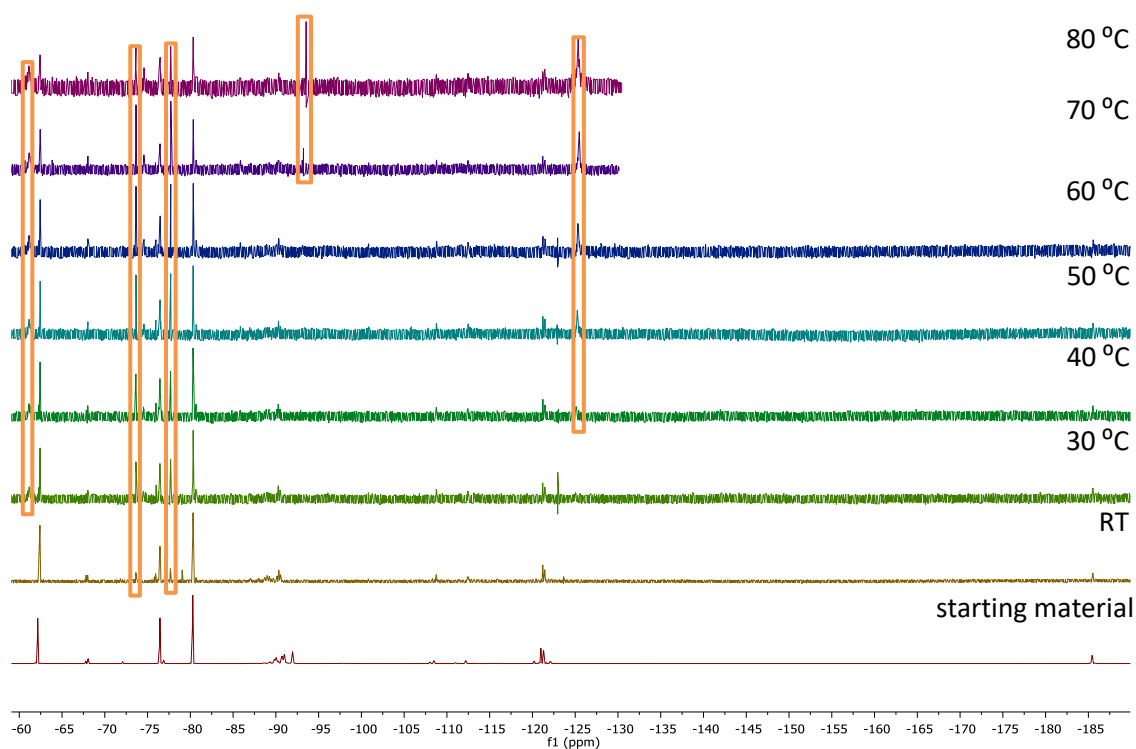


Figure 150: ¹⁹F NMR spectra over time of the reaction of 2-*tert*-butyl-1,1,3,3-tetramethylguanidine with CF₃CF₂CF(CF₃)(CH₂CF₂)₂-7F (new peaks are highlighted in orange)

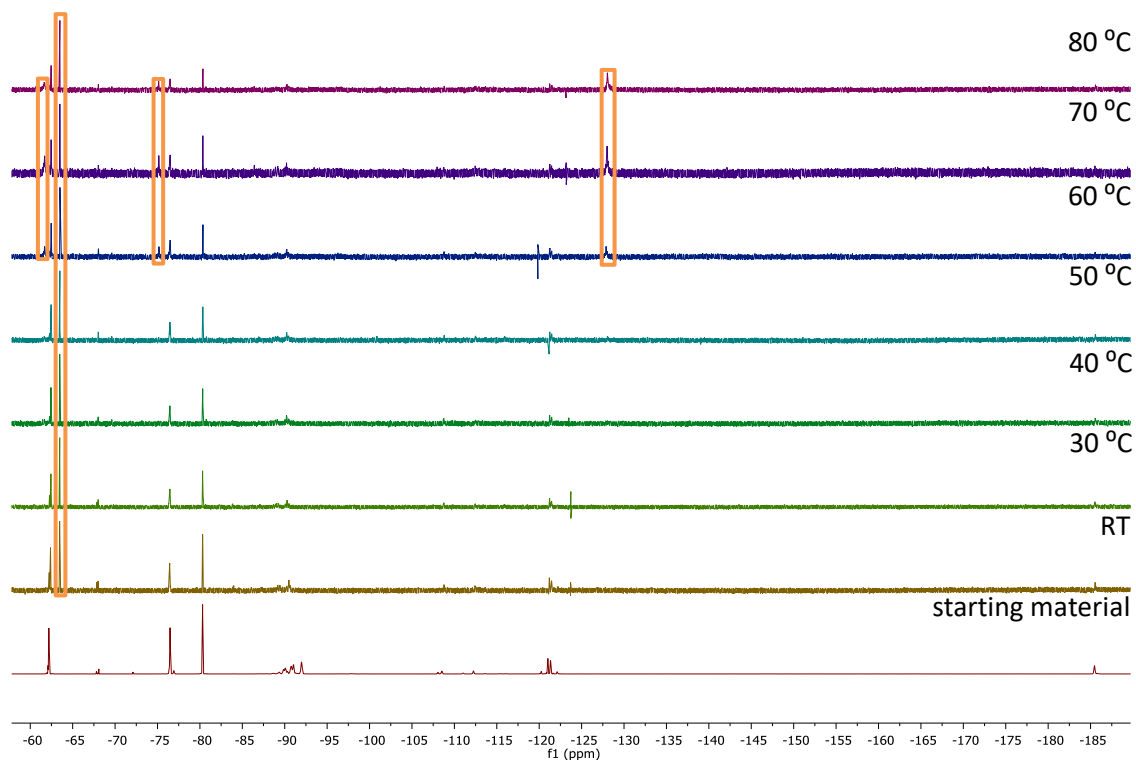


Figure 151: ^{19}F NMR spectra over time of the reaction of DBU with $\text{CF}_3\text{CF}_2\text{CF}(\text{CF}_3)(\text{CH}_2\text{CF}_2)_{2.7}\text{F}$ (new peaks are highlighted in orange)

The ^{19}F NMR spectra from each of these reactions show a significant number of new peaks from the decomposition products of **68** (highlighted in orange). In particular, the spectra of both product mixtures have peaks at $-60 - -62$, $-73 - -78$ and $-125 - -129$ ppm that were not present in the starting material. Unfortunately, detailed information about the structures of the decomposition products cannot be obtained from the ^{19}F NMR spectra.

However, analysis of the product mixtures by GC-MS provided more useful information (Fig. 152).

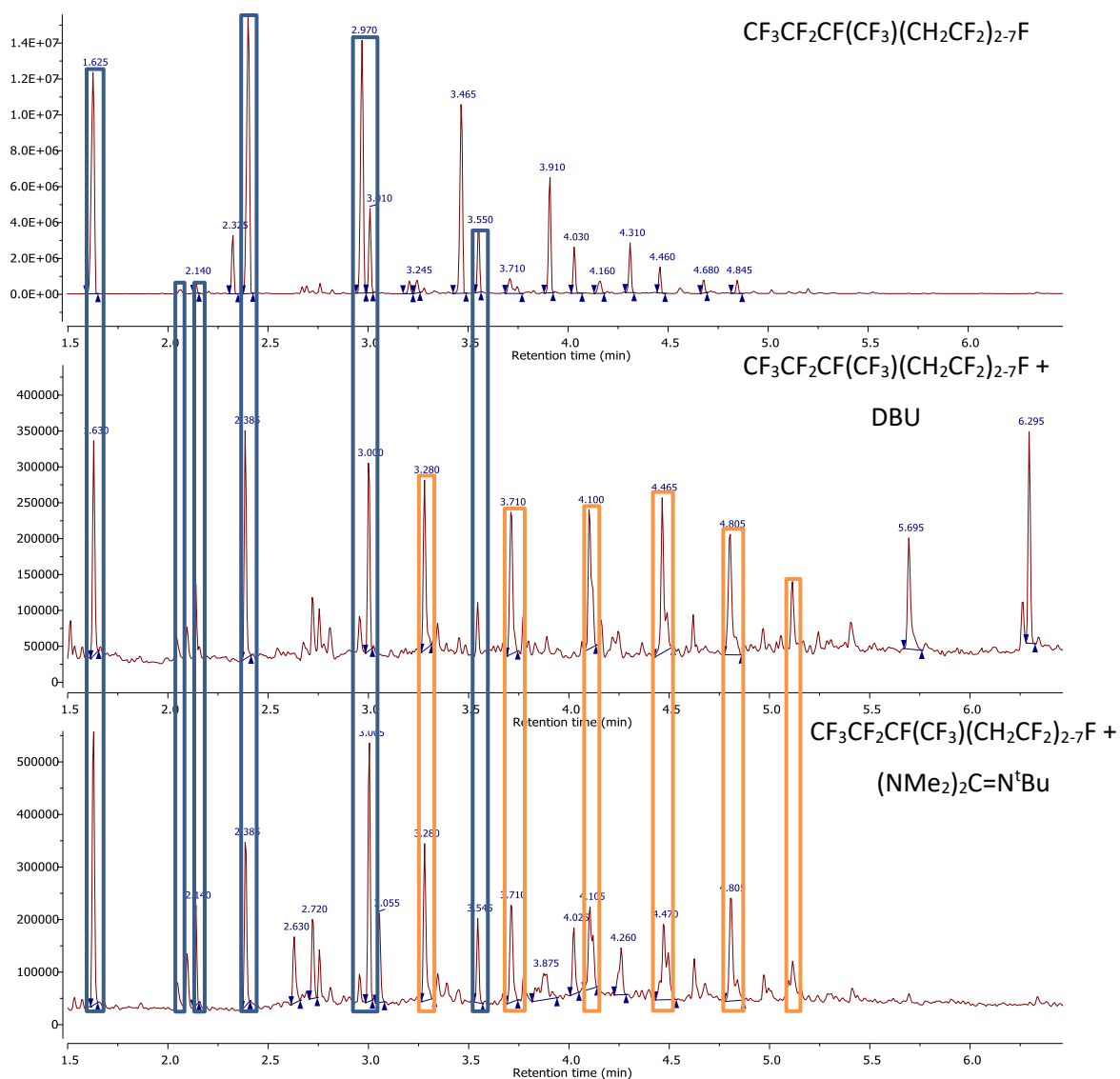


Figure 152: Comparison of the gas chromatogram of $\text{CF}_3\text{CF}_2\text{CF}(\text{CF}_3)(\text{CH}_2\text{CF}_2)_2\text{-7F}$ (a) with those of the product mixture after reaction with DBU (b) and 2-*tert*-butyl-1,1,3,3-tetramethylguanidine (c)
Blue = compounds in all three gas chromatograms
Orange = compounds found only in both product mixture gas chromatograms

As the gas chromatogram above indicates, low molecular weight Viton® model compounds ($\text{CF}_3\text{CF}_2\text{CF}(\text{CF}_3)(\text{CH}_2\text{CF}_2)_2\text{-3F}$, highlighted in blue) did not react extensively with DBU or 2-*tert*-butyl-1,1,3,3-tetramethylguanidine. However, higher molecular weight compounds ($\text{CF}_3\text{CF}_2\text{CF}(\text{CF}_3)(\text{CH}_2\text{CF}_2)_4\text{-7F}$) did react and produced the series of products highlighted in orange (Fig. 152). The retention times of these compounds increase with molecular weight; each peak contains fragment ions that are 64 mass units heavier than the previous species, indicative of the incorporation of another molecule of VDF into each subsequent compound.

As examples, the GC-MS of the compounds at retention times of 3.280 and 3.710 are detailed in Fig. 153 and 154.

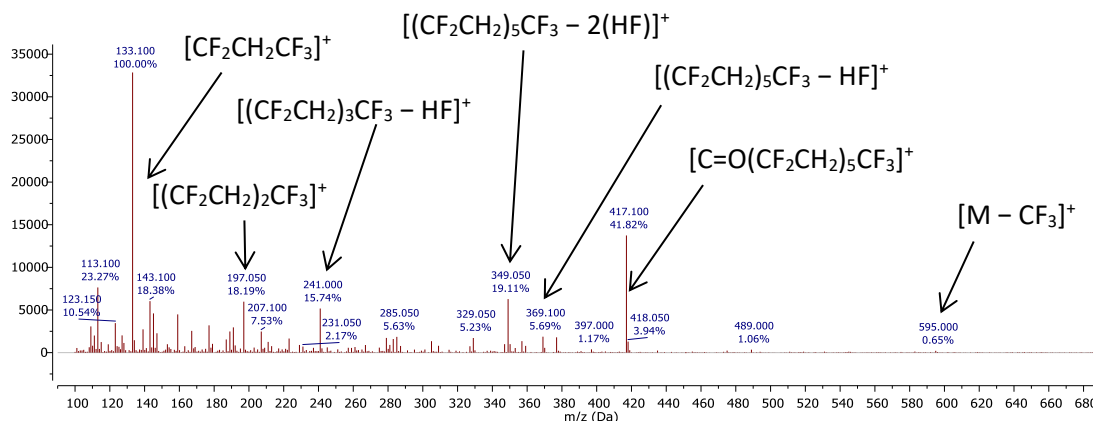


Figure 153: GC-MS of the compound at retention time = 3.280, (a) (possibly $\text{CF}_3\text{CF}_2\text{CF}(\text{CF}_3)\text{CH}_2\text{CF}=\text{CHC}=\text{O}(\text{CH}_2\text{CF}_2)_5\text{F}$)

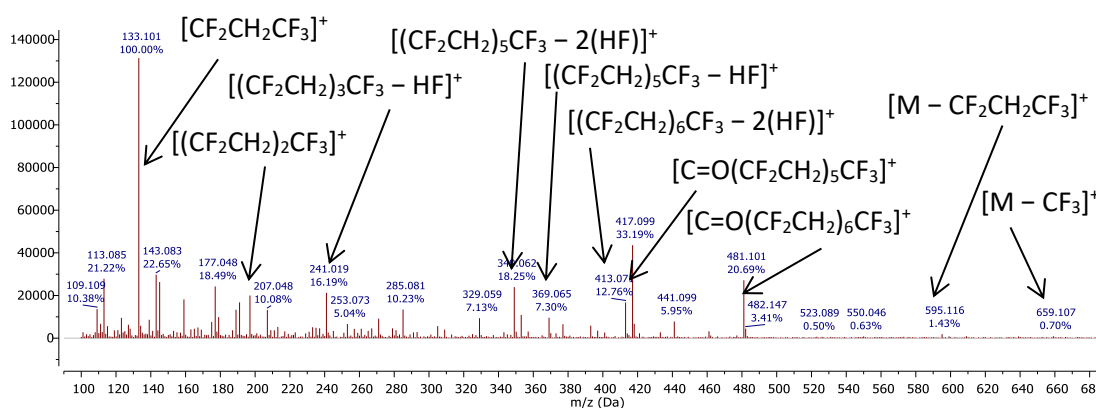


Figure 154: GC-MS of the compound at retention time = 3.710, (b) (possibly $\text{CF}_3\text{CF}_2\text{CF}(\text{CF}_3)\text{CH}_2\text{CF}=\text{CHC}=\text{O}(\text{CH}_2\text{CF}_2)_6\text{F}$)

Both GC-MS contain fragment ions from dehydrofluorinated compounds, such as those fragments with an $m/z = 241.0$, 349.1 and 369.1 in compound (a), and additionally at 413.1 in compound (b). However, there are additional fragments with $m/z = 417.1$ in both compounds, and 481.1 in compound (b). These are the fragments with structures $[\text{C}=\text{O}(\text{CF}_2\text{CH}_2)_5\text{CF}_3]^+$ and $[\text{C}=\text{O}(\text{CF}_2\text{CH}_2)_6\text{CF}_3]^+$ respectively, suggesting that these decomposition products contain carbonyl groups, formed by reaction of dehydrofluorinated **68** with $\text{H}_2\text{O}/\text{OH}^-$ ions.

Hydrolysis could occur by several pathways, depending on which dehydrofluorinated compounds were present in the product mixture. A possible structure for these compounds is $\text{CF}_3\text{CF}_2\text{CF}(\text{CF}_3)\text{CH}_2\text{CF}=\text{CHC}=\text{O}(\text{CH}_2\text{CF}_2)_{2-6}\text{F}$ (**71**), formed by the reaction of $\text{CF}_3\text{CF}_2\text{CF}(\text{CF}_3)\text{CH}_2\text{CF}_2\text{CH}=\text{CF}(\text{CH}_2\text{CF}_2)_{2-6}\text{F}$ (**70**) with hydroxide, the mechanism for which is described in Fig. 155.

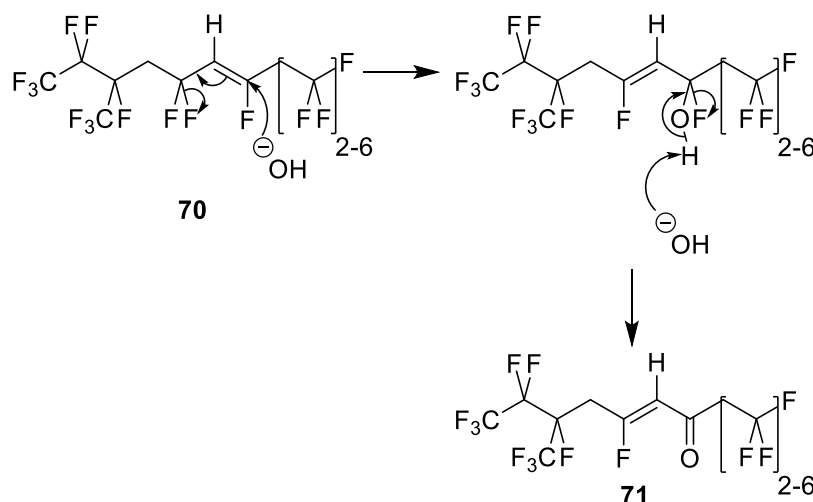


Figure 155: Carbonyl containing products, synthesised by attack of $\text{H}_2\text{O}/\text{OH}^-$ on various dehydrofluorinated compounds

The presence of carbonyl compounds is supported by the IR spectrum of the product mixture (Fig. 156).

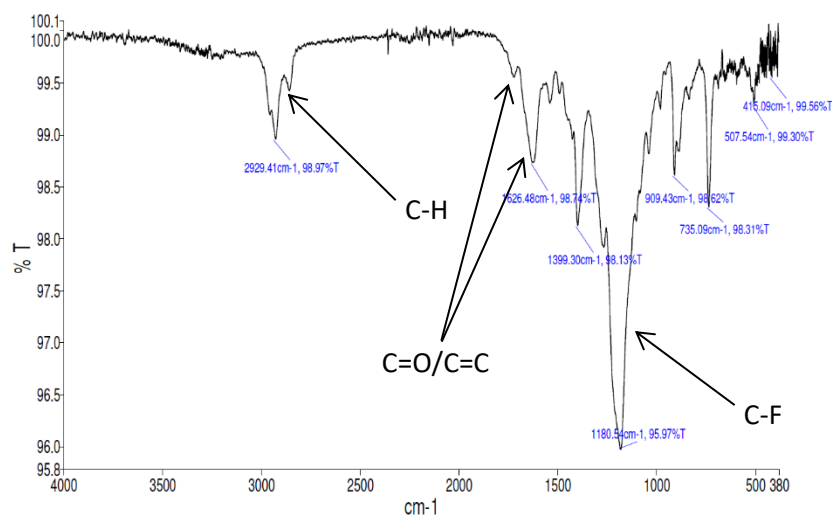


Figure 156: IR spectrum from the reaction of DBU with $\text{CF}_3\text{CF}_2\text{CF}(\text{CF}_3)(\text{CH}_2\text{CF}_2)_{2-7}\text{F}$

The IR spectrum contains a strong signal at 1181 cm^{-1} for the C – F bonds in the product, and a second at 2929 cm^{-1} for the C – H bonds. However, there is another strong signal at 1626 cm^{-1} , and other weaker signals close to this one, that are assigned to C = O bonds. Unfortunately,

any signals for C = C bonds in dehydrofluorinated **68** would also appear in this region, so the assigned structures of the products are tentative.

The products obtained suggest that Viton® polymers that are dehydrofluorinated by exposure to basic compounds can be further degraded by water. Therefore, excluding water from systems exposed to basic petroleum additives may increase the lifetime of Viton® seals. They also suggest that Viton® molecules containing long poly VDF units are more susceptible to attack by basic compounds as, in the reactions above, only the higher molecular weight Viton® model compounds ($\text{CF}_3\text{CF}_2\text{CF}(\text{CF}_3)(\text{CH}_2\text{CF}_2)_{4-7}\text{F}$) underwent extensive decomposition.

The reactions of *N,N'*-dimethyl ethylenediamine ($\text{p}K_a = 10.16$) and triethylamine ($\text{p}K_a = 11.01$) with **68** were repeated at higher temperature (80 – 120 °C), using petroleum ether 100 – 120 °C as the reaction solvent. The branched Viton® model compounds were heated to 80 °C in petroleum ether, the amines were added, and the reactions were heated for 5 days. The temperature was increased by 10 °C each day, to a maximum of 120 °C, after which the reactions were stirred for a further 2 days at 120 °C (Fig. 157).

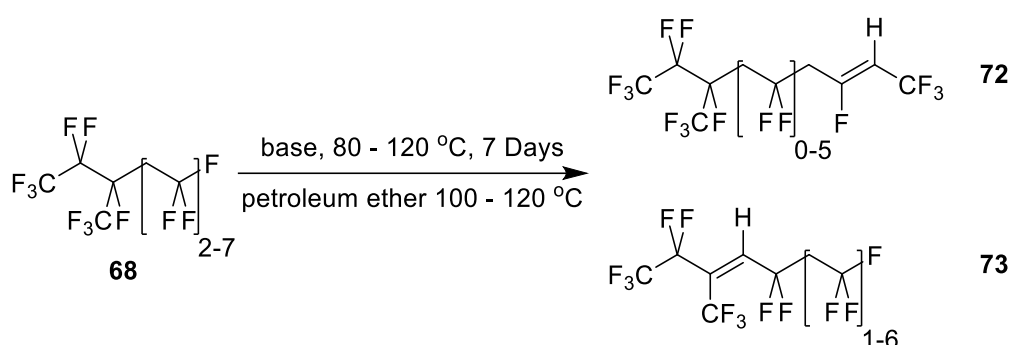


Figure 157: Reaction of $\text{CF}_3\text{CF}_2\text{CF}(\text{CF}_3)(\text{CH}_2\text{CF}_2)_{2-7}\text{F}$ with amine bases at high temperature

The reactions were monitored by ^{19}F NMR spectroscopy and both showed significant discolouration over time (clear to yellow/brown). However, as previously, there was no observable reaction between triethylamine and **68** by ^{19}F NMR spectroscopy.

By contrast, **68** did react with *N,N'*-dimethyl ethylenediamine (Fig. 158).

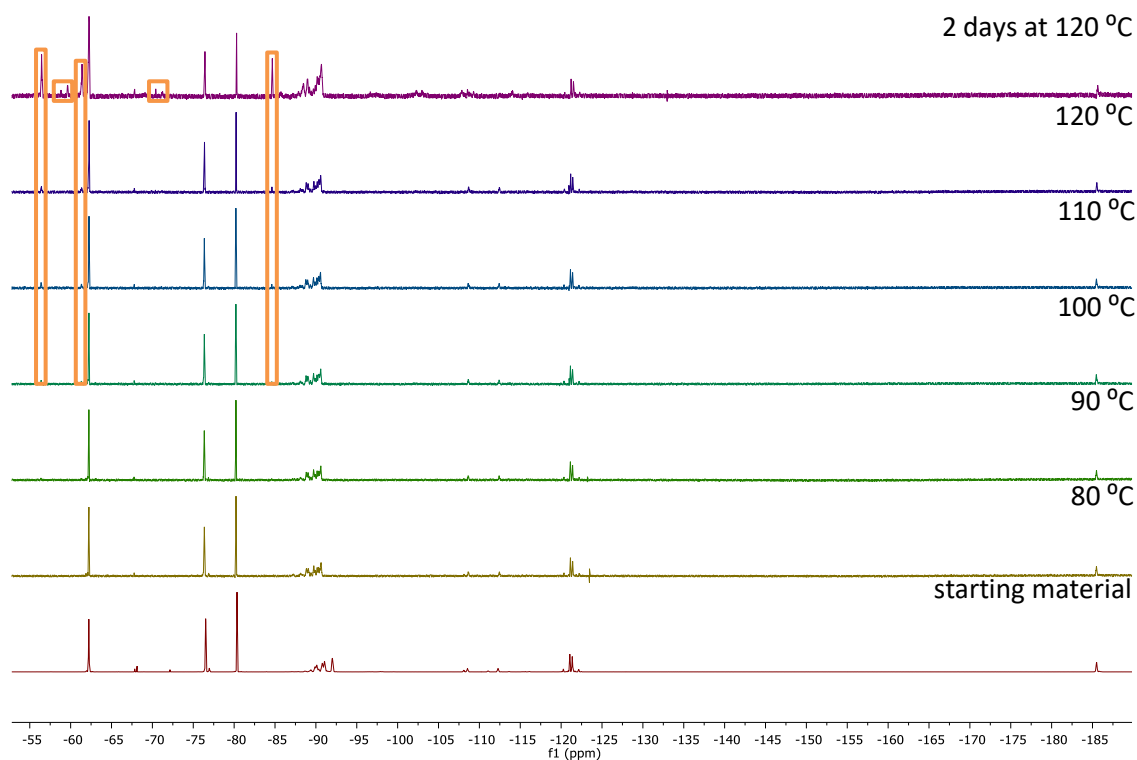


Figure 158: ^{19}F NMR spectra over time of the reaction of *N,N'*-dimethyl ethylenediamine with $\text{CF}_3\text{CF}_2\text{CF}(\text{CF}_3)(\text{CH}_2\text{CF}_2)_{2.7}\text{F}$

At temperatures above 100 °C, several new peaks begin to appear in the ^{19}F NMR spectra for dehydrofluorinated products. In particular, there are multiplets at $-56.07 - -56.38$ and $-61.05 - -61.30$ ppm that are indicative of $\text{CF}=\text{CH}-\text{CF}_3$ groups, and a multiplet at $-84.39 - -84.53$ ppm, that is from $\text{CF}_3\text{CF}_2\text{C}(\text{CF}_3)=\text{CHCF}_2$ groups. It is therefore likely that the products of this reaction are a mixture of $\text{CF}_3\text{CF}_2\text{CF}(\text{CF}_3)(\text{CH}_2\text{CF}_2)_{0-5}\text{CH}_2\text{CF}=\text{CHCF}_3$ (**72**) and $\text{CF}_3\text{CF}_2\text{C}(\text{CF}_3)=\text{CHCF}_2(\text{CH}_2\text{CF}_2)_{1-6}\text{F}$ (**73**), formed by dehydrofluorination adjacent to the terminal CF_3 group and to the $\text{CF}_3\text{CF}_2\text{CF}(\text{CF}_3)$ R_f chain respectively. These results indicate that mildly basic petroleum additives ($\text{p}K_a > 10$) can cause dehydrofluorination of Viton® seals at high temperatures.

$\text{CF}_3\text{CF}_2\text{CF}(\text{CF}_3)(\text{CH}_2\text{CF}_2)_{2-7}\text{F}$ (**68**) was reacted with two mixtures of petroleum additives supplied by Afton Chemical® (HiTEC® 307 and HiTEC® 317). The reactions were first carried out from rt – 80 °C and then from 80 – 120 °C, using the two methods described previously (Fig. 159).

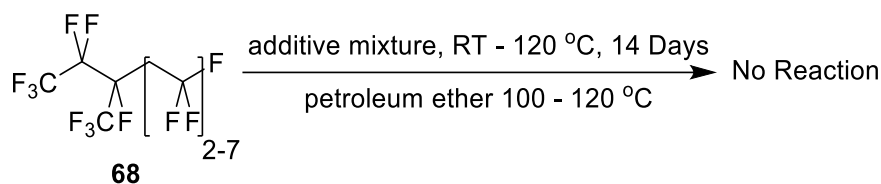


Figure 159: Reaction of $\text{CF}_3\text{CF}_2\text{CF}(\text{CF}_3)(\text{CH}_2\text{CF}_2)_{2-7}\text{F}$ with additive mixtures HiTEC® 307 and HiTEC® 317, supplied by Afton Chemical®

These reactions were first carried out using 10 mL of a 1:9 mixture of the additive mixture to petroleum ether 100 – 120 °C, and 0.1 g of **68**. The reaction mixtures were first heated from rt – 80 °C and monitored by ^{19}F NMR spectroscopy. On examination, no observable reaction had occurred. The reactions were subsequently heated from 80 – 120 °C over 5 days, before being stirred for two days at 120 °C. However, on examination by ^{19}F NMR spectroscopy, no observable reaction had occurred under these conditions.

These reactions were repeated using 10 mL of a 1:1 mixture of the additive mixture to petroleum ether 100 – 120 °C, and 0.1 g of **68**. However, once again, no reaction was observed, as seen by ^{19}F NMR spectroscopy.

4.5. Conclusion

Branched Viton® model compounds, containing the poly VDF units $(\text{CH}_2\text{CF}_2)_n$ from structures (a), (b) and (c) and the HFP-VDF group $(\text{CF}_2\text{CF}(\text{CF}_3)\text{CH}_2\text{CF}_2)$ of structures (d) and (e) were synthesised in a two-step process. Perfluoro-2-iodobutane (**61**) was reacted with either 5 or 9 equivalents VDF at high temperature and pressure to produce several different mixtures of branched VDF telomer iodides. These were subsequently reacted with SbF_5 to give the intended branched VDF telomer fluorides $(\text{CF}_3\text{CF}_2\text{CF}(\text{CF}_3)(\text{CH}_2\text{CF}_2)_{1-4}\text{F}$ (**67**), $\text{CF}_3\text{CF}_2\text{CF}(\text{CF}_3)(\text{CH}_2\text{CF}_2)_{2-5}\text{F}$ (**69**) and $\text{CF}_3\text{CF}_2\text{CF}(\text{CF}_3)(\text{CH}_2\text{CF}_2)_{2-7}\text{F}$ (**68**) in moderate yields (Fig. 160).

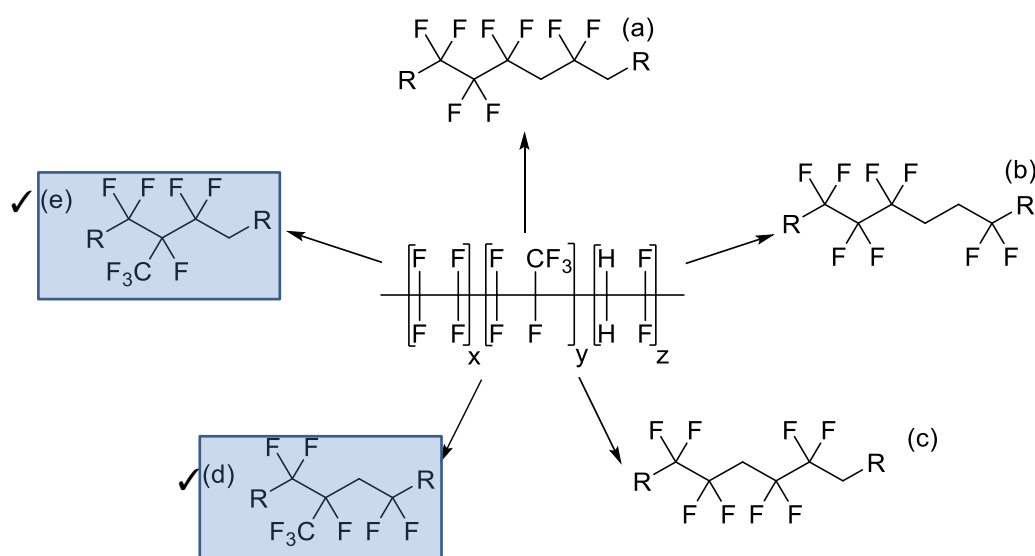


Figure 160: Structures found within Viton®

Reactions of KO^tBu , LDA and $n\text{-BuLi}$ with **68** and **69** produced viscous polymeric tars that could not be analysed. However, reactions with DBU and 2-*tert*-butyl-1,1,3,3-tetramethylguanidine produced a mixture of decomposition products that contained carbonyl groups, probably formed by the reaction of water or hydroxide ions with the dehydrofluorinated Viton® model compounds. In addition, *N,N'*-dimethyl ethylenediamine reacted with **68** at temperatures above $100\text{ }^\circ\text{C}$, despite not reacting at all with $\text{C}_8\text{F}_{17}(\text{CH}_2\text{CF}_2)_{1-4}\text{F}$ (**49**).

The results of these reactions indicate that the presence of the HFP-VDF group $(\text{CF}_2\text{CF}(\text{CF}_3)\text{CH}_2\text{CF}_2)$ in Viton® seals increases their vulnerability to dehydrofluorination by basic petroleum additives ($\text{p}K_a > 10$). They also demonstrate that exposure of these dehydrofluorinated seals to water can cause subsequent degradation of the Viton® seals through the formation of reactive carbonyl groups along the polymer backbone.

5. Synthesis of Discrete RCF(CF₃)R Compounds

A second route to Viton[®] model compounds that contain the -CF(CF₃)CH₂- group found in structure (d) was investigated. The proposed pathway involved a two-step synthesis by sequential reaction of alkyl carbonyl compounds with Me₃SiCF₃ (**74**) and DAST (**75**). Unlike the other syntheses of Viton[®] model compounds that used radical chain reactions to produce mixtures of products, described in previous chapters, this strategy would produce individual compounds that could be purified and analysed in detail.

The reactions of Me₃SiCF₃ with alkyl ketones are known to produce 1-trifluoromethyl alcohols (RCOH(CF₃)R') in moderate to excellent yields^{72,73}. Once synthesised, these compounds could be further reacted with DAST to produce the corresponding RCF(CF₃)R' compounds (Fig. 161).

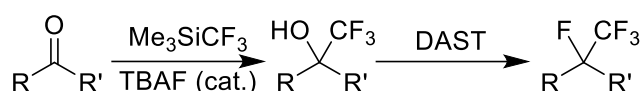


Figure 161: Sequential reaction of carbonyl compounds with Me₃SiCF₃ and DAST to synthesise RCF(CF₃)R' systems

Of particular interest are those compounds that contain the RCF(CF₃)CH₂R' group found in structure (d), a model of the HFP-VDF unit of Viton[®] elastomers. These systems have not been widely explored, with only limited examples of RCF(CF₃)CH₂R' compounds synthesised using DAST in the literature. Specifically, the synthesis of several potential antiviral compounds (**78**) containing RCF(CF₃)CH₂R' groups was reported by Alios BioPharma Inc. in 2015⁷⁴ (Fig. 162).

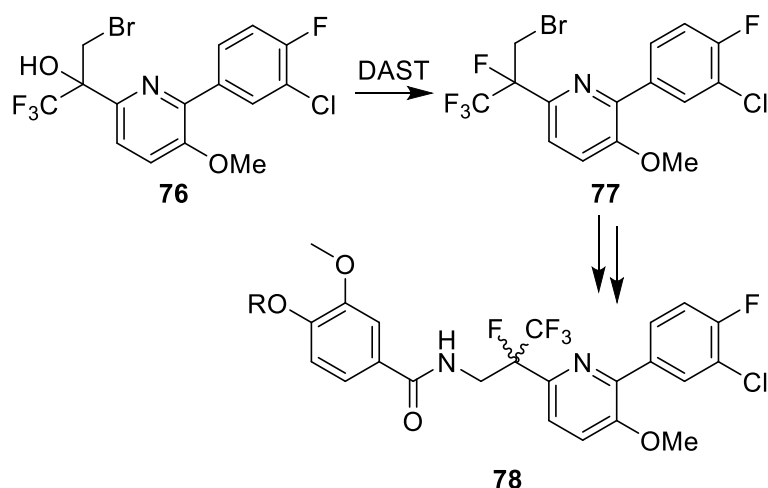


Figure 162: Synthesis of a series of potential antiviral compounds using DAST⁷⁴

In addition, a series of patents filed by Imperial Chemical Industries (ICI) between 1988 and 1993 detail the synthesis of several ether, thioether, sulfoxide and sulfone herbicides that contain the $\text{RCF}(\text{CF}_3)\text{CH}_2\text{R}'$ group⁷⁵⁻⁷⁸ (Fig. 163).

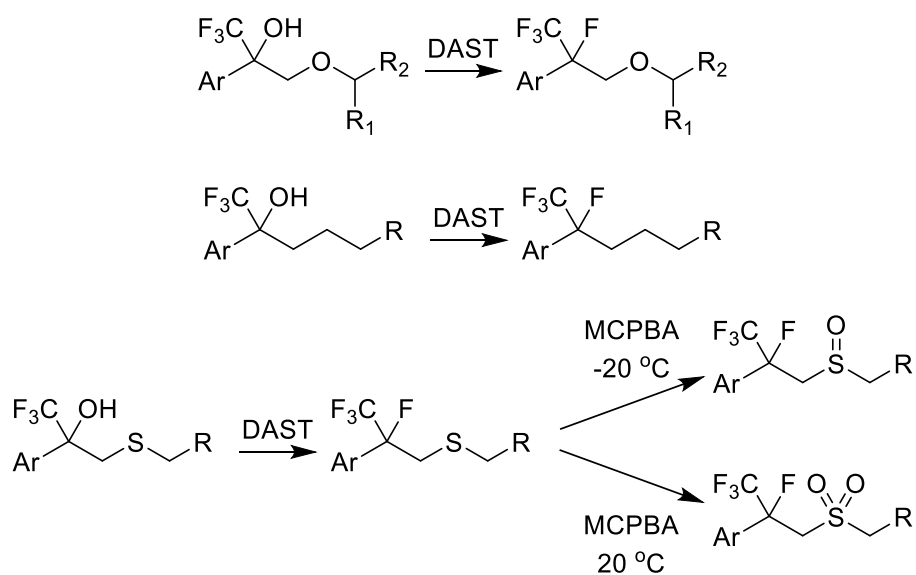


Figure 163: Synthesis of $\text{RCF}(\text{CF}_3)\text{CH}_2\text{R}'$ containing ethers, thioethers, sulfoxides and sulfones⁷⁵⁻⁷⁸

The limited literature on these compounds highlights both the lack of research in these systems and their potential uses outside of simply being Viton® model compounds.

5.1. Introduction – Me_3SiCF_3 and DAST

The work in this chapter makes extensive use of both the Ruppert – Prakash reagent (Me_3SiCF_3) and diethylaminosulfur trifluoride (DAST) (Fig. 164). Consequently, a brief overview of the chemistry of these reagents is given below.



Figure 164: Reagents used in this chapter, Me_3SiCF_3 and DAST

5.1.1. Trifluoromethylation – The Ruppert – Prakash Reagent

The trifluoromethyl (CF₃) group is a common structural moiety in pharmaceutical and agrochemical compounds. In particular, the presence of one or more CF₃ groups is known to improve the lipophilicity of drug molecules and it is found in several widely used drugs such as Nexavar (**79**), an anticancer drug (Fig. 165), and Tipranavir (**80**), a component of HIV treatments⁷⁹ (Fig. 166).

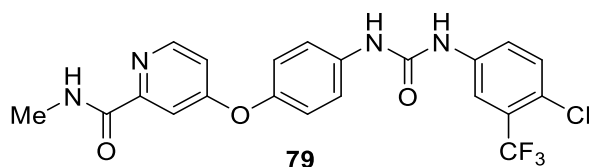


Figure 165: Nexavar, anticancer drug⁷⁹

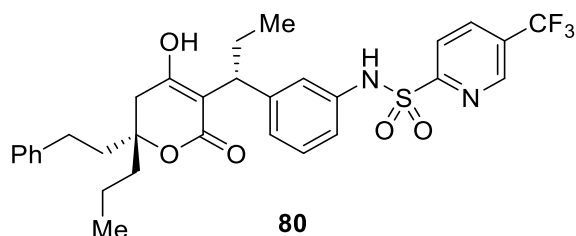


Figure 166: Tipranavir, component of HIV treatments⁷⁹

The majority of industrially relevant aromatic CF₃ compounds are synthesised using a variation of the Swarts reaction. This was first developed by Frédéric Swarts in 1892 and used a mixture of SbF₃ and SbCl₅ to convert trichloromethyl aromatics (**82**) (synthesised by chlorination of the appropriate toluene derivative (**81**)) to trifluoromethyl aromatics (**83**)⁸⁰. This process was developed further by Kinetic Chem. Inc. in 1934 to use anhydrous HF, and this method is still widely used today due to the ready availability of the starting materials (Fig. 167)⁸¹.

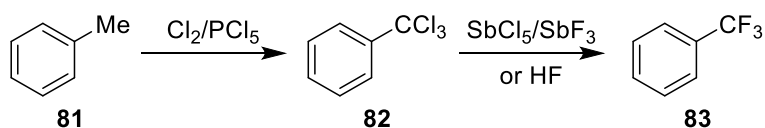


Figure 167: Synthesis of aromatic trifluoromethyl compounds using the Swarts reaction

However, at research and discovery scales, reagents such as chlorine gas and anhydrous HF can be difficult to handle. Consequently, a range of different trifluoromethylating agents have subsequently been developed⁸², and one of the most widely used of these is trifluoromethyltrimethylsilane (Me₃SiCF₃), more commonly known as the Ruppert – Prakash

reagent. The molecule was first isolated by Ingo Ruppert in 1984⁸³ and its chemistry as trifluoromethylating agent was developed by G. K. Surya Prakash from 1988 onwards^{72,73}.

Me_3SiCF_3 is synthesised by the reaction of Me_3SiCl with XCF_3 ($\text{X} = \text{Br}/\text{I}$), using a phosphine (III) compound (typically $\text{P}(\text{NEt}_2)_3$) as a halogen acceptor (Fig. 168)^{73,83}.

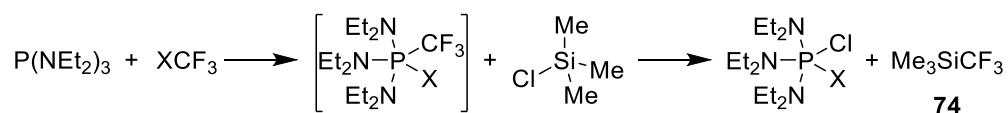


Figure 168: Synthesis of Me_3SiCF_3 from Me_3SiCl using XCF_3 ^{73,83}

Me_3SiCF_3 is a nucleophilic trifluoromethylating agent (a source of CF_3^-) and reacts with a wide variety of electrophiles such as carbonyl group containing compounds. For example, the mechanism of reaction with aldehydes and ketones is detailed in Fig. 169.^{72,73}

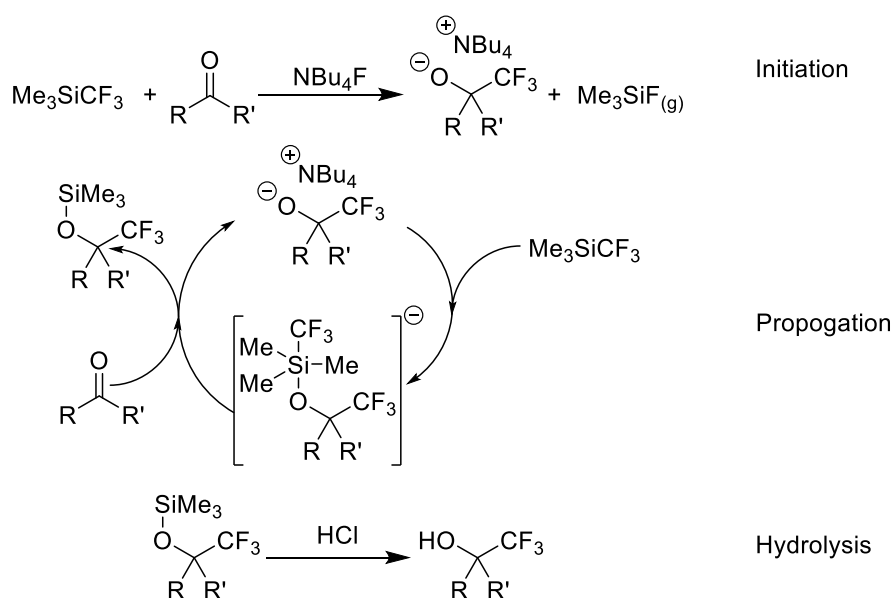


Figure 169: Mechanism for the reaction of ketones and aldehydes with Me_3SiCF_3 ^{72,73}

The reaction proceeds by an anionic chain mechanism through a negatively charged pentacoordinate silicon intermediate, initiated by a fluoride ion source e.g. tetrabutylammonium fluoride (TBAF). The principal product is the silylated compound $\text{RC}(\text{OSiMe}_3)(\text{CF}_3)\text{R}$, which is hydrolysed by HCl to produce the corresponding alcohol, $\text{RCOH}(\text{CF}_3)\text{R}$. A wide range of carbonyl substrates can be used in this reaction, including aliphatic and aromatic ketones⁷³, steroids⁸⁴, sugars^{85,86} (open chain form), carboxylic acid halides⁸⁷ and succinimides⁷³. In addition, Me_3SiCF_3 can be reacted with iodobenzene derivatives and CuI to produce trifluoromethyl aromatic compounds⁸².

5.1.2. Deoxofluorination Reactions – DAST

One of the most widely studied classes of nucleophilic fluorinating agents are the deoxofluorinating reagents. These sulfur – fluorides substitute oxygen atoms for fluorine and include both neutral and charged molecules (Fig. 170). The most readily available of these species is diethylaminosulfur trifluoride (DAST, **75**), the reagent used in this project.

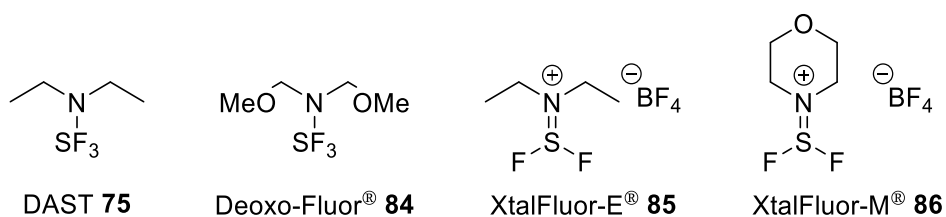


Figure 170: Various deoxofluorination reagents

The most commonly used substrates for deoxofluorination reactions are alcohols, although some aldehydes and ketones can be converted to geminal difluorides with an excess of a deoxofluorinating agent⁸⁸.

The reactions of DAST with primary alcohols is an S_N2 process, giving the corresponding fluorides with few side products⁸⁸ (Fig. 171).

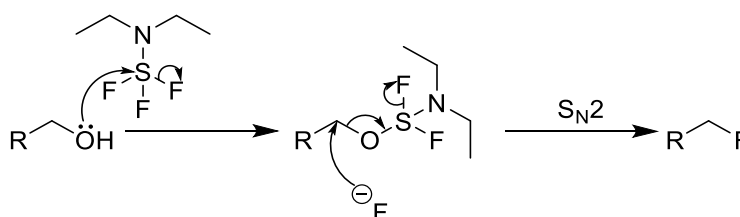


Figure 171: S_N2 reaction of DAST and a primary alcohol

Reactions with secondary alcohols produce secondary fluorides by the same method. These reactions are typically also S_N2 processes, confirmed by inversion of stereochemistry when using enantiomerically pure alcohol starting materials^{89–91} (Fig. 172).

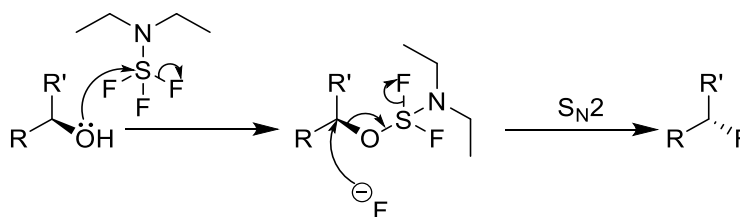


Figure 172: S_N2 reaction of DAST and a secondary alcohol with inversion of stereochemistry

However, the Et_2NOSF_2 moiety is a good leaving group, and this can lead to side reactions if the starting alcohol has any β hydrogen atoms. Instead of acting as a nucleophile the fluoride ion acts as a base and attacks the β hydrogen, leading to an E2 elimination reaction to produce an alkene product^{89,91} (Fig. 173).

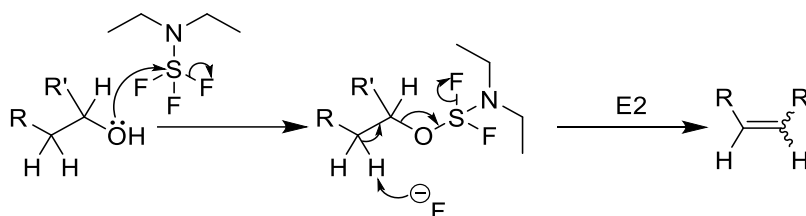


Figure 173: E2 elimination reaction of DAST and a secondary alcohol to give an alkene product

This reaction was reported by Leroy *et al.* when reacting 2-octanol (**87**) with DAST. The reaction produced a mixture of the intended 2-fluorooctane (**88**) product and several 2-octene elimination products (**89**) in a 48:52 ratio. These octene by-products were separated by converting them to the corresponding di-bromo compounds (**90**) and distilling the subsequent mixture⁸⁹ (Fig. 174).

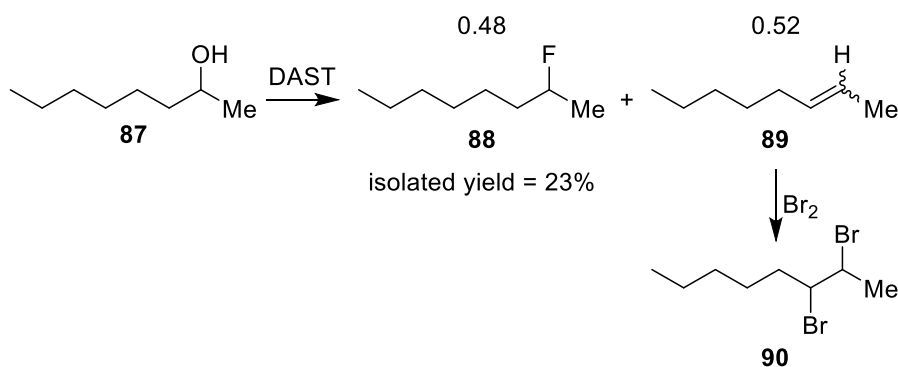


Figure 174: Reaction of 2-octanol with DAST, synthesising a mixture of 2-fluorooctane and 2-octenes⁸⁹

Eliminations were also observed by Sutherland *et al.* during the reaction of an amino acid derivative (**91**) with DAST. The first attempt at the reaction, using freshly distilled DAST, produced only the elimination product (**92**). However, reaction with DAST containing trace amounts of water produced a mixture consisting mainly of the intended fluorinated product (**93**) (with inversion of stereochemistry), as well as the intermediate (**94**) and only a small amount of **92**⁹¹ (Fig. 175).

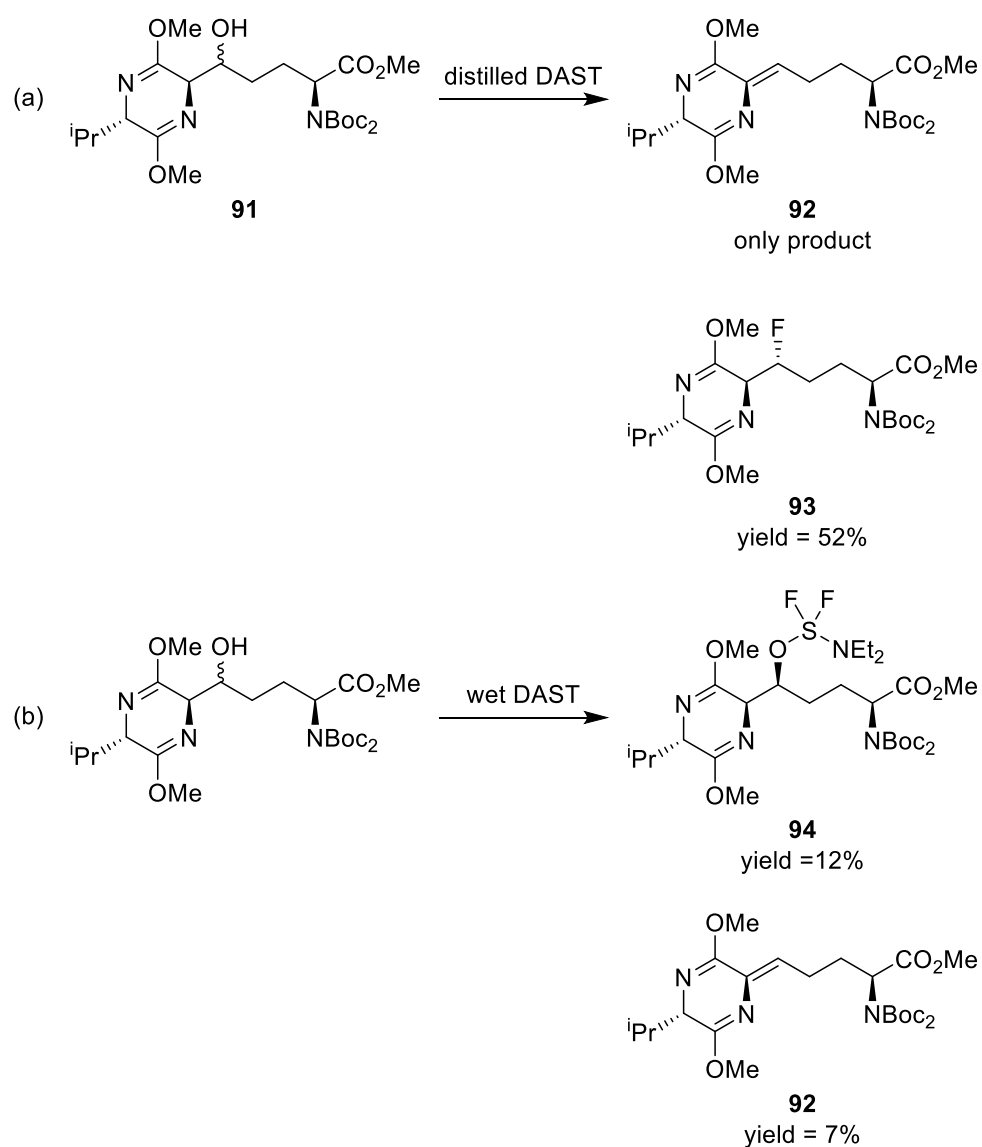


Figure 175: Reactions of an amino acid derivative with distilled (a) and wet (b) DAST and the products obtained⁹¹

Reactions of DAST with tertiary alcohols have not been widely explored as discussed previously, due to the forcing conditions required by the increased steric bulk of the alcohol starting materials. This can be problematic as DAST is known to explosively decompose at temperatures above 80 °C.

5.2. Reactions of Aldehydes and Ketones with Me₃SiCF₃

The first reactions investigated were those of nine different aldehydes and ketones with Me₃SiCF₃, based on a literature procedure^{72,73}. A wide range of substrates were used, including aromatic species, both cyclic and non-cyclic aliphatic compounds and three 1-substituted butan-1-ones (C₃H₇COR), in order to provide a variety of CF₃ containing substrates. The carbonyl compound was stirred in THF at room temperature and Me₃SiCF₃ was added, followed by a catalytic amount of TBAF. In the majority of cases, the reaction was stirred for three hours after which 6 M HCl was added and the aqueous mixture was stirred for a further 48 hours to hydrolyse the intermediate RC(OSiMe₃)(CF₃)R' species. The organic layer was extracted and the solvent removed *in vacuo* to yield the corresponding alcohol (Fig. 176, Table 23). However, the reactions with the C₃H₇COR required elevated reaction and hydrolysis times and temperatures due to the increased steric bulk of the side groups (Fig. 177, Table 24).

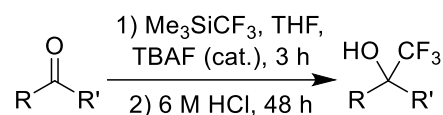
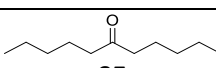
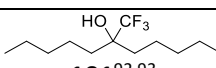
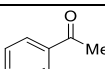
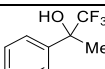
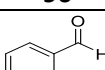
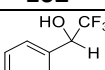
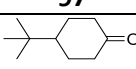
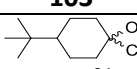
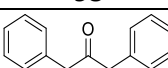
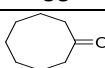
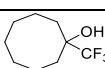


Figure 176: Reactions of aldehydes and ketones with Me₃SiCF₃

Table 23: Results from the reactions of aldehydes and ketones with Me₃SiCF₃

Starting Material	Product	Yield/ %
 95	 101 ^{92,93}	62
 96	 102 ⁸⁷	50
 97	 103 ⁸⁷	82
 98	 104 ⁹⁴	87
 99	Mixture	N.A.
 100	 105	47 (impure)

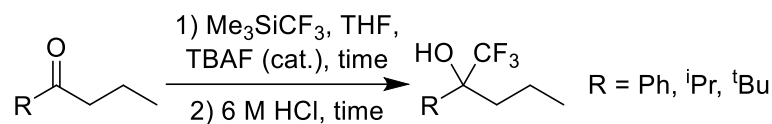


Figure 177: Reaction of 1-substituted butan-1-ones compounds with Me₃SiCF₃

Table 24: Reaction conditions for the synthesis of C₃H₇COH(CF₃)R

R	Product	Yield/%	Reaction with Me ₃ SiCF ₃		Hydrolysis with HCl	
			Time / h	Temperature/ °C	Time / h	Temperature/ °C
Ph, 106	109 ⁹⁵	26	24	rt	72	50
ⁱ Pr, 107	110	23	48	rt	120	50
^t Bu, 108	Not isolated	N.A.	72	50	504 (3 weeks)	50

As shown above, the majority of the carbonyl substrates produced the intended 1-trifluoromethyl alcohols in moderate to excellent yields, confirmed by comparing the ¹H, ¹⁹F and ¹³C NMR spectra of the compounds to literature data. However, deoxofluorination reactions with 1,3-diphenylpropanone (**99**) and C₃H₇CO^tBu (**108**) produced a complex mixture of products. This is due to the increased steric bulk of the side groups in these species leading to incomplete reaction and hydrolysis; the material extracted contained a mixture of the starting material, intermediate and 1-trifluoromethyl alcohol product that could not be separated. In addition, small amounts of 4-chloro-1-butanol (**112**), formed by the ring opening reaction of THF (**111**) with HCl, were observed in reactions that required elevated temperatures and durations for hydrolysis (Fig. 178).

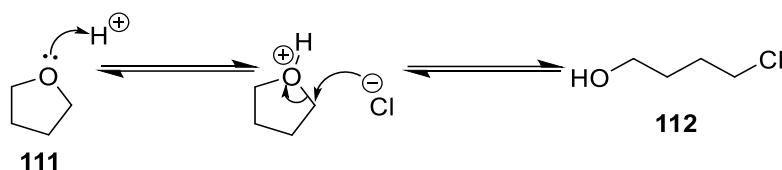


Figure 178: Ring opening of THF by HCl

The reaction of 4-*t*-butylcyclohexanone (**98**) with Me₃SiCF₃ formed two products in a 4:1 ratio as observed by ¹⁹F NMR spectroscopy resonances at -77.76 (major) and -84.78 (minor) ppm (Fig. 179).

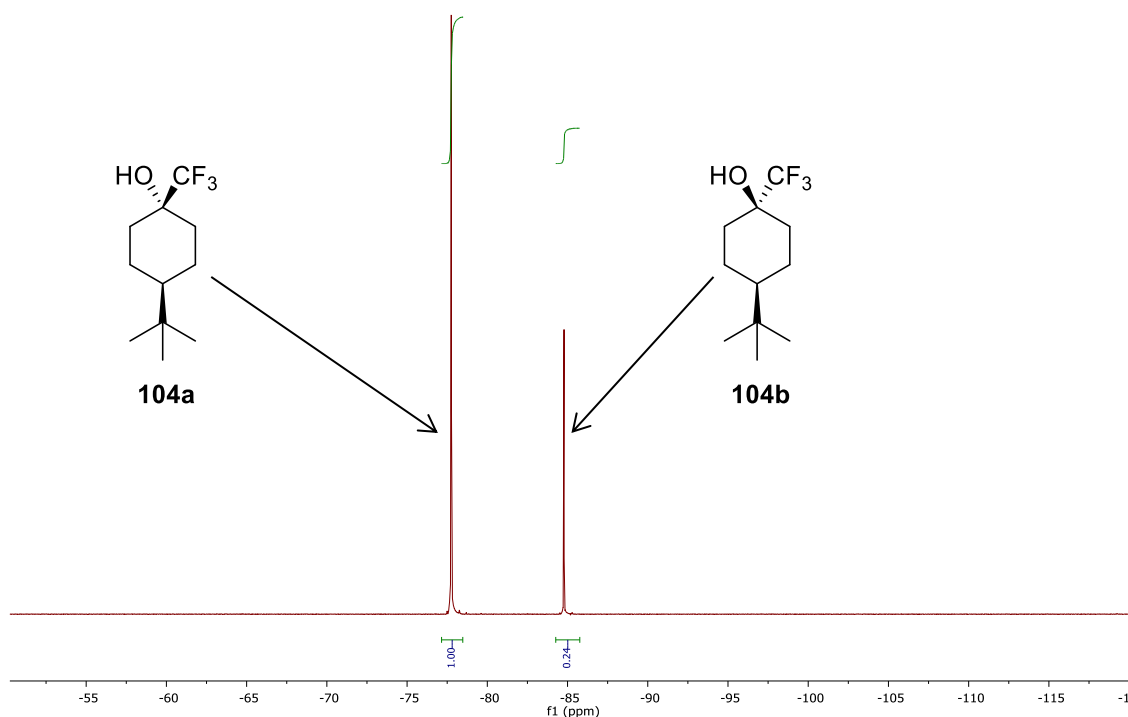


Figure 179: ¹⁹F NMR spectrum of 1-trifluoromethyl-4-*t*-butylcyclohexanol

The two products are the *cis* (**104a**) and *trans* (**104b**) alcohols, formed by attack of Me₃SiCF₃ on both faces of the ketone starting material. The major product is **104a**, confirmed by the molecular and crystal structures of 1-trifluoromethyl-4-*t*-butylcyclohexanol (**104**), and this selectivity is in agreement with literature syntheses of this species⁹⁴ (Fig. 180 and 181).

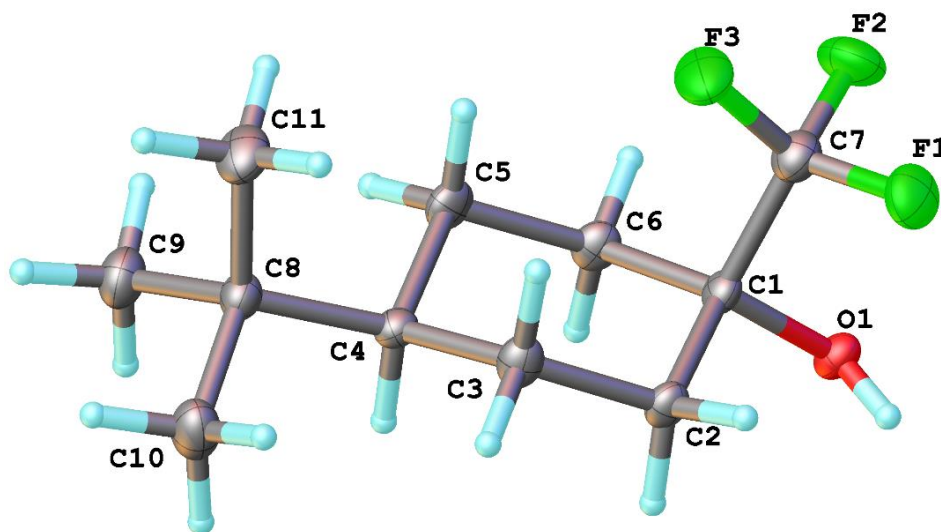


Figure 180: Molecular structure of 1-trifluoromethyl-4-*t*-butylcyclohexanol, determined by X-ray crystallography

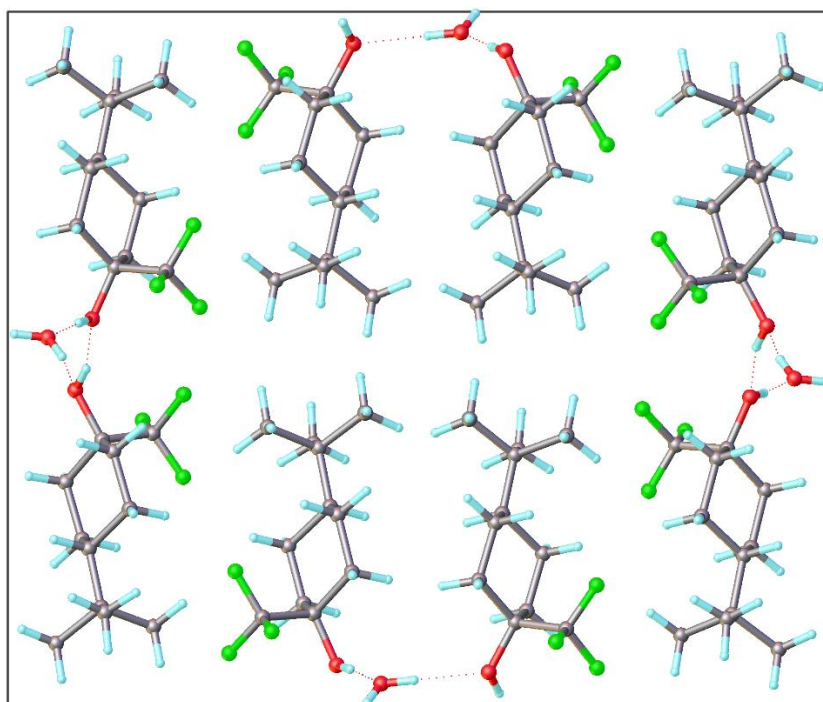


Figure 181: X-ray crystal structure of the semi-hydrate of 1-trifluoromethyl-4-*t*-butylcyclohexanol

This selectivity is due to the steric interactions in the pentacoordinate $[\text{ROSiMe}_3\text{CF}_3]^-$ intermediate of the reaction mechanism, as well as with the ROSiMe_3 species that forms before acid hydrolysis. The $\text{ROSiMe}_3/[\text{ROSiMe}_3\text{CF}_3]^-$ and CF_3 groups of the intermediates are both sterically bulky, but the observed selectivity indicates that the $\text{OSiMe}_3/[\text{ROSiMe}_3\text{CF}_3]^-$ groups have the strongest steric interactions with the protons of the cyclohexyl ring under these conditions. This leads to preferential formation of the *trans* alcohol by acid hydrolysis (Fig. 182).

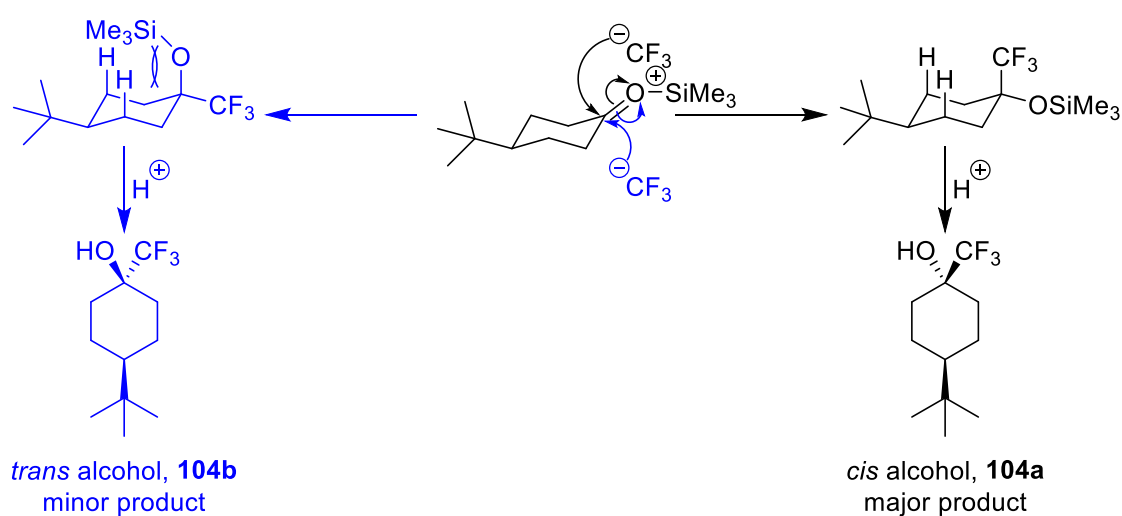


Figure 182: Explanation for the *cis* selectivity in the reaction of Me_3SiCF_3 with 4-*t*-butylcyclohexanone

Reactions of a range of aldehydes and ketones with Me_3SiCF_3 produced the desired $\text{RCOH}(\text{CF}_3)\text{R}'$ compounds in moderate yields. These species would be further reacted with DAST in an attempt to produce the corresponding $\text{RCF}(\text{CF}_3)\text{R}'$ species that are models of the $\text{CF}(\text{CF}_3)\text{CH}_2$ groups found in Viton[®] elastomers.

5.2.1. Reactions of Dicarbonyl Compounds with Me_3SiCF_3

In an attempt to synthesise Viton[®] model compounds that contained multiple $\text{CF}(\text{CF}_3)$ groups, two methods for the reactions of dicarbonyl compounds with Me_3SiCF_3 were investigated to produce systems with two $\text{C}(\text{OH})\text{CF}_3$ groups.

The reactions of dicarbonyl substrates were first attempted with the conditions used previously for the reactions of carbonyl compounds with Me_3SiCF_3 ^{72,73}. Due to the presence of multiple carbonyl groups, three equivalents of Me_3SiCF_3 were used and the reactions were carried out at elevated temperature (50 °C) for 48 hours, followed by hydrolysis with 6 M HCl for a further 48 hours (Fig. 183).

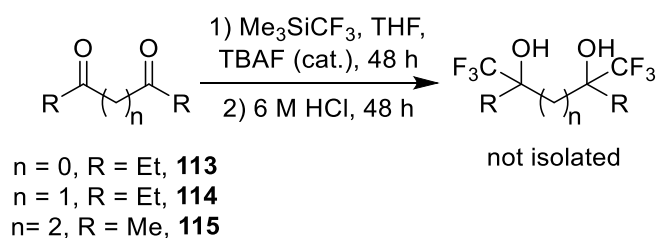


Figure 183: Reaction of a range of dicarbonyl compounds with Me_3SiCF_3 using TBAF as a catalyst

The ¹H and ¹⁹F NMR spectra and the GC-MS data from each of the reactions were indicative of complex mixtures of products. Due to the presence of multiple carbonyl groups in the starting material, it is likely that the extracted residues contain a mixture of the mono and di-addition products, as well as a mixture of fully and partially hydrolysed compounds (Fig. 184).

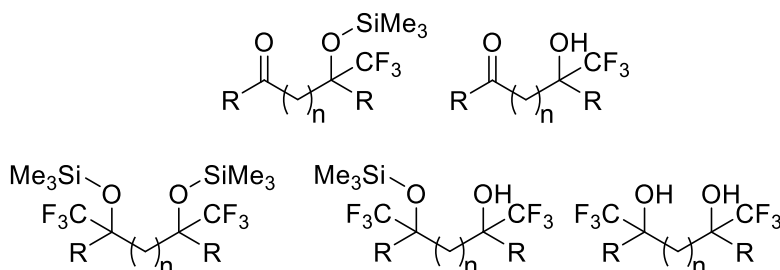


Figure 184: Possible products from the reactions of dicarbonyl compounds with Me_3SiCF_3

In an attempt to better control the mixture of products formed, reaction of $\text{MeCOCH}_2\text{CH}_2\text{COMe}$ (**115**) was repeated using one equivalent of Me_3SiCF_3 . By reducing the equivalents of Me_3SiCF_3 , it was hoped that the reaction would stop after one addition of CF_3 , producing only one product. However, as the ^{19}F NMR spectrum from the reaction shows, a mixture of trifluoromethylated products was still obtained, with a product profile similar to that observed when three equivalents of Me_3SiCF_3 was used (Fig. 185).

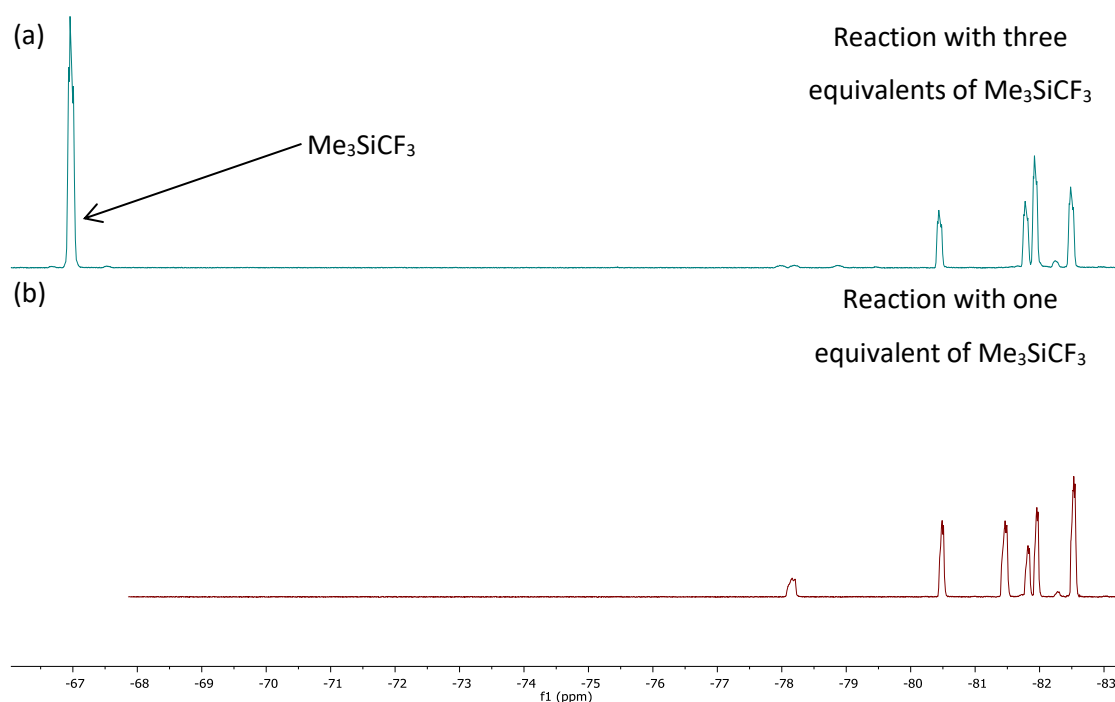


Figure 185: ^{19}F NMR spectra (before hydrolysis) from the reactions of $\text{MeCOCH}_2\text{CH}_2\text{COMe}$ with 3 equivalents (a) and 1 equivalents (b) of Me_3SiCF_3

A second route to model compounds containing multiple $\text{CF}(\text{CF}_3)$ groups was investigated using CsF as a catalyst⁹⁶. However, reaction of **115** with 3.25 equivalents of Me_3SiCF_3 and catalytic CsF led to a complex mixture of products by ^{19}F NMR spectroscopy and GC-MS analysis from which pure products could not be isolated. Due to the difficulties encountered in these syntheses, this strategy was abandoned.

5.3. Reactions of $\text{RCOH}(\text{CF}_3)\text{R}$ Compounds with DAST

Having synthesised a range of different $\text{RCOH}(\text{CF}_3)\text{R}$ derivatives, these species were subsequently reacted with the deoxofluorination reagent DAST in attempts to synthesise $\text{RCF}(\text{CF}_3)\text{CH}_2\text{R}'$ compounds that are models of structure (d) found in Viton[®] elastomers.

The first reactions that were investigated were those in Table 25. The alcohol was dissolved in DCM at 0 °C and 2.2 equivalents of DAST in DCM was added. The reactions were allowed to warm to room temperature and stirred for 48 hours after which excess DAST was hydrolysed with sat. NaHCO₃ and the product was extracted *in vacuo* (Fig. 186, Table 25).

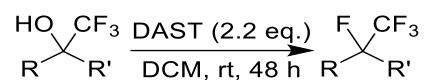
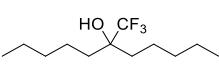
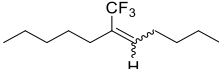
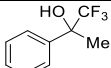
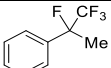
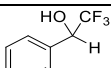
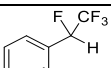
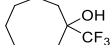


Figure 186: Reaction of trifluoromethyl alcohols with DAST

Table 25: Results from the reactions of trifluoromethyl alcohols with DAST

Starting Material	Product	Yield/ %
 101	 116	48
 102	 117 ⁹⁷	44
 103	 118 ⁹⁸	39
 104	 119 ⁹⁴	61
 105	mixture	N.A.

Of the five alcohols reacted, only 1-trifluoromethyl-1-phenylethanol (**102**) and 1-trifluoromethyl-1-phenylmethanol (**103**) were converted to the intended RCF(CF₃)R products, producing 1-trifluoromethyl-1-fluoro-1-phenylethane (PhCF(CF₃)Me, **117**) and 1-trifluoromethyl-1-fluoro-1-phenylmethane (PhCF(CF₃)H, **118**) respectively. ¹H, ¹⁹F and ¹³C NMR spectroscopy confirms the structure of these products. For example, in the case of **118**, conversion to the intended product is confirmed by the presence of a doublet of quartets (5.60 ppm, PhCF(CF₃)H, ²J_{HF} = 44.2 Hz, ³J_{HF} = 6.1 Hz) in the ¹H NMR spectra, and a quartet of doublets (122.25 ppm, PhCF(CF₃)H, ¹J_{CF} = 280.7 Hz, ²J_{CF} = 28.2 Hz) and doublet of quartets (88.96 ppm, PhCF(CF₃)H, ¹J_{CF} = 186.2 Hz, ²J_{CF} = 34.9 Hz) in the ¹³C NMR spectra of **118**. There is also a new signal in the ¹⁹F NMR spectra of **118**, a doublet of quartets at -194.62 ppm (²J_{FH} = 44.1 Hz, ³J_{FF} = 12.8 Hz) for the tertiary fluorine atom (PhCF(CF₃)H).

However, all other alcohols that were reacted did not produce the intended deoxofluorination products. Reaction of DAST with 1-trifluoromethyl-4-*t*-butylcyclohexanol (**104**) yielded 1-trifluoromethyl-4-*t*-butylcyclohex-1-ene (**119**), the dehydrofluorinated derivative of the intended product, as confirmed by ^{19}F and ^{13}C NMR spectroscopy (Fig. 187 and 188).

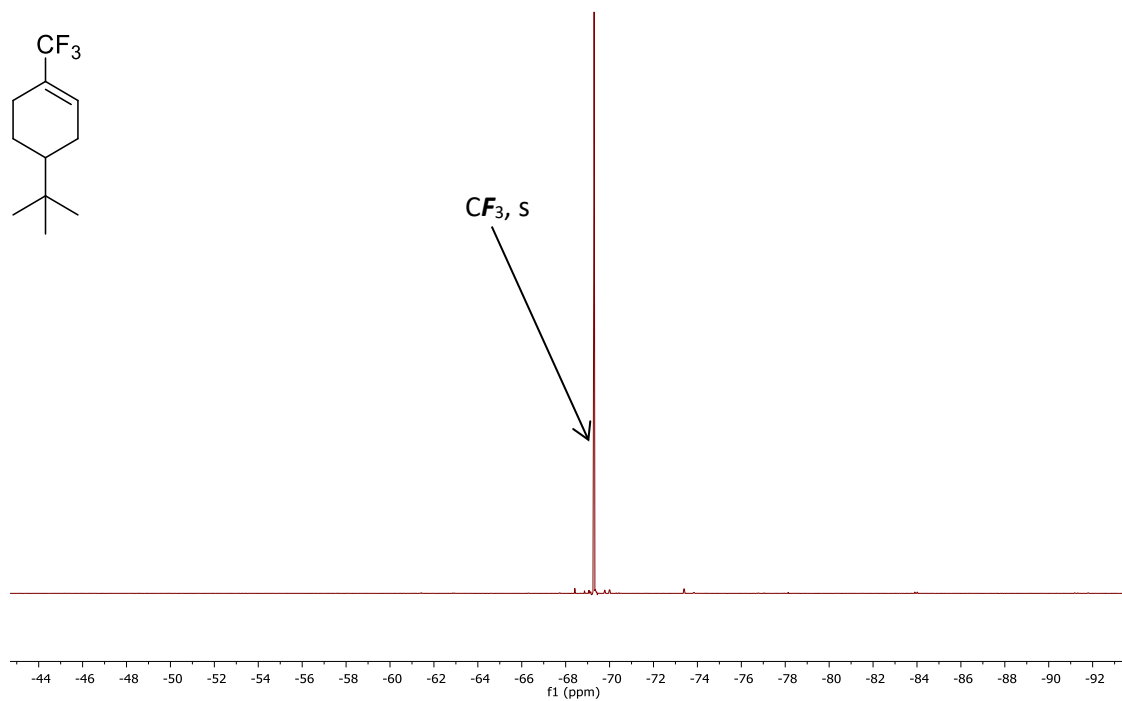


Figure 187: ^{19}F NMR spectrum of 1-trifluoromethyl-4-*t*-butylcyclohex-1-ene

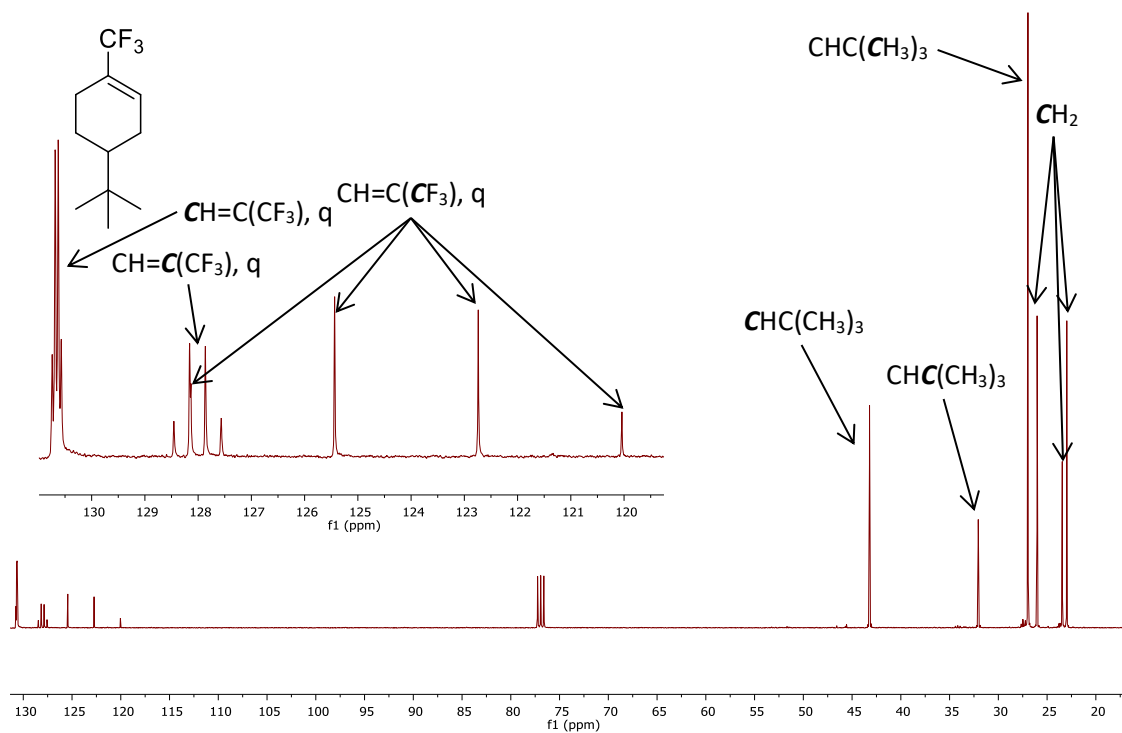


Figure 188: ^{13}C NMR spectrum of 1-trifluoromethyl-4-*t*-butylcyclohex-1-ene and expansion of the region between 131 and 119 ppm

The ^{19}F NMR spectra contains only a singlet at -69.30 ppm for the CF_3 group of the actual product, trifluoromethyl-4-*t*-butylcyclohex-1-ene (**119**), and this structure is confirmed by the three quartets present in the ^{13}C NMR spectra at 130.66 ($^3J_{\text{CF}} = 5.7$ Hz, $\text{CH}=\text{C}(\text{CF}_3)$), 128.01 ($^3J_{\text{CF}} = 29.8$ Hz, $\text{CH}=\text{C}(\text{CF}_3)$) and 124.09 ppm ($^1J_{\text{CF}} = 271.4$ Hz, $\text{CH}=\text{C}(\text{CF}_3)$), indicative of the presence of an alkene group.

Additionally, the reaction of 6-trifluoromethylundecan-6-ol (**101**) with DAST produced two products, both of which are consistent with 6-trifluoromethylundec-5-ene ($\text{C}_4\text{H}_9\text{CH}=\text{C}(\text{CF}_3)\text{C}_5\text{H}_{11}$, **116**), as observed by GC-MS and ^1H and ^{19}F NMR spectroscopy (Fig. 189 – 191).

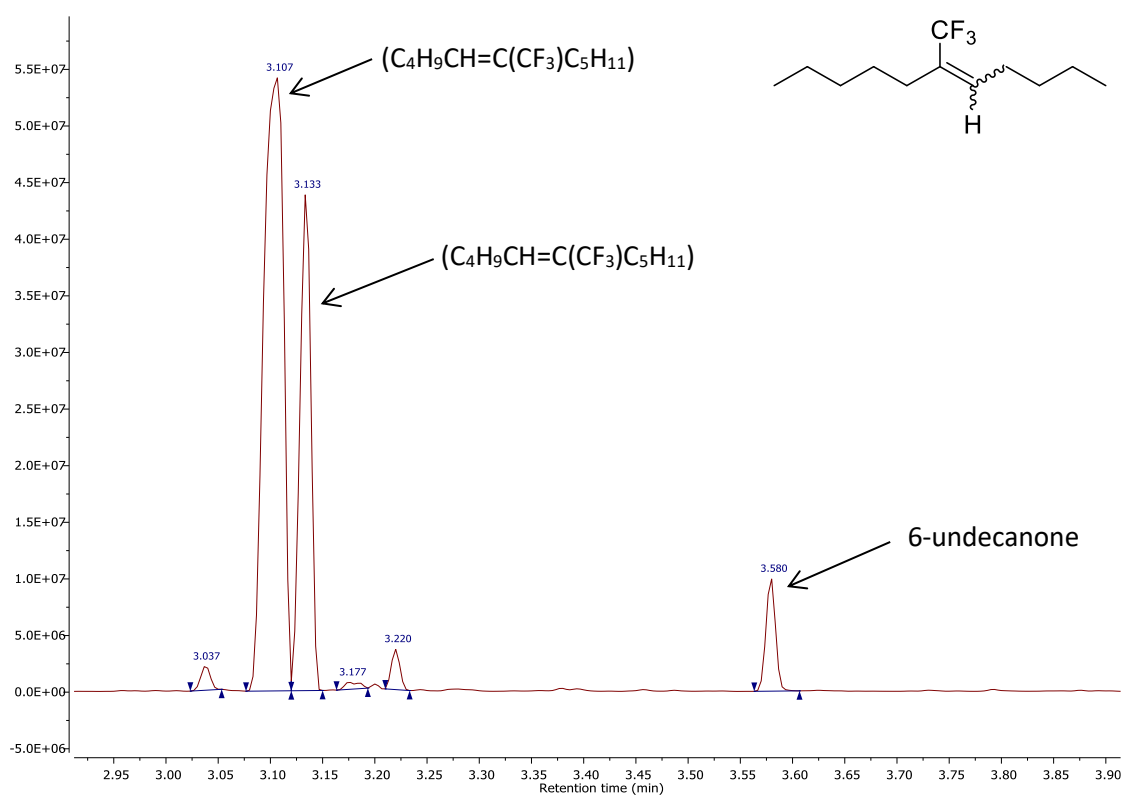


Figure 189: Gas chromatogram of $\text{C}_4\text{H}_9\text{CH}=\text{C}(\text{CF}_3)\text{C}_5\text{H}_{11}$

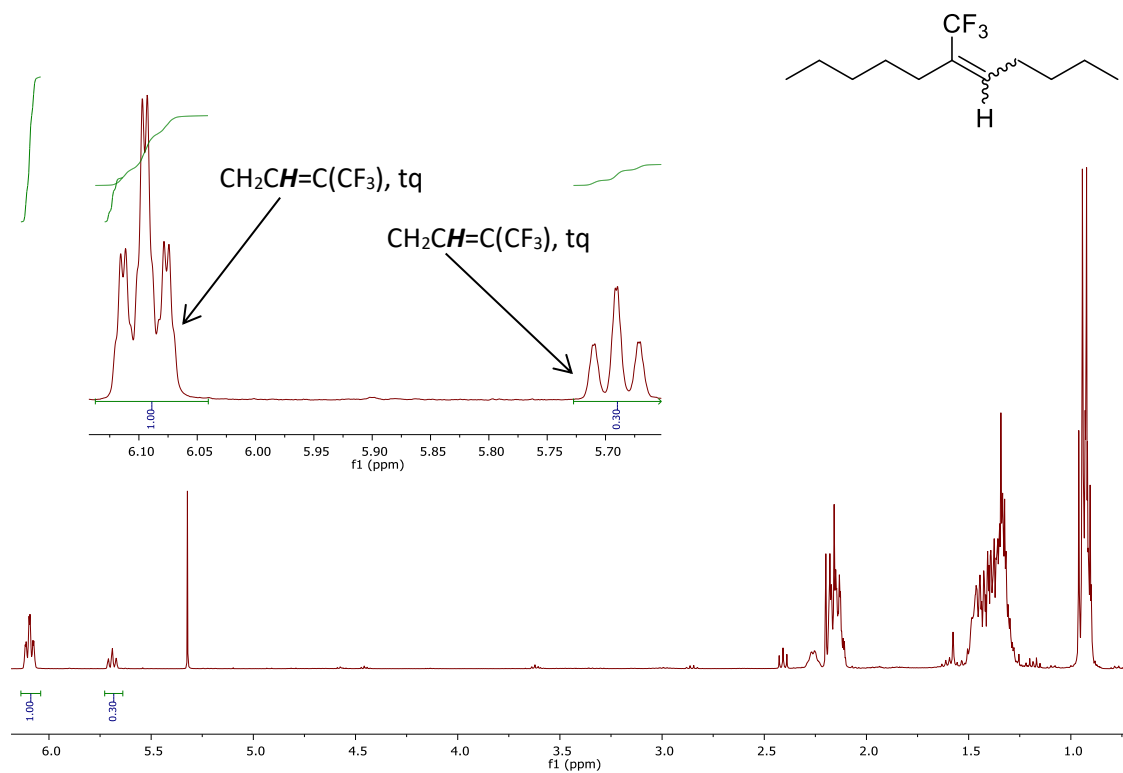


Figure 190: ^1H NMR spectrum of $\text{C}_4\text{H}_9\text{CH}=\text{C}(\text{CF}_3)\text{C}_5\text{H}_{11}$

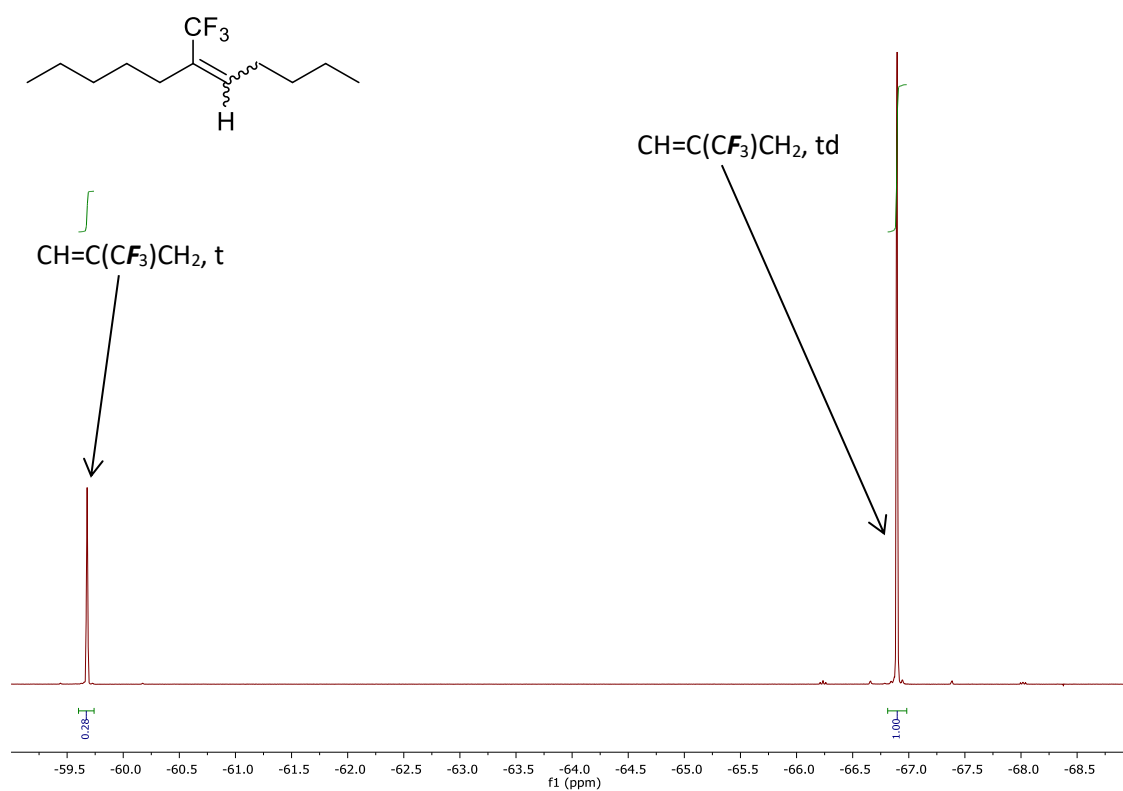


Figure 191: ^{19}F NMR spectrum of $\text{C}_4\text{H}_9\text{CH}=\text{C}(\text{CF}_3)\text{C}_5\text{H}_{11}$

The two products are the *cis* and *trans* isomers of **116** in a 1:4 ratio. However, it is not certain from the above data which isomer is the major product. In the ^1H NMR spectrum, the $\text{CH}_2\text{CH}=\text{C}(\text{CF}_3)$ resonances for both isomers are triplets of quartets, the first at 6.09 ppm ($^3J_{\text{HH}} = 7.4$ Hz, $^4J_{\text{HF}} = 1.8$ Hz) and the second at 5.69 ppm ($^3J_{\text{HH}} = 7.8$ Hz, $^4J_{\text{HF}} = 1.1$ Hz), giving no indication as to which signal corresponds to which isomer. By contrast, the $\text{CH}=\text{C}(\text{CF}_3)\text{CH}_2$ resonances for the two isomers in the ^{19}F NMR spectrum are different; there is a triplet at -59.74 ppm ($^4J_{\text{FH}} = 2.2$ Hz) and triplet of doublets at -66.97 ppm ($^4J_{\text{FH}} = 2.2$ Hz, $^4J_{\text{FH}} = 1.9$ Hz). The absence of a second coupling in the resonance at -59.74 ppm (from the minor product) suggests that this may be the *cis* isomer as groups that are *cis* typically have weak or non-existent couplings to each other.

There are two possible methods by which these dehydrofluorinated products could form in these reactions; either by elimination of Et_2NSOF and HF during the reaction with DAST, or elimination of HF from the intended deoxofluorination product during workup with NaHCO_3 (Fig. 192).

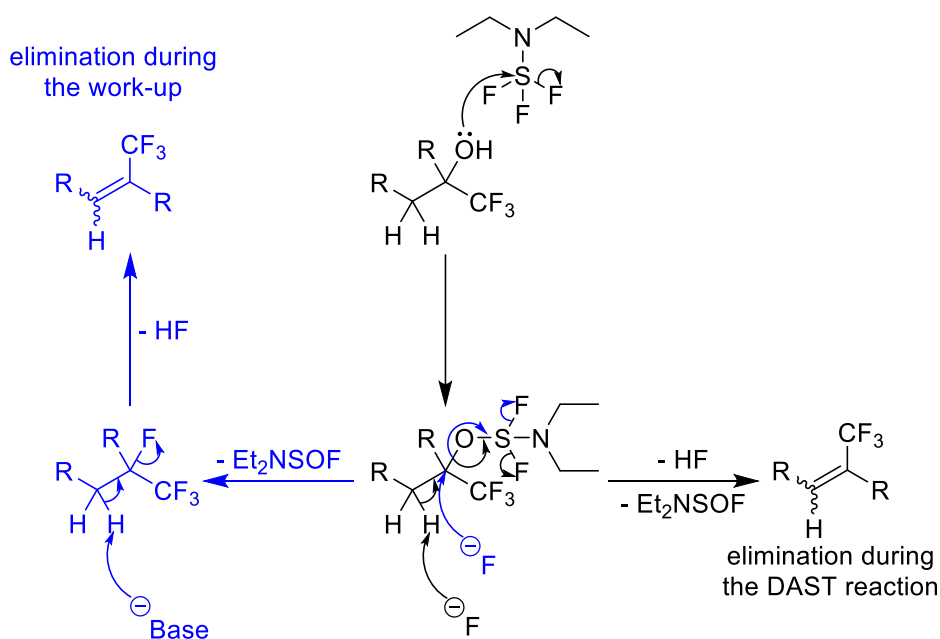


Figure 192: Possible mechanisms for the formation of dehydrofluorinated products during reactions with DAST

In order to further investigate these dehydrofluorination reactions, the previously synthesised 1-substituted 1-trifluorobutan-1-ols ($C_3H_7COH(CF_3)Ph$ and $C_3H_7COH(CF_3)^iPr$) were reacted with DAST under similar conditions (Fig. 193). The reactions were analysed by ^{19}F NMR spectroscopy before and after work-up with $NaHCO_3$ so that the mechanisms of the dehydrofluorination processes could be determined.

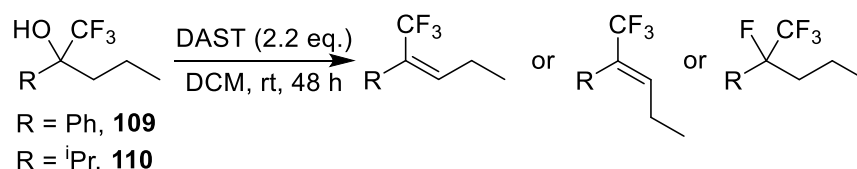


Figure 193: Reaction of $C_3H_7COH(CF_3)R$ compounds with DAST

The first reaction that was investigated was that of $C_3H_7COH(CF_3)Ph$ (**109**) with DAST. The ^{19}F NMR spectra of the product of this reaction before and after work-up are shown in Fig. 194.

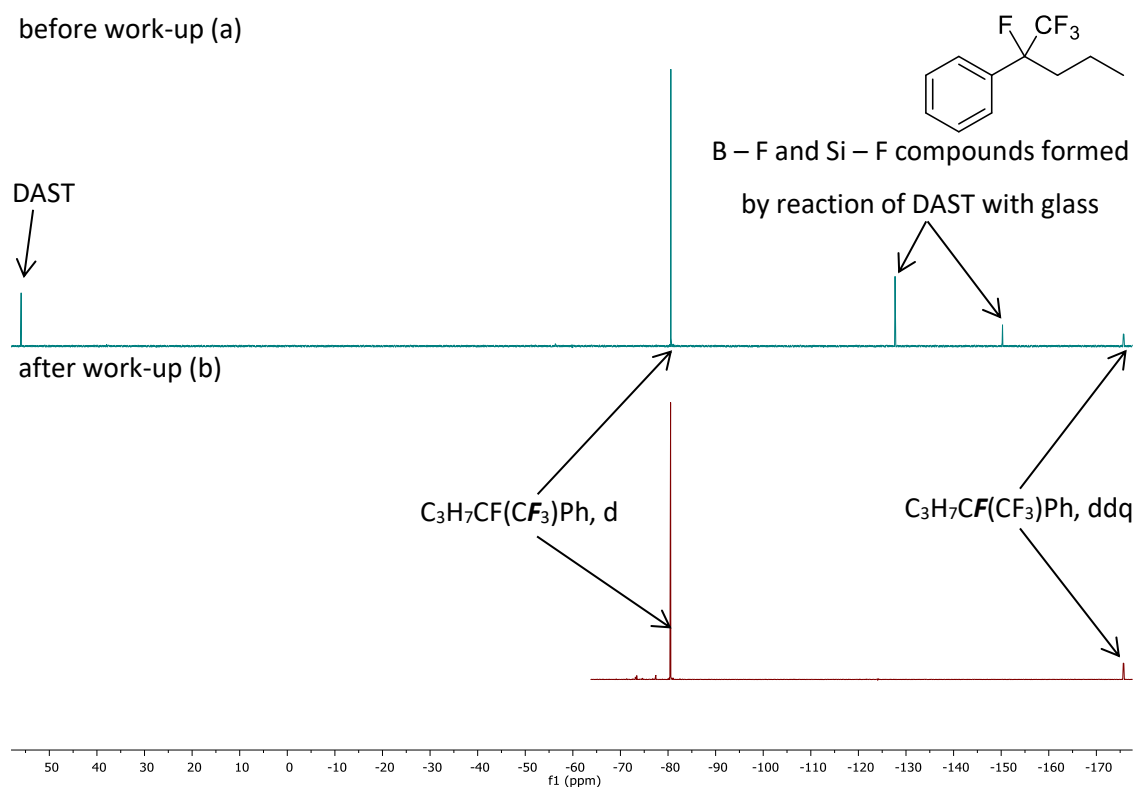


Figure 194: ^{19}F NMR spectra of the products of the reaction of $C_3H_7COH(CF_3)Ph$ with DAST before (a) and after (b) work-up

As the ^{19}F NMR spectra show, $C_3H_7CF(CF_3)Ph$ (**120**) was successfully synthesised by deoxofluorination of **109**, and no dehydrofluorination occurred during either the reaction with DAST or the work-up. This is confirmed by the splitting patterns and chemical shifts of the two fluorine signals. There is a doublet at -80.53 ppm ($^3J_{FF} = 6.9$ Hz) for the $CF(CF_3)$ group, and a doublet of doublet of quartets at -175.71 ppm ($^3J_{FH} = 37.4$ Hz, $^3J_{FH} = 13.9$ Hz, $^3J_{FF} = 7.0$ Hz) for

the $CF(CF_3)$ group. The complex splitting pattern of this signal is due to the ${}^3J_{FF}$ coupling to the neighbouring CF_3 , and the two unique ${}^3J_{FH}$ couplings to the two neighbouring diastereotopic protons (Fig. 195).

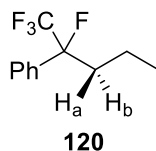


Figure 195: Diastereotopic protons coupling to the fluorine in $PhCF(CF_3)CH_2CH_2CH_3$

The second reaction that was investigated was that of $C_3H_7COH(CF_3)^iPr$ (**110**) with DAST. The reaction produced a mixture of different products, as observed in the ${}^{19}F$ NMR spectra before and after work-up (Fig. 196).

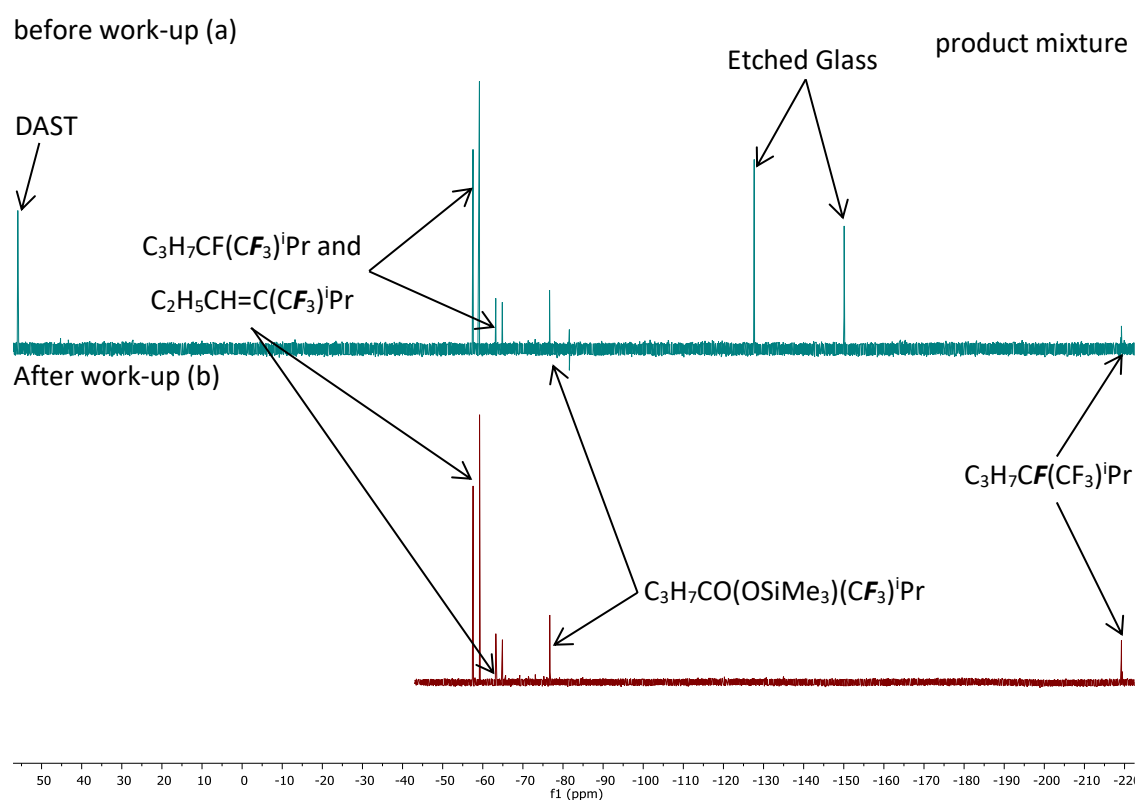


Figure 196: ${}^{19}F$ NMR spectra of the products from the reaction of $C_3H_7COH(CF_3)^iPr$ with DAST before (a) and after (b) work-up

As the ${}^{19}F$ NMR spectra show, a mixture of different products including the intended deoxofluorination product and dehydrofluorinated elimination products were all formed before the addition of $NaHCO_3$, suggesting that the dehydrofluorinated products are formed during the deoxofluorination reactions with DAST.

The results above can be used to explain the selectivity of the different reactions of $RCH_2COH(CF_3)R$ compounds with DAST. Depending on the substrate, both S_N1 and S_N2 reactions are possible when reacting DAST with tertiary alcohols, as detailed in Fig. 197.

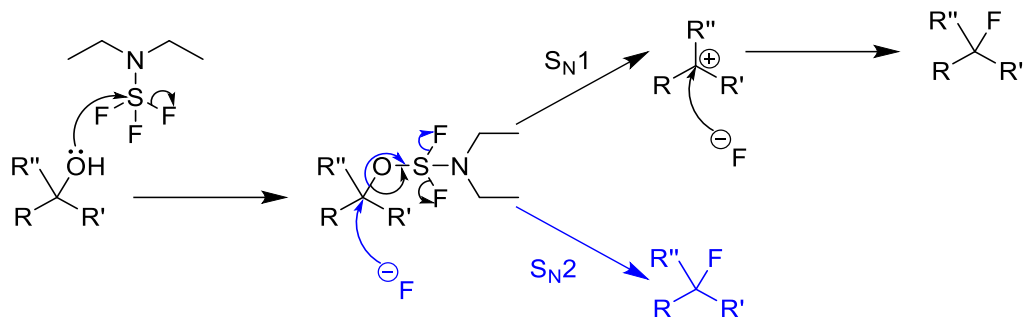


Figure 197: Mechanism for the reaction of DAST with an alcohol

However, the CF_3 group is relatively sterically demanding, as observed previously by Nagal *et al.* while investigating the dehydration of homoallyl CF_3 alcohols (Fig. 198)⁹⁹. The results from these reactions are detailed in Table 26 and indicate that CF_3 groups have a steric bulk similar to cyclohexyl groups.

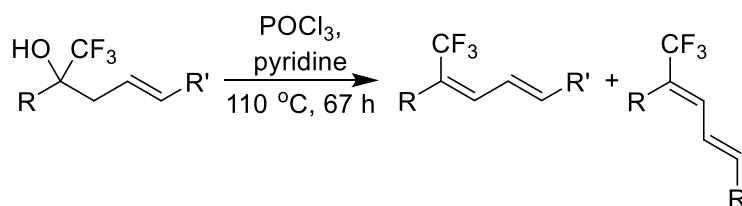


Figure 198: Dehydration of homoallyl CF_3 alcohols⁹⁹

Table 26: Results from the dehydration of homoallyl CF_3 alcohols⁹⁹

R	H	Me	Ph	ⁿ Bu	ⁱ Bu	cyclohexyl	^s Bu	hexyl
R'	ⁿ Pr	SiMe ₃						
<i>cis:trans</i>	13:2	9:2	3:1	2:1	5:2	7:8	2:3	1:10

The CF_3 group is also electron withdrawing and would destabilise a neighbouring carbocation centre. This can inhibit both the S_N1 and S_N2 mechanisms of the DAST reaction, as was the case for the reaction with $C_3H_7COH(CF_3)^iPr$ (**110**) (Fig. 199).

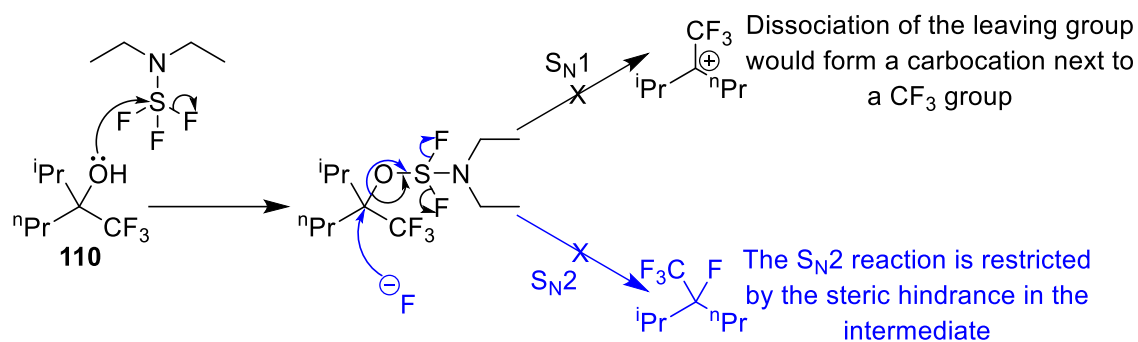


Figure 199: Reasons for the lack of formation of $\text{C}_3\text{H}_7\text{CF}(\text{CF}_3)\text{iPr}$ from $\text{C}_3\text{H}_7\text{COH}(\text{CF}_3)\text{iPr}$ using DAST

Instead, the intermediate undergoes an elimination reaction, producing a mixture of alkene products (Fig. 200).

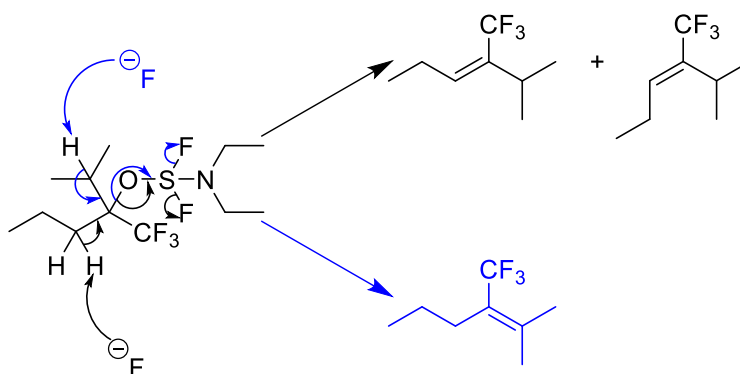


Figure 200: Elimination of Et_2NSOF from $\text{C}_3\text{H}_7\text{C}(\text{OSF}_2\text{NEt}_2)(\text{CF}_3)\text{iPr}$ to give a mixture of alkene products

The elimination of Et_2NSOF from DAST reaction intermediates has been reported as discussed earlier in this chapter^{89,91}, and $\text{C}_5\text{H}_{11}\text{COH}(\text{CF}_3)\text{C}_5\text{H}_{11}$ (**101**) underwent a similar elimination reaction to form the mixture of *cis* and *trans* $\text{C}_4\text{H}_9\text{CH}=\text{C}(\text{CF}_3)\text{C}_5\text{H}_{11}$ (**116**) observed previously.

In the case of $C_3H_7COH(CF_3)Ph$ (**109**), the intended deoxofluorination product ($C_3H_7CF(CF_3)Ph$ (**120**)) was synthesised without any evidence of elimination reactions having occurred. This is due to resonance stabilisation of the carbocation intermediate from the S_N1 process, and the reduced steric hindrance of the S_N2 intermediate (although the S_N1 mechanism is most plausible) (Fig. 201).

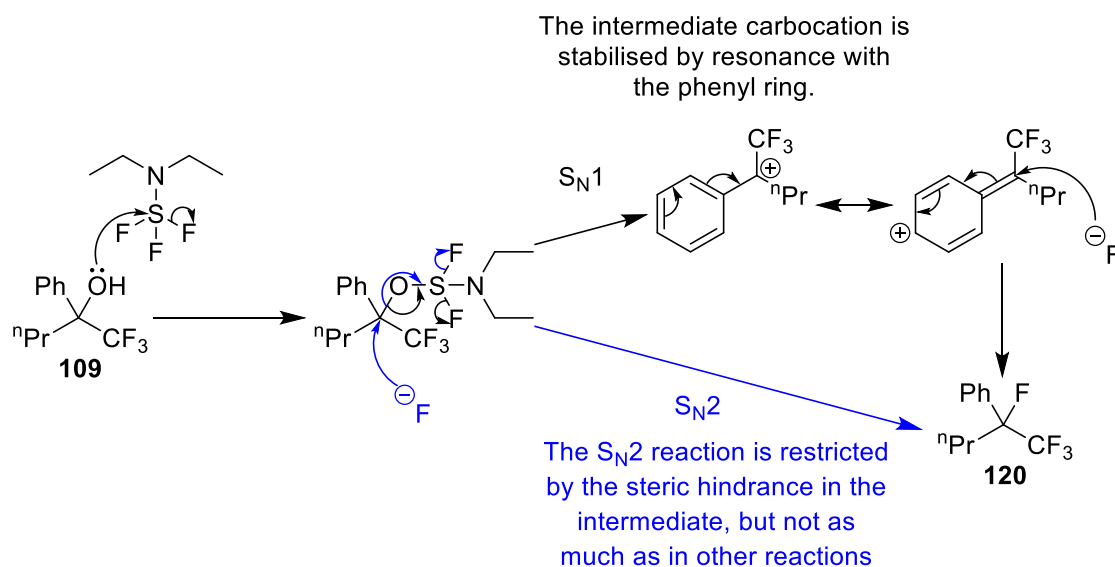


Figure 201: Mechanism for the synthesis of $C_3H_7CF(CF_3)Ph$ from $C_3H_7COH(CF_3)Ph$ using DAST

The proposed mechanisms above explain why the reaction of $C_3H_7COH(CF_3)Ph$ (**109**) with DAST synthesised the intended deoxofluorination product, whereas reaction with $C_3H_7COH(CF_3)Pr$ (**110**) and $C_5H_{11}COH(CF_3)C_5H_{11}$ (**101**) formed alkene elimination products instead. Alkene products are formed by the E2 elimination of Et_2NSOF from the intermediate species in the reactions of DAST with $RCH_2COH(CF_3)R'$, not by dehydrofluorination of $RCH_2CF(CF_3)R'$ as previously hypothesised. These reactions occur when the groups R and R' are sterically bulky and not capable of stabilising an intermediate carbocation by resonance, such as alkyl groups, favouring elimination over substitution. By contrast, the reaction of **109** with DAST produced the intended deoxofluorination product ($C_3H_7CF(CF_3)Ph$ (**120**)), most likely by an S_N1 substitution at the intermediate species in the DAST reaction via a carbocation that is stabilised by resonance with the neighbouring phenyl group.

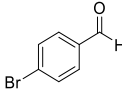
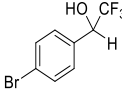
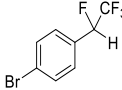
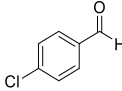
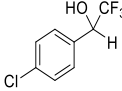
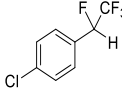
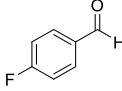
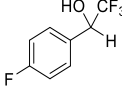
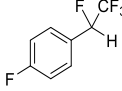
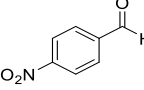
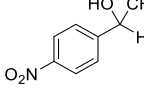
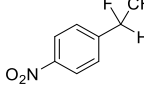
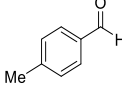
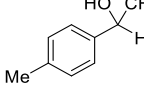
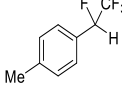
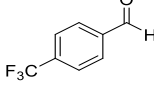
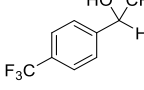
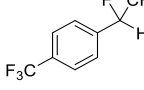
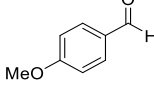
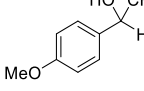
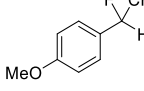
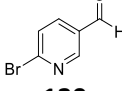
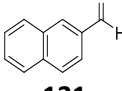
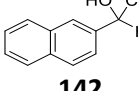
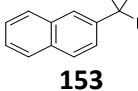
5.4. Conclusion

As a possible route to models of the $\text{CF}(\text{CF}_3)\text{CH}_2$ group found in Viton[®] elastomers, reactions of carbonyl compounds with the Me_3SiCF_3 , and subsequent deoxofluorination reactions of the alcohol products with DAST, were investigated. A range of aromatic and aliphatic ketones and aldehydes were reacted with Me_3SiCF_3 , producing the intended $\text{RCH}_2\text{COH}(\text{CF}_3)\text{R}'$ products in the majority of cases. However, subsequent reactions of these alcohols with DAST produced a mixture of the intended $\text{RCH}_2\text{CF}(\text{CF}_3)\text{R}'$ deoxofluorination products and $\text{RCH}=\text{C}(\text{CF}_3)\text{R}'$ compounds that are produced through elimination reactions depending on the structure of the substrate.

The chemoselectivity of these reactions can be explained by the nature of the substituent groups R and R'. In the case where R' is a phenyl group, the intended deoxofluorination product is formed by an $\text{S}_{\text{N}}1$ substitution, as the carbocation intermediate in this reaction is stabilised by the neighbouring aromatic group. However, when R and R' are both aliphatic, the intended substitution reaction is inhibited by the presence of the electron withdrawing CF_3 group and the other sterically bulky side groups. Under these circumstances, the elimination reaction is favoured, producing a mixture of alkene products.

Due to the competing dehydrofluorination reactions, the required $\text{RCH}_2\text{CF}(\text{CF}_3)\text{R}'$ species could not be produced by these reactions for use as models of structure (d) found in Viton[®] elastomers. However, the reactions of benzaldehydes with Me_3SiCF_3 and DAST have been investigated further in Durham following on from the work described in this thesis. Specifically, the reactions of a range of benzaldehyde derivatives have been investigated by D. Cooper (M.Sc), synthesising the corresponding $\text{ArCHF}(\text{CF}_3)$ in good yields (Table 27). These compounds have been used in conformational analysis studies and for further reactions such as nitrations. They are also potentially useful as starting materials for the synthesis of agrochemical and pharmaceutical compounds.

Table 27: ArCHF(CF₃) derivatives synthesised by D. Cooper

Starting Material	Alcohol Intermediate	Yield of Alcohol/ %	Final Product	Yield of Product/ %
 97	 103	70	 118	42
 121	 132	36	 143	49
 122	 133	85	 144	49
 123	 134	51	 145	81
 124	 135	36	 146	94
 125	 136	37	 147	21
 126	 137	67	 148	12
 127	 138	74	 149	65
 128	 139	59	 150	43
 129	 140	51	 151	58
 130	 141	72	 152	85
 131	 142	46	 153	74

6. Conclusion

A variety of different Viton® model compounds were synthesised by the reactions of perfluoroalkyl iodides with VDF and subsequent capping with SbF₅ (Fig. 202). Specifically models of structures (a) – (e) were synthesised (Fig. 203).

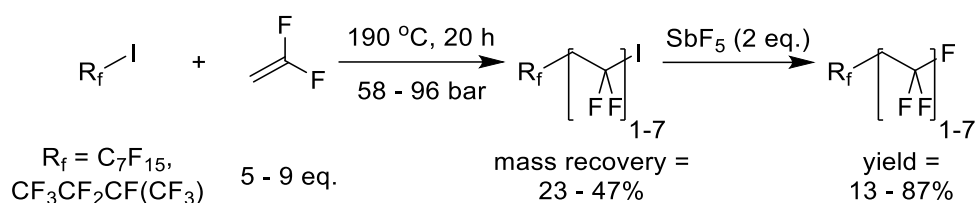


Figure 202: Synthesis of Viton® model compounds

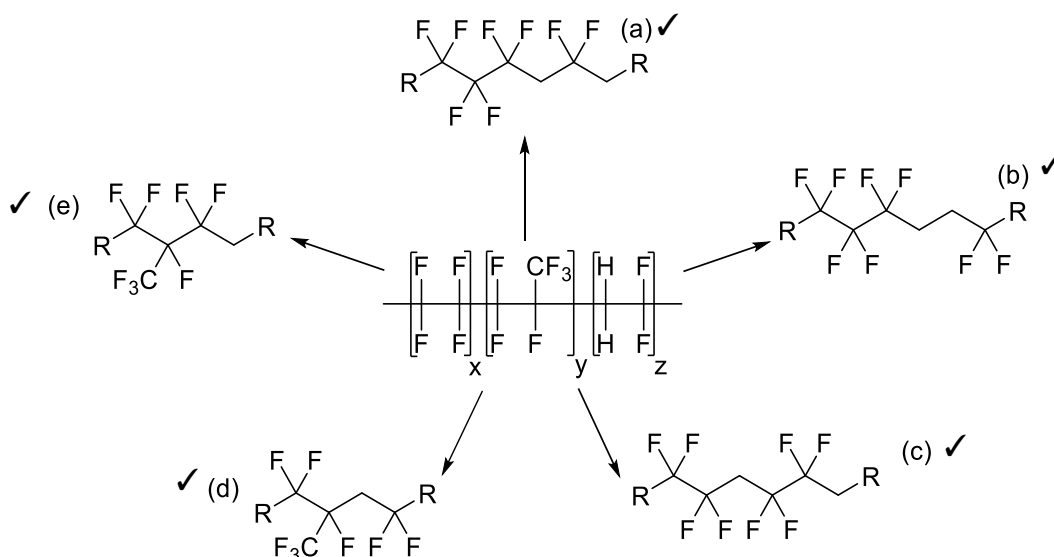


Figure 203: Structures found within Viton® that were synthesised in this project

Models of structures (a) – (d) were subsequently reacted with a range of bases and the products were characterised by NMR spectroscopy and mass spectrometry.

Models of structure (a) were the major components of the product mixture formed in the reaction of $C_8F_{17}I$ (**45**) with VDF (**1**) and SbF_5 , synthesising $C_8F_{17}(CH_2CF_2)_{1-4}F$ (**49**). These compounds were reacted with both organic (amine) and inorganic bases causing dehydrofluorination, and the principal products depended on which base was used (Fig. 204).

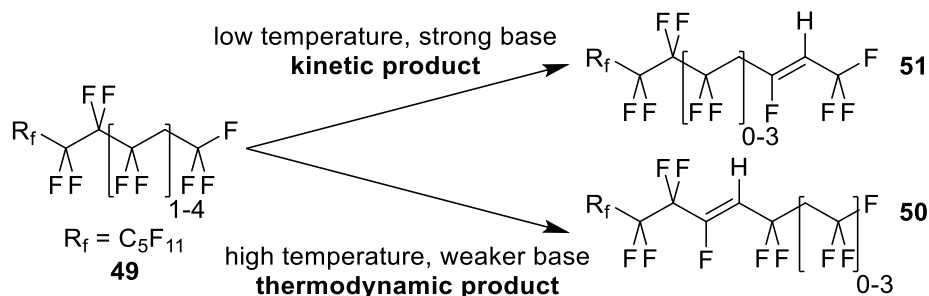


Figure 204: Major products from the reactions of $C_8F_{17}(CH_2CF_2)_{1-4}F$, a model of structure (a), with different bases

In addition, reaction of **49** with KOMe produced several products with the structure $C_7F_{15}C(OMe)=CH(CF_2CH_2)_{0-3}CF_3$ (**56**), formed by nucleophilic attack of methoxide ions on the dehydrofluorinated species (Fig. 205).

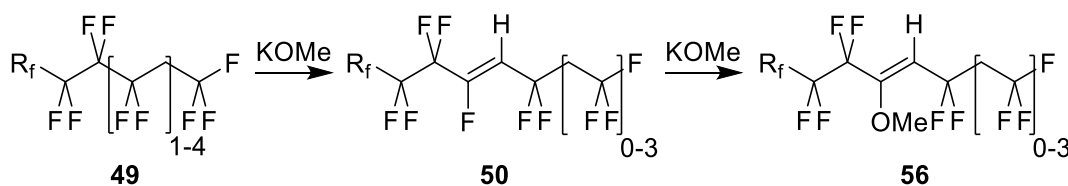


Figure 205: Reaction of $C_8F_{17}(CH_2CF_2)_{1-4}F$ with KOMe

$C_7F_{15}CF_2CH_2CF_2CF_2CH_2CH_2CF_2I$ (**53**), a compound modelling structures (b) and (c), was formed as a minor side product in the synthesis of $C_8F_{17}(CH_2CF_2)_{1-4}I$ (**47**) by internal head to head addition of VDF. This compound reacts with SbF_5 and was subsequently dehydrofluorinated on exposure to DBU (Fig. 206).

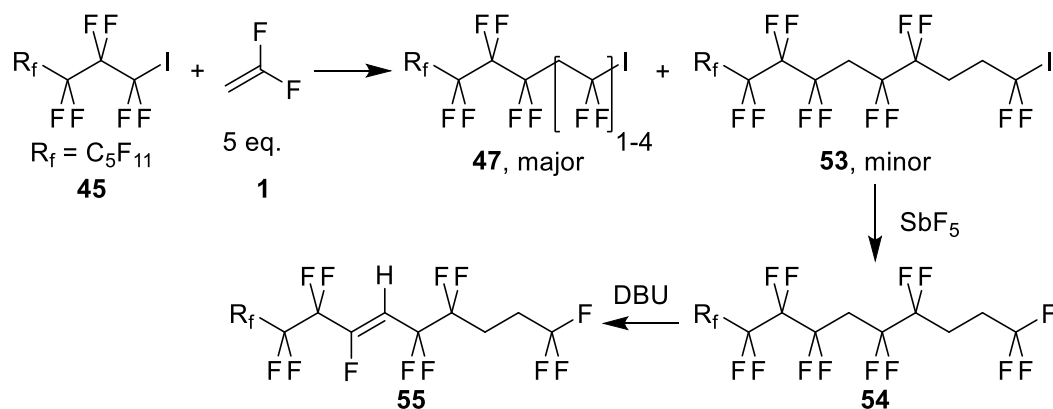


Figure 206: Synthesis of $C_7F_{15}CF_2CH_2CF_2CF_2CH_2CH_2CF_2I$ and subsequent reaction with DBU

$\text{CF}_3\text{CF}_2\text{CF}(\text{CF}_3)(\text{CH}_2\text{CF}_2)_{2-7}\text{F}$ (**68**), models of structure (d), were synthesised by reaction of $\text{CF}_3\text{CF}_2\text{CF}(\text{CF}_3)\text{I}$ (**61**) with VDF and SbF_5 . Trace amounts of $\text{CF}_3\text{CF}_2\text{CF}(\text{CF}_3)\text{CF}_2\text{CH}_2\text{I}$, a model of structure (e), were also synthesised in the first step of this reaction. However, this compound was not observed after subsequent reaction due to its high volatility and low abundance (Fig. 207).

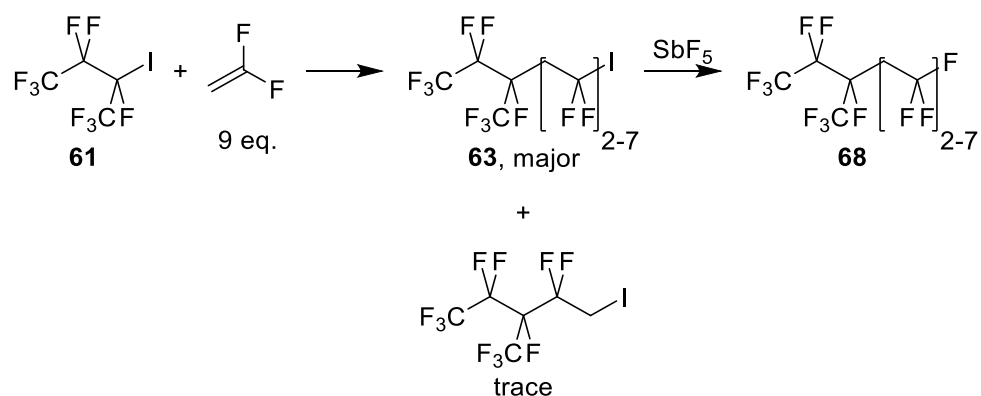


Figure 207: Synthesis of $\text{CF}_3\text{CF}_2\text{CF}(\text{CF}_3)(\text{CH}_2\text{CF}_2)_{2-7}\text{F}$, a model of structure (d) along with trace amounts of $\text{CF}_3\text{CF}_2\text{CF}(\text{CF}_3)\text{CF}_2\text{CH}_2\text{I}$, a model of structure (e)

These models of structure (d) were also reacted with bases and gave products including simple dehydrofluorinated species (**72** and **73**), polymeric tars and carbonyl group containing molecules (**71**) depending on the base and the reaction conditions (Fig. 208).

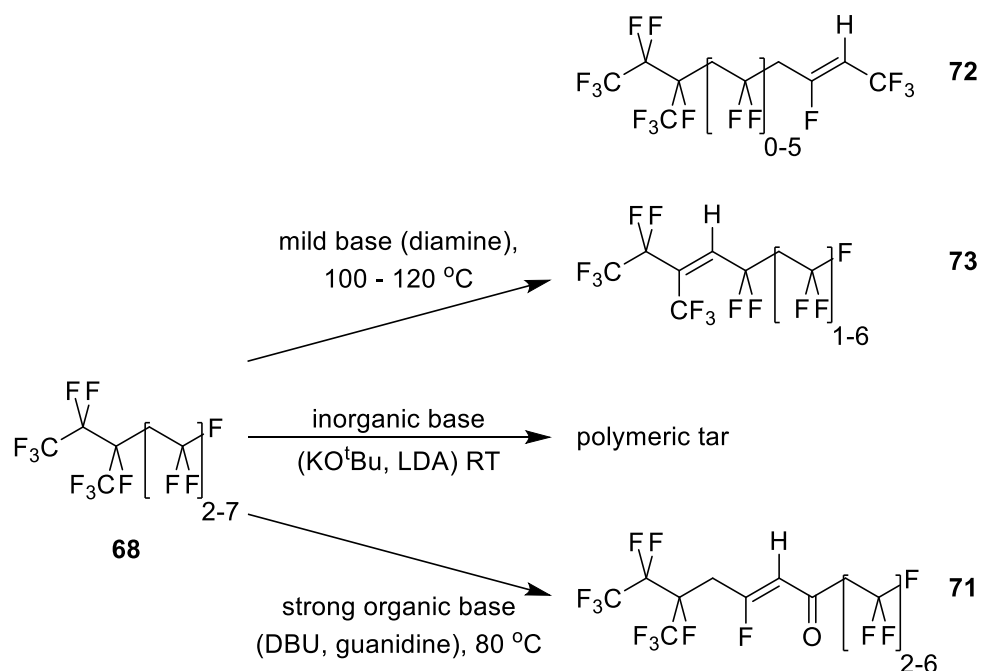


Figure 208: Major products from the reactions of $\text{CF}_3\text{CF}_2\text{CF}(\text{CF}_3)(\text{CH}_2\text{CF}_2)_{2-7}\text{F}$ with different bases

A second route to structure (d) was investigated; a two-step synthesis by sequential reaction of alkyl carbonyl compounds ($\text{RCOCH}_2\text{R}'$) with Me_3SiCF_3 (**74**) and DAST (**75**). However, this strategy produced a mixture of both the intended $\text{RCF}(\text{CF}_3)\text{CH}_2\text{R}'$ systems and several different dehydrofluorinated products, the composition of which depended on the groups R and R' (Fig. 209).

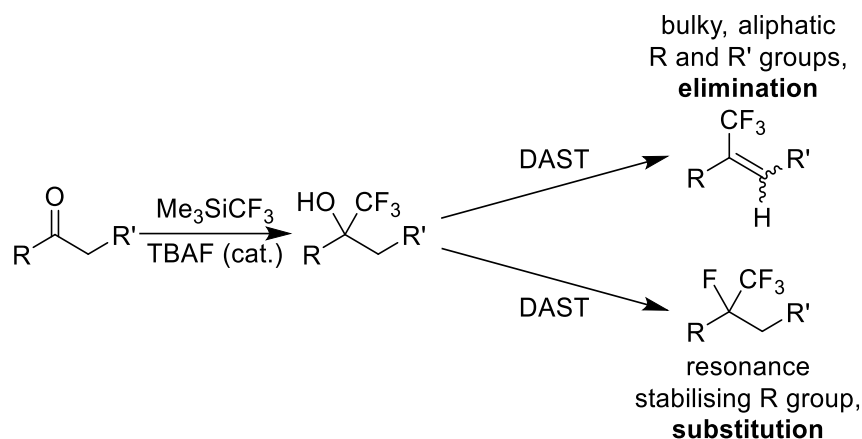


Figure 209: Sequential reaction of RCOCH_2R compounds with Me_3SiCF_3 and DAST to synthesise $\text{RCF}(\text{CF}_3)\text{CH}_2\text{R}$ systems, models of structure (d), and the dehydrofluorinated by-products that also formed

The reactions of Viton[®] model compounds with bases indicate that exposure to petroleum additives containing basic groups can cause dehydrofluorination of Viton[®] seals within engines and other mechanical components. These reactions would occur at the poly VDF ($(\text{CH}_2\text{CF}_2)_n$, structure (a) – (c)) and HFP-VDF ($\text{CF}_2\text{CF}(\text{CF}_3)\text{CH}_2\text{CF}_2$, structure (d)) groups of the elastomer, particularly at structure (d) which reacted with relatively mild bases (*N,N'*-dimethyl ethylenediamine). Dehydrofluorinated polymers could be further degraded by nucleophilic additive compounds, as shown by the reactions of **49** with KOMe that produced $\text{C}_7\text{F}_{15}\text{C}(\text{OMe})=\text{CH}(\text{CF}_2\text{CH}_2)_{0-3}\text{CF}_3$ (**56**). The presence of residual water in a system could also cause degradation by the production of reactive carbonyl groups along the polymer backbone, as observed in the reaction of **68** with DBU while exposed to atmospheric moisture.

All reactions of the Viton[®] model compounds were carried out under relatively mild conditions (atmospheric pressure, temperature ≤ 120 °C, time ≤ 1 week). Long term exposure of Viton[®] seals to even low concentrations of mildly basic petroleum additives could cause seal degradation and eventual failure, particularly if these systems were operating at high temperatures and pressures. Therefore, these results indicate that contact between Viton[®] seals and basic or nucleophilic petroleum additives should be minimised wherever possible.

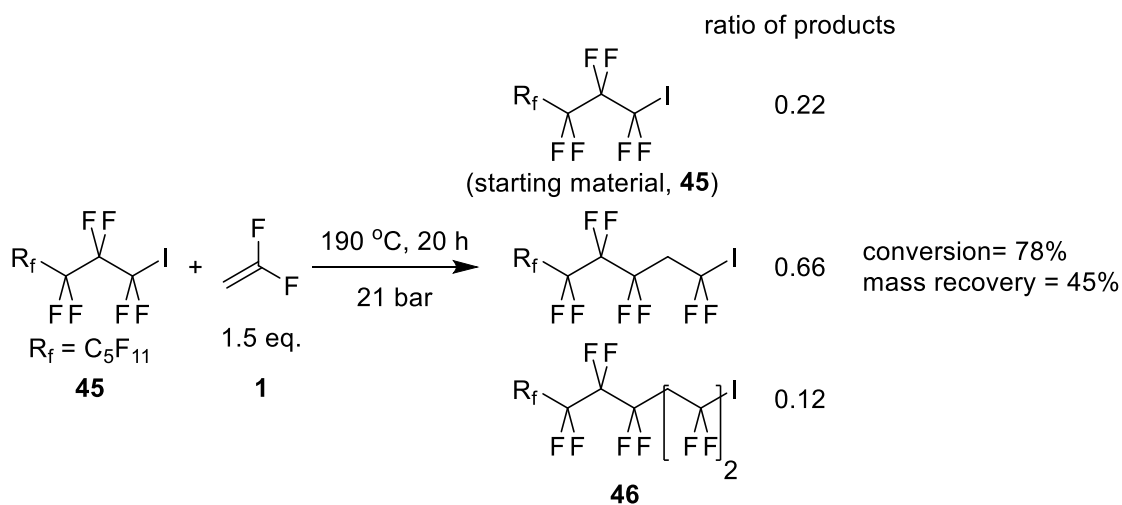
7. Experimental

Chemicals were purchased from Apollo Scientific, Fluorochem or Sigma Aldrich and, unless otherwise stated, were used without any further purification. Dry solvents were obtained using an Innovative Technology Inc. Solvent Purification System. All column chromatography was carried out using Silicagel LC60A (40 – 63 micron) purchased from Fluorochem.

Proton, carbon and fluorine nuclear magnetic resonance spectra (^1H NMR, ^{13}C NMR and ^{19}F NMR) were recorded on a Bruker 400 Ultrashield (^1H NMR at 400 MHz; ^{13}C NMR at 101 MHz; ^{19}F NMR at 376 MHz) spectrometer or a Varian VNMRS-700 (^1H NMR at 700 MHz; ^{13}C NMR at 176 MHz) with residual solvent peaks as the internal standard (^1H NMR, CHCl_3 at 7.26 ppm; ^{13}C NMR, CHCl_3 at 77.36 ppm). In addition, 2d NMR spectra (HMBC and HSQC) were recorded on a Varian VNMRS-700 in order to aid characterisation. ^1H , ^{13}C and ^{19}F spectroscopic data are reported as follows: chemical shift (ppm), integration, multiplicity (s = singlet, d = doublet, t = triplet, q = quartet, p = pentet, m = multiplet), coupling constant (Hz) and assignment. All GC-MS data was acquired on a Shimadzu QP2010*Ultra with an expanded mass range to accommodate high molecular weight telomers.

Reagents were degassed on a Schlenk Line by freeze-pump-thaw at 5 mbar, before being transferred to the appropriate reaction vessel. Gaseous and low boiling reagents were vacuum transferred to the appropriate reaction vessel via Young's Tubes, tested to 6 bar, on a Schlenk Line at 5 mbar. High pressure reactions were contained in a 160 mL Hastelloy autoclave tested to 300 bar and fitted with a Forward Acting Rupture Disk, rated to 200 bar. High pressure reactions were carried out in the High Pressure Lab, a unique facility at Durham University. The autoclave was heated in a rocking furnace that was remotely controlled using a Eurotherm control box connected to two K thermocouples, a control thermocouple attached to the rear of the furnace, and an indicator thermocouple placed inside the autoclave.

Reaction of Perfluorooctyl Iodide with VDF (1.5 equivalents)



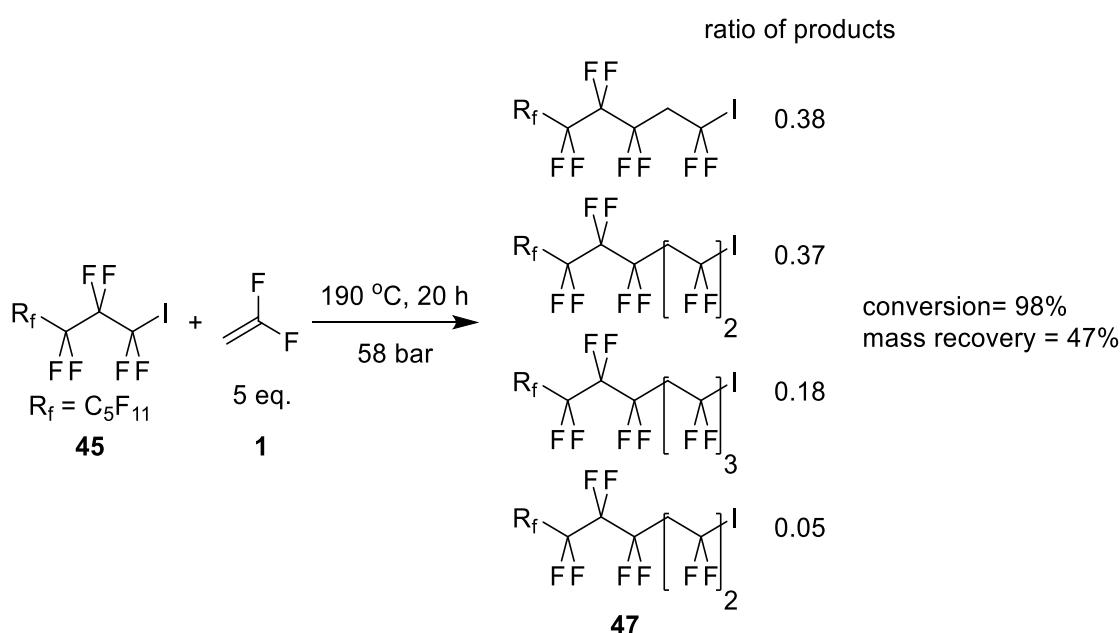
Perfluorooctyl iodide (19.60 g, 35.9 mmol), was degassed and transferred to an autoclave (160 mL, Hastelloy) and vinylidene fluoride (3.35 g, 52.5 mmol) was added by vacuum transfer. The autoclave was transferred to a rocking furnace and heated to 190 °C for 20 hours. The autoclave was allowed to cool, and a brown solid was recovered (18.47 g). This was dissolved in DCM (100 mL) and washed with aq. sodium thiosulfate, water and brine to yield $C_8F_{17}(CH_2CF_2)_{0-2}I$ (13.14 g, 78% conversion, 45% mass recovery) as a yellow solid; 1H NMR (400 MHz, Chloroform-*d*) δ 3.41 (2 H, p, $^3J_{HF} = 15.6$, $CF_2CH_2CF_2I$), 3.39 (2 H, p, $^3J_{HF} = 15.1$, $CF_2CH_2CF_2I$), 2.83 (2 H, p, $^3J_{HF} = 16.1$, $CF_2CH_2CF_2$); ^{19}F NMR (376 MHz, Chloroform-*d*) δ -38.26 – -38.43 (2 F, m, $CF_2CH_2CF_2I$), -39.08 (2 F, ttt, $^3J_{FH} = 15.6$, $^4J_{FF} = 9.4$, $^5J_{FH} = 3.0$, $(CF_2CH_2)_2CF_2I$), -81.32 – -81.43 (3 F, m, CF_2CF_3), -88.26 – -90.88 (2 F, m, CF_2CH_2), -112.53 – -112.90 (2 F, m, CF_2CF_2), -121.69 – -122.43 (4 F, m, CF_2CF_2), -122.93 – -123.26 (2 F, m, CF_2CF_2), -123.58 – -123.92 (2 F, m, CF_2CF_2) -126.47 – -126.70 (2 F, m, CF_2CF_2); ^{13}C NMR (101 MHz, Chloroform-*d*) δ 117.37 (qt, $^1J_{CF} = 288.7$, $^2J_{CF} = 33.7$, CF_2CF_3), 114.04 – 104.94 (m, CF_2CF_2) 88.73 (t, $^1J_{CF} = 315.3$, CH_2CF_2I), 54.76 – 54.04 (m, $CF_2CH_2CF_2$), 48.45 (p, $^2J_{CF} = 21.3$, $CF_2CH_2CF_2I$), 37.81 – 37.06 (m, $CF_2CH_2CF_2$). The GC-MS data for each product, and the percentage of each compound in the product mixture determined by ^{19}F NMR spectroscopy, are given below:

2H,2H 1-iodoperfluorodecane (66%): GC-MS: 2.4 mins $m/z = 590.9$ (1%, $[M - F]^+$), 483.0 (100, $[M - I]^+$), 176.9 (11, $[ICF_2]^+$), 133.0 (41, $[CF_2CH_2CF_3]^+$), 131.0 (15, $[C_3F_5]^+$).

2H,2H,4H,4H 1-iodoperfluorododecane (12%): GC-MS: 3.0 mins $m/z = 654.9$ (1%, $[M - F]^+$), 547.0 (36, $[M - I]^+$), 176.9 (11, $[ICF_2]^+$), 133.0 (100, $[CF_2CH_2CF_3]^+$), 113.0 (13, $[CF_2CHCF_2]^+$).

In addition, perfluorooctyl iodide, the starting material, was observed in the product mixture (22%): ^{19}F NMR (376 MHz, Chloroform-*d*) δ -59.25 – -59.42 (2 F, m, CF_2I), -81.45 (3 F, tt, $^3J_{\text{FF}} = 10.1$, $^4J_{\text{FF}} = 2.4$, CF_3), -113.28 – -113.58 (2 F, m, CF_2), -121.16 – -121.53 (2 F, m, CF_2I), -122.03 – -122.50 (4 F, m, CF_2), -122.96 – -123.33 (2 F, m, CF_2), -126.56 – -126.79 (2 F, m, CF_2); ^{13}C NMR (101 MHz, Chloroform-*d*) δ 117.07 (qt, $^1J_{\text{CF}} = 287.9$, $^2J_{\text{CF}} = 32.9$, CF_3), 114.06–104.60 (m, CF_2) 93.26 (tt, $^1J_{\text{CF}} = 321.1$, $^2J_{\text{CF}} = 41.9$, CF_2I); GC-MS: 1.5 mins $m/z = 545.9$ (29%, $[\text{M}]^+$), 419.0 (100, $[\text{M} - \text{I}]^+$), 331.0 (24, $[\text{C}_7\text{F}_{13}]^+$), 176.9 (32, $[\text{ICF}_2]^+$), 169.0 (87, $[\text{CF}_2\text{CF}_2\text{CF}_3]^+$), 131.0 (73, $[\text{C}_3\text{F}_5]^+$).

Reaction of Perfluorooctyl Iodide with VDF (5 equivalents)



Perfluorooctyl iodide (21.84 g, 40.0 mmol), was degassed and transferred to an autoclave (160 mL, Hastelloy) and vinylidene fluoride (12.92 g, 202 mmol) was added by vacuum transfer. The autoclave was transferred to a rocking furnace and heated to 190 °C for 20 hours. The autoclave was allowed to cool and a pink solid was recovered (22.46 g). This was dissolved in DCM (100 mL) and washed with aq. sodium thiosulfate, water and brine to yield $\text{C}_8\text{F}_{17}(\text{CH}_2\text{CF}_2)_{1-4}\text{I}$ (16.58 g, 98% conversion, 47% mass recovery) as a white solid; ^1H NMR (600 MHz, Chloroform-*d*) δ 3.49 – 3.25 (2 H, m, $\text{CF}_2\text{CH}_2\text{CF}_2\text{I}$), 2.99 – 2.62 (2 H, m, $\text{CF}_2\text{CH}_2\text{CF}_2$); ^{19}F NMR (376 MHz, Chloroform-*d*) δ -38.34 (2 F, tt, $^3J_{\text{FH}} = 13.7$, $^4J_{\text{FF}} = 12.6$, $\text{CF}_2\text{CH}_2\text{CF}_2\text{I}$), -38.43 – -38.52 (2 F, m, $(\text{CF}_2\text{CH}_2)_4\text{CF}_2\text{I}$), -38.51 – -38.70 (2 F, m, $(\text{CF}_2\text{CH}_2)_3\text{CF}_2\text{I}$), -39.06 (2 F, ttt, $^3J_{\text{FH}} = 15.7$, $^4J_{\text{FF}} = 9.5$, $^5J_{\text{FH}} = 3.1$, $(\text{CF}_2\text{CH}_2)_2\text{CF}_2\text{I}$), -81.38 (3 F, t, $^3J_{\text{FF}} = 10.1$, CF_2CF_3), -88.27 – -90.92 (2 F, m, CF_2CH_2), -112.57 – -112.86 (2 F, m, CF_2CF_2), -121.68 – -122.00 (4 F,

m, CF_2CF_2), -122.96 – -123.25 (2 F, m, CF_2CF_2), -123.59 – -123.94 (2 F, m, CF_2CF_2) -126.46 – -126.71 (2 F, m, CF_2CF_2); ^{13}C NMR (101 MHz, Chloroform-*d*) δ 121.07 – 105.39 (m, CF_2CF_2), 117.39 (qt, $^1J_{\text{CF}} = 287.7$, $^2J_{\text{CF}} = 32.8$, CF_2CF_3), 91.02 (tt, $^1J_{\text{CF}} = 313.4$, $^3J_{\text{CF}} = 5.1$, $(\text{CF}_2\text{CH}_2)_3\text{CF}_2\text{I}$), 90.69 (tt, $^1J_{\text{CF}} = 313.3$, $^3J_{\text{CF}} = 5.1$, $(\text{CF}_2\text{CH}_2)_2\text{CF}_2\text{I}$), 88.78 (t, $^1J_{\text{CF}} = 315.4$, $\text{CF}_2\text{CH}_2\text{CF}_2\text{I}$), 55.19– 54.15 (m, $\text{CF}_2\text{CH}_2\text{CF}_2$), 48.51 (p, $^2J_{\text{CF}} = 21.7$, $\text{CF}_2\text{CH}_2\text{CF}_2\text{I}$), 44.15 – 43.24 (m, $\text{CF}_2\text{CH}_2\text{CF}_2$), 38.25 – 37.35 (m, $\text{CF}_2\text{CH}_2\text{CF}_2$). The GC-MS data for each product, and the percentage of each compound in the product mixture determined by ^{19}F NMR spectroscopy, are given below:

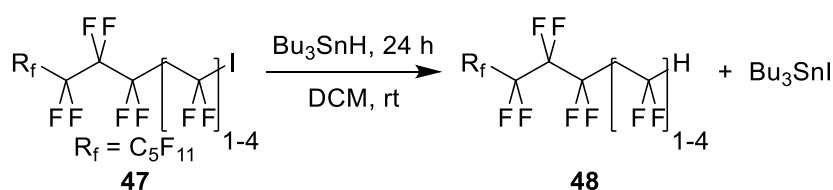
2H,2H 1-iodoperfluorodecane (38%): GC-MS: 2.4 mins $m/z = 590.9$ (1%, $[\text{M} - \text{F}]^+$), 483.0 (100, $[\text{M} - \text{I}]^+$), 176.9 (14, $[\text{ICF}_2]^+$), 133.0 (59, $[\text{CF}_2\text{CH}_2\text{CF}_3]^+$), 131.0 (19, $[\text{C}_3\text{F}_5]^+$).

2H,2H,4H,4H 1-iodoperfluorododecane (37%): GC-MS: 3.0 mins $m/z = 655.0$ (1%, $[\text{M} - \text{F}]^+$), 547.0 (33, $[\text{M} - \text{I}]^+$), 527.0 (3, $[\text{M} - \text{I} - \text{HF}]^+$), 176.9 (10, $[\text{ICF}_2]^+$), 133.0 (100, $[\text{CF}_2\text{CH}_2\text{CF}_3]^+$), 113.0 (9, $[\text{CF}_2\text{CHCF}_2]^+$).

2H,2H,4H,4H,6H,6H 1-iodoperfluorotetradecane (18%): GC-MS: 3.5 mins $m/z = 719.0$ (1%, $[\text{M} - \text{F}]^+$), 611.1 (28, $[\text{M} - \text{I}]^+$), 591.0 (6, $[\text{M} - \text{I} - \text{HF}]^+$), 483.0 (24, $[\text{M} - (\text{CF}_2\text{CH}_2)_2\text{I}]^+$), 241.0 (18, $[\text{ICF}_2\text{CH}_2\text{CF}_2]^+$), 197.0 (21, $[\text{CF}_2\text{CH}_2\text{CF}_2\text{CH}_2\text{CF}_3]^+$), 177.0 (21, $[\text{ICF}_2]^+$), 133.1 (100, $[\text{CF}_2\text{CH}_2\text{CF}_3]^+$), 113.0 (20, $[\text{CF}_2\text{CHCF}_2]^+$).

2H,2H,4H,4H,6H,6H,8H,8H 1-iodoperfluorohexadecane (5%): GC-MS: 3.9 mins $m/z = 783.0$ (1%, $[\text{M} - \text{F}]^+$), 675.1 (9, $[\text{M} - \text{I}]^+$), 655.1 (18, $[\text{M} - \text{I} - \text{HF}]^+$), 527.0 (15, $[\text{M} - (\text{CF}_2\text{CH}_2)_2\text{I}]^+$), 483.0 (4, $[\text{M} - (\text{CF}_2\text{CH}_2)_3\text{I}]^+$), 305.0 (10, $[\text{ICF}_2\text{CH}_2\text{CF}_2\text{CH}_2\text{CF}_2]^+$), 241.0 (15, $[\text{ICF}_2\text{CH}_2\text{CF}_2]^+$), 197.0 (42, $[\text{CF}_2\text{CH}_2\text{CF}_2\text{CH}_2\text{CF}_3]^+$), 177.0 (36, $[\text{ICF}_2]^+$), 133.1 (100, $[\text{CF}_2\text{CH}_2\text{CF}_3]^+$), 113.0 (24, $[\text{CF}_2\text{CHCF}_2]^+$).

Reaction of Telomer Iodides with Bu_3SnH



The mixture of telomer iodides ($\text{C}_8\text{F}_{17}(\text{CH}_2\text{CF}_2)_{1-4}$) (2.69 g, 4 mmol) and Bu_3SnH (1.16 g, 4 mmol) were dissolved in DCM (20 mL) and stirred under argon for 24 hours. The reaction mixture was worked up in the following ways:

Work Up 1

KF (2 g) dissolved in water (20 mL) was added to the reaction mixture, which was stirred for a further 30 minutes. The solution was filtered, the organic phase was separated and the solvent removed in vacuo to yield a crude product (ratio of product:tin residues = 4:6). The crude product was dissolved in hexane (20 mL) and stirred with KF (2 g) dissolved in water (20 mL) for a further 5 hours. The solution was filtered through celite, the organic phase was separated and the solvent removed in vacuo to yield a crude product (ratio of product:tin residues = 9:1). The crude product was dissolved in hexane (20 mL) and to this was added iodine (3 g). The mixture was stirred for 3 hours, after which Na₂S₂O₃ (10 g) dissolved in water (20 mL) was added. The organic layer was separated and concentrated in vacuo. The solution was filtered through a column of silica and K₂CO₃ (ratio 9:1) using neat hexane as the solvent. After filtration, the solvent was removed in vacuo to yield C₈F₁₇(CH₂CF₂)₁₋₄H (ratio of product:tin residues = 97:3) (0.23 g, 10%) as an off white solid.

Work Up 2

Iodine (3 g) was added to the reaction mixture, which was stirred for 3 hours, after which Na₂S₂O₃ (10 g) dissolved in water (20 mL) was added. The organic layer was separated and concentrated in vacuo. The solution was filtered through a column of silica and K₂CO₃ (ratio 9:1) using neat hexane as the solvent. After filtration, the solvent was removed in vacuo to yield a crude product (ratio of product:tin residues = 3:7). Perfluorohexane (20 mL) and hexane (20 mL) were added to the product which dissolved all materials present. The fluororous phase was separated and the solvent was removed in vacuo to yield C₈F₁₇(CH₂CF₂)₁₋₄H (ratio of product:tin residues = 96:4) (0.35 g, 15%) as an off white solid.

Work Up 3

Iodine (3 g) was added to the reaction mixture, which was stirred for 3 hours, after which Na₂S₂O₃ (10 g) dissolved in water (20 mL) was added. The organic layer was separated and the solvent removed in vacuo. Perfluorohexane (20 mL) and hexane (20 mL) were added to the product which dissolved all materials present. The fluororous phase was separated and the solvent was removed in vacuo to yield C₈F₁₇(CH₂CF₂)₁₋₄H (ratio of product:tin residues = 9:1) (0.74 g, 30%) as an off white solid.

¹H NMR (400 MHz, Chloroform-*d*) δ 6.09 (1 H, tt, ²J_{HF} = 55.0, ³J_{HH} = 4.6, CF₂H), 6.08 (1 H, tt, ²J_{HF} = 55.0, ³J_{HH} = 4.6, CF₂H), 6.07 (1 H, tt, ²J_{HF} = 55.1, ³J_{HH} = 4.5, CF₂H), 3.04 – 2.42 (m, CF₂CH₂CF₂);

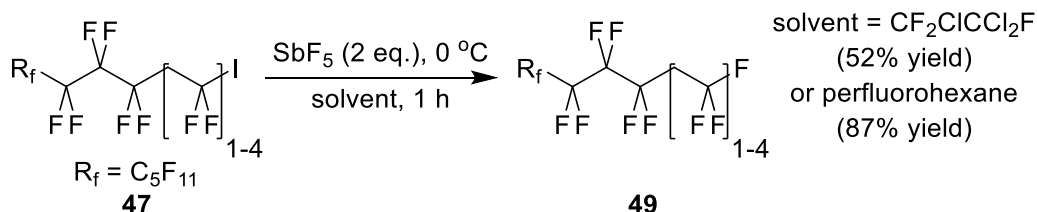
^{19}F NMR (376 MHz, Chloroform-*d*) -81.43 (tt, $^3J_{\text{FF}} = 9.8$, $^4J_{\text{FF}} = 2.0$, CF_2CF_3), $-88.46 - -92.75$ (m, CF_2CH_2), $-112.59 - -113.17$ (m, CF_2CF_2), -114.34 (dttt, $^2J_{\text{FH}} = 54.6$, $^3J_{\text{FH}} = 14.3$, $^4J_{\text{FF}} = 5.6$, $^5J_{\text{FH}} = 1.6$, $\text{CH}_2\text{CF}_2\text{H}$), -115.36 (dtt, $^2J_{\text{FH}} = 55.3$, $^3J_{\text{FH}} = 15.2$, $^4J_{\text{FF}} = 5.6$, $\text{CH}_2\text{CF}_2\text{H}$), -115.59 (dttt, $^2J_{\text{FH}} = 55.1$, $^3J_{\text{FH}} = 15.0$, $^4J_{\text{FF}} = 5.5$, $^5J_{\text{FH}} = 1.5$, $\text{CH}_2\text{CF}_2\text{H}$), $-121.68 - -122.15$ (m, CF_2CF_2), $-122.18 - -122.56$ (m, CF_2CF_2), $-123.01 - -123.37$ (m, CF_2CF_2), $-123.61 - -124.17$ (m, CF_2CF_2), $-126.48 - -126.82$ (m, CF_2CF_2). ^{13}C NMR (101 MHz, Chloroform-*d*) δ $120.53 - 105.40$ (m, CF_2CF_2), 117.08 (qt, $^1J_{\text{CF}} = 288.0$, $^2J_{\text{CF}} = 33.4$, CF_2CF_3), $43.97 - 42.93$ (m, $\text{CF}_2\text{CH}_2\text{CF}_2$), $42.32 - 41.14$ (m, $\text{CF}_2\text{CH}_2\text{CF}_2\text{H}$), $38.05 - 36.99$ (m, $\text{CF}_2\text{CH}_2\text{CF}_2$). The GC-MS data for each product, and the percentage of each compound in the product mixture determined by ^1H NMR spectroscopy, are given below ($\text{C}_8\text{F}_{17}\text{CH}_2\text{CF}_2\text{H}$ (22%) was not observed by GC-MS):

$\text{C}_8\text{F}_{17}(\text{CH}_2\text{CF}_2)_2\text{H}$ (47%): GC-MS: 2.1 mins $m/z = 529.0$ (2%, $[\text{M} - \text{F}]^+$), 483.0 (10, $[\text{M} - \text{CH}_2\text{CF}_2\text{H}]^+$), 179.1 (38, $[\text{CF}_2\text{CH}_2\text{CF}_2\text{CH}_2\text{CF}_2\text{H}]^+$), 133.1 (83, $[\text{CF}_2\text{CH}_2\text{CF}_3]^+$), 115.1 (100, $[\text{CF}_2\text{CH}_2\text{CF}_2\text{H}]^+$).

$\text{C}_8\text{F}_{17}(\text{CH}_2\text{CF}_2)_3\text{H}$ (23%): 2.7 mins $m/z = 573.0$ (4%, $[\text{M} - \text{HF}_2]^+$), 478.0 (11, $[\text{C}_8\text{F}_{17}\text{CH}_2\text{CFCH}_2]^+$), 223.0 (16, $[(\text{CF}_2\text{CH}_2\text{CF}_2\text{CH}_2\text{CF}_2\text{CH}_2\text{CF}_2\text{H}) - \text{HF}]^+$), 179.1 (10, $[\text{CF}_2\text{CH}_2\text{CF}_2\text{CH}_2\text{CF}_2\text{H}]^+$), 133.1 (81, $[\text{CF}_2\text{CH}_2\text{CF}_3]^+$), 115.1 (100, $[\text{CF}_2\text{CH}_2\text{CF}_2\text{H}]^+$).

$(\text{C}_8\text{F}_{17}(\text{CH}_2\text{CF}_2)_4\text{H})$ (8%): GC-MS: 3.2 mins $m/z = 637.0$ (4%, $[\text{M} - \text{HF}_2]^+$), 527.0 (7, $[(\text{C}_8\text{F}_{17}\text{CH}_2\text{CF}_2\text{CH}_2\text{CF}_2) - \text{HF}]^+$), 478.0 (17, $[\text{C}_8\text{F}_{17}\text{CH}_2\text{CFCH}_2]^+$), 307.0 (15, $[(\text{CF}_2\text{CH}_2\text{CF}_2\text{CH}_2\text{CF}_2\text{CH}_2\text{CF}_2\text{CH}_2\text{CF}_2\text{H}) - \text{HF}]^+$), 223.0 (6, $[(\text{CF}_2\text{CH}_2\text{CF}_2\text{CH}_2\text{CF}_2\text{CH}_2\text{CF}_2\text{H}) - \text{HF}]^+$), 179.0 (28, $[\text{CF}_2\text{CH}_2\text{CF}_2\text{CH}_2\text{CF}_2\text{H}]^+$), 133.1 (100, $[\text{CF}_2\text{CH}_2\text{CF}_3]^+$), 115.1 (59, $[\text{CF}_2\text{CH}_2\text{CF}_2\text{H}]^+$).

Reactions of Telomer Iodides with SbF_5



The mixture of telomer iodides ($\text{C}_8\text{F}_{17}(\text{CH}_2\text{CF}_2)_{1-4}\text{I}$) (2.69 g, 4 mmol) was dissolved in $\text{CF}_2\text{ClCCl}_2\text{F}$ (10 mL) at 0°C and SbF_5 (1.79 g, 8 mmol) dissolved in $\text{CF}_2\text{ClCCl}_2\text{F}$ (10 mL) was added dropwise over 20 minutes. The reaction mixture was stirred for an hour, after which water (30 mL) was added. The solution was allowed to warm to rt and neutralised with solid NaHCO_3 . The fluorocarbon layer was extracted and the solvent was removed in vacuo to yield $\text{C}_8\text{F}_{17}(\text{CH}_2\text{CF}_2)_{1-4}\text{F}$ as an orange oil (1.19 g, 52%).

The mixture of telomer iodides ($C_8F_{17}(CH_2CF_2)_{1-4}I$) (16.14 g, 24 mmol) was dissolved in perfluorohexane (20 mL) at 0 °C. To this was added SbF_5 (10.73 g, 48 mmol) dissolved in perfluorohexane (40 mL) dropwise over 20 minutes. The reaction mixture was stirred for an hour, after which water (50 mL) was added. The solution was allowed to warm to rt and neutralised with solid $NaHCO_3$. The fluorocarbon layer was extracted and the solvent was removed in vacuo to yield $C_8F_{17}(CH_2CF_2)_{1-4}F$ as an orange oil (11.92 g, 87%). Both reactions produced the same mixture of products; 1H NMR (400 MHz, deuterium oxide) δ 3.04 – 2.43 (m, $CF_2CH_2CF_2$); ^{19}F NMR (376 MHz, deuterium oxide) –63.27 (p, $^3J_{FH} = 9.4$, $CF_2CH_2CF_3$), –63.89 (p, $^3J_{FH} = 9.5$, $(CF_2CH_2)_4CF_3$), –64.24 (p, $^3J_{FH} = 9.7$, $(CF_2CH_2)_3CF_3$), –64.34 (p, $^3J_{FH} = 9.6$, $(CF_2CH_2)_2CF_3$), –83.26 (t, $^3J_{FF} = 10.3$, CF_2CF_3), –90.02 – –93.49 (m, CH_2CF_2), –113.76 – –115.73 (m, CF_2CF_2), –115.41 – –115.80 (m, CF_2CF_2), –122.92 – –123.21 (m, CF_2CF_2), –123.24 – –123.69 (m, CF_2CF_2), –124.19 – –124.54 (m, CF_2CF_2), –125.07 – –125.40 (m, CF_2CF_2), –127.89 – –128.33 (m, CF_2CF_2); ^{13}C NMR (101 MHz, deuterium oxide) δ 122.70 (qt, $^1J_{CF} = 275.4$, $^3J_{CF} = 6.7$, $(CF_2CH_2)_{1-4}CF_3$), 122.37 (q, $^1J_{CF} = 276.5$, $CF_2CH_2CF_3$), 120.38 – 104.90 (m, CF_2CF_2), 116.94 (qt, $^1J_{CF} = 287.2$, $^2J_{CF} = 32.9$, CF_2CF_3), 43.33 – 41.74 (m, CH_2CF_2), 41.10 – 39.53 (m, CH_2CF_2), 37.66 – 35.86 (m, CH_2CF_2), 35.64 – 34.12 (m, CH_2CF_2). The GC-MS data for each product are given below:

$C_8F_{17}CH_2CF_2F$: GC-MS: 0.9 mins $m/z = 483.0$ (1%, $[M - F]^+$), 133.1 (100, $[CF_2CH_2CF_3]^+$), 131.0 (12, $[C_3F_5]^+$);

$C_8F_{17}(CH_2CF_2)_2F$: GC-MS: 1.9 mins $m/z = 547.0$ (1%, $[M - F]^+$), 483.0 (3, $[M - CH_2CF_3]^+$), 197.0 (26, $[CF_2CH_2CF_2CH_2CF_3]^+$), 133.1 (100, $[CF_2CH_2CF_3]^+$), 113.0 (6, $[CF_2CHCF_2]^+$);

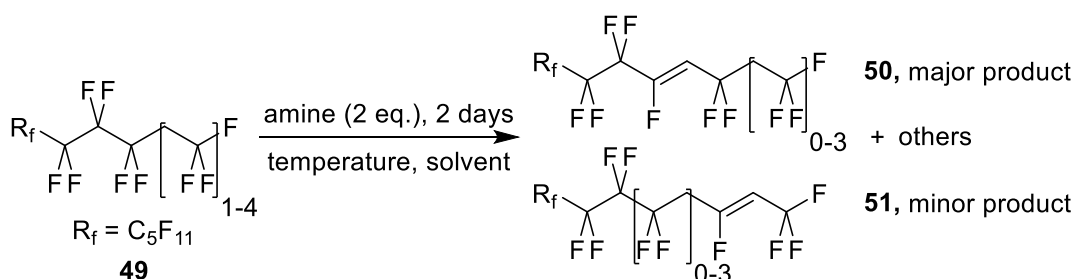
$C_8F_{17}(CH_2CF_2)_3F$: GC-MS: 2.6 mins $m/z = 611.0$ (1%, $[M - F]^+$), 547.0 (1, $[M - CH_2CF_3]^+$), 483.0 (5, $[M - CH_2CF_2CH_2CF_3]^+$), 261.0 (7, $[CF_2CH_2CF_2CH_2CF_2CH_2CF_3]^+$) 197.0 (13, $[CF_2CH_2CF_2CH_2CF_3]^+$), 133.1 (100, $[CF_2CH_2CF_3]^+$), 109.1 (15, $[CF_2CF_3]^+$);

$C_8F_{17}(CH_2CF_2)_4F$: GC-MS: 3.1 mins $m/z = 655.1$ (1%, $[M - HF_2]^+$), 483.0 (3, $[M - (CH_2CF_2)_2CH_2CF_3]^+$), 478.0 (5, $[C_8F_{17}CH_2CFCH_2]^+$), 305.1 (6, $[(CF_2CH_2CF_2CH_2CF_2CH_2CF_2CH_2CF_3) - HF]^+$), 197.0 (41, $[CF_2CH_2CF_2CH_2CF_3]^+$), 177.0 (15, $[(CF_2CH_2CF_2CH_2CF_3) - HF]^+$), 133.1 (100, $[CF_2CH_2CF_3]^+$), 109.1 (9, $[CF_2CF_3]^+$);

$C_8F_{17}CH_2CF_2CF_2CH_2I$: GC-MS: 3.2 mins $m/z = 674.0$ (40%, $[M]^+$), 635.0 (3, $[M - HF_2]^+$), 463.1 (17, $[C_7F_{15}CF=CHCF_2]^+$), 305.0 (5, $[CF_2CH_2CF_2CF_2CH_2I]^+$), 190.9 (100, $[CF_2CH_2I]^+$), 169.0 (7, $[CF_3CF_2CF_2]^+$), 133.1 (80, $[CF_2CH_2CF_3]^+$), 119.0 (13, $[CF_3CF_2]^+$);

$C_8F_{17}(CH_2CF_2)_2CF_2CH_2I$: GC-MS: 3.5 mins $m/z = 737.9$ (53%, $[M]^{+}$), 699.0 (9, $[M - HF_2]^+$), 527.0 (7, $[C_7F_{15}CFCHCF_2CH_2CF_2]^+$), 348.9 (26, $[(CF_2CH_2CF_2CH_2CF_2CF_2CH_2I) - HF]^+$), 284.9 (6, $[(CF_2CH_2CF_2CF_2CH_2I) - HF]^+$) 197.0 (12, $[CF_2CH_2CF_2CF_2CH_2F]^+$) 190.9 (51, $[CF_2CH_2I]^+$), 177.0 (13, $[(CF_2CH_2CF_2CF_2CH_2F) - HF]^+$, 133.1 (100, $[CF_2CH_2CF_3]^+$), 131.0 (7, $[C_3F_5]^+$), 119.0 (6, $[CF_3CF_2]^+$), 113 (12, $[CF_2CHCF_2]^+$).

General Procedure for the Reactions of Telomer Fluorides with Amines



The mixture of telomer fluorides ($C_8F_{17}(CH_2CF_2)_{1-4}F$) (1.00 g, 1.77 mmol) were stirred with an amine (4.00 mmol) in petroleum ether (30 mL) at various temperatures for 2 days. 1 M HCl (20 mL) was added, the organic layer was separated and washed with water and brine. The solvent was removed in vacuo and the products were analysed by 1H and ^{19}F NMR.

$C_8F_{17}(CH_2CF_2)_{1-4}F$ was reacted with N,N-dimethyl aniline (0.48 g), Pyridine (0.32 g), Morpholine (0.35 g), DABCO (0.45 g) and DBU (0.61 g) in petroleum ether 40 – 60 °C at rt. Only the reaction with DBU caused observable dehydrofluorination (7%); 1H NMR (400 MHz, Chloroform-*d*) δ 5.94 (dq, $^3J_{HF} = 28.7$, $^3J_{HF} = 6.8$, $CF=CH-CF_3$), 3.09 – 2.62 (m, CH_2CF_2); ^{19}F NMR (376 MHz, Chloroform-*d*) δ -59.60 (ddt, $^3J_{FH} = 17.4$, $^4J_{FF} = 6.9$, $^5J_{FH} = 1.9$, $CH_2CF=CH-CF_3$), -60.95 (p, $^3J_{FH} = 9.2$, $CF_2CH_2CF_3$), -61.92 – -62.15 (m, $(CF_2CH_2)_{2-4}CF_3$), -81.15 (t, $^3J_{FF} = 10.0$ Hz, CF_2CF_3), -88.20 – -91.91 (m, CH_2CF_2), -112.55 – -112.96 (m, CF_2CF_2), -121.52 – -121.94 (m, CF_2CF_2), -122.02 – -122.36 (m, CF_2CF_2), -122.85 – -123.17 (m, CF_2CF_2), -123.54 – -123.87 (m, CF_2CF_2), -126.30 – -126.59 (m, CF_2CF_2).

$C_8F_{17}(CH_2CF_2)_{1-4}F$ (1 g, 1.770 mmol) was reacted with N,N-dimethyl aniline (0.48 g), pyridine (0.32 g), morpholine (0.35 g), DABCO (0.45 g), N,N'-dimethyl ethylenediamine (0.45 g), triethylamine (0.40 g), 2-tert-Butyl-1,1,3,3-tetramethylguanidine (0.69 g) and DBU (0.61 g) in petroleum ether 60 – 80 °C (30 mL) for 2 days at 80 °C. Only the reaction with DBU caused observable dehydrofluorination (35%); 1H NMR (400 MHz, Chloroform-*d*) δ 6.33 (dd,

-122.65 – -123.44 (m, CF_2CF_2), -123.69 (s, CF_2CF_2), -125.06 – -128.41 (m, CF_2CF_2). The GC-MS data for each product is given below:

$\text{C}_7\text{F}_{15}\text{CF}=\text{CHCF}_2\text{CH}_2\text{CF}_3$: GC-MS: 1.6 mins $m/z = 527.0$ (15%, $[\text{M} - \text{F}]^+$), 463.0 (61, $[\text{C}_7\text{F}_{15}\text{CF}=\text{CHCF}_2]^+$), 227.0 (100, $[\text{CF}_2\text{CF}=\text{CHCF}_2\text{CH}_2\text{CF}_3]^+$), 207.0 (37, $[\text{CF}_2\text{CF}=\text{CHCF}=\text{CHCF}_3]^+$), 163.0 (100, $[\text{CF}_2\text{CF}=\text{CHCF}_3]^+$), 157.0 (15, $[\text{CF}=\text{CHCF}=\text{CHCF}_3]^+$), 144.0 (11, $[\text{CF}_2\text{CF}=\text{CHCF}_2]^+$), 133.1 (19, $[\text{CF}_2\text{CH}_2\text{CF}_3]^+$), 131.0 (18, $[\text{C}_3\text{F}_5]^+$), 119.1 (26, $[\text{C}_2\text{F}_5]^+$), 113.1 (34, $[\text{CF}=\text{CHCF}_3]^+$);

$\text{C}_7\text{F}_{15}\text{CF}_2\text{CH}_2\text{CF}_2\text{CH}_2\text{CF}_3$: GC-MS: 1.8 mins $m/z = 547.0$ (1%, $[\text{M} - \text{F}]^+$), 483.0 (5, $[\text{M} - \text{CH}_2\text{CF}_3]^+$), 197.0 (30, $[\text{CF}_2\text{CH}_2\text{CF}_2\text{CH}_2\text{CF}_3]^+$), 133.1 (100, $[\text{CF}_2\text{CH}_2\text{CF}_3]^+$), 113.0 (8, $[\text{CF}_2\text{CHCF}_2]^+$);

$\text{C}_7\text{F}_{15}\text{CF}=\text{CHCF}=\text{CHCF}_3$: GC-MS: 1.9 mins $m/z = 526.0$ (19%, $[\text{M}]^{++}$), 507.0 (18, $[\text{M} - \text{F}]^+$), 207.0 (100, $[\text{CF}_2\text{CF}=\text{CHCF}=\text{CHCF}_3]^+$), 157.1 (37, $[\text{CF}=\text{CHCF}=\text{CHCF}_3]^+$), 119.1 (21, $[\text{C}_2\text{F}_5]^+$);

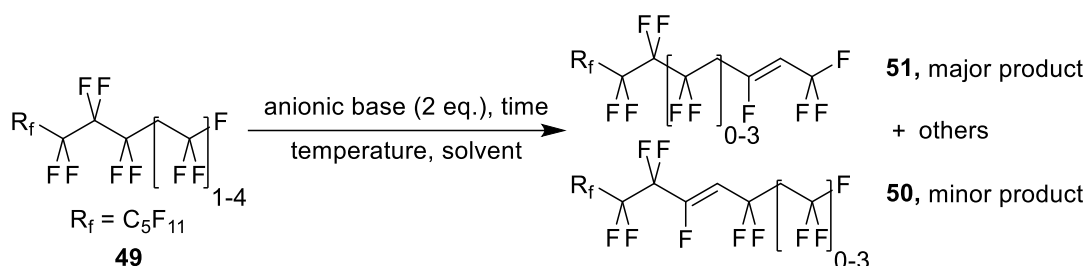
$\text{C}_7\text{F}_{15}\text{CF}=\text{CHCF}_2\text{CF}_2\text{CH}_2\text{CH}_2\text{CF}_3$: GC-MS: 2.0 mins $m/z = 591.0$ (2%, $[\text{M} - \text{F}]^+$), 571.1 (3, $[\text{M} - \text{HF}_2]^+$), 463.0 (22, $[\text{C}_7\text{F}_{15}\text{CF}=\text{CHCF}_2]^+$), 147.1 (100, $[\text{CF}_2\text{CH}_2\text{CH}_2\text{CF}_3]^+$), 127.1 (75, $[(\text{CF}_2\text{CH}_2\text{CH}_2\text{CF}_3) - \text{HF}]^+$);

$\text{C}_7\text{F}_{15}\text{CF}=\text{CHCF}_2\text{CH}_2\text{CF}_2\text{CH}_2\text{CF}_3$: GC-MS: 2.3 mins $m/z = 591.1$ (1%, $[\text{M} - \text{F}]^+$), 527.0 (6%, $[\text{C}_7\text{F}_{15}\text{CF}=\text{CHCF}_2\text{CH}_2\text{CF}_2]^+$), 463.0 (100, $[\text{C}_7\text{F}_{15}\text{CF}=\text{CHCF}_2]^+$), 291.1 (13, $[\text{CF}_2\text{CF}=\text{CHCF}_2\text{CH}_2\text{CF}_2\text{CH}_2\text{CF}_3]^+$), 163.1 (47, $[\text{CF}_2\text{CF}=\text{CHCF}_3]^+$), 133.1 (33.1, $[\text{CF}_2\text{CH}_2\text{CF}_3]^+$), 113.1 (18, $[\text{CF}=\text{CHCF}_3]^+$);

$\text{C}_7\text{F}_{15}\text{CF}_2\text{CF}_2\text{CH}_2\text{I}$: GC-MS: 2.5 mins $m/z = 610.0$ (96%, $[\text{M}]^{++}$), 190.9 (100, $[\text{CF}_2\text{CH}_2\text{I}]^+$), 141.0 (11, $[\text{CH}_2\text{I}]^+$), 131.0 (14, $[\text{C}_3\text{F}_5]^+$), 119.0 (14, $[\text{C}_2\text{F}_5]^+$);

$\text{C}_7\text{F}_{15}\text{CF}=\text{CHCF}_2\text{CF}_2\text{CH}_2\text{I}$: GC-MS: 2.8 mins $m/z = 653.9$ (44%, $[\text{M}]^{++}$), 463.0 (39, $[\text{C}_7\text{F}_{15}\text{CF}=\text{CHCF}_2]^+$), 225.0 (10, $[\text{C}_6\text{F}_8\text{H}]^+$), 190.9 (100, $[\text{CF}_2\text{CH}_2\text{I}]^+$), 163.0 (10, $[\text{CF}_2\text{CF}=\text{CHCF}_3]^+$), 119.0 (10, $[\text{C}_2\text{F}_5]^+$), 113.0 (10, $[\text{CF}=\text{CHCF}_3]^+$).

General Procedure for the Reactions of Telomer Fluorides with Anionic Bases

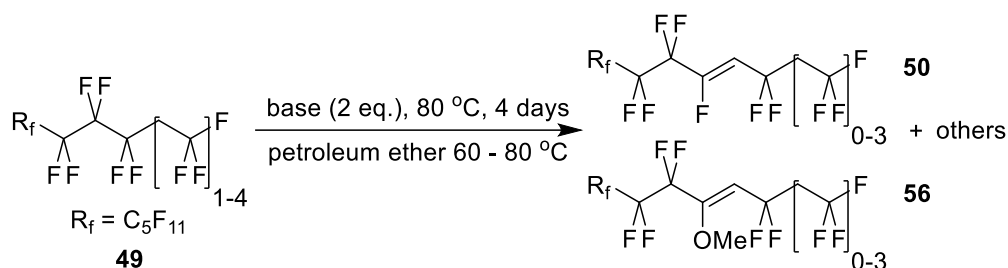


The mixture of telomer fluorides ($\text{C}_8\text{F}_{17}(\text{CH}_2\text{CF}_2)_{1-4}\text{F}$) (1.00 g, 1.77 mmol) were stirred with a base (4.00 mmol) in a solvent (30 mL) at various temperatures for 2 days. 1 M HCl (20 mL) was added, the organic layer was separated and washed with water and brine. The solvent was removed in vacuo and the products were analysed by ^1H and ^{19}F NMR.

$\text{C}_8\text{F}_{17}(\text{CH}_2\text{CF}_2)_{1-4}\text{F}$ was reacted with NaOEt (0.27 g), LHMDS (0.67 g), NaH, (0.10 g) and KO^tBu (0.45 g) in diethyl ether at rt. Only the reaction with KO^tBu caused observable dehydrofluorination (30%); ^1H NMR (400 MHz, Chloroform-*d*) δ 5.91 (dq, $^3J_{\text{HF}} = 28.7$, $^3J_{\text{HF}} = 6.8$, $\text{CF}=\text{CH}-\text{CF}_3$), 3.08 – 2.61 (m, CH_2CF_2); ^{19}F NMR (376 MHz, Chloroform-*d*) δ -58.60 (dd, $^3J_{\text{FH}} = 16.8$, $^4J_{\text{FF}} = 7.3$, $\text{CF}=\text{CH}-\text{CF}_3$), -59.24 – -59.37 (m, $\text{CF}=\text{CH}-\text{CF}_3$), -59.54 (ddt, $^3J_{\text{FH}} = 17.4$, $^4J_{\text{FF}} = 6.9$, $^5J_{\text{FH}} = 2.0$, $\text{CF}=\text{CH}-\text{CF}_3$), -60.89 (p, $^3J_{\text{FH}} = 9.3$, CH_2CF_3), -61.91 (p, $^3J_{\text{FH}} = 9.5$, CH_2CF_3), -62.01 (p, $^3J_{\text{FH}} = 9.5$, CH_2CF_3), -62.31 (p, $^3J_{\text{FH}} = 9.2$, CH_2CF_3), -81.08 (t, $^3J_{\text{FF}} = 9.8$, CF_2CF_3), -88.56 – -88.81 (m, CH_2CF_2), -88.82 – -89.03 (m, CH_2CF_2), -89.23 – -89.53 (m, CH_2CF_2), -91.48 – -91.75 (m, CH_2CF_2), -111.62 – -112.87 (m, CF_2CF_2), -113.65 – -114.00 (m, CF_2CF_2), -118.35 (q, $^3J_{\text{FH}} = 13.0$, $\text{CH}=\text{CF}$), -118.72 – -118.88 (m, $\text{CH}=\text{CF}$), -119.15 (q, $^3J_{\text{FH}} = 12.0$, $\text{CH}=\text{CF}$), -121.49 – -121.86 (m, CF_2CF_2), -121.87 – -122.33 (m, CF_2CF_2), -122.79 – -123.13 (m, CF_2CF_2), -123.46 – -123.78 (m, CF_2CF_2), -126.25 – -126.55 (m, CF_2CF_2).

$\text{C}_8\text{F}_{17}(\text{CH}_2\text{CF}_2)_{1-4}\text{F}$ was reacted with n-BuLi (2.5 M in hexanes, 0.80 mL, 2.00 mmol) and LDA (synthesised in situ from diisopropylamine [0.28 mL, 2 mmol] and n-BuLi [2.5 M in hexanes, 0.88 mL, 2.20 mmol]) in THF at -78 °C. The reaction with n-BuLi produced a viscous black tar that could not be dissolved in a solvent for analysis. The reaction with LDA caused observable dehydrofluorination (20%); ^1H NMR (400 MHz, Chloroform-*d*) δ 5.90 (dq, $^3J_{\text{HF}} = 28.8$, $^3J_{\text{HF}} = 6.9$, $\text{CF}=\text{CH}-\text{CF}_3$), 3.03 – 2.65 (m, CH_2CF_2); ^{19}F NMR (376 MHz, Chloroform-*d*) δ -55.76 (dt, $^3J_{\text{FH}} = 8.2$, $^4J_{\text{FF}} = 2.2$, $\text{CF}=\text{CH}-\text{CF}_3$), -59.80 (ddt, $^3J_{\text{FH}} = 17.5$, $^4J_{\text{FF}} = 6.9$, $^5J_{\text{FH}} = 2.0$, $\text{CF}=\text{CH}-\text{CF}_3$), -61.14 (p, $^3J_{\text{FH}} = 9.4$, CH_2CF_3), -62.16 (t, $^3J_{\text{FH}} = 9.5$, CH_2CF_3), -62.25 (p, $^3J_{\text{FH}} = 9.4$, CH_2CF_3),

-81.20 – -81.45 (m, CF₂CF₃), -88.77 – -88.99 (m, CH₂CF₂), -89.43 – -89.70 (m, CH₂CF₂), -91.66 – -91.93 (m, CH₂CF₂), -111.84 – -112.18 (m, CF₂CF₂), -112.66 – -113.02 (m, CF₂CF₂), -113.87 – -114.14 (m, CF₂CF₂), -119.25 – -119.43 (m, CH=CF), -121.61 – -122.01 (m, CF₂CF₂), -122.06 – -122.53 (m, CF₂CF₂), -122.90 – -123.30 (m, CF₂CF₂), -123.65 – -123.95 (m, CF₂CF₂), -126.41 – -126.73 (m, CF₂CF₂).



C₈F₁₇(CH₂CF₂)₁₋₄F was reacted with NaO^tBu (0.38 g), and KOMe (0.28 g) in diethyl ether at 80 °C in petroleum ether 60 – 80 °C. Both the reaction with NaO^tBu and with KOMe caused observable dehydrofluorination as described below;

Reaction with NaO^tBu (>50% dehydrofluorination): ¹H NMR (400 MHz, Chloroform-*d*) δ 7.03 – 6.93 (m, CF=CH-CF_n) 6.58 (dddd, ³J_{HF} = 30.0, ³J_{HF} = 28.4, ³J_{HF} = 8.6, ³J_{HF} = 1.3, CF=CH-CF_n), 6.36 (dd, ³J_{HF} = 29.8, ³J_{HF} = 27.1, CF=CH-CF), 6.12 – 5.81 (m, CF=CH-CF_n), 5.80 – 5.49 (m, CF=CH-CF_n), 3.74 – 3.50 (m, CH₂l), 3.13 – 2.68 (m, CH₂CF₂); ¹⁹F NMR (376 MHz, Chloroform-*d*) δ -56.35 – -56.60 (m, CF=CH-CF₃), -57.11 (dd, ³J_{FH} = 11.3, ⁴J_{FF} = 8.2, CF=CH-CF₃), -57.73 (dd, ³J_{FH} = 16.3, ⁴J_{FF} = 7.7, CF=CH-CF₃), -58.04 (dd, ³J_{FH} = 16.5, ⁴J_{FF} = 7.6, CF=CH-CF₃), -58.08 – -58.16 (m, CF=CH-CF₃), -58.64 (dd, ³J_{FH} = 16.9, ⁴J_{FF} = 7.3, CF=CH-CF₃), -59.53 – -59.63 (m, CF=CH-CF₃), -61.91 – -62.12 (m, CH₂CF₃), -62.22 (t, ³J_{FH} = 9.5, CH₂CF₃), -62.35 (p, ³J_{FH} = 9.3, CH₂CF₃), -80.99 – -81.24 (m, CF₂CF₃), -86.50 – -87.56 (m, CH₂CF₂), -87.84 – -89.53 (m, CH₂CF₂), -90.55 – -91.94 (m, CH₂CF₂), -98.77 – -99.12 (m, CH=CF), -100.77 (q, ³J_{FH} = 13.6, CH=CF), -112.19 – -112.88 (m, CH=CF), -118.16 (h, ³J_{FH} = 13.6, CH=CF), -118.40 (q, ³J_{FH} = 13.8, CH=CF), -118.74 – -118.92 (m, CF₂CF₂), -121.74 (s, CF₂CF₂), -122.16 (s, CF₂CF₂), -122.63 – -122.87 (m, CF₂CF₂), -122.97 (s, CF₂CF₂), -123.68 (s, CF₂CF₂), -126.26 – -126.56 (m, CF₂CF₂).

Reaction with KOMe (>50% dehydrofluorination): ¹H NMR (400 MHz, Chloroform-*d*) δ 6.16 (d, ³J_{HF} = 22.6, C(OMe)=CH-CF₂), 6.01 – 5.82 (m, CF=CH-CF₂), 5.71 (q, ³J_{HF} = 8.1, C(OMe)=CH-CF₃), 5.62 (q, ³J_{HF} = 7.8, C(OMe)=CH-CF₃), 5.55 (dq, ³J_{HF} = 31.5, ³J_{HF} = 7.5, CF=CH-CF₃), 3.98 (s, OMe), 3.93 – 3.89 (m, OMe) 3.68 – 3.51 (m, CH₂l) 3.07 – 2.65 (m, CH₂CF₂); ¹⁹F NMR (376 MHz, Chloroform-*d*) δ -55.27(t, ³J_{HF} = 7.5, C(OMe)=CH-CF₃), -56.24 – -56.41 (m, CF=CH-CF₃), -56.25 – -56.39 (m, CF=CH-CF₃), -57.30 – -57.37 (m, CF=CH-CF₃),

-57.76 – -57.85 (m, CF=CH-CF₃), -57.89 – -57.97 (m, CF=CH-CF₃), -58.26 (dd, ³J_{FH} = 16.8, ⁴J_{FF} = 7.4, CF=CH-CF₃), -58.61 – -58.71 (m, CF=CH-CF₃), -61.92 – -62.12 (m, CH₂CF₃), -62.13 – -62.31 (m, CH₂CF₃), -62.37 (q, ³J_{FH} = 8.8, CH₂CF₃), -81.12 (t, ³J_{FH} = 8.5, CF₂CF₃), -86.51 – -89.53 (m, CH₂CF₂), -90.37 – -91.92 (m, CH₂CF₂), -112.17 – -112.89 (m, CF₂CF₂), -114.98 – -116.36 (m, CF₂), -115.10 (t, ³J_{FH} = 14.4, CH=CF), -115.28 (t, ³J_{FH} = 14.1, CH=CF), -115.97 (t, ³J_{FH} = 13.9, CH=CF), -116.06 (t, ³J_{FH} = 12.2, CH=CF), -118.84 (s, CF₂CF₂), -121.75 (s, CF₂CF₂), -121.87 – -122.50 (m, CF₂CF₂), -122.98 (s, CF₂CF₂), -123.69 (s, CF₂CF₂), -126.41 (s, CF₂CF₂); The GC-MS data for each product is given below:

C₇F₁₅C(OMe)=CHCF₃: GC-MS: 1.7 mins *m/z* = 494.1 (37%, [M]⁺), 475.1 (28, [M - F]⁺), 225.0 (13, [CF₂CF₂C(OMe)=CHCF₂]⁺), 175.1 (100, [CF₂C(OMe)=CHCF₂]⁺), 131.1 (13, [C₃F₅]⁺), 125.1 (36, [C(OMe)=CHCF₂]⁺), 119.1 (22, [C₂F₅]⁺);

C₇F₁₅CF=CHCF₂CH₂CF₃: GC-MS: 1.7 mins *m/z* = 527.1 (5%, [M - F]⁺), 463.1 (32, [C₇F₁₅CF=CHCF₂]⁺), 227.0 (61, [CF₂CF=CHCF₂CH₂CF₃]⁺), 163.1 (100, [CF₂CF=CHCF₃]⁺), 144.1 (8, [CF₂CF=CHCF₂]⁺), 133.1 (15, [CF₂CH₂CF₃]⁺), 131.1 (11, [C₃F₅]⁺), 119.1 (14, [C₂F₅]⁺), 113.1 (26, [CF=CHCF₃]⁺);

C₇F₁₅CF₂CH₂CF₂CH₂CF₃: GC-MS: 1.9 mins *m/z* = 547.0 (0.5%, [M - F]⁺), 483.1 (2, [M - CH₂CF₃]⁺), 197.0 (16, [CF₂CH₂CF₂CH₂CF₃]⁺), 133.1 (100, [CF₂CH₂CF₃]⁺), 131.1 (5, [C₃F₅]⁺);

C₇F₁₅CF=CHCF=CHCF₃: GC-MS: 2.0 mins *m/z* = 526.1 (6%, [M]⁺), 507.1 (7, [M - F]⁺), 207.0 (100, [CF₂CF=CHCF=CHCF₃]⁺), 157.1 (46, [CF=CHCF=CHCF₃]⁺), 131.1 (11, [C₃F₅]⁺), 119.1 (21, [C₂F₅]⁺);

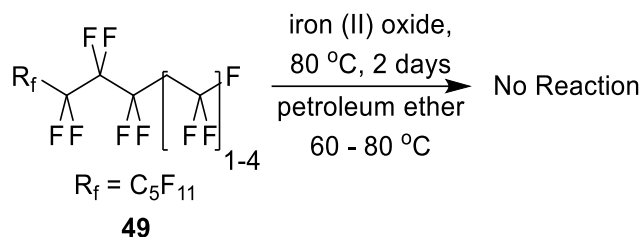
C₇F₁₅C(OMe)C=CHCF₂CH₂CF₃: GC-MS: 2.4 mins *m/z* = 538.1 (35%, [M - HF]⁺), 519.1 (25, [M - HF₂]⁺), 455.0 (100, [(C₇F₁₅C(OMe)C=CHCF₂) - HF]⁺);

C₇F₁₅CF=CHCF₂CH₂CF₂CH₂CF₃: GC-MS: 2.4 mins *m/z* = 591.0 (1%, [M - F]⁺), 463.1 (63, [C₇F₁₅CF=CHCF₂]⁺), 291.1 (14, [CF₂CF=CHCF₂CH₂CF₂CH₂CF₃]⁺), 163.0 (100, [CF₂CF=CHCF₃]⁺), 133.1 (69, [CF₂CH₂CF₃]⁺), 119.1 (16, [C₂F₅]⁺), 113.1 (37, [CF=CHCF₃]⁺);

C₇F₁₅C(OMe)C=CH(CF₂CH₂)₂CF₃: GC-MS: 2.6 mins *m/z* = 538.1 (28%, [C₇F₁₅C(OMe)C=CHCF₂CH=CF₂]⁺), 519.1 (22, [C₇F₁₅C(OMe)C=CHCF₂CH=CF]⁺), 455.1 (100, [(C₇F₁₅C(OMe)C=CHCF₂) - HF]⁺), 219.0 (15, [CF₃CF₂CF₂CF₂]⁺), 169.0 (29, [CF₃CF₂CF₂]⁺), 119.0 (25, [CF₃CF₂]⁺);

C₇F₁₅CF₂CH₂CF₂CH₂CF₂CH₂CF₃: GC-MS: 2.6 mins *m/z* = 611.0 (0.2%, [M - F]⁺), 547.0 (1, [M - CH₂CF₃]⁺), 483.0 (4, [M - CH₂CF₂CH₂CF₃]⁺), 261.1 (7, [CF₂CH₂CF₂CH₂CF₂CH₂CF₃]⁺), 197.0 (16, [CF₂CH₂CF₂CH₂CF₃]⁺), 131.1 (5, [C₃F₅]⁺).

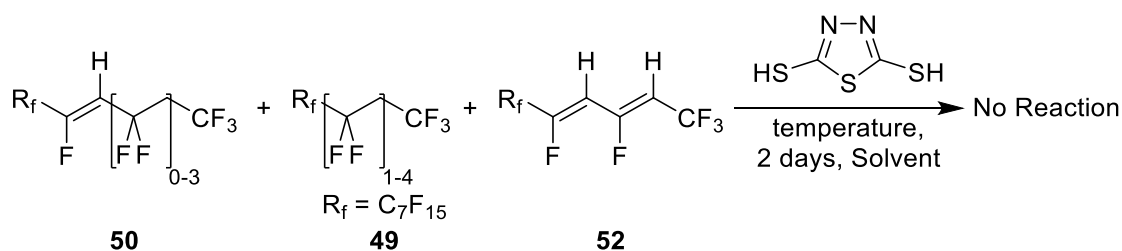
Reaction of Telomer Fluorides with Iron Oxide



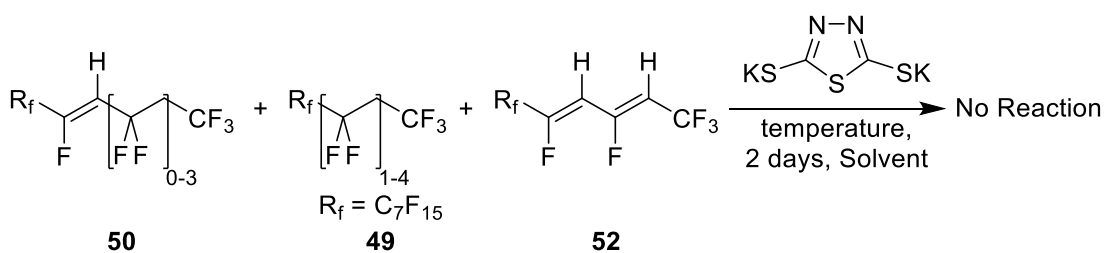
The mixture of telomer fluorides ($\text{C}_8\text{F}_{17}(\text{CH}_2\text{CF}_2)_{1-4}\text{F}$) (2 g, 3.54 mmol) was stirred with FeO (1.28 g, 8 mmol) in petroleum ether 60 – 80 °C (30 mL) for 2 days at 80 °C. The Iron (II) oxide was filtered and the solvent was removed in vacuo. On examination, no reaction had occurred.

Reactions of Dehydrofluorinated Telomer Fluorides with Dithio

Thiodiazole

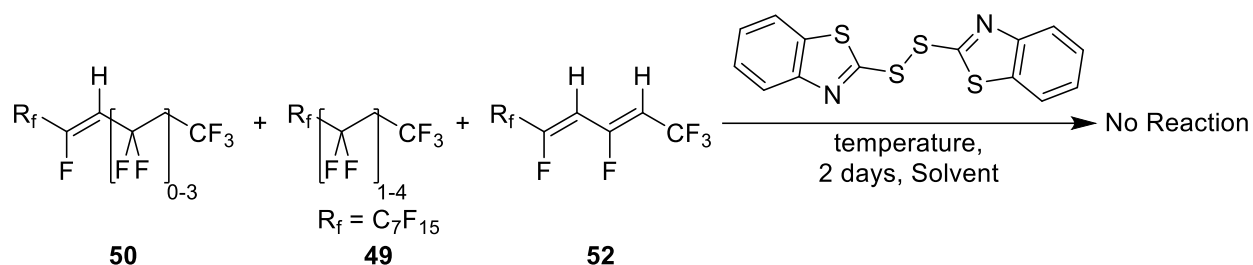


The mixture of dehydrofluorinated telomer fluorides (principally $\text{C}_8\text{F}_{17}(\text{CH}_2\text{CF}_2)_{1-4}\text{F}$, $\text{C}_7\text{F}_{15}\text{CF}=\text{CHCF}_2(\text{CH}_2\text{CF}_2)_{0-3}\text{F}$ and $\text{C}_7\text{F}_{15}\text{CF}=\text{CHCF}=\text{CHCF}_3$) (0.25 g, 0.45 mmol) was stirred with dithio thiodiazole (0.15 g, 1.00 mmol) in petroleum ether 60 – 80 °C (30 mL) for 2 days at rt. The organic layer was separated, washed with water and brine and the solvent was removed in vacuo. Analysis of the product mixture by ^{19}F NMR showed that no reaction had occurred. The reaction was repeated at 80 °C in ethyl acetate (30 mL) for 2 days. Analysis of the product mixture by ^{19}F NMR showed that no reaction had occurred.



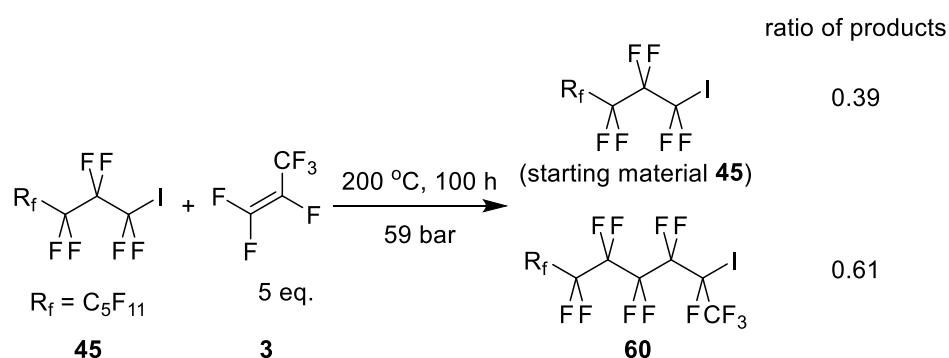
The mixture of dehydrofluorinated telomer fluorides (principally $\text{C}_8\text{F}_{17}(\text{CH}_2\text{CF}_2)_{1-4}\text{F}$, $\text{C}_7\text{F}_{15}\text{CF}=\text{CHCF}_2(\text{CH}_2\text{CF}_2)_{0-3}\text{F}$ and $\text{C}_7\text{F}_{15}\text{CF}=\text{CHCF}=\text{CHCF}_3$) (0.25 g, 0.45 mmol) was stirred with

1,3,4-thiadiazole-2,5-dithiol dipotassium salt (0.23 g, 1.00 mmol) in petroleum ether 60 – 80 °C (30 mL) for 2 days at rt. The organic layer was separated, washed with water and brine and the solvent was removed in vacuo. Analysis of the product mixture by ^{19}F NMR showed that no reaction had occurred. The reaction was repeated at 80 °C in ethyl acetate (30 mL) for 2 days. Analysis of the product mixture by ^{19}F NMR showed that no reaction had occurred.



The mixture of dehydrofluorinated telomer fluorides (principally $\text{C}_8\text{F}_{17}(\text{CH}_2\text{CF}_2)_{1-4}\text{F}$, $\text{C}_7\text{F}_{15}\text{CF=CHCF}_2(\text{CH}_2\text{CF}_2)_{0-3}\text{F}$ and $\text{C}_7\text{F}_{15}\text{CF=CHCF=CHCF}_3$) (0.25 g, 0.45 mmol) was stirred with 2,2'-dithiobis(benzothiazole) (0.33 g, 1.00 mmol) in petroleum ether 60 – 80 °C (30 mL) for 2 days at rt. The organic layer was separated, washed with water and brine and the solvent was removed in vacuo. Analysis of the product mixture by ^{19}F NMR showed that no reaction had occurred. The reaction was repeated at 80 °C in ethyl acetate (30 mL) for 2 days. Analysis of the product mixture by ^{19}F NMR showed that no reaction had occurred.

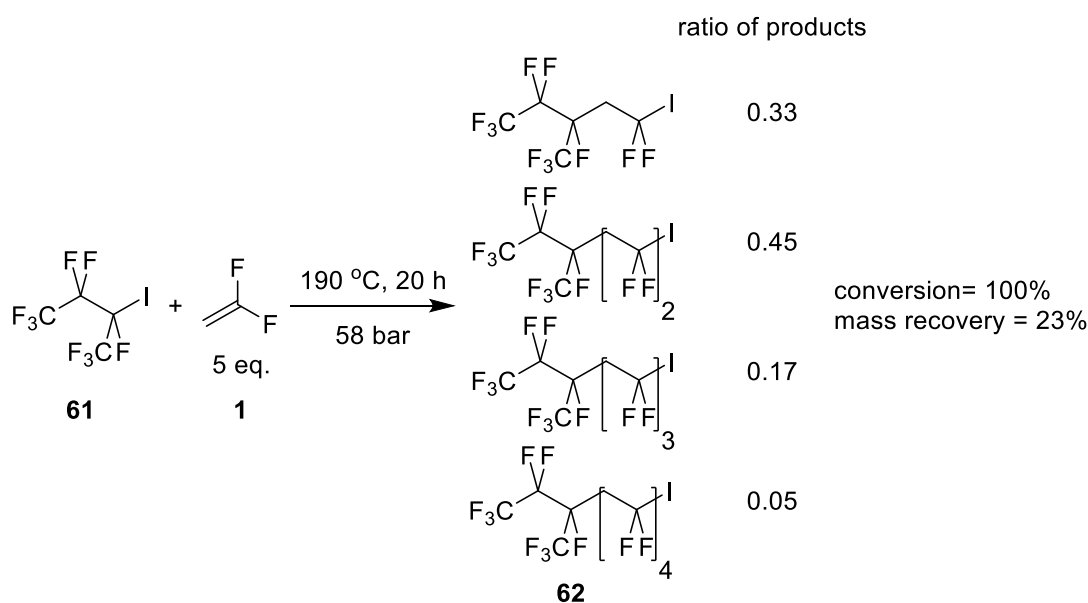
Reaction of Perfluorooctyl Iodide with HFP



Perfluorooctyl iodide (21.84 g, 40 mmol), was degassed and transferred to an autoclave (160 mL, Hastelloy) and hexafluoropropylene (30.00 g, 200 mmol) was added by vacuum transfer. The autoclave was transferred to a rocking furnace and heated to 200 °C for 100 hours. The autoclave was allowed to cool and a black liquid was recovered. This was dissolved in DCM (100 mL) and washed with aq. sodium thiosulfate, water and brine. However, on

filtration, this had failed to purify the product, which remained a black liquid ($C_8F_{17}(CF_2CF(CF_3))_{0-1}$); ^{19}F NMR (376 MHz, Chloroform-*d*) δ -59.53 (tp, $^3J_{FF} = 15.5$, $^4J_{FF} = 3.8$, CF_2I), -69.47 (ddd, $^3J_{FF} = 21.3$, $^3J_{FF} = 13.2$, $^4J_{FF} = 8.4$, $CF_2CF(CF_3)I$), -73.74 (dtd, $^3J_{FF} = 19.3$, $^3J_{FF} = 12.0$, $^4J_{FF} = 7.4$, $CF_2CF(CF_3)I$), -74.88 – -75.03 (m, $CF_2CF(CF_3)I$), -81.90 – -82.13 (m, CF_2CF_3), -113.56 – -113.80 (m, CF_2CF_2), -121.46 – -121.80 (m, CF_2CF_2), -122.31 – -122.90 (m, CF_2CF_2), -123.29 – -123.80 (m, CF_2CF_2), -126.92 – -127.27 (m, CF_2CF_2), -145.32 (dh, $^3J_{FF} = 28.2$, $^3J_{FF} = 13.8$, $CF_2CF(CF_3)I$); ^{13}C NMR (101 MHz, Chloroform-*d*) δ 119.76 (qd, $^1J_{CF} = 282.1$, $^2J_{CF} = 25.8$, $CF_2CF(CF_3)I$), 116.97 (qt, $^1J_{CF} = 287.0$, $^2J_{CF} = 32.6$, CF_2CF_3), 114.44 – 104.41 (m, CF_2), 92.62 (tt, $^1J_{CF} = 320.4$, $^2J_{CF} = 41.4$, CF_2I), 84.33 – 80.73 (m, $CF_2CF(CF_3)I$).

Reaction of Perfluoro-2-iodobutane with 5 eq. of VDF



Perfluoro-2-iodobutane (13.8 g, 40 mmol), was degassed and transferred to an autoclave (160 mL, Hastelloy) and vinylidene fluoride (12.8 g, 200 mmol) was added by vacuum transfer. The autoclave was transferred to a rocking furnace and heated to 190 °C for 20 hours. The autoclave was allowed to cool and a brown liquid was recovered. This was dissolved in DCM (100 mL), washed with aq. sodium thiosulfate, water and brine and the solvent removed in vacuo to yield $CF_3CF_2CF(CF_3)(CH_2CF_2)_{1-4}I$ (6.2 g, 100% conversion, 22% mass recovery) as a yellow liquid; 1H NMR (400 MHz, Chloroform-*d*) δ 3.69 – 3.43 (m, $CF(CF_3)CH_2CF_2I$), 3.38 (tt, $^3J_{HF} = 15.8$, $^3J_{HF} = 14.2$ Hz, $CF(CF_3)(CH_2CF_2)_{0-3}CH_2CF_2I$), 3.06 – 2.66 (m, $CF(CF_3)(CH_2CF_2)_{0-3}CH_2CF_2I$); ^{19}F NMR (376 MHz, Chloroform-*d*) δ -37.51 – -37.83 (m, CH_2CF_2I), -38.45 – -38.74 (m, CH_2CF_2I), -76.13 – -76.38 (m, $CF(CF_3)$), -76.47 – -76.68 (m, $CF(CF_3)$), -79.99 – -80.24 (m, $CF_3CF_2CF(CF_3)$), -88.56 (s, $CF(CF_3)(CH_2CF_2)_{0-3}CH_2CF_2I$), -89.10 – -89.69 (m,

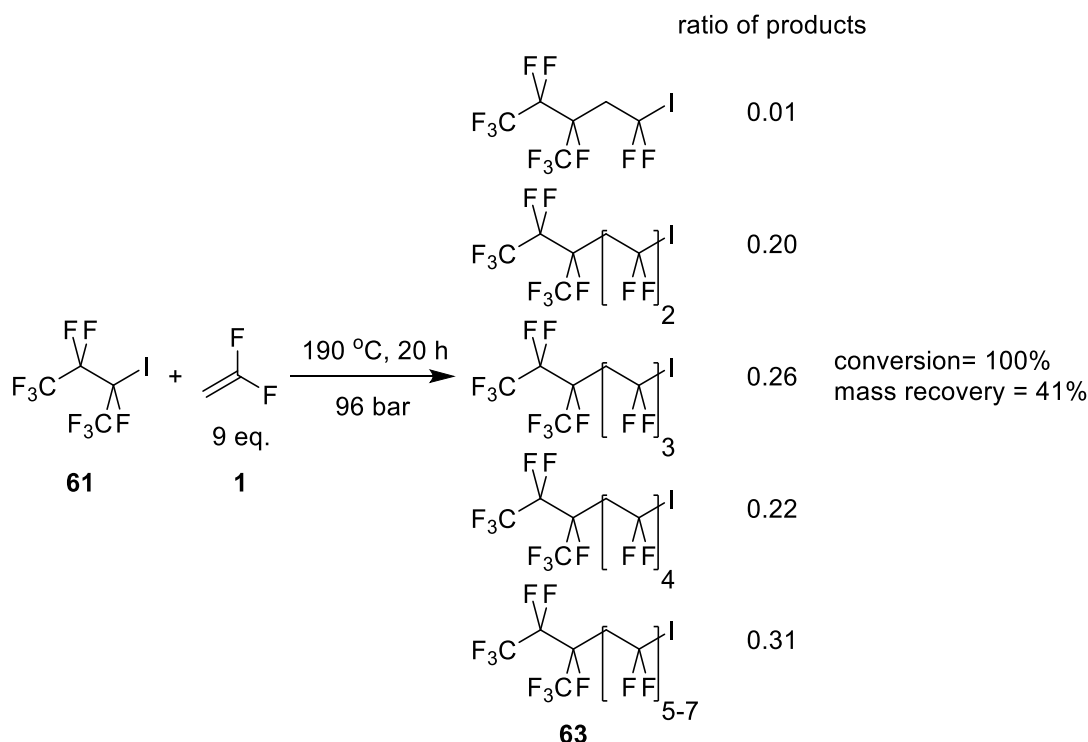
$\text{CF}(\text{CF}_3)(\text{CH}_2\text{CF}_2)_{0-3}\text{CH}_2\text{CF}_2\text{I}$, $-89.91 - -90.36$ (m, $\text{CF}(\text{CF}_3)(\text{CH}_2\text{CF}_2)_{0-3}\text{CH}_2\text{CF}_2\text{I}$), -120.24 (p, $^3J_{\text{FF}} = 7.8$, $\text{CF}_3\text{CF}_2\text{CF}(\text{CF}_3)$), -121.03 (p, $^3J_{\text{FF}} = 7.7$, $\text{CF}_3\text{CF}_2\text{CF}(\text{CF}_3)$), $-121.22 - -121.39$ (m, $\text{CF}_3\text{CF}_2\text{CF}(\text{CF}_3)$), -121.61 (qq, $^3J_{\text{FF}} = 11.8$, $^4J_{\text{FF}} = 3.8$, $\text{CF}_3\text{CF}_2\text{CF}(\text{CF}_3)$), -122.39 (qq, $^3J_{\text{FF}} = 12.6$, $^4J_{\text{FF}} = 4.3$, $\text{CF}_3\text{CF}_2\text{CF}(\text{CF}_3)$), $-185.39 - -185.89$ (m, $\text{CF}(\text{CF}_3)$); ^{13}C NMR (101 MHz, Chloroform-*d*) δ 120.11 (qdd, $^1J_{\text{CF}} = 286.6$, $^2J_{\text{CF}} = 27.4$, $^3J_{\text{CF}} = 3.5$, $\text{CF}_2\text{CF}(\text{CF}_3)\text{CH}_2$), 117.65 (qt, $^1J_{\text{CF}} = 287.7$, $^2J_{\text{CF}} = 34.3$, CF_2CF_3), 113.83 – 107.21 (m, CF_3CF_2), 92.66 – 89.35 (m, $\text{CF}_2\text{CF}(\text{CF}_3)\text{CH}_2$), 90.40 (tt, $^1J_{\text{CF}} = 313.7$, $^3J_{\text{CF}} = 4.7$, $\text{CH}_2\text{CF}_2\text{I}$), 89.26 (td, $^1J_{\text{CF}} = 317.2$, $^3J_{\text{CF}} = 4.6$, $\text{CF}(\text{CF}_3)\text{CH}_2\text{CF}_2\text{I}$), 55.31 – 54.12 (m, CH_2CF_2), 46.33 (q, $^2J_{\text{CF}} = 20.8$, CH_2CF_2), 35.92 – 34.94 (m, CH_2CF_2). The GC-MS data for each product, and the percentage of each compound in the product mixture determined by ^{19}F NMR spectroscopy, are given below:

$\text{CF}_3\text{CF}_2\text{CF}(\text{CF}_3)\text{CH}_2\text{CF}_2\text{I}$ (33%): GC-MS: 1.4 mins $m/z = 283.0$ (100%, $[\text{M} - \text{I}]^+$), 195.0 (13, $[\text{CF}_3\text{CF}=\text{CFCH}_2\text{CF}_2]^+$) 176.9 (7, $[\text{ICF}_2]^+$), 133.0 (23, $[\text{CF}_2\text{CH}_2\text{CF}_3]^+$) 119.0 (17, $[\text{CF}_2\text{CF}_3]^+$).

$\text{CF}_3\text{CF}_2\text{CF}(\text{CF}_3)(\text{CH}_2\text{CF}_2)_2\text{I}$ (45%): GC-MS: 2.3 mins $m/z = 455.0$ (1%, $[\text{M} - \text{F}]^+$), 347.0 (100, $[\text{M} - \text{I}]^+$), 283.0 (25, $[\text{M} - \text{CH}_2\text{CF}_2\text{I}]^+$), 263.0 (32, $[\text{CF}_3\text{CF}_2\text{C}(\text{CF}_3)=\text{CHCF}_2]^+$), 195.0 (21, $[\text{CF}_3\text{CF}=\text{CFCH}_2\text{CF}_2]^+$), 176.9 (17, $[\text{ICF}_2]^+$), 145 (12, $[\text{C}_4\text{H}_2\text{F}_5]^+$), 133.0 (51, $[\text{CF}_2\text{CH}_2\text{CF}_3]^+$), 119.0 (18, $[\text{CF}_2\text{CF}_3]^+$), 113.0 (16, $[\text{CF}_2\text{CHCF}_2]^+$).

$\text{CF}_3\text{CF}_2\text{CF}(\text{CF}_3)(\text{CH}_2\text{CF}_2)_3\text{I}$ (17%): GC-MS: 3.0 mins $m/z = 411.1$ (50%, $[\text{M} - \text{I}]^+$), 327.1 (22, $[\text{CF}_3\text{CF}_2\text{C}(\text{CF}_3)=\text{CHCF}_2\text{CH}_2\text{CF}_2]^+$), 283.1 (100, $[\text{M} - (\text{CH}_2\text{CF}_2)_2\text{I}]^+$), 263.0 (18, $[\text{CF}_3\text{CF}_2\text{C}(\text{CF}_3)=\text{CHCF}_2]^+$), 195.0 (28, $[\text{CF}_3\text{CF}=\text{CFCH}_2\text{CF}_2]^+$), 177.0 (20, $[\text{ICF}_2]^+$), 145 (8, $[\text{C}_4\text{H}_2\text{F}_5]^+$), 133.0 (83, $[\text{CF}_2\text{CH}_2\text{CF}_3]^+$), 119.0 (9, $[\text{CF}_2\text{CF}_3]^+$), 113.0 (28, $[\text{CF}_2\text{CHCF}_2]^+$).

Reaction of Perfluoro-2-iodobutane with 9 eq. of VDF



Perfluoro-2-iodobutane (13.8 g, 40 mmol), was degassed and transferred to an autoclave (160 mL, Hastelloy) and vinylidene fluoride (23.0 g, 360 mmol) was added by vacuum transfer. The autoclave was transferred to a rocking furnace and heated to 190 °C for 20 hours. The autoclave was allowed to cool and a brown liquid was recovered. This was dissolved in DCM (100 mL), washed with aq. sodium thiosulfate, water and brine and the solvent removed in vacuo to yield $\text{CF}_3\text{CF}_2\text{CF}(\text{CF}_3)(\text{CH}_2\text{CF}_2)_{2-7}\text{I}$ (15.24 g, 100% conversion, 41% mass recovery) as a yellow liquid; ^1H NMR (400 MHz, Chloroform-*d*) δ 3.44 – 3.26 (m, $\text{CF}(\text{CF}_3)(\text{CH}_2\text{CF}_2)_{1-6}\text{CH}_2\text{CF}_2\text{I}$), 3.12 – 2.53 (m, $\text{CF}(\text{CF}_3)(\text{CH}_2\text{CF}_2)_{1-6}\text{CH}_2\text{CF}_2\text{I}$); ^{19}F NMR (376 MHz, Chloroform-*d*) δ -38.24 – -38.70 (m, $\text{CH}_2\text{CF}_2\text{I}$), -76.00 – -76.27 (m, $\text{CF}(\text{CF}_3)$), -76.36 – -76.52 (m, $\text{CF}(\text{CF}_3)$), -76.54 – -76.75 (m, $\text{CF}(\text{CF}_3)$), -79.88 – -80.05 (m, $\text{CF}_3\text{CF}_2\text{CF}(\text{CF}_3)$), -87.85 – -89.08 (m, $\text{CF}(\text{CF}_3)(\text{CH}_2\text{CF}_2)_{1-6}\text{CH}_2\text{CF}_2\text{I}$), -89.10 – -89.79 (m, $\text{CF}(\text{CF}_3)(\text{CH}_2\text{CF}_2)_{1-6}\text{CH}_2\text{CF}_2\text{I}$), -89.90 – -90.55 (m, $\text{CF}(\text{CF}_3)(\text{CH}_2\text{CF}_2)_{1-6}\text{CH}_2\text{CF}_2\text{I}$), -119.91 – -120.05 (m, $\text{CF}_3\text{CF}_2\text{CF}(\text{CF}_3)$), -120.17 (dhept, $^3J_{\text{FF}} = 15.7$, $^3J_{\text{FF}} = 8.1$, $\text{CF}_3\text{CF}_2\text{CF}(\text{CF}_3)$), -120.84 – -121.06 (m, $\text{CF}_3\text{CF}_2\text{CF}(\text{CF}_3)$), -121.10 – -121.38 (m, $\text{CF}_3\text{CF}_2\text{CF}(\text{CF}_3)$), -121.52 (ddtt, $^3J_{\text{FF}} = 31.0$, $^3J_{\text{FF}} = 17.7$, $^4J_{\text{FF}} = 13.2$, $^4J_{\text{FF}} = 4.2$, $\text{CF}_3\text{CF}_2\text{CF}(\text{CF}_3)$), -121.89 – -122.15 (m, $\text{CF}_3\text{CF}_2\text{CF}(\text{CF}_3)$), -122.32 (dddq, $^3J_{\text{FF}} = 30.8$, $^3J_{\text{FF}} = 13.2$, $^4J_{\text{FF}} = 8.5$, $^4J_{\text{FF}} = 4.1$, $\text{CF}_3\text{CF}_2\text{CF}(\text{CF}_3)$), -185.70 (s, $\text{CF}(\text{CF}_3)$). ^{13}C NMR (101 MHz, Chloroform-*d*) δ 120.11 (qdd, $^1J_{\text{CF}} = 287.6$, $^2J_{\text{CF}} = 27.5$, $^3J_{\text{CF}} = 3.5$, $\text{CF}_2\text{CF}(\text{CF}_3)\text{CH}_2$), 117.74 (qt, $^1J_{\text{CF}} = 287.7$, $^2J_{\text{CF}} = 34.3$, CF_2CF_3), 113.84 – 107.18 (m, CF_3CF_2), 92.66 – 89.35 (m, $\text{CF}_2\text{CF}(\text{CF}_3)\text{CH}_2$), 90.76 (tt, $^1J_{\text{CF}} = 313.7$, $^3J_{\text{CF}} = 4.6$, $\text{CH}_2\text{CF}_2\text{I}$), 90.42 (tt, $^1J_{\text{CF}} = 313.7$, $^3J_{\text{CF}} = 5.1$,

CH₂CF₂I), 55.31 – 53.89 (m, CH₂CF₂), 44.47 – 43.06 (m, CH₂CF₂), 36.02 – 34.96 (m, CH₂CF₂). The GC-MS data for each product, and the percentage of each compound in the product mixture determined by ¹⁹F NMR spectroscopy, are given below:

CF₃CF₂CF(CF₃)CH₂CF₂I (1%): GC-MS: 1.3 mins *m/z* = 283.1 (100%, [M – I]⁺), 195.0 (13, [CF₂=C(CF₃)CH₂CF₂]⁺) 176.9 (7, [ICF₂]⁺), 133.1 (21, [CF₂CH₂CF₃]⁺) 119.0 (15, [CF₂CF₃]⁺), 113.1 (10, [CF₃CH₂CF₂ – HF]⁺).

CF₃CF₂CF(CF₃)(CH₂CF₂)₂I (20%): GC-MS: 2.3 mins *m/z* = 454.9 (1%, [M – F]⁺), 347.1 (100, [M – I]⁺), 283.1 (23, [CF₃CF₂CF(CF₃)CH₂CF₂]⁺), 263.0 (28, [CF₃CF₂CF(CF₃)CH₂CF₂ – HF]⁺), 195.0 (20, [CF₂=C(CF₃)CH₂CF₂]⁺), 176.9 (14, [ICF₂]⁺), 145.1 (10, [C₄H₂F₅]⁺), 133.0 (41, [CF₂CH₂CF₃]⁺), 119.0 (15, [CF₂CF₃]⁺), 113.0 (14, [CF₂CHCF₂]⁺).

CF₃CF₂CF(CF₃)(CH₂CF₂)₃I (26%): GC-MS: 2.9 mins *m/z* = 411.1 (37%, [M – I]⁺), 327.1 (14, [CF₃CF₂CF(CF₃)(CH₂CF₂)₂ – HF]⁺), 283.1 (70, [CF₃CF₂CF(CF₃)CH₂CF₂]⁺), 263.0 (15, [CF₃CF₂CF(CF₃)CH₂CF₂ – HF]⁺), 195.0 (23, [CF₂=C(CF₃)CH₂CF₂]⁺), 177.0 (21, [ICF₂]⁺), 145.1 (9, [C₄H₂F₅]⁺), 133.0 (100, [CF₂CH₂CF₃]⁺), 119.0 (12, [CF₂CF₃]⁺), 113.0 (29, [CF₂CHCF₂]⁺).

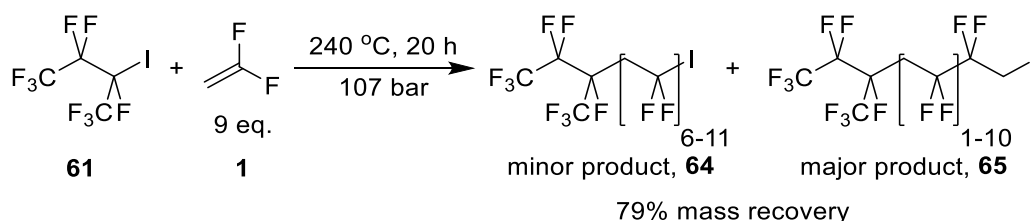
CF₃CF₂CF(CF₃)(CH₂CF₂)₄I (22%): GC-MS: 3.5 mins *m/z* = 475.0 (14%, [M – I]⁺), 455.0 (30, [M – I – HF]⁺), 347.1 (17, [CF₃CF₂C(CF₃)FCH₂CF₂CH₂CF₂]⁺), 327.1 (27, [CF₃CF₂C(CF₃)FCH=CFCH₂CF₂]⁺), 283.1 (39, [CF₃CF₂CF(CF₃)CH₂CF₂]⁺), 263.0 (9, [CF₃CF₂CF(CF₃)CH₂CF₂ – HF]⁺), 241.0 (14, [CF₂CH₂CF₂I]⁺), 197.0 (35, [CF₃(CH₂CF₂)₂]⁺) 195.0 (17, [CF₂=C(CF₃)CH₂CF₂]⁺), 177.0 (38, [ICF₂]⁺), 145 (6, [C₄H₂F₅]⁺), 133.1 (100, [CF₂CH₂CF₃]⁺), 119.0 (8, [CF₂CF₃]⁺), 113.0 (37, [CF₂CHCF₂]⁺).

CF₃CF₂CF(CF₃)(CH₂CF₂)₅I (17%): GC-MS: 4.0 mins *m/z* = 539.1 (2%, [M – I]⁺), 519.1 (19, [M – I – HF]⁺), 347.1 (8, [CF₃CF₂C(CF₃)FCH₂CF₂CH₂CF₂]⁺), 327.1 (17, [CF₃CF₂C(CF₃)FCH=CFCH₂CF₂]⁺), 283.1 (32, [CF₃CF₂CF(CF₃)CH₂CF₂]⁺), 261.1 (9, [CF₃(CH₂CF₂)₃]⁺), 241.0 (26, [CF₂CH₂CF₂I]⁺), 197.0 (18, [CF₃(CH₂CF₂)₂]⁺) 195.0 (12, [CF₂=C(CF₃)CH₂CF₂]⁺), 177.0 (32, [ICF₂]⁺), 133.0 (100, [CF₂CH₂CF₃]⁺), 119.0 (5, [CF₂CF₃]⁺), 113.0 (41, [CF₂CHCF₂]⁺).

CF₃CF₂CF(CF₃)(CH₂CF₂)₆I (9%): GC-MS: 4.4 mins *m/z* = 603.1 (2%, [M – I]⁺), 583.1 (30, [M – I – HF]⁺), 391.1 (9, [CF₃CF₂CF(CF₃)(CH₂CF₂)₃ – HF]⁺), 347.1 (9, [CF₃CF₂C(CF₃)FCH₂CF₂CH₂CF₂]⁺), 327.0 (20, [CF₃CF₂CF(CF₃)(CH₂CF₂)₂ – HF]⁺), 305.1 (14, [(CF₂CH₂)₂CF₂I]⁺), 283.1 (43, [CF₃CF₂CF(CF₃)CH₂CF₂]⁺), 261.1 (10, [CF₃(CH₂CF₂)₃]⁺), 241.0 (31, [CF₂CH₂CF₂I]⁺), 197.0 (35, [CF₃(CH₂CF₂)₂]⁺) 195.0 (12, [CF₂=C(CF₃)CH₂CF₂]⁺), 177.0 (41, [ICF₂]⁺), 133.1 (100, [CF₂CH₂CF₃]⁺), 119.0 (4, [CF₂CF₃]⁺), 113.0 (46, [CF₂CHCF₂]⁺).

CF₃CF₂CF(CF₃)(CH₂CF₂)₇I (5%): GC-MS: 4.8 mins *m/z* = 667.2 (1% , [M - I]⁺), 647.2 (24, [M - I - HF]⁺), 455.1 (7, [CF₃CF₂CF(CF₃)(CH₂CF₂)₄ - HF]⁺), 391.1 (9, [CF₃CF₂CF(CF₃)(CH₂CF₂)₃ - HF]⁺), 369.1 (7, [(CF₂CH₂)₃CF₂I]⁺), 349.1 (7, [CF₃(CH₂CF₂)₅ - 2HF]⁺), 347.1 (9, [CF₃CF₂CF(CF₃)(CH₂CF₂)₂]⁺), 327.1 (20, [CF₃CF₂CF(CF₃)(CH₂CF₂)₂ - HF]⁺), 305.1 (19, [(CF₂CH₂)₂CF₂I]⁺), 283.1 (45, [CF₃CF₂CF(CF₃)CH₂CF₂]⁺), 261.1 (12, [CF₃(CH₂CF₂)₃]⁺), 241.1 (36, [CF₂CH₂CF₂I]⁺), 197.1 (45, [CF₃(CH₂CF₂)₂]⁺), 177.0 (46, [ICF₂]⁺), 133.1 (100, [CF₃CH₂CF₂]⁺), 119.0 (4, [CF₂CF₃]⁺), 113.1 (50, [CF₃CH₂CF₂ - HF]⁺).

Reaction of Perfluoro-2-iodobutane with 9eq. of VDF at 240 °C



Perfluoro-2-iodobutane (13.8 g, 40 mmol), was degassed and transferred to an autoclave (160 mL, Hastelloy) and vinylidene fluoride (23.0 g, 360 mmol) was added by vacuum transfer. The autoclave was transferred to a rocking furnace and heated to 240 °C for 20 hours. The autoclave was allowed to cool and a brown liquid was recovered. This was dissolved in DCM (100 mL), washed with aq. sodium thiosulfate, water and brine and the solvent removed in vacuo to yield a mixture of CF₃CF₂CF(CF₃)(CH₂CF₂)₁₋₁₀CF₂CH₂I (major product) and CF₃CF₂CF(CF₃)(CH₂CF₂)₆₋₁₁I (minor product) (21.65 g, 79% mass recovery) as a brown, viscous liquid; ¹H NMR (400 MHz, Chloroform-*d*) δ 3.63 (t, ³J_{HF} = 17.6, CF(CF₃)(CH₂CF₂)₁₋₁₀CF₂CH₂I), 3.61 (t, ³J_{HF} = 17.5, CF(CF₃)(CH₂CF₂)₁₋₁₀CF₂CH₂I), 3.37 (p, ³J_{HF} = 14.8, CF(CF₃)(CH₂CF₂)₅₋₁₀CH₂CF₂I), 3.11 – 2.52 (m, CF(CF)₃(CH₂CF₂)₁₋₁₀); ¹⁹F NMR (376 MHz, Chloroform-*d*) δ -38.11 – -38.33 (m, CH₂CF₂I), -38.36 – -38.54 (m, CH₂CF₂I), -75.84 – -76.19 (m, CF(CF₃)), -79.68 – -79.99 (m, CF₃CF₂CF(CF₃)), -88.43 – -88.94 (m, CF(CF₃)(CH₂CF₂)_n), -89.14 – -89.66 (m, CF(CF₃)(CH₂CF₂)_n), -89.90 – -90.56 (m, CF(CF₃)(CH₂CF₂)_n), -91.57 – -91.92 (m, CF(CF₃)(CH₂CF₂)_n), -107.44 – -107.63 (m, CF(CF₃)(CH₂CF₂)₁₋₁₀CF₂CH₂I), -107.90 – -108.26 (m, CF(CF₃)(CH₂CF₂)₁₋₁₀CF₂CH₂I), -111.84 – -112.22 (m, CF(CF₃)(CH₂CF₂)₁₋₁₀CF₂CH₂I), -114.76 – -115.16 (m, CF(CF₃)(CH₂CF₂)₁₋₁₀CF₂CH₂I), -120.00 – -120.16 (m, CF₃CF₂CF(CF₃)), -120.58 – -120.72 (m, CF₃CF₂CF(CF₃)), -120.86 (hept, ³J_{FF} = 7.9, CF₃CF₂CF(CF₃)), -121.03 – -121.33 (m, CF₃CF₂CF(CF₃)), -121.44 (dtt, ³J_{FF} = 13.4, ³J_{FF} = 8.8, ⁴J_{FF} = 4.7, CF₃CF₂CF(CF₃)), -121.83 – -122.06 (m, CF₃CF₂CF(CF₃)), -185.58 (s, CF(CF₃)). The GC-MS data for each product is given below:

CF₃CF₂CF(CF₃)CH₂CF₂CF₂CH₂I: GC-MS: 2.3 mins *m/z* = 474.0 (100% , M⁺), 283.1 (23, [CF₃CF₂CF(CF₃)CH₂CF₂]⁺), 191.0 (84, [CF₂CH₂I]⁺), 133.1 (31, [CF₃CH₂CF₂]⁺), 119.1 (16, [CF₃CF₂]⁺).

CF₃CF₂CF(CF₃)(CH₂CF₂)₂CF₂CH₂I: GC-MS: 3.0 mins *m/z* = 538.0 (100% , M⁺), 347.1 (10, [CF₃CF₂CF(CF₃)(CH₂CF₂)₂]⁺), 327.1 (15, [CF₃CF₂CF(CF₃)(CH₂CF₂)₂ - HF]⁺), 283.1 (41, [CF₃CF₂CF(CF₃)CH₂CF₂]⁺), 191.0 (77, [CF₂CH₂I]⁺), 133.1 (99, [CF₃CH₂CF₂]⁺), 119.1 (14, [CF₃CF₂]⁺), 113.1 (17, [CF₃CH₂CF₂ - HF]⁺).

CF₃CF₂CF(CF₃)(CH₂CF₂)₃CF₂CH₂I: GC-MS: 3.6 mins *m/z* = 602.0 (50% , M⁺), 349.0 (12, [(CF₂CH₂)₂CF₂CF₂CH₂I] - HF]⁺, 283.1 (41, [CF₃CF₂CF(CF₃)CH₂CF₂]⁺), 191.0 (42, [CF₂CH₂I]⁺), 133.1 (100, [CF₃CH₂CF₂]⁺), 119.1 (8, [CF₃CF₂]⁺), 113.1 (19, [CF₃CH₂CF₂ - HF]⁺).

CF₃CF₂CF(CF₃)(CH₂CF₂)₄CF₂CH₂I: GC-MS: 4.0 mins *m/z* = 666.0 (44% , M⁺), 413.0 (9, [(CF₂CH₂)₃CF₂CF₂CH₂I] - HF]⁺, 349.0 (14, [(CF₂CH₂)₂CF₂CF₂CH₂I] - HF]⁺, 347.1 (12, [CF₃CF₂CF(CF₃)(CH₂CF₂)₂]⁺), 327.1 (20, [CF₃CF₂CF(CF₃)(CH₂CF₂)₂ - HF]⁺), 283.1 (30, [CF₃CF₂CF(CF₃)CH₂CF₂]⁺), 197.0 (22, [CF₃(CH₂CF₂)₂]⁺), 191.0 (39, [CF₂CH₂I]⁺), 133.1 (100, [CF₃CH₂CF₂]⁺), 119.1 (7, [CF₃CF₂]⁺), 113.1 (22, [CF₃CH₂CF₂ - HF]⁺).

CF₃CF₂CF(CF₃)(CH₂CF₂)₅CF₂CH₂I: GC-MS: 4.5 mins *m/z* = 730.1 (30% , M⁺), 413.0 (10, [(CF₂CH₂)₃CF₂CF₂CH₂I] - HF]⁺, 349.0 (15, [(CF₂CH₂)₂CF₂CF₂CH₂I] - HF]⁺, 347.1 (9, [CF₃CF₂CF(CF₃)(CH₂CF₂)₂]⁺), 327.1 (18, [CF₃CF₂CF(CF₃)(CH₂CF₂)₂ - HF]⁺), 283.1 (39, [CF₃CF₂CF(CF₃)CH₂CF₂]⁺), 197.0 (22, [CF₃(CH₂CF₂)₂]⁺), 191.0 (32, [CF₂CH₂I]⁺), 133.1 (100, [CF₃CH₂CF₂]⁺), 119.1 (5, [CF₃CF₂]⁺), 113.1 (26, [CF₃CH₂CF₂ - HF]⁺).

CF₃CF₂CF(CF₃)(CH₂CF₂)₆CF₂CH₂I: GC-MS: 4.9 mins *m/z* = 794.1 (30% , M⁺), 477.0 (6, [(CF₂CH₂)₃CF₂CF₂CH₂I] - HF]⁺, 413.0 (13, [(CF₂CH₂)₃CF₂CF₂CH₂I] - HF]⁺, 349.0 (17, [(CF₂CH₂)₂CF₂CF₂CH₂I] - HF]⁺, 347.1 (9, [CF₃CF₂CF(CF₃)(CH₂CF₂)₂]⁺), 327.1 (18, [CF₃CF₂CF(CF₃)(CH₂CF₂)₂ - HF]⁺), 283.1 (39, [CF₃CF₂CF(CF₃)CH₂CF₂]⁺), 241.1 (14, [CF₂CF₂CH₂I]⁺), 197.0 (30, [CF₃(CH₂CF₂)₂]⁺), 191.0 (29, [CF₂CH₂I]⁺), 133.1 (100, [CF₃CH₂CF₂]⁺), 119.1 (5, [CF₃CF₂]⁺), 113.1 (30, [CF₃CH₂CF₂ - HF]⁺).

CF₃CF₂CF(CF₃)(CH₂CF₂)₇CF₂CH₂I: GC-MS: 5.2 mins *m/z* = 858.1 (10% , M⁺), 477.0 (6, [(CF₂CH₂)₃CF₂CF₂CH₂I] - HF]⁺, 413.0 (14, [(CF₂CH₂)₃CF₂CF₂CH₂I] - HF]⁺, 349.0 (15, [(CF₂CH₂)₂CF₂CF₂CH₂I] - HF]⁺, 347.1 (9, [CF₃CF₂CF(CF₃)(CH₂CF₂)₂]⁺), 327.1 (17, [CF₃CF₂CF(CF₃)(CH₂CF₂)₂ - HF]⁺), 283.1 (38, [CF₃CF₂CF(CF₃)CH₂CF₂]⁺), 261.1 (10, [CF₃(CH₂CF₂)₃]⁺), 241.1 (19, [CF₂CF₂CH₂I]⁺), 197.1 (35, [CF₃(CH₂CF₂)₂]⁺), 191.0 (24, [CF₂CH₂I]⁺), 133.1 (100, [CF₃CH₂CF₂]⁺), 113.1 (33, [CF₃CH₂CF₂ - HF]⁺).

CF₃CF₂CF(CF₃)(CH₂CF₂)₈CF₂CH₂I: GC-MS: 5.5 mins *m/z* = 922.2 (6% , M⁺•), 477.0 (8, [(CF₂CH₂)₃CF₂CF₂CH₂I] - HF)⁺, 413.0 (14, [(CF₂CH₂)₃CF₂CF₂CH₂I] - HF)⁺, 349.0 (18, [(CF₂CH₂)₂CF₂CF₂CH₂I] - HF)⁺, 347.1 (9, [CF₃CF₂CF(CF₃)(CH₂CF₂)₂]⁺), 327.1 (17, [CF₃CF₂CF(CF₃)(CH₂CF₂)₂ - HF]⁺), 305.1 (17, [CF₂CH₂CF₂CF₂CH₂I]⁺), 283.1 (36, [CF₃CF₂CF(CF₃)CH₂CF₂]⁺), 261.1 (13, [CF₃(CH₂CF₂)₃]⁺), 241.1 (23, [CF₂CF₂CH₂I]⁺), 197.1 (39, [CF₃(CH₂CF₂)₂]⁺), 191.0 (22, [CF₂CH₂I]⁺), 133.1 (100, [CF₃CH₂CF₂]⁺), 113.1 (35, [CF₃CH₂CF₂ - HF]⁺).

CF₃CF₂CF(CF₃)(CH₂CF₂)₆I: GC-MS: 4.4 mins *m/z* = 730.1 (3% , M⁺•), 583.1 (24, [M - I - HF]⁺), 391.1 (8, [CF₃CF₂CF(CF₃)(CH₂CF₂)₃ - HF]⁺), 347.1 (11, [CF₃CF₂CF(CF₃)(CH₂CF₂)₂]⁺), 327.1 (22, [CF₃CF₂CF(CF₃)(CH₂CF₂)₂ - HF]⁺), 283.1 (43, [CF₃CF₂CF(CF₃)CH₂CF₂]⁺), 261.1 (9, [CF₃(CH₂CF₂)₃]⁺), 241.1 (24, [CF₂CF₂CH₂I]⁺), 197.1 (30, [CF₃(CH₂CF₂)₂]⁺), 177.1 (29, [CF₃(CH₂CF₂)₂ - HF]⁺), 133.1 (100, [CF₃CH₂CF₂]⁺), 113.1 (48, [CF₃CH₂CF₂ - HF]⁺).

CF₃CF₂CF(CF₃)(CH₂CF₂)₇I: GC-MS: 4.8 mins *m/z* = 794.1 (2% , M⁺•), 647.2 (24, [M - I - HF]⁺), 455.1 (7, [CF₃CF₂CF(CF₃)(CH₂CF₂)₄ - HF]⁺), 391.1 (9, [CF₃CF₂CF(CF₃)(CH₂CF₂)₃ - HF]⁺), 347.1 (9, [CF₃CF₂CF(CF₃)(CH₂CF₂)₂]⁺), 327.1 (17, [CF₃CF₂CF(CF₃)(CH₂CF₂)₂ - HF]⁺), 305.1 (15, [CF₂CH₂CF₂CF₂CH₂I]⁺), 283.1 (39, [CF₃CF₂CF(CF₃)CH₂CF₂]⁺), 261.1 (11, [CF₃(CH₂CF₂)₃]⁺), 241.1 (32, [CF₂CF₂CH₂I]⁺), 197.1 (37, [CF₃(CH₂CF₂)₂]⁺), 177.1 (35, [CF₃(CH₂CF₂)₂ - HF]⁺), 133.1 (100, [CF₃CH₂CF₂]⁺), 113.1 (45, [CF₃CH₂CF₂ - HF]⁺).

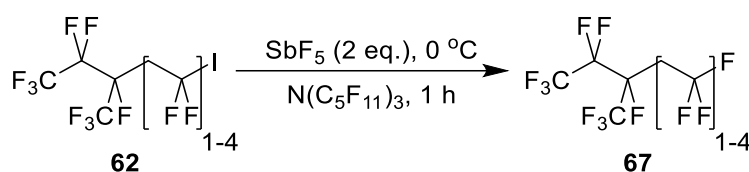
CF₃CF₂CF(CF₃)(CH₂CF₂)₈I: GC-MS: 5.1 mins *m/z* = 858.1 (1% , M⁺•), 711.2 (21, [M - I - HF]⁺), 455.1 (6, [CF₃CF₂CF(CF₃)(CH₂CF₂)₄ - HF]⁺), 391.1 (7, [CF₃CF₂CF(CF₃)(CH₂CF₂)₃ - HF]⁺), 369.1 (7, [(CF₂CH₂)₂CF₂CF₂CH₂I]⁺), 347.1 (8, [CF₃CF₂CF(CF₃)(CH₂CF₂)₂]⁺), 327.1 (15, [CF₃CF₂CF(CF₃)(CH₂CF₂)₂ - HF]⁺), 305.1 (15, [CF₂CH₂CF₂CF₂CH₂I]⁺), 283.1 (35, [CF₃CF₂CF(CF₃)CH₂CF₂]⁺), 261.1 (12, [CF₃(CH₂CF₂)₃]⁺), 241.1 (33, [CF₂CF₂CH₂I]⁺), 197.1 (39, [CF₃(CH₂CF₂)₂]⁺), 177.1 (39, [CF₃(CH₂CF₂)₂ - HF]⁺), 133.1 (100, [CF₃CH₂CF₂]⁺), 113.1 (47, [CF₃CH₂CF₂ - HF]⁺).

CF₃CF₂CF(CF₃)(CH₂CF₂)₉I: GC-MS: 5.5 mins *m/z* = 922.1 (1% , M⁺•), 775.2 (15, [M - I - HF]⁺), 519.1 (7, [CF₃CF₂CF(CF₃)(CH₂CF₂)₅ - HF]⁺), 455.1 (9, [CF₃CF₂CF(CF₃)(CH₂CF₂)₄ - HF]⁺), 433.1 (5, [(CF₂CH₂)₃CF₂CF₂CH₂I]⁺), 411.1 (6, [CF₃CF₂CF(CF₃)(CH₂CF₂)₃]⁺), 391.1 (9, [CF₃CF₂CF(CF₃)(CH₂CF₂)₃ - HF]⁺), 369.1 (11, [(CF₂CH₂)₂CF₂CF₂CH₂I]⁺), 349.1 (11, [(CF₂CH₂)₂CF₂CF₂CH₂I] - HF)⁺, 347.1 (11, [CF₃CF₂CF(CF₃)(CH₂CF₂)₂]⁺), 327.1 (20, [CF₃CF₂CF(CF₃)(CH₂CF₂)₂ - HF]⁺), 305.1 (21, [CF₂CH₂CF₂CF₂CH₂I]⁺), 285.1 (17, [CF₂CH₂CF₂CF₂CH₂I] - HF)⁺, 283.1 (40, [CF₃CF₂CF(CF₃)CH₂CF₂]⁺), 261.1 (17, [CF₃(CH₂CF₂)₃]⁺),

241.1 (39, [CF₂CF₂CH₂I]⁺), 197.1 (48, [CF₃(CH₂CF₂)₂]⁺), 177.0 (42, [CF₃(CH₂CF₂)₂ - HF]⁺), 133.1 (100, [CF₃CH₂CF₂]⁺), 113.1 (50, [CF₃CH₂CF₂ - HF]⁺).

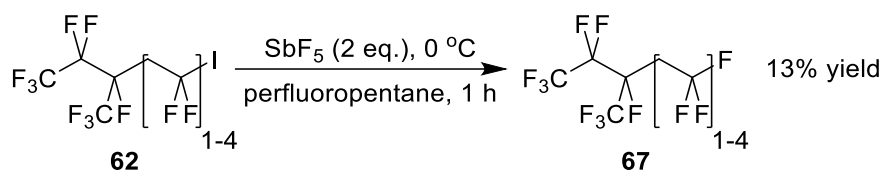
CF₃CF₂CF(CF₃)(CH₂CF₂)₁₀I: GC-MS: 5.8 mins *m/z* = 986.2 (1% , M⁺•), 839.2 (11, [M - I - HF]⁺), 583.2 (4, [CF₃CF₂CF(CF₃)(CH₂CF₂)₆ - HF]⁺), 519.1 (9, [CF₃CF₂CF(CF₃)(CH₂CF₂)₅ - HF]⁺), 497.1 (4, [(CF₂CH₂)₄CF₂CF₂CH₂I]⁺), 455.1 (9, [CF₃CF₂CF(CF₃)(CH₂CF₂)₄ - HF]⁺), 433.1 (7, [(CF₂CH₂)₃CF₂CF₂CH₂I]⁺), 411.1 (8, [CF₃CF₂CF(CF₃)(CH₂CF₂)₃]⁺), 391.1 (10, [CF₃CF₂CF(CF₃)(CH₂CF₂)₃ - HF]⁺), 369.1 (12, [(CF₂CH₂)₂CF₂CF₂CH₂I]⁺), 349.1 (13, [(CF₂CH₂)₂CF₂CF₂CH₂I - HF]⁺), 347.1 (11, [CF₃CF₂CF(CF₃)(CH₂CF₂)₂]⁺), 327.1 (21, [CF₃CF₂CF(CF₃)(CH₂CF₂)₂ - HF]⁺), 305.1 (25, [CF₂CH₂CF₂CF₂CH₂I]⁺), 285.1 (20, [CF₂CH₂CF₂CF₂CH₂I - HF]⁺), 283.1 (41, [CF₃CF₂CF(CF₃)CH₂CF₂]⁺), 261.1 (21, [CF₃(CH₂CF₂)₃]⁺), 241.1 (42, [CF₂CF₂CH₂I]⁺), 197.0 (48, [CF₃(CH₂CF₂)₂]⁺), 177.0 (36, [CF₃(CH₂CF₂)₂ - HF]⁺), 133.1 (100, [CF₃CH₂CF₂]⁺), 113.1 (48, [CF₃CH₂CF₂ - HF]⁺).

Reaction of CF₃CF₂CF(CF₃)(CH₂CF₂)₁₋₄I with SbF₅ in N(C₅F₁₁)₃



The mixture of telomer iodides (CF₃CF₂CF(CF₃)(CH₂CF₂)₁₋₄I) (2 g, 4.2 mmol) was dissolved in N(C₅F₁₁)₃ (5 mL) at 0 °C and SbF₅ (1.73 g, 8 mmol) in N(C₅F₁₁)₃ (10 mL) was added dropwise over 20 minutes. The reaction mixture was stirred for an hour, after which water (30 mL) was added. The solution was neutralised with Sat. NaHCO₃ solution (30 mL) and the fluorocarbon layer was extracted. The product was distilled from the solvent; however, only one drop of product was extracted; ¹H NMR (400 MHz, Chloroform-*d*) δ 3.17 – 2.74 (m, CF(CF₃)(CH₂CF₂)₁₋₄F); ¹⁹F NMR (376 MHz, Chloroform-*d*) δ -59.95 – -60.13 (m, CH₂CF₃), -61.66 (pd, ³J_{FH} = 9.6, ⁴J_{FF} = 2.2, CH₂CF₃), -76.07 (dp, ³J_{FF} = 21.2, ⁴J_{FH} = 7.7, CF(CF₃)CH₂CF₃), -76.44 (dh, ³J_{FF} = 18.9, ⁴J_{FH} = 6.4, CF(CF₃)(CH₂CF₂)₂F), -79.88 (dt, ³J_{FF} = 10.8, ⁴J_{FF} = 6.4, CF₃CF₂CF(CF₃)), -79.97 (dq, ³J_{FF} = 12.2, ⁴J_{FF} = 6.4, CF₃CF₂CF(CF₃)), -88.91 – -89.10 (m, CF(CF₃)(CH₂CF₂)₀₋₃CH₂CF₃), -89.25 – -89.63 (m, CF(CF₃)(CH₂CF₂)₀₋₃CH₂CF₃), -89.94 – -90.59 (m, CF(CF₃)(CH₂CF₂)₀₋₃CH₂CF₃), -90.91 – -91.27 (m, CF(CF₃)(CH₂CF₂)₀₋₃CH₂CF₃), -120.27 (dt, ³J_{FF} = 13.7, ³J_{FF} = 7.0, CF₃CF₂CF(CF₃)), -120.95 (h, ³J_{FF} = 7.8, CF₃CF₂CF(CF₃)), -121.05 – -121.26 (m, CF₃CF₂CF(CF₃)), -121.58 (qp, ³J_{FF} = 12.2, ³J_{FF} = 3.7, CF₃CF₂CF(CF₃)), -121.77 – -122.08 (m, CF₃CF₂CF(CF₃)), -122.37 (tdt, ³J_{FF} = 12.5, ³J_{FF} = 8.2, ⁴J_{FF} = 3.6, CF₃CF₂CF(CF₃)), -185.54 (s, CF(CF₃)CH₂CF₂), -185.87 – -186.13 (m, CF(CF₃)CH₂CF₃).

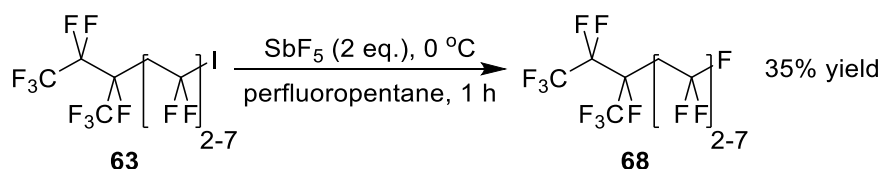
Reactions of $\text{CF}_3\text{CF}_2\text{CF}(\text{CF}_3)(\text{CH}_2\text{CF}_2)_n\text{I}$ with SbF_5 in Perfluoropentane



The mixture of telomer iodides $(\text{CF}_3\text{CF}_2\text{CF}(\text{CF}_3)(\text{CH}_2\text{CF}_2)_{1-4})\text{I}$ (2 g, 4.2 mmol) was dissolved in C_5F_{12} (10 mL) at $0 \text{ }^\circ\text{C}$ and SbF_5 (1.73 g, 8 mmol) in C_5F_{12} (10 mL) was added dropwise over 20 minutes. The reaction mixture was stirred for an hour, after which water (30 mL) was added. The solution was neutralised with NaHCO_3 and the fluorocarbon layer was extracted. The solvent was removed in vacuo to yield $\text{CF}_3\text{CF}_2\text{CF}(\text{CF}_3)(\text{CH}_2\text{CF}_2)_{2-7}\text{F}$ (0.20 g, 13%) as a yellow oil; ^1H NMR (400 MHz, Deuterium Oxide) δ 3.20 – 2.66 (m, $\text{CF}(\text{CF}_3)(\text{CH}_2\text{CF}_2)_{2-7}\text{F}$); ^{19}F NMR (376 MHz, Deuterium Oxide) δ -62.09 – -62.29 (m, CH_2CF_3), -77.33 – -77.16 (m, $\text{CF}(\text{CF}_3)\text{CH}_2\text{CF}_2$), -80.19 – -80.38 (m, $\text{CF}_3\text{CF}_2\text{CF}(\text{CF}_3)$), -89.57 – -91.78 (m, $\text{CF}(\text{CF}_3)(\text{CH}_2\text{CF}_2)_{1-6}\text{CH}_2\text{CF}_3$), -120.13 – -122.72 (m, $\text{CF}_2\text{CF}(\text{CF}_3)$), -185.49 – -185.99 (m, $\text{CF}(\text{CF}_3)\text{CH}_2\text{CF}_2$). The GC-MS data for the two observed products are given below:

$\text{CF}_3\text{CF}_2\text{CF}(\text{CF}_3)(\text{CH}_2\text{CF}_2)_2\text{F}$: GC-MS: 0.8 mins $m/z = 347.0$ (3 %, $[\text{M} - \text{F}]^+$), 283.1 (29, $[\text{CF}_3\text{CF}_2\text{C}(\text{CF}_3)\text{FCH}_2\text{CF}_2]^+$), 263.0 (6, $[\text{CF}_3\text{CF}_2\text{C}(\text{CF}_3)\text{FCH}=\text{CF}]^+$), 195.0 (11, $[\text{CF}=\text{CCF}_3\text{FCH}_2\text{CF}_2]^+$), 145.1 (5, $[\text{C}_4\text{H}_2\text{F}_5]^+$), 133.0 (100, $[\text{CF}_2\text{CH}_2\text{CF}_3]^+$), 119.0 (7, $[\text{CF}_2\text{CF}_3]^+$), 113.0 (7, $[\text{CF}_2\text{CHCF}_2]^+$).

$\text{CF}_3\text{CF}_2\text{CF}(\text{CF}_3)(\text{CH}_2\text{CF}_2)_3\text{F}$: GC-MS: 1.7 mins $m/z = 411.0$ (1 %, $[\text{M} - \text{F}]^+$), 347.1 (7, $[\text{M} - \text{CH}_2\text{CF}_3]^+$), 283.1 (47, $[\text{CF}_3\text{CF}_2\text{C}(\text{CF}_3)\text{FCH}_2\text{CF}_2]^+$), 263.0 (5, $[\text{CF}_3\text{CF}_2\text{C}(\text{CF}_3)\text{FCH}=\text{CF}]^+$), 195.0 (13, $[\text{CF}=\text{CCF}_3\text{FCH}_2\text{CF}_2]^+$), 145.1 (5, $[\text{C}_4\text{H}_2\text{F}_5]^+$), 133.0 (100, $[\text{CF}_2\text{CH}_2\text{CF}_3]^+$), 119.0 (7, $[\text{CF}_2\text{CF}_3]^+$), 113.0 (9, $[\text{CF}_2\text{CHCF}_2]^+$).



The mixture of telomer iodides $(\text{CF}_3\text{CF}_2\text{CF}(\text{CF}_3)(\text{CH}_2\text{CF}_2)_{2-7})\text{I}$ (8.2 g, 13.6 mmol) was dissolved in C_5F_{12} (20 mL) at $0 \text{ }^\circ\text{C}$ and SbF_5 (5.98 g, 28 mmol) in C_5F_{12} (30 mL) was added dropwise over 20 minutes. The reaction mixture was stirred for an hour, after which water (50 mL) was added. The solution was neutralised with NaHCO_3 and the fluorocarbon layer was extracted. The

solvent was removed in vacuo to yield $\text{CF}_3\text{CF}_2\text{CF}(\text{CF}_3)(\text{CH}_2\text{CF}_2)_2\text{-F}$ (2.36 g, 35%) as a yellow oil; ^1H NMR (400 MHz, Deuterium Oxide) δ 3.02 – 2.22 (m, $\text{CF}(\text{CF}_3)(\text{CH}_2\text{CF}_2)_{2-7}\text{F}$); ^{19}F NMR (376 MHz, Deuterium Oxide) δ -63.42 – -63.63 (m, CH_2CF_3), -77.63 – -78.00 (m, $\text{CF}(\text{CF}_3)\text{CH}_2\text{CF}_2$), -81.50 – -81.80 (m, $\text{CF}_3\text{CF}_2\text{CF}(\text{CF}_3)$), -89.93 (s, $\text{CF}(\text{CF}_3)(\text{CH}_2\text{CF}_2)_{1-6}\text{CH}_2\text{CF}_3$), -90.07 (s, $\text{CF}(\text{CF}_3)(\text{CH}_2\text{CF}_2)_{1-6}\text{CH}_2\text{CF}_3$), -90.33 – -90.87 (m, $\text{CF}(\text{CF}_3)(\text{CH}_2\text{CF}_2)_{1-6}\text{CH}_2\text{CF}_3$), -91.00 – -91.81 (m, $\text{CF}(\text{CF}_3)(\text{CH}_2\text{CF}_2)_{1-6}\text{CH}_2\text{CF}_3$), -91.86 – -92.74 (m, $\text{CF}(\text{CF}_3)(\text{CH}_2\text{CF}_2)_{1-6}\text{CH}_2\text{CF}_3$), -93.10 – -93.59 (m, $\text{CF}(\text{CF}_3)(\text{CH}_2\text{CF}_2)_{1-6}\text{CH}_2\text{CF}_3$), -121.48 – -121.67 (m, $\text{CF}_2\text{CF}(\text{CF}_3)$), -122.26 – -122.50 (m, $\text{CF}_2\text{CF}(\text{CF}_3)$), -122.54 – -122.79 (m, $\text{CF}_2\text{CF}(\text{CF}_3)$), -122.91 – -123.08 (m, $\text{CF}_2\text{CF}(\text{CF}_3)$), -123.32 – -123.55 (m, $\text{CF}_2\text{CF}(\text{CF}_3)$), -186.81 (s, $\text{CF}(\text{CF}_3)\text{CH}_2\text{CF}_2$); ^{13}C NMR (101 MHz, Chloroform-*d*) δ 122.98 (qd, $^1J_{\text{CF}} = 275.8$, $^2J_{\text{CF}} = 5.5$, $\text{CF}_2\text{CF}(\text{CF}_3)\text{CH}_2$), 121.19 – 114.11 (m, CH_2CF_2 , CH_2CF_3), 117.86 (q, $^1J_{\text{CF}} = 286.8$, CH_2CF_3), 110.42 (tqd, $^1J_{\text{CF}} = 267.3$, $^2J_{\text{CF}} = 39.3$, $^2J_{\text{CF}} = 26.1$, CF_3CF_2), 90.86 (dq, $^1J_{\text{CF}} = 210.0$, $^2J_{\text{CF}} = 30.6$, $\text{CF}_2\text{CF}(\text{CF}_3)\text{CH}_2$), 44.11 – 41.84 (m, CH_2CF_2), 40.25 (h, $^2J_{\text{CF}} = 29.1$, CH_2CF_2), 34.95 (td, $^2J_{\text{CF}} = 25.9$, $^2J_{\text{CF}} = 20.3$, $\text{CF}_2\text{CF}(\text{CF}_3)\text{CH}_2\text{CF}_2$). The GC-MS data for each product, and the percentage of each compound in the product mixture determined by $\{^1\text{H}\}^{19}\text{F}$ NMR spectroscopy, are given below:

$\text{CF}_3\text{CF}_2\text{CF}(\text{CF}_3)(\text{CH}_2\text{CF}_2)_2\text{F}$ (5%): GC-MS: 0.7 mins $m/z = 347.1$ (3%, $[\text{M} - \text{F}]^+$), 283.0 (27, $[\text{CF}_3\text{CF}_2\text{CF}(\text{CF}_3)\text{CH}_2\text{CF}_2]^+$), 263.0 (7, $[\text{CF}_3\text{CF}_2\text{CF}(\text{CF}_3)\text{CH}_2\text{CF}_2 - \text{HF}]^+$), 195.0 (11, $[\text{CF}_2=\text{C}(\text{CF}_3)\text{CH}_2\text{CF}_2]^+$), 145.1 (6, $[\text{C}_4\text{H}_2\text{F}_5]^+$), 133.1 (100, $[\text{CF}_2\text{CH}_2\text{CF}_3]^+$), 119.0 (7, $[\text{CF}_2\text{CF}_3]^+$), 113.0 (8, $[\text{CF}_3\text{CH}_2\text{CF}_2 - \text{HF}]^+$).

$\text{CF}_3\text{CF}_2\text{CF}(\text{CF}_3)(\text{CH}_2\text{CF}_2)_3\text{F}$ (21%): GC-MS: 1.6 mins $m/z = 411.0$ (1%, $[\text{M} - \text{F}]^+$), 347.1 (7, $[\text{CF}_3\text{CF}_2\text{CF}(\text{CF}_3)(\text{CH}_2\text{CF}_2)_2]^+$), 283.1 (42, $[\text{CF}_3\text{CF}_2\text{CF}(\text{CF}_3)\text{CH}_2\text{CF}_2]^+$), 263.0 (5, $[\text{CF}_3\text{CF}_2\text{CF}(\text{CF}_3)\text{CH}_2\text{CF}_2 - \text{HF}]^+$), 197.0 (22, $[\text{CF}_3(\text{CH}_2\text{CF}_2)_2]^+$), 195.0 (13, $[\text{CF}_2=\text{C}(\text{CF}_3)\text{CH}_2\text{CF}_2]^+$), 145.1 (5, $[\text{C}_4\text{H}_2\text{F}_5]^+$), 133.1 (100, $[\text{CF}_2\text{CH}_2\text{CF}_3]^+$), 119.0 (6, $[\text{CF}_2\text{CF}_3]^+$), 113.1 (10, $[\text{CF}_3\text{CH}_2\text{CF}_2 - \text{HF}]^+$).

$\text{CF}_3\text{CF}_2\text{CF}(\text{CF}_3)(\text{CH}_2\text{CF}_2)_4\text{F}$ (25%): GC-MS: 2.4 mins $m/z = 455.1$ (2%, $[\text{M} - \text{HF}_2]^+$), 411.1 (1, $[\text{M} - \text{CH}_2\text{CF}_3]^+$), 347.1 (11, $[\text{CF}_3\text{CF}_2\text{CF}(\text{CF}_3)(\text{CH}_2\text{CF}_2)_2]^+$), 327.1 (8, $[\text{CF}_3\text{CF}_2\text{CF}(\text{CF}_3)(\text{CH}_2\text{CF}_2)_2 - \text{HF}]^+$), 283.1 (37, $[\text{CF}_3\text{CF}_2\text{C}(\text{CF}_3)\text{FCH}_2\text{CF}_2]^+$), 197.0 (27, $[\text{CF}_3(\text{CH}_2\text{CF}_2)_2]^+$), 195.0 (10, $[\text{CF}_2=\text{C}(\text{CF}_3)\text{CH}_2\text{CF}_2]^+$), 177.0 (7, $[\text{CF}_3(\text{CH}_2\text{CF}_2)_2 - \text{HF}]^+$), 145.1 (3, $[\text{C}_4\text{H}_2\text{F}_5]^+$), 133.0 (100, $[\text{CF}_2\text{CH}_2\text{CF}_3]^+$), 119.0 (5, $[\text{CF}_2\text{CF}_3]^+$), 113.0 (10, $[\text{CF}_3\text{CH}_2\text{CF}_2 - \text{HF}]^+$).

$\text{CF}_3\text{CF}_2\text{CF}(\text{CF}_3)(\text{CH}_2\text{CF}_2)_5\text{F}$ (22%): GC-MS: 3.0 mins $m/z = 519.1$ (2%, $[\text{M} - \text{HF}_2]^+$), 455.1 (2, $[\text{CF}_3\text{CF}_2\text{CF}(\text{CF}_3)(\text{CH}_2\text{CF}_2)_4 - \text{HF}]^+$), 411.1 (3, $[\text{CF}_3\text{CF}_2\text{CF}(\text{CF}_3)(\text{CH}_2\text{CF}_2)_3]^+$), 347.1 (10, $[\text{CF}_3\text{CF}_2\text{CF}(\text{CF}_3)(\text{CH}_2\text{CF}_2)_2]^+$), 327.1 (11, $[\text{CF}_3\text{CF}_2\text{CF}(\text{CF}_3)(\text{CH}_2\text{CF}_2)_2 - \text{HF}]^+$), 283.1

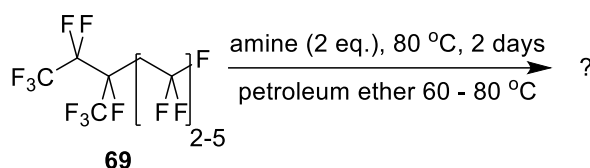
(37, [CF₃CF₂CF(CF₃)CH₂CF₂]⁺), 197.0 (39, [CF₃(CH₂CF₂)₂]⁺), 195.0 (9, [CF₂=C(CF₃)CH₂CF₂]⁺), 177.0 (13, [CF₃(CH₂CF₂)₂ - HF]⁺), 145.1 (3, [C₄H₂F₅]⁺), 133.1 (100, [CF₂CH₂CF₃]⁺), 113.0 (14, [CF₃CH₂CF₂ - HF]⁺).

CF₃CF₂CF(CF₃)(CH₂CF₂)₆F (16%): GC-MS: 3.5 mins *m/z* = 583.1 (2%, [M - HF₂]⁺), 519.1 (2, [CF₃CF₂CF(CF₃)(CH₂CF₂)₅ - HF]⁺), 455.1 (4, [CF₃CF₂CF(CF₃)(CH₂CF₂)₄ - HF]⁺), 411.1 (4, [CF₃CF₂CF(CF₃)(CH₂CF₂)₃]⁺), 391.1 (4, [CF₃CF₂CF(CF₃)(CH₂CF₂)₃ - HF]⁺), 347.1 (10, [CF₃CF₂CF(CF₃)(CH₂CF₂)₂]⁺), 327.1 (15, [CF₃CF₂CF(CF₃)(CH₂CF₂)₂ - HF]⁺), 283.1 (37, [CF₃CF₂CF(CF₃)CH₂CF₂]⁺), 261.1 (15, [CF₃(CH₂CF₂)₃]⁺), 241.1 (16, [CF₃(CH₂CF₂)₃ - HF]⁺), 197.0 (46, [CF₃(CH₂CF₂)₂]⁺), 195.0 (9, [CF₂=C(CF₃)CH₂CF₂]⁺), 177.0 (16, [CF₃(CH₂CF₂)₂ - HF]⁺), 133.1 (100, [CF₂CH₂CF₃]⁺), 113.0 (17, [CF₃CH₂CF₂ - HF]⁺).

CF₃CF₂CF(CF₃)(CH₂CF₂)₇F (8%): GC-MS: 3.9 mins *m/z* = 647.1 (2%, [M - HF₂]⁺), 583.1 (2, [CF₃CF₂CF(CF₃)(CH₂CF₂)₆ - HF]⁺), 519.1 (4, [CF₃CF₂CF(CF₃)(CH₂CF₂)₅ - HF]⁺), 455.1 (6, [CF₃CF₂CF(CF₃)(CH₂CF₂)₄ - HF]⁺), 411.1 (5, [CF₃CF₂CF(CF₃)(CH₂CF₂)₃]⁺), 391.1 (7, [CF₃CF₂CF(CF₃)(CH₂CF₂)₃ - HF]⁺), 369.1 (5, [CF₃(CH₂CF₂)₅ - HF]⁺), 347.1 (10, [CF₃CF₂CF(CF₃)(CH₂CF₂)₂]⁺), 327.1 (16, [CF₃CF₂CF(CF₃)(CH₂CF₂)₂ - HF]⁺), 305.1 (13, [CF₃(CH₂CF₂)₄ - HF]⁺), 283.1 (37, [CF₃CF₂CF(CF₃)CH₂CF₂]⁺), 261.1 (18, [CF₃(CH₂CF₂)₃]⁺), 241.1 (24, [CF₃(CH₂CF₂)₃ - HF]⁺), 197.0 (52, [CF₃(CH₂CF₂)₂]⁺), 195.0 (8, [CF₂=C(CF₃)CH₂CF₂]⁺), 177.0 (19, [CF₃(CH₂CF₂)₂ - HF]⁺), 133.1 (100, [CF₂CH₂CF₃]⁺), 113.0 (20, [CF₃CH₂CF₂ - HF]⁺).

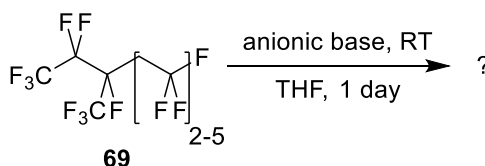
CF₃CF₂CF(CF₃)(CH₂CF₂)₈F (3%): GC-MS: 4.3 mins *m/z* = 611.1 (2%, [M - HF₂]⁺), 647.1 (2, [CF₃CF₂CF(CF₃)(CH₂CF₂)₆ - HF]⁺), 583.1 (4, [CF₃CF₂CF(CF₃)(CH₂CF₂)₆ - HF]⁺), 519.1 (5, [CF₃CF₂CF(CF₃)(CH₂CF₂)₅ - HF]⁺), 455.1 (8, [CF₃CF₂CF(CF₃)(CH₂CF₂)₄ - HF]⁺), 433.1 (5, [CF₃(CH₂CF₂)₆ - HF]⁺), 411.1 (6, [CF₃CF₂CF(CF₃)(CH₂CF₂)₃]⁺), 391.1 (7, [CF₃CF₂CF(CF₃)(CH₂CF₂)₃ - HF]⁺), 369.1 (8, [CF₃(CH₂CF₂)₅ - HF]⁺), 347.1 (10, [CF₃CF₂CF(CF₃)(CH₂CF₂)₂]⁺), 327.1 (17, [CF₃CF₂CF(CF₃)(CH₂CF₂)₂ - HF]⁺), 305.1 (18, [CF₃(CH₂CF₂)₄ - HF]⁺), 283.1 (35, [CF₃CF₂CF(CF₃)CH₂CF₂]⁺), 261.1 (22, [CF₃(CH₂CF₂)₃]⁺), 241.1 (27, [CF₃(CH₂CF₂)₃ - HF]⁺), 197.0 (51, [CF₃(CH₂CF₂)₂]⁺), 195.0 (8, [CF₂=C(CF₃)CH₂CF₂]⁺), 177.0 (21, [CF₃(CH₂CF₂)₂ - HF]⁺), 133.1 (100, [CF₂CH₂CF₃]⁺), 113.0 (22, [CF₃CH₂CF₂ - HF]⁺).

Reactions of $\text{CF}_3\text{CF}_2\text{CF}(\text{CF}_3)(\text{CH}_2\text{CF}_2)_n\text{F}$ with Amines at Fixed Temperature



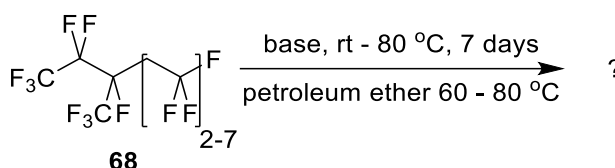
$\text{CF}_3\text{CF}_2\text{CF}(\text{CF}_3)(\text{CH}_2\text{CF}_2)_{2-5}\text{F}$ (1 g, 2.32 mmol) was dissolved in petroleum ether 60 – 80 °C (30 mL) and either DBU (0.76 g, 5mmol) or NEt_3 (0.48 g, 5 mmol) was added. The reaction was heated to 80 °C for two days after which the product mixture was extracted and analysed by ^{19}F NMR spectroscopy. On examination, despite a slight discolouration of the solution, no reaction between NEt_3 and $\text{CF}_3\text{CF}_2\text{CF}(\text{CF}_3)(\text{CH}_2\text{CF}_2)_{2-5}\text{F}$ was observed by ^{19}F NMR. However, the reaction with DBU produced a viscous black and severe degradation was observed by ^{19}F NMR spectroscopy. Unfortunately, the spectrum of the product mixture was too complex to extract any useful data about the structure of the decomposition products.

Reactions of $\text{CF}_3\text{CF}_2\text{CF}(\text{CF}_3)(\text{CH}_2\text{CF}_2)_n\text{F}$ with Anionic Bases at Fixed Temperature



$\text{CF}_3\text{CF}_2\text{CF}(\text{CF}_3)(\text{CH}_2\text{CF}_2)_{2-5}\text{F}$ (1 g, 2.32 mmol) was dissolved in petroleum THF (30 mL) and either KO^tBu (0.28 g, 2.5 mmol), $n\text{-BuLi}$ (2.5 M in hexanes, 1 mL, 2.5 mmol) or LDA (made in situ from 0.38 mL of diisopropyl amine, 2.5 mmol) was added. The reaction was stirred at rt for two days after which the product mixture was extracted and analysed by ^{19}F NMR spectroscopy. In all reactions, the product was a viscous, black tar. However, there was no change in the products observed by ^{19}F NMR, suggesting that the decomposition products that had formed were polymeric mixtures that were insoluble in the NMR solvent.

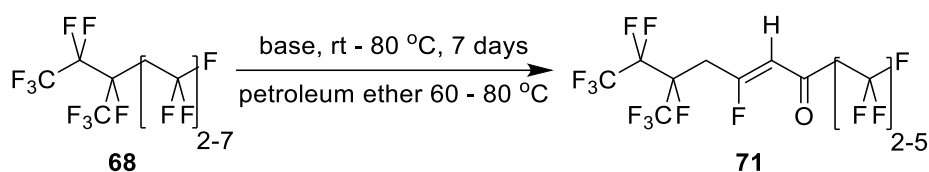
General Procedure for the Reactions of $\text{CF}_3\text{CF}_2\text{CF}(\text{CF}_3)(\text{CH}_2\text{CF}_2)_n\text{F}$ with Bases Using Increasingly Forcing Conditions



$\text{CF}_3\text{CF}_2\text{CF}(\text{CF}_3)(\text{CH}_2\text{CF}_2)_{2-7}\text{F}$ (0.1 g, 0.20 mmol) was dissolved in petroleum ether 60 – 80 (10 mL) and a base (0.50 mmol) was added. The reaction was stirred for 7 days, and the temperature was increased each day, first from rt to 30 °C and then by 10 °C each day to a maximum of 80 °C. The reaction was monitored by ^{19}F NMR and, after 7 days the product mixtures were extracted and analysed by GC-MS.

N,N-dimethyl aniline (0.060 g), pyridine (0.040 g), morpholine (0.044 g), DABCO (0.056 g), *N,N'*-dimethyl ethylenediamine (0.044 g) and triethylamine (0.051 g) were reacted with $\text{CF}_3\text{CF}_2\text{CF}(\text{CF}_3)(\text{CH}_2\text{CF}_2)_{2-7}\text{F}$. The reaction mixtures had discoloured, but on analysis by ^{19}F NMR and GC-MS, no observable reaction had occurred.

KO^tBu (0.056 g), *n*-BuLi (2.5 M in hexanes, 0.20 mL, 0.50 mmol) or LDA (synthesised in situ from diisopropylamine [0.10 mL, 0.72 mmol] and *n*-BuLi [2.5 M in hexanes, 0.30 mL, 0.75mmol]) were reacted with $\text{CF}_3\text{CF}_2\text{CF}(\text{CF}_3)(\text{CH}_2\text{CF}_2)_{2-7}\text{F}$. The reactions produced black tars after stirring for 15 minutes at rt. These mixtures were insoluble and therefore could not be examined by ^{19}F NMR or GC-MS.



DBU (0.076 g) and 2-*tert*-butyl-1,1,3,3-tetramethylguanidine (0.086 g) were reacted with $\text{CF}_3\text{CF}_2\text{CF}(\text{CF}_3)(\text{CH}_2\text{CF}_2)_{2-7}\text{F}$. By ^{19}F NMR, both reactions produced a mixture of decomposition products; however, the identity of the products could not be determined. The final products were examined by GC-MS, and each mixture contained the same decomposition products. The GC-MS data for each product are given below:

$\text{CF}_3\text{CF}_2\text{CF}(\text{CF}_3)(\text{CH}_2\text{CF}_2)_3\text{F}$: GC-MS: 1.6 mins $m/z = 411.0$ (1%, $[\text{M} - \text{F}]^+$), 347.1 (5, $[\text{CF}_3\text{CF}_2\text{CF}(\text{CF}_3)(\text{CH}_2\text{CF}_2)_2]^+$), 283.1 (42, $[\text{CF}_3\text{CF}_2\text{CF}(\text{CF}_3)\text{CH}_2\text{CF}_2]^+$), 263.0

(4, [CF₃CF₂CF(CF₃)CH₂CF₂ - HF]⁺), 197.0 (16, [CF₃(CH₂CF₂)₂]⁺), 195.0 (10, [CF₂=C(CF₃)CH₂CF₂]⁺), 145.1 (5, [C₄H₂F₅]⁺), 133.1 (100, [CF₂CH₂CF₃]⁺), 119.0 (7, [CF₂CF₃]⁺), 113.1 (9, [CF₃CH₂CF₂ - HF]⁺).

CF₃CF₂CF(CF₃)(CH₂CF₂)₄F: GC-MS: 2.4 mins *m/z* = 455.1 (1%, [M - HF₂]⁺), 411.1 (1, [CF₃CF₂CF(CF₃)(CH₂CF₂)₃]⁺), 347.1 (7, [CF₃CF₂CF(CF₃)(CH₂CF₂)₂]⁺), 327.1 (6, [CF₃CF₂CF(CF₃)(CH₂CF₂)₂ - HF]⁺), 283.1 (24, [CF₃CF₂CF(CF₃)CH₂CF₂]⁺), 197.0 (18, [CF₃(CH₂CF₂)₂]⁺), 195.0 (7, [CF₂=C(CF₃)CH₂CF₂]⁺), 177.0 (6, [CF₃(CH₂CF₂)₂ - HF]⁺), 145.1 (4, [C₄H₂F₅]⁺), 133.0 (100, [CF₂CH₂CF₃]⁺), 119.0 (5, [CF₂CF₃]⁺), 113.0 (9, [CF₃CH₂CF₂ - HF]⁺).

CF₃CF₂CF(CF₃)(CH₂CF₂)₅F: GC-MS: 3.0 mins *m/z* = 519.1 (2%, [M - HF₂]⁺), 455.1 (2, [CF₃CF₂CF(CF₃)(CH₂CF₂)₄ - HF]⁺), 411.1 (3, [CF₃CF₂CF(CF₃)(CH₂CF₂)₃]⁺), 347.1 (7, [CF₃CF₂CF(CF₃)(CH₂CF₂)₂]⁺), 327.1 (9, [CF₃CF₂CF(CF₃)(CH₂CF₂)₂ - HF]⁺), 283.1 (26, [CF₃CF₂CF(CF₃)CH₂CF₂]⁺), 197.0 (28, [CF₃(CH₂CF₂)₂]⁺), 195.0 (10, [CF₂=C(CF₃)CH₂CF₂]⁺), 177.0 (9, [CF₃(CH₂CF₂)₂ - HF]⁺), 145.1 (3, [C₄H₂F₅]⁺), 133.1 (100, [CF₂CH₂CF₃]⁺), 113.0 (15, [CF₃CH₂CF₂ - HF]⁺).

CF₃CF₂CF(CF₃)CH₂CH₂C=O(CF₂CH₂)₅CF₃: GC-MS: 3.3 mins *m/z* = 595.0 (1%, [M - CF₃]⁺), 417.1 (42, [C=O(CF₂CH₂)₅CF₃]⁺), 369.1 (6, [CF₃(CH₂CF₂)₅ - HF]⁺), 349.1 (19, [CF₃(CH₂CF₂)₅ - 2HF]⁺), 329.1 (5, [CF₃(CH₂CF₂)₅ - 3HF]⁺), 305.0 (4, [CF₃(CH₂CF₂)₄ - HF]⁺), 285.0 (7, [CF₃(CH₂CF₂)₄ - 2HF]⁺), 261.0 (2, [CF₃(CH₂CF₂)₃]⁺), 241.0 (4, [CF₃(CH₂CF₂)₃ - HF]⁺), 197.0 (18, [CF₃(CH₂CF₂)₂]⁺), 177.0 (10, [CF₃(CH₂CF₂)₂ - HF]⁺), 133.1 (100, [CF₂CH₂CF₃]⁺), 113.0 (23, [CF₃CH₂CF₂ - HF]⁺).

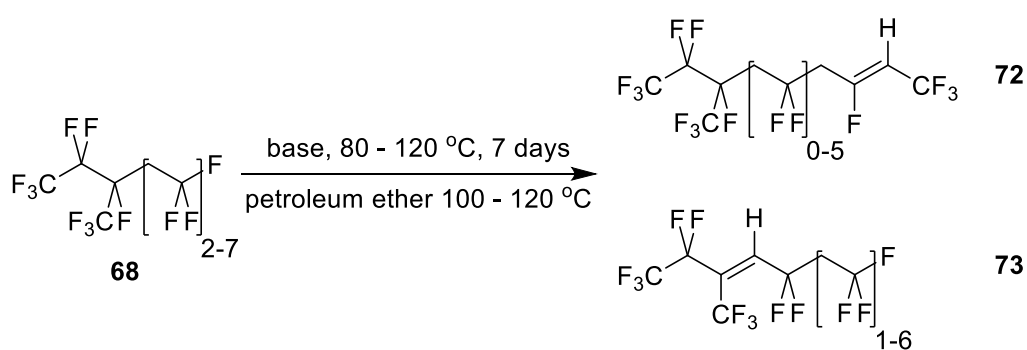
CF₃CF₂CF(CF₃)CH₂CH₂C=O(CF₂CH₂)₆CF₃: GC-MS: 3.7 mins *m/z* = 659.1 (1%, [M - CF₃]⁺), 595.0 (1, [M - CF₂CH₂CF₃]⁺), 481.1 (21, [C=O(CF₂CH₂)₆CF₃]⁺), 441.1 (6, [C=O(CF₂CH₂)₆CF₃ - 2HF]⁺), 417.1 (33, [C=O(CF₂CH₂)₅CF₃]⁺), 413.1 (19, [CF₃(CH₂CF₂)₆ - 2HF]⁺), 369.1 (7, [CF₃(CH₂CF₂)₅ - HF]⁺), 349.1 (18, [CF₃(CH₂CF₂)₅ - 2HF]⁺), 329.1 (7, [CF₃(CH₂CF₂)₅ - 3HF]⁺), 305.0 (4, [CF₃(CH₂CF₂)₄ - HF]⁺), 285.0 (10, [CF₃(CH₂CF₂)₄ - 2HF]⁺), 241.0 (16, [CF₃(CH₂CF₂)₃ - HF]⁺), 197.0 (15, [CF₃(CH₂CF₂)₂]⁺), 177.0 (19, [CF₃(CH₂CF₂)₂ - HF]⁺), 133.1 (100, [CF₂CH₂CF₃]⁺), 113.0 (21, [CF₃CH₂CF₂ - HF]⁺).

CF₃CF₂CF(CF₃)CH₂CH₂C=O(CF₂CH₂)₇CF₃: GC-MS: 4.1 mins *m/z* = 723.1 (1%, [M - CF₃]⁺), 659.1 (1, [M - CF₂CH₂CF₃]⁺), 595.0 (1, [M - (CF₂CH₂)₂CF₃]⁺), 545.1 (1, [C=O(CF₂CH₂)₇CF₃]⁺), 481.1 (27, [C=O(CF₂CH₂)₆CF₃]⁺), 441.1 (6, [C=O(CF₂CH₂)₆CF₃ - 2HF]⁺), 417.1 (31, [C=O(CF₂CH₂)₅CF₃]⁺), 413.1 (14, [CF₃(CH₂CF₂)₆ - 2HF]⁺), 369.1 (5, [CF₃(CH₂CF₂)₅ - HF]⁺), 349.1 (4, [CF₃(CH₂CF₂)₅ - 2HF]⁺), 329.1 (5, [CF₃(CH₂CF₂)₅ - 3HF]⁺), 305.0 (4, [CF₃(CH₂CF₂)₄ - HF]⁺), 285.0 (12, [CF₃(CH₂CF₂)₄ - 2HF]⁺), 241.0 (13, [CF₃(CH₂CF₂)₃ - HF]⁺), 197.0 (20, [CF₃(CH₂CF₂)₂]⁺), 177.0 (24, [CF₃(CH₂CF₂)₂ - HF]⁺), 133.1 (100, [CF₂CH₂CF₃]⁺), 113.0 (18, [CF₃CH₂CF₂ - HF]⁺).

CF₃CF₂CF(CF₃)CH₂CH₂C=O(CF₂CH₂)₈CF₃: GC-MS: 4.5 mins *m/z* = 787.1 (1%, [M - CF₃]⁺), 767.1 (1, [M - CF₃ - HF]⁺), 723.1 (1, [M - CF₂CH₂CF₃]⁺), 659.1 (1, [M - (CF₂CH₂)₂CF₃]⁺), 545.2 (32, [C=O(CF₂CH₂)₇CF₃]⁺), 505.1 (17, [C=O(CF₂CH₂)₇CF₃ - 2HF]⁺), 481.1 (33, [C=O(CF₂CH₂)₆CF₃]⁺), 441.1 (5, [C=O(CF₂CH₂)₆CF₃ - 2HF]⁺), 413.1 (15, [CF₃(CH₂CF₂)₆ - 2HF]⁺), 369.1 (4, [CF₃(CH₂CF₂)₅ - HF]⁺), 349.1 (3, [CF₃(CH₂CF₂)₅ - 2HF]⁺), 329.1 (8, [CF₃(CH₂CF₂)₅ - 3HF]⁺), 305.0 (5, [CF₃(CH₂CF₂)₄ - HF]⁺), 285.0 (14, [CF₃(CH₂CF₂)₄ - 2HF]⁺), 241.0 (26, [CF₃(CH₂CF₂)₃ - HF]⁺), 197.0 (24, [CF₃(CH₂CF₂)₂]⁺), 177.0 (22, [CF₃(CH₂CF₂)₂ - HF]⁺), 133.1 (100, [CF₂CH₂CF₃]⁺), 113.0 (21, [CF₃CH₂CF₂ - HF]⁺).

CF₃CF₂CF(CF₃)CH₂CH₂C=O(CF₂CH₂)₉CF₃: GC-MS: 4.8 mins *m/z* = 851.1 (1%, [M - CF₃]⁺), 787.1 (1, [M - CF₂CH₂CF₃]⁺), 723.1 (1, [M - (CF₂CH₂)₂CF₃]⁺), 659.1 (1, [M - (CF₂CH₂)₃CF₃]⁺), 609.2 (6, [C=O(CF₂CH₂)₈CF₃]⁺), 569.1 (8, [C=O(CF₂CH₂)₇CF₃ - 2HF]⁺), 545.2 (27, [C=O(CF₂CH₂)₇CF₃]⁺), 505.1 (18, [C=O(CF₂CH₂)₇CF₃ - 2HF]⁺), 481.1 (20, [C=O(CF₂CH₂)₆CF₃]⁺), 441.2 (4, [C=O(CF₂CH₂)₆CF₃ - 2HF]⁺), 413.1 (7, [CF₃(CH₂CF₂)₆ - 2HF]⁺), 369.1 (6, [CF₃(CH₂CF₂)₅ - HF]⁺), 329.1 (7, [CF₃(CH₂CF₂)₅ - 3HF]⁺), 305.0 (6, [CF₃(CH₂CF₂)₄ - HF]⁺), 285.0 (16, [CF₃(CH₂CF₂)₄ - 2HF]⁺), 241.0 (27, [CF₃(CH₂CF₂)₃ - HF]⁺), 197.0 (33, [CF₃(CH₂CF₂)₂]⁺), 177.0 (23, [CF₃(CH₂CF₂)₂ - HF]⁺), 133.1 (100, [CF₂CH₂CF₃]⁺), 113.0 (24, [CF₃CH₂CF₂ - HF]⁺).

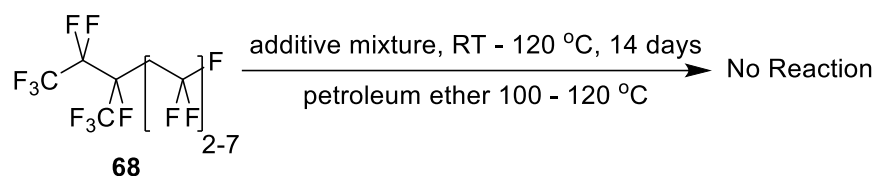
General Procedure for the Reactions of CF₃CF₂CF(CF₃)(CH₂CF₂)_nF with Bases at High Temperature



CF₃CF₂CF(CF₃)(CH₂CF₂)₂₋₇F (0.1 g, 0.20 mmol) was dissolved in petroleum ether 100 – 120 (10 mL) and N,N'-dimethyl ethylenediamine (0.044 g, 0.50 mmol) or triethylamine (0.051 g, 0.50 mmol) was added. The reactions were heated to 80 °C and stirred for 7 days. The temperature was increased by 10 °C each day to a maximum of 120 °C on the 5th day, after which the reactions were heated for 2 more days, and monitored by ¹⁹F NMR throughout. Upon analysis, the reaction mixture with triethylamine had discoloured but no observable reaction had occurred. However, the reaction with N,N'-dimethyl ethylenediamine had caused

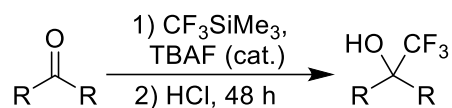
decomposition, as observed by ^{19}F NMR; ^{19}F NMR (376 MHz, Deuterium Oxide) δ -56.07 – -56.38 (m, $\text{CF}=\text{CH}-\text{CF}_3$), -59.28 – -59.54 (m, $\text{CF}=\text{CH}-\text{CF}_3$), -61.05 – -61.30 (m, $\text{CF}=\text{CH}-\text{CF}_3$), -61.87 – -62.17 (m, CH_2CF_3), -76.08 – -76.37 (m, $\text{CF}_3\text{CF}_2\text{CF}(\text{CF}_3)\text{CH}_2\text{CF}_2$), -80.00 – -80.16 (m, $\text{CF}_3\text{CF}_2\text{CF}(\text{CF}_3)$), -84.39 – -84.53 (m $\text{CF}_3\text{CF}_2\text{C}(\text{CF}_3)=\text{CHCF}_2$), -87.92 – -88.47 (m $\text{CF}(\text{CF}_3)(\text{CH}_2\text{CF}_2)_{1-6}\text{CH}_2\text{CF}_3$), -88.57 – -89.12 (m $\text{CF}(\text{CF}_3)(\text{CH}_2\text{CF}_2)_{1-6}\text{CH}_2\text{CF}_3$), -89.35 – -90.71 (m $\text{CF}(\text{CF}_3)(\text{CH}_2\text{CF}_2)_{1-6}\text{CH}_2\text{CF}_3$), -120.93 – -121.08 (m, $\text{CF}_2\text{CF}(\text{CF}_3)$), -121.22 – -121.38 (m, $\text{CF}_2\text{CF}(\text{CF}_3)$), -185.29 – -185.59 (m, $\text{CF}(\text{CF}_3)\text{CH}_2\text{CF}_2$).

General Procedure for the Reactions of $\text{CF}_3\text{CF}_2\text{CF}(\text{CF}_3)(\text{CH}_2\text{CF}_2)_n\text{F}$ with Afton Chemical® Additive Mixtures



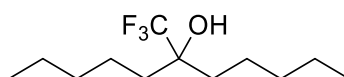
$\text{CF}_3\text{CF}_2\text{CF}(\text{CF}_3)(\text{CH}_2\text{CF}_2)_{2-7}\text{F}$ (0.1 g, 0.20 mmol) was dissolved in a mixture of petroleum ether 100 – 120 (9 mL) and an Afton Chemical® additive mixture (additive mixture HiTEC® 307, 1 mL or additive mixture HiTEC® 317, 1 mL) was added. The reactions were stirred for 7 days, the temperature was increased each day, first from rt to 30 °C and then by 10 °C each day to a maximum of 80 °C, and the reactions were monitored by ^{19}F NMR. Upon analysis, no observable reaction had occurred. The reactions were heated to 80 °C and stirred for a further 7 days. The temperature was increased by 10 °C each day to a maximum of 120 °C on the 5th day, after which the reactions were heated for 2 more days, and monitored by ^{19}F NMR throughout. Upon analysis, no observable reaction had occurred. The reactions were repeated as described above, using petroleum ether 100 – 120 (5 mL) and an Afton Chemical® additive mixture (additive mixture HiTEC® 307, 5 mL or additive mixture HiTEC® 317, 5 mL). Upon analysis, no observable reaction had occurred.

General Procedure for the Reactions of Carbonyl Compounds with CF_3SiMe_3



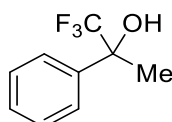
The carbonyl compound (30 mmol) and CF_3SiMe_3 (5.1 g, 36 mmol) were dissolved in THF (30 mL) at 0 °C. TBAF (0.1 g) was added, the reaction was allowed to warm to rt and stirred for 3 hours. The intermediate was hydrolysed with 6 M HCl (6 mL) for 48 hours. The product was isolated with ether (3 x 30 mL), washed with water (2 x 50 mL) and brine 50 mL. The organic layer was dried with MgSO_4 and the solvent removed in vacuo to yield the alcohol product.

6-(Trifluoromethyl)-6-undecanol (101)



6-undecanone (5.1 g) reacted to give 6-(trifluoromethyl)-6-undecanol (5.6 g, 78%) as a yellow oil; ^1H NMR (400 MHz, Chloroform-*d*) δ 2.37 (1 H, s, **OH**), 1.74 – 1.53 (4 H, m, $\text{CH}_2\text{COH}(\text{CF}_3)\text{CH}_2$), 1.44 – 1.21 (12 H, m, $\text{CH}_2\text{CH}_2\text{CH}_2$), 0.89 (6 H, t, $^3J_{\text{HH}} = 7.0$, **CH**₃); ^{19}F NMR (376 MHz, Chloroform-*d*) δ -79.74 (s, **CF**₃); ^{13}C NMR (101 MHz, Chloroform-*d*) δ 126.93 (q, $^1J_{\text{CF}} = 285.5$, **CF**₃), 75.58 (q, $^2J_{\text{CF}} = 26.6$, $\text{CH}_2\text{COH}(\text{CF}_3)\text{CH}_2$), 33.52 (s, **CH**₂), 32.36 (s, **CH**₂), 22.56 (s, **CH**₂), 22.46 (q, $^3J_{\text{CF}} = 1.1$, $\text{CH}_2\text{COH}(\text{CF}_3)\text{CH}_2$), 14.03 (s, **CH**₃); GC-MS: 3.6 mins $m/z = 222.2$ (1%, $[\text{M} - \text{H}_2\text{O}]^+$), 171.2 (63, $[\text{M} - \text{CF}_3]^+$), 99.1 (13, $[\text{C}_5\text{H}_{11}\text{CO}]^+$), 71.1 (37, $[\text{C}_5\text{H}_{11}]^+$), 69.1 (27, $[\text{CF}_3]^+$), 57.1 (49, $[\text{C}_4\text{H}_9]^+$), 56.1 (100, $[\text{C}_4\text{H}_8]^+$), 55.1 (59, $[\text{C}_4\text{H}_8]^+$), 43.1 (26, $[\text{C}_3\text{H}_7]^+$). In agreement with literature data^{92,93}.

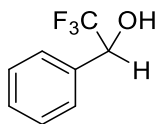
1-Trifluoromethyl-1-phenylethanol (102)



Acetophenone (3.6 g) reacted to give 1-trifluoromethyl-1-phenylethanol (2.8 g, 50%) as a brown oil; ^1H NMR (400 MHz, Chloroform-*d*) δ 7.66 – 7.60 (2 H, m, **Ar-H**), 7.47 – 7.36 (3 H, m, **Ar-H**), 1.80 (3H, q, $^4J_{\text{HF}} = 1.2$, $\text{COH}(\text{CF}_3)\text{CH}_3$); ^{19}F NMR (376 MHz, Chloroform-*d*) δ -80.86 (s, **CF**₃); ^{13}C NMR (101 MHz, Chloroform-*d*) δ 128.55 (s, **Ar-C**), 128.33(s, **Ar-C**), 125.82 (q, $^1J_{\text{CF}} = 285.4$,

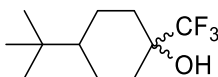
PhCOH(CF₃)CH₃, 74.73 (q, ²J_{CF} = 29.1, PhCOH(CF₃)CH₃), 23.78 (q, ³J_{CF} = 1.3 Hz, PhCOH(CF₃)CH₃); GC-MS: 3.0 mins *m/z* = 189.9 (12%, M⁺), 121.0 (93, [M - CF₃]⁺), 105.0 (21, [PhCO]⁺), 77.0 (20, [Ph]⁺), 43.0 (100, [MeCO]⁺). In agreement with literature data⁸⁷.

1-Trifluoromethyl-1-phenylmethanol (103)



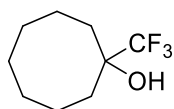
Benzaldehyde (3.2 g) reacted to give 1-trifluoromethyl-1-phenylmethanol (4.3 g, 82%) as a brown oil; ¹H NMR (400 MHz, Chloroform-*d*) δ 7.54 – 7.47 (2 H, m, Ar-**H**), 7.45 – 7.40 (3 H, m, Ar-**H**), 4.97 (1H, q, ³J_{HF} = 6.6, CHOH(CF₃)); ¹⁹F NMR (376 MHz, Chloroform-*d*) δ -78.28 (d, ³J_{FH} = 6.8, CF₃); ¹³C NMR (101 MHz, Chloroform-*d*) δ 129.3 (s, Ar-**C**), 128.50 (s, Ar-**C**), 127.52 (q, ⁴J_{CF} = 1.1, ortho Ar-**C**), 124.47 (q, ¹J_{CF} = 282.1, PhCHOH(CF₃)), 74.73 (q, ²J_{CF} = 31.6, PhCHOH(CF₃)); GC-MS: 3.0 mins *m/z* = 176.1 (47%, M⁺), 107.1 (100, [M - CF₃]⁺), 79.1 (74, [C₂F₂HO]⁺), 77.1 (50, [Ph]⁺). In agreement with literature data⁸⁷.

1-Trifluoromethyl-4-t-butylcyclohexanol (104)



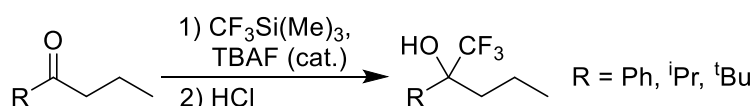
4-t-Butylcyclohexanone (4.6 g) reacted to give 1-trifluoromethyl-4-t-butylcyclohexanol (5.8 g, 87%) as a yellow powder (note that all NMR peaks had a small shoulder due to a mixture of axial and equatorial products being present); ¹H NMR (400 MHz, Chloroform-*d*) δ 2.27 – 2.16 (2 H, m, CH₂), 1.77 – 1.65 (2 H, m, CH₂), 1.56 – 1.44 (2 H, m, CH₂), 1.42 – 1.24 (2 H, m, CH₂), 1.15 – 1.04 (1 H, m, CHCMe₃) 0.86 (9 H, m, C(CH₃)₃); ¹⁹F NMR (376 MHz, Chloroform-*d*) δ -77.76 (s, *cis* CF₃), -84.78 (s, *trans* CF₃); ¹³C NMR (101 MHz, Chloroform-*d*) δ 126.96 (q, ¹J_{CF} = 286.1, CF₃), 72.06 (q, ²J_{CF} = 27.5, CH₂COH(CF₃)CH₂), 46.27 (s, CHCMe₃), 33.29 (s, CH₂CHCMe₃CH₂), 32.32 (s, C(Me)₃), 27.52 (s, C(CH₃)₃), (q, ³J_{CF} = 1.5, CH₂COH(CF₃)CH₂); GC-MS: 3.4 mins *m/z* = 209.1 (1%, [M - CH₃]⁺), 191.1 (13, [M - H₂O - CH₃]⁺), 149.1 (19, [M - H₂O - C(CH₃)₃]⁺), 57.2 (100, [C(CH₃)₃]⁺), 56.1 (66, [CH₂=C(CH₃)₂]⁺), 41.1 (26, [C₃H₅]⁺). In agreement with literature data⁹⁴.

1-Trifluoromethylcyclooctanol (105)



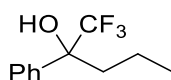
Cyclooctanone (3.8 g) reacted to give 1-trifluoromethylcyclooctanol (2.8 g, 47%) as a yellow oil; ^1H NMR (400 MHz, Chloroform-*d*) δ 2.58 (1 H, s, OH), 2.03 – 0.92 (16 H, m, CH₂); ^{19}F NMR (376 MHz, Chloroform-*d*) δ -81.72 (s, CF₃); ^{13}C NMR (101 MHz, Chloroform-*d*) δ 126.95 (q, $^1J_{\text{CF}} = 286.5$, CF₃), 75.62 (q, $^2J_{\text{CF}} = 26.3$, CH₂COH(CF₃)CH₂), 29.93 (s, CH₂), 27.74 (s, CH₂), 24.54 (s, CH₂), 20.96 (q, $^3J_{\text{CF}} = 1.0$, CH₂COH(CF₃)CH₂); GC-MS: 3.2 mins $m/z = 178.1$ (3%, [M - H₂O]⁺), 150.1 (61, [M - H₂O - CH₂=CH₂]⁺), 127.2 (100, [M - CF₃]⁺), 109.1 (71, [M - H₂O - CF₃]⁺), 69.1 (66, [CF₃]⁺), 56.1 (94, [C₄H₈]⁺), 41.2 (69, [C₃H₅]⁺).

General Procedure for the Reactions of C₃H₇COR with CF₃SiMe₃



The ketones (20 mmol) and CF₃SiMe₃ (3.4 g, 24 mmol) were dissolved in THF (50 mL) at 0 °C. TBAF (0.1 g) was added, the reactions were allowed to warm to rt and stirred for varying times, heating to 50 °C if needed. The products were hydrolysed with 6 M HCl (10 mL) for varying times at 50 °C. The products were isolated with ether (3 x 30 mL) washed with water (2 x 50 mL) and brine 50 mL. The organic layers were dried with MgSO₄ and the solvent removed *in vacuo* to yield the alcohol product.

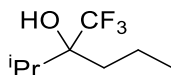
Phenyl-2-trifluoromethylbutan-2-ol (109)



Butyrophenone (2.96 g), was reacted for 24 hours at rt and hydrolysed for 72 hours to yield 1-phenyl-2-trifluoromethylbutan-2-ol (1.12g, 26%) as a yellow oil; ^1H NMR (400 MHz, Chloroform-*d*) δ 7.59 – 7.53 (2 H, m, Ar-*H*), 7.44 – 7.33 (3 H, m, Ar-*H*), 2.59 (1 H, s, OH), 2.28 – 2.11 (1 H, m, PhCOH(CF₃)CH₂), 2.05 – 1.92 (1 H, m, PhCOH(CF₃)CH₂), 1.48 – 1.31 (1 H, m, PhCOH(CF₃)CH₂CH₂), 1.15 – 0.97 (1 H, m, PhCOH(CF₃)CH₂CH₂), 0.91 (3 H, t, $^3J_{\text{HH}} = 7.3$, CH₂CH₂CH₃); ^{19}F NMR (376 MHz, Chloroform-*d*) δ -80.08 (s, CF₃); GC-MS: 3.4 mins $m/z = 218.1$

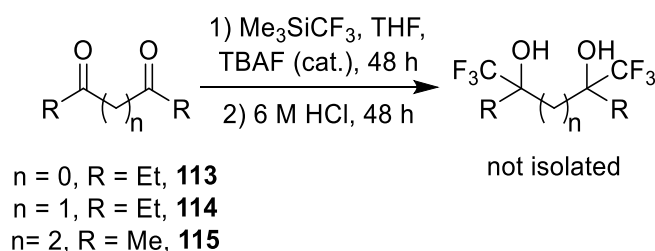
(9%, M⁺), 175.1 (78, [M - C₃H₇]⁺), 149.3 (31, [M - CF₃]⁺), 105.1 (99, [PhCO]⁺), 77.1 (35, [Ph]⁺), 71.1 (29, [COIC₃H₇]⁺), 69.0 (10, [CF₃]⁺), 43.1 (29, [C₃H₇]⁺). In agreement with literature data⁹⁵.

2-Methyl-3-trifluoromethylhexan-3-ol (110)

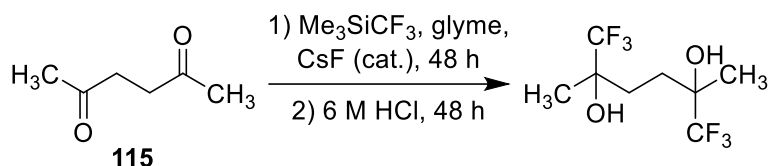


2,2-dimethyl-3-hexanone (2.56 g), was reacted for 48 hours at rt and hydrolysed for 120 hours to yield 2-methyl-3-trifluoromethylhexan-3-ol (0.86, 23%) as a yellow oil; ¹H NMR (400 MHz, Chloroform-*d*) δ 2.34 (1 H, s, *OH*), 2.10 (1 H, hept, ³J_{HH} = 6.9, (CH₃)₂CH), 1.70 – 1.62 (2 H, m, ⁱPrCOH(CF₃)CH₂), 1.50 – 1.36 (2 H, m, ⁱPrCOH(CF₃)CH₂), 1.03 (3 H, dq, ³J_{HH} = 7.3, ⁴J_{HH} = 1.3, (CH₃)₂CH), 1.02 (3 H, dq, ³J_{HH} = 7.3, ⁴J_{HH} = 1.3, (CH₃)₂CH), 0.96 (3 H, t, ³J_{HH} = 7.3, CH₂CH₂CH₃); ¹⁹F NMR (376 MHz, Chloroform-*d*) δ -74.58 (s, CF₃); GC-MS: 2.3 mins *m/z* = 167.1 (1%, [M - OH]⁺), 141.1 (73, [M - C₃H₇]⁺), 123.1 (90, [M - H₂O - C₃H₇]⁺), 115.2 (31, [M - CF₃]⁺), 71.1 (35, [COC₃H₇]⁺), 69.1 (6, [CF₃]⁺), 59.1 (25, [OC₃H₇]⁺), 43.1 (100, [C₃H₇]⁺).

Reactions of Dicarboxyl Carbonyl Compounds with Me₃SiCF₃

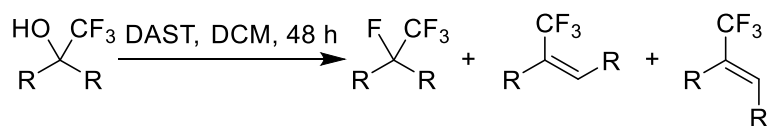


3,4-hexanedione (3.42 g, 30 mmol), 3,5-heptanedione (3.84 g, 30 mmol) and 2,5-hexanedione (3.42 g, 30 mmol) were individually dissolved in THF (30 mL) at 0 °C with CF₃SiMe₃ (12.8 g, 90 mmol). TBAF (0.2 g) was added and the reactions were allowed to warm to rt and stirred for 48 hours. The product was hydrolysed with 6 M HCl (12 mL) for 48 hours, isolated with ether (3 x 30 mL), washed with water (2 x 50 mL) and brine 50 mL. The organic layer was dried with MgSO₄ and the solvent removed in vacuo to yield the product mixtures. The isolated liquids contained a mixture of compounds that could not be purified. The reaction with MeCOCH₂CH₂COMe was repeated using 1 eq. (4.3 g, 30 mmol) of CF₃SiMe₃. This reaction also produced a mixture of compounds that could not be purified.



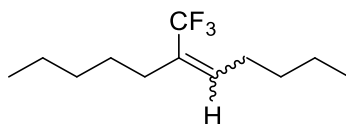
2,5-hexanedione (1.14 g, 10 mmol) and CF_3SiMe_3 (4.62 g, 32.5 mmol) were dissolved in glyme (10 mL) at 0 °C. CsF (0.03 g) was added, the reaction was allowed to warm to rt, and subsequently heated to 60 °C and stirred for 48 hours. The glyme was removed in vacuo, the residue was cooled to 0 °C and THF (4 mL) and 6 M HCl (16 mL) were added. The product was stirred at rt for 48 hours, isolated with ether (3 x 30 mL) washed with water (2 x 50 mL) and brine 50 mL. The organic layer was dried with MgSO_4 and the solvent removed in vacuo to yield the product mixture. The isolated liquid contained a mixture of compounds that could not be purified.

General Procedure for the Reactions of 1-Trifluoromethyl alcohols with DAST



The alcohol (10 mmol) was dissolved in DCM (40 mL) and stirred at 0 °C. DAST (3.54 g, 22 mmol) in DCM (10 mL) was added to the reaction mixture, the reaction was allowed to warm to rt and stirred overnight. Water (50 mL) and DCM (50 mL) were added, followed by neutralisation with sat. NaHCO_3 . The organic layer was washed with water (2 x 50 mL) and brine (50 mL) and the solvent removed in vacuo to yield the fluorinated product.

6-Trifluoromethylundec-5-ene (116)



6-(Trifluoromethyl)-6-undecanol (2.40 g) reacted to yield 6-trifluoromethylundec-5-ene (1.16 g, 52%) as a yellow oil as a mixture of *cis* and *trans* isomers; ^1H NMR (400 MHz, Chloroform-*d*) δ 6.07 (1 H, tq, $^3J_{\text{HH}} = 7.4$, $^4J_{\text{HF}} = 1.8$, *trans* $\text{CH}=\text{C}(\text{CF}_3)\text{CH}_2$), 5.67 (1 H, tq, $^3J_{\text{HH}} = 7.8$, $^4J_{\text{HF}} = 1.1$, *cis* $\text{CH}=\text{C}(\text{CF}_3)\text{CH}_2$), 2.20 – 2.08 (2 H, m, $\text{CH}=\text{C}(\text{CF}_3)\text{CH}_2$), 1.51 – 1.23 (12 H, m, $\text{CH}_2\text{CH}_2\text{CH}_2$), 0.96 – 0.87 (6 H, m, CH_3); ^{19}F NMR (376 MHz, Chloroform-*d*) δ -59.74 (t, $^4J_{\text{FH}} = 2.2$,

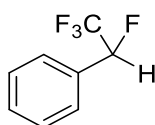
cis CH=C(CF₃), -66.97 (td, ⁴J_{FH} = 2.2, ⁴J_{FH} = 1.9, *trans* CH=C(CF₃)); ¹³C NMR (101 MHz, Chloroform-*d*) δ 137.67 (q, ³J_{CF} = 3.7, *cis* CH=C(CF₃)), 134.42 (q, ³J_{CF} = 6.2, *trans* CH=C(CF₃)), 129.71 (q, ²J_{CF} = 27.4, CH=C(CF₃)), 124.95 (q, ¹J_{CF} = 273.1, CF₃), 32.00 (s, CH₂), 31.15 (s, CH₂), 28.87 (s, CH₂), 27.17 (s, CH₂), 25.89 (s, CH₂), 22.53 (s, CH₂), 14.08 (s, CH₃), 13.99 (s, CH₃); 3.2 mins *m/z* = 222.2 (12%, [M]⁺), 70.1 (49, [CF₃H]⁺), 69.1 (28, [CF₃]⁺), 57.1 (67, [CH₃(CH₂)₃]⁺), 56.2 (100, [(CH₂)₄]⁺), 43.1 (47, [C₃H₇]⁺), 41.1 (55, [C₃H₅]⁺); GC-MS: 3.3 mins *m/z* = 222.2 (10%, [M]⁺), 70.1 (39, [CF₃H]⁺), 69.1 (25, [CF₃]⁺), 57.1 (47, [CH₃(CH₂)₃]⁺), 56.1 (100, [(CH₂)₄]⁺), 43.1 (48, [C₃H₇]⁺), 41.1 (49, [C₃H₅]⁺).

1-Trifluoromethyl-1-phenyl-1-fluoroethane (117)



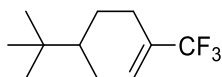
1-Trifluoromethyl-1-phenylethanol (1.90 g) reacted to yield 1-trifluoromethyl-1-phenyl-1-fluoroethane (0.85 g, 44%) as a brown oil; ¹H NMR (400 MHz, Chloroform-*d*) δ 7.54 – 7.49 (2 H, m, Ar-**H**), 7.48 – 7.40 (3 H, m, Ar-**H**), 1.80 (3H, d, ³J_{HF} = 23.0, CF(CF₃)CH₃); ¹⁹F NMR (376 MHz, Chloroform-*d*) δ -81.49 (3F, d, ³J_{FF} = 6.9, CF₃), -163.62 (1F, qq, ³J_{FF} = 23.0, ³J_{FH} = 6.9, CF(CF₃)); GC-MS: 2.3 mins *m/z* = 192.1 (62%, M⁺), 127.1 (13, [CCF(CF₃)Me]⁺) 123.2 (100, [M - CF₃]⁺), 103.1 (40, [PhCCH₂]⁺), 77.0 (17, [Ph]⁺). In agreement with literature data⁹⁷.

1-Trifluoromethyl-1-phenyl-1-fluoromethane (118)



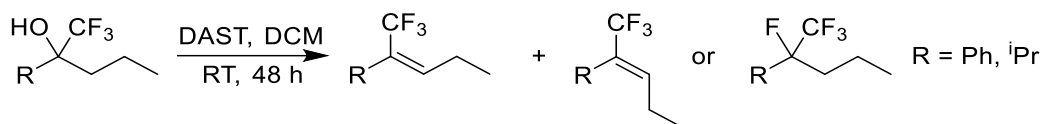
1-Trifluoromethyl-1-phenylmethanol (1.76 g) reacted to yield 1-trifluoromethyl-1-phenyl-1-fluoromethane (0.69 g, 48%) as a brown oil; ¹H NMR (400 MHz, Chloroform-*d*) δ 7.51 – 7.42 (5 H, m, Ar-**H**), 5.60 (1H, dq, ²J_{HF} = 44.2, ³J_{HF} = 6.1, CHF(CF₃)); ¹⁹F NMR (376 MHz, Chloroform-*d*) δ -88.83 (3F, dd, ³J_{FF} = 12.9, ³J_{FH} = 6.1, CF₃), -194.62 (1F, dq, ²J_{FH} = 44.1, ³J_{FF} = 12.8, CHF(CF₃)); ¹³C NMR (101 MHz, Chloroform-*d*) δ 130.42 (d, ⁴J_{CF} = 1.6, meta Ar-**C**), 128.71 (s, para Ar-**C**), 127.16 (dq, ³J_{CF} = 6.7, ⁴J_{CF} = 0.9, ortho Ar-**C**), 122.25 (dq, ¹J_{CF} = 280.7, ²J_{CF} = 28.2, PhCHF(CF₃)), 88.95 (dq, ¹J_{CF} = 186.2, ²J_{CF} = 34.9, PhCHF(CF₃)); GC-MS: 3.0 mins *m/z* = 177.9 (38%, M⁺), 109.0 (100, [M - CF₃]⁺), 83.0 (15, [CH₂CF₃]⁺). In agreement with literature data⁹⁸.

1-Trifluoromethyl-4-t-butylcyclohex-1-ene (119)



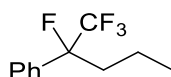
1-Trifluoromethyl-4-t-butylcyclohexanol (2.24 g) reacted to yield 1-trifluoromethyl-4-t-butylcyclohex-1-ene (1.263 g, 61%) as a brown oil; ^1H NMR (400 MHz, Chloroform-*d*) δ 6.39 – 6.31 (1H, m, $\text{C}(\text{CF}_3)=\text{CH}$), 2.34 – 2.26 (1 H, m, CHCMe_3), 2.26 – 2.05 (2 H, m, CH_2), 2.01 – 1.82 (2 H, m, CH_2), 1.40 – 1.12 (2 H, m, CH_2), 0.92 (9 H, m, $\text{C}(\text{CH}_3)_3$); ^{19}F NMR (376 MHz, Chloroform-*d*) δ -69.29 (s, CF_3); ^{13}C NMR (101 MHz, Chloroform-*d*) δ 130.66 (q, $^3J_{\text{CF}} = 5.7$, $\text{CH}=\text{C}(\text{CF}_3)$), 128.01 (q, $^3J_{\text{CF}} = 29.8$, $\text{CH}=\text{C}(\text{CF}_3)$), 124.09 (q, $^1J_{\text{CF}} = 271.4$, $\text{CH}=\text{C}(\text{CF}_3)$), 43.21 (s, $\text{CHC}(\text{CH}_3)_3$), 32.06 (s, $\text{CHC}(\text{CH}_3)_3$), 26.97 (s, $\text{CHC}(\text{CH}_3)_3$), 26.02 (s, CH_2), 23.45 (q, $^3J_{\text{CF}} = 1.2$, CH_2), 22.98 (s, CH_2); GC-MS: 3.0 mins $m/z = 206.2$ (8%, M^+), 191.1 (11, $[\text{M} - \text{CH}_3]^+$), 149.1 (27, $[\text{M} - \text{C}(\text{CH}_3)_3]^+$), 135.1 (33, $[\text{M} - \text{CF}_3 - \text{H}_2]^+$), 69.1 (26, $[\text{CF}_3]^+$), 58.1 (88, $[\text{CH}(\text{CH}_3)_3]^+$), 57.2 (100, $[\text{C}(\text{CH}_3)_3]^+$), 56.1 (54, $[\text{CH}_2=\text{C}(\text{CH}_3)_2]^+$), 43.1 (33, $[\text{C}_3\text{H}_7]^+$), 41.1 (70, $[\text{C}_3\text{H}_5]^+$). In agreement with literature data⁹⁴.

General Procedure for the Reactions of $\text{C}_3\text{H}_7\text{COH}(\text{CF}_3)\text{R}$ with DAST



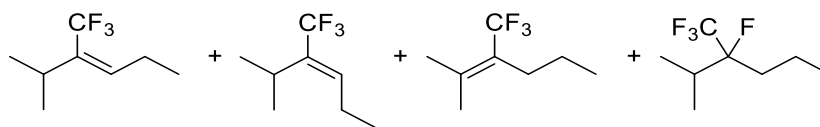
The alcohol (5 mmol) was dissolved in DCM (40 mL) and stirred at 0 °C. DAST (1.77 g, 11 mmol) in DCM (10 mL) was added to the reaction mixture, the reaction was allowed to warm to rt and stirred overnight. Water (50 mL) and DCM (50 mL) were added, followed by neutralisation with sat. NaHCO_3 . The organic layer was washed with water (2 x 50 mL) and brine (50 mL). The products were analysed in solution by ^{19}F NMR and are awaiting purification.

1-Phenyl-2-trifluoromethyl-2-fluorobutane (120)



1-phenyl-2-trifluoromethylbutan-2-ol (1.09 g) reacted to yield 1-phenyl-2-trifluoromethyl-2-fluorobutane; ^{19}F NMR (376 MHz, Chloroform-*d*) δ -80.53 (d, $^3J_{\text{FF}} = 6.9$, $\text{CF}(\text{CF}_3)$), -175.71 (ddq, $^3J_{\text{FH}} = 37.4$, $^3J_{\text{FH}} = 13.9$, $^3J_{\text{FF}} = 7.0$, $\text{CF}(\text{CF}_3)$).

Reaction of 2-methyl-3-trifluoromethylhexan-3-ol with DAST



2-methyl-3-trifluoromethylhexan-3-ol (0.86 g) reacted to yield a mixture of *cis* and *trans* 2-methyl-3-trifluoromethylundec-3-ene, 2-methyl-3-trifluoromethylundec-2-ene and 2-methyl-3-trifluoromethyl-3-fluorohexane which could not be identified individually; ^{19}F NMR (376 MHz, Chloroform-*d*) δ -57.58 (p, $^3J_{\text{FH}} = 2.5$, CF_3), -59.19 (t, $^3J_{\text{FH}} = 2.4$, CF_3), -63.25 (s, CF_3), -64.90 (t, $^3J_{\text{FH}} = 10.1$, CF_3), -219.01 – -219.46 (m, $\text{CF}(\text{CF}_3)$).

8. References

- 1 Petroleum consumption by countries, 2019 - knoema.com, <https://knoema.com/atlas/topics/Energy/Oil/Petroleum-consumption>, (accessed 28 June 2019).
- 2 H. Schobert, in *Chemistry of Fossil Fuels and Biofuels*, Cambridge University Press, Cambridge, 1st edn., 2013, pp. 103–131.
- 3 N. J. Hyne, *Nontechnical guide to petroleum geology, exploration, drilling, and production*, PennWell Corporation, Tulsa, 3rd edn., 2012.
- 4 J. G. Speight, *The Chemistry and Technology of Petroleum*, Taylor & Francis Group, Boca Raton, 4th edn., 2007.
- 5 Use of Oil - Energy Explained, https://www.eia.gov/energyexplained/index.php?page=oil_use, (accessed 28 June 2019).
- 6 J. S. Eow, *Environ. Prog.*, 2002, **21**, 143–162.
- 7 W. Letzsch, in *Handbook of Petroleum Processing*, eds. S. A. Treese, P. R. Pujado and D. S. J. Jones, Springer International Publishing, New York, 2nd edn., 2015, pp. 261–316.
- 8 T. Mang, J. Braun, W. Dresel and J. Omeis, in *Ullmann's Encyclopedia of Industrial Chemistry*, ed. B. Elvers, Wiley-VCH, Weinheim, 6th edn., 2011.
- 9 F. Elastomers, in *Kirk-Othmer Encyclopedia of Chemical Technology*, John Wiley & Sons, Inc, Hoboken, 2000.
- 10 Viton® and Vamac families: Chemical structure and monomer composition, https://www.ber-pa.it/UserFiles/Download/BER-PA_Viton_Vamac_Product_Line.pdf, (accessed 28 June 2019).
- 11 T. Sugama, T. Pyatina, E. Redline, J. McElhanon and D. Blankenship, *Polym. Degrad. Stab.*, 2015, **120**, 328–339.
- 12 D. Li and M. Liao, *J. Fluor. Chem.*, 2017, **201**, 55–67.
- 13 Global Fluorochemicals Market Size | Industry Analysis Report, 2024, <https://www.grandviewresearch.com/industry-analysis/fluorochemical-market>, (accessed 28 June 2019).
- 14 A. Harsanyi and G. Sandford, *Green Chem.*, 2015, **17**, 2081–2086.
- 15 G. Villalba, R. U. Ayres and H. Schroder, *J. Ind. Ecol.*, 2008, **11**, 85–101.
- 16 M. J. Molina and F. S. Rowland, *Nature*, 1974, **249**, 810–812.
- 17 G. J. M. Velders, D. W. Fahey, J. S. Daniel, M. McFarland and S. O. Andersen, *Proc. Natl. Acad. Sci. U. S. A.*, 2009, **106**, 10949–54.
- 18 J. Park, A. Benning, F. Downing, J. Laucius and R. McHarness, *Ind. Eng. Chem.*, 1947, **39**, 354–358.
- 19 A. L. Henne and T. P. Waalkes, *J. Am. Chem. Soc.*, 1946, **68**, 496–497.
- 20 J. G. Drobny, *Technology of Fluoropolymers*, CRC Press, Boca Raton, 2nd edn., 2008.
- 21 S. Ebnesajjad, in *Applied Plastics Engineering Handbook: Processing, Materials, and Applications*, ed. M. Kutz, Elsevier, Amsterdam, 2nd edn., 2016, pp. 55–72.
- 22 P. W. Atkins, T. Overton, J. P. Rourke, M. Weller and F. A. Armstrong, *Shriver & Atkins' Inorganic Chemistry*, Oxford University Press, Oxford, 5th edn., 2010.
- 23 D. O'Hagan, *Chem. Soc. Rev.*, 2008, **37**, 308–319.
- 24 P. Shah and A. D. Westwell, *J. Enzyme Inhib. Med. Chem.*, 2007, **22**, 527–540.
- 25 J.-P. Bégué and D. Bonnet-Delpon, *Bioorganic and Medicinal Chemistry of Fluorine*, John Wiley & Sons, Inc., Hoboken, 2007.
- 26 FKM Rubber Crumb - J. Allcock & Sons Ltd., <http://www.allcocks.co.uk/en/products/rubber-crumb-and-granule/fkm-crumb-new.htm>, (accessed 28 June 2019).

- 27 R. Honma, H. Hori, F. R. da Cunha, N. Horiike, L. Steinbach and B. Ameduri, *Ind. Eng. Chem. Res.*, 2019, **58**, 13030–13040.
- 28 Kalrez® Perfluoroelastomer Parts | DuPont™, <http://www.dupont.co.uk/products-and-services/plastics-polymers-resins/parts-shapes/brands/kalrez-perfluoroelastomer.html>, (accessed 28 June 2019).
- 29 Chemraz® Perfluoroelastomer | Greene Tweed, <https://www.gtweed.com/markets/oilfield/products/sealing-systems/materials/chemraz-perfluoroelastomer/>, (accessed 28 June 2019).
- 30 FKM Rubber compounds, [https://www.polycomp.nl/fkm-advantages/#Monomers for FKM](https://www.polycomp.nl/fkm-advantages/#Monomers%20for%20FKM), (accessed 28 June 2019).
- 31 E. E. Lewis and M. A. Naylor, *J. Am. Chem. Soc.*, 1947, **69**, 1968–1970.
- 32 US Pat., US20040034259A1, 2004.
- 33 US Pat., US 2004/0082822 A1, 2004.
- 34 US Pat., US20040002621A1, 2004.
- 35 B. Atkinson and A. B. Trenwith, *J. Chem. Soc.*, 1953, 2082.
- 36 B. Atkinson and V. A. Atkinson, *J. Chem. Soc.*, 1957, **VII**, 2086–2094.
- 37 I. D. Kushina, M. U. Fedurtsa, V. M. Gida, V. G. Barabanov and O. M. Nefedov, *Bull. Acad. Sci. USSR Div. Chem. Sci.*, 1989, **38**, 1312–1315.
- 38 US Pat., US3114778A, 1963.
- 39 CNIPA Pat., CN 105367392 A, 2015.
- 40 J. G. Drobny, *Fluoroelastomers Handbook : the Definitive User's Guide*, William Andrew, Norwich, NY, 2nd edn., 2016.
- 41 US Pat., US4380618A, 1983.
- 42 US Pat., US5639837A, 1997.
- 43 J. Balague, B. Ameduri, B. Boutevin and G. Caporiccio, *J. Fluor. Chem.*, 1995, **70**, 215–223.
- 44 J. Balagué, B. Améduri, B. Boutevin and G. Caporiccio, *J. Fluor. Chem.*, 1995, **74**, 49–58.
- 45 A. Taguet, L. Sauguet, B. Ameduri and B. Boutevin, *J. Fluor. Chem.*, 2007, **128**, 619–630.
- 46 A. Taguet, B. Ameduri and B. Boutevin, Springer, Berlin, Heidelberg, 2005, pp. 127–211.
- 47 W. W. Schmiegel, *Angew. Makromol. Chemie*, 1979, **76**, 39–65.
- 48 US Pat., US4035565A, 1977.
- 49 Viton Fluoroelastomers Selection Guide, https://www.chemours.com/Viton/en_US/assets/downloads/viton-selection-guide.pdf, (accessed 28 June 2019).
- 50 W. E. Hanford and R. M. Joyce, *J. Am. Chem. Soc.*, 1946, **68**, 2082–2085.
- 51 Viton Fluid Resistance Guide, <https://plastomatic.com/viton-fluid-resistance-guide.pdf>, (accessed 28 June 2019).
- 52 N. O. Brace, *J. Fluor. Chem.*, 1999, **93**, 1–25.
- 53 R. N. Haszeldine, *J. Chem. Soc.*, 1953, 3761–3768.
- 54 V. A. Petrov and C. G. Krespan, *J. Org. Chem.*, 1996, **61**, 9605–9607.
- 55 R. D. Chambers, J. Hutchinson, R. H. Mobbs and W. K. R. Musgrave, *Tetrahedron*, 1964, **20**, 497–506.
- 56 M. Hauptschein, M. Braid and F. E. Lawlor, *J. Am. Chem. Soc.*, 1957, **79**, 2549–2553.
- 57 W. R. Dolbier, *Chem. Rev.*, 1996, **96**, 1557–1584.
- 58 M. Matsugi, M. Hasegawa, S. Hasebe, S. Takai, R. Suyama, Y. Wakita, K. Kudo, H. Imamura, T. Hayashi and S. Haga, *Tetrahedron Lett.*, 2008, **49**, 4189–4191.
- 59 P. M. Murphy, C. S. Baldwin and R. C. Buck, *J. Fluor. Chem.*, 2012, **138**, 3–23.
- 60 T. Rawner, E. Lutsker, C. A. Kaiser and O. Reiser, *ACS Catal.*, 2018, **8**, 3950–3956.
- 61 D. V. Avila, K. U. Ingold, J. Luszytk, W. R. Dolbier, H. Q. Pan and M. Muir, *J. Am. Chem. Soc.*, 1994, **116**, 99–104.

- 62 D. V. Avila, K. U. Ingold, J. Luszytk, W. R. Dolbier and H. Q. Pan, *J. Org. Chem.*, 1996, **61**, 2027–2030.
- 63 N. O. Brace, *J. Fluor. Chem.*, 1999, **96**, 101–127.
- 64 N. O. Brace, *J. Am. Chem. Soc.*, 1964, **86**, 523–524.
- 65 N. O. Brace, *J. Org. Chem.*, 1966, **31**, 2879–2885.
- 66 N. O. Brace, *J. Org. Chem.*, 1973, **38**, 3167–3172.
- 67 M. Iizuka and M. Yoshida, *J. Fluor. Chem.*, 2009, **130**, 926–932.
- 68 J. Balagué, B. Améduri, B. Boutevin and G. Caporiccio, *J. Fluor. Chem.*, 1995, **73**, 237–245.
- 69 G. C. Apsey, R. D. Chambers and P. Odello, *J. Fluor. Chem.*, 1996, **77**, 127–132.
- 70 G. C. Apsey, R. D. Chambers and M. J. Salisbury, *J. Fluor. Chem.*, 1988, **40**, 261–282.
- 71 E. Le Grogneq, J.-M. Chrétien, F. Zammattio and J.-P. Quintard, *Chem. Rev.*, 2015, **115**, 10207–10260.
- 72 G. K. S. Prakash, R. Krishnamurti and G. A. Olah, *J. Am. Chem. Soc.*, 1989, **111**, 393–395.
- 73 G. K. S. Prakash and A. K. Yudin, *Chem. Rev.*, 1997, **97**, 757–786.
- 74 WIPO Pat., WO 2015/026792 A1, 2015.
- 75 EU Pat., EP0273549 (A1), 1988.
- 76 US Pat., US4791139A, 1988.
- 77 US Pat., US4937388A, 1990.
- 78 US Pat., US005225607A, 1993.
- 79 J. Wang, M. Sánchez-Roselló, J. L. Aceña, C. del Pozo, A. E. Sorochinsky, S. Fustero, V. A. Soloshonok and H. Liu, *Chem. Rev.*, 2014, **114**, 2432–2506.
- 80 F. Swarts, *Bull. Acad. R. Belg.*, 1892, **24**, 309.
- 81 US Pat., US1967244A, 1934.
- 82 W. Zhu, J. Wang, S. Wang, Z. Gu, J. L. Aceña, K. Izawa, H. Liu and V. A. Soloshonok, *J. Fluor. Chem.*, 2014, **167**, 37–54.
- 83 I. Ruppert, K. Schlich and W. Volbach, *Tetrahedron Lett.*, 1984, **25**, 2195–2198.
- 84 Z. Wang and B. Ruan, *J. Fluor. Chem.*, 1994, **69**, 1–3.
- 85 R. C. Bansal, B. Dean, S. Hakomori and T. Toyokuni, *J. Chem. Soc. Chem. Commun.*, 1991, 796–797.
- 86 P. Munier, D. Picq and D. Anker, *Tetrahedron Lett.*, 1993, **34**, 8241–8244.
- 87 R. Krishnamurti, D. R. Bellew and G. K. S. Prakash, *J. Org. Chem.*, 1991, **56**, 984–989.
- 88 R. P. Singh and J. M. Shreeve, *Synthesis (Stuttg.)*, 2002, **2002**, 2561–2578.
- 89 J. Leroy, E. Hebert and C. Wakselman, *J. Org. Chem.*, 1979, **44**, 3406–3408.
- 90 D. F. Shellhamer, A. A. Briggs, B. M. Miller, J. M. Prince, D. H. Scott and V. L. Heasley, *J. Chem. Soc. Perkin Trans. 2*, 1996, 973–977.
- 91 A. Sutherland and J. C. Vederas, *Chem. Commun.*, 1999, **7**, 1739–1740.
- 92 J. Joubert, S. Roussel, C. Christophe, T. Billard, B. R. Langlois and T. Vidal, *Angew. Chemie Int. Ed.*, 2003, **42**, 3133–3136.
- 93 T. Shono, M. Ishifune, T. Okada and S. Kashimura, *J. Org. Chem.*, 1991, **56**, 2–4.
- 94 Y. Carcenac, M. Tordeux, C. Wakselman and P. Diter, *J. Fluor. Chem.*, 2005, **126**, 1347–1355.
- 95 S. Mizuta, N. Shibata, S. Akiti, H. Fujimoto, S. Nakamura and T. Takeshi, *Org. Lett.*, 2007, **9**, 3707–3710.
- 96 R. P. Singh, J. M. Leitch, B. Twamley and J. M. Shreeve, *J. Org. Chem.*, 2001, **66**, 1436–1440.
- 97 Canadian Pat., CA1022573A, 1977.
- 98 E. Emer, J. Twilton, M. Tredwell, S. Calderwood, T. L. Collier, B. Liégault, M. Taillefer and V. Gouverneur, *Org. Lett.*, 2014, **16**, 6004–6007.
- 99 T. Nagai, G. Nishioka, M. Koyama, A. Ando, T. Miki and I. Kumadaki, *J. Fluor. Chem.*, 1992, **57**, 229–237.

Appendix 1: Crystallographic data for compound 102a

Identification code	17srv190
Empirical formula	C ₁₁ H ₁₉ F ₃ O × 0.5 H ₂ O
Formula weight	233.27
Temperature/K	120.0
Crystal system	monoclinic
Space group	P2 ₁ /n
a/Å	6.6068(4)
b/Å	20.8211(11)
c/Å	17.5521(10)
α/°	90
β/°	96.155(2)
γ/°	90
Volume/Å ³	2400.6(2)
Z	8
ρ _{calc} /cm ³	1.291
μ/mm ⁻¹	0.114
F(000)	1000.0
Crystal size/mm ³	0.29 × 0.08 × 0.04
Radiation	MoKα (λ = 0.71073)
2θ range for data collection/°	4.556 to 54.99
Index ranges	-8 ≤ h ≤ 8, -27 ≤ k ≤ 26, -22 ≤ l ≤ 22
Reflections collected	33264
Independent reflections	5514 [R _{int} = 0.0732, R _{sigma} = 0.0598]
Data/restraints/parameters	5514/0/292
Goodness-of-fit on F ²	1.010
Final R indexes [I >= 2σ (I)]	R ₁ = 0.0518, wR ₂ = 0.0964
Final R indexes [all data]	R ₁ = 0.1028, wR ₂ = 0.1145
Largest diff. peak/hole / e Å ⁻³	0.28/-0.30

Table 2 Fractional Atomic Coordinates ($\times 10^4$) and Equivalent Isotropic Displacement Parameters ($\text{\AA}^2 \times 10^3$) for 17srv190. U_{eq} is defined as 1/3 of the trace of the orthogonalised U_{ij} tensor.

Atom	<i>x</i>	<i>y</i>	<i>z</i>	$U(\text{eq})$
F1	3943.3(18)	2128.0(5)	4474.3(6)	31.8(3)
F2	6505.3(17)	1631.7(6)	4098.1(7)	34.4(3)
F3	4398.8(19)	2121.5(5)	3281.3(6)	34.2(3)
O1	3684.7(19)	817.6(6)	4535.6(7)	18.5(3)
C1	3261(3)	1141.5(8)	3816.5(10)	16.3(4)
C2	995(3)	1276.4(9)	3651.3(10)	18.0(4)
C3	317(3)	1474.0(9)	2824.4(10)	20.4(4)
C4	974(3)	981.6(9)	2248.5(10)	16.2(4)
C5	3282(3)	897.6(9)	2382.4(10)	20.0(4)
C6	3996(3)	699.5(9)	3208.7(10)	19.8(4)
C7	4521(3)	1756.1(9)	3912.8(11)	23.5(4)
C8	166(3)	1130.8(9)	1401.3(10)	18.9(4)
C9	744(3)	584.2(10)	881.4(11)	27.6(5)
C10	-2154(3)	1173.2(11)	1326.6(11)	29.6(5)
C11	1025(3)	1760.5(10)	1121.3(11)	29.3(5)
F1A	3290.7(17)	3192.5(6)	1050.8(7)	32.7(3)
F2A	5884.5(18)	2677.8(5)	736.2(7)	35.2(3)
F3A	5375.0(19)	2752.8(5)	1919.0(6)	35.3(3)
O1A	6143(2)	3979.0(6)	565.5(7)	22.1(3)
C1A	6498(3)	3702.0(9)	1309.9(10)	16.9(4)
C2A	5815(3)	4161.6(9)	1909.3(10)	20.1(4)
C3A	6597(3)	3992.3(9)	2737.2(10)	20.1(4)
C4A	8902(3)	3898.9(9)	2854.4(10)	17.1(4)
C5A	9509(3)	3395.2(9)	2284.8(10)	20.3(4)
C6A	8777(3)	3576.7(9)	1455.5(10)	19.2(4)
C7A	5270(3)	3081.1(10)	1255.8(10)	23.6(4)
C8A	9737(3)	3759.5(9)	3701.7(10)	20.1(4)
C9A	12052(3)	3697.9(11)	3763.9(11)	30.3(5)
C10A	9230(3)	4323.2(10)	4207.5(11)	29.6(5)
C11A	8841(3)	3143.8(10)	4003.9(11)	33.1(5)
O1W	2524(2)	4516.7(7)	297.5(10)	39.4(4)

Table 3 Anisotropic Displacement Parameters ($\text{\AA}^2 \times 10^3$) for 17srv190. The Anisotropic displacement factor exponent takes the form: $-2\pi^2[h^2a^2U_{11}+2hka*b*U_{12}+...]$.						
Atom	U₁₁	U₂₂	U₃₃	U₂₃	U₁₃	U₁₂
F1	42.3(8)	23.8(6)	29.3(6)	-7.1(5)	3.4(5)	-3.8(5)
F2	19.7(7)	40.9(7)	42.0(7)	3.4(6)	0.8(5)	-8.3(5)
F3	47.4(8)	28.1(7)	26.3(6)	9.6(5)	1.1(6)	-12.4(6)
O1	18.8(7)	21.7(7)	15.5(6)	3.9(6)	3.7(5)	3.2(5)
C1	18.5(10)	18.3(10)	12.0(9)	2.8(7)	1.5(7)	0.6(7)
C2	16.7(10)	22.3(10)	15.6(9)	0.0(8)	4.2(7)	3.9(8)
C3	18.2(10)	24.3(10)	18.6(10)	-0.6(8)	2.3(8)	6.7(8)
C4	16.8(10)	16.5(9)	15.8(9)	1.9(7)	3.3(7)	-0.3(7)
C5	21.2(10)	22(1)	18.0(9)	-2.2(8)	7.0(8)	4.7(8)
C6	16.8(10)	22.4(10)	20.5(10)	1.0(8)	3.3(8)	5.8(8)
C7	27.4(12)	23.6(10)	19.7(10)	2.6(9)	3.4(8)	-0.1(9)
C8	22.8(11)	19.1(10)	15.0(9)	-0.1(8)	2.2(8)	-0.7(8)
C9	34.5(12)	28.9(11)	19.3(10)	-2.7(9)	2.8(9)	1.1(9)
C10	25.2(12)	40.1(13)	22.9(11)	-3.9(10)	-0.4(9)	1.4(9)
C11	40.1(13)	25.8(11)	21.8(10)	6.4(9)	2.4(9)	-3.2(10)
F1A	20.1(6)	36.3(7)	41.0(7)	1.6(6)	-0.2(5)	-8.3(5)
F2A	43.4(8)	27.9(7)	33.8(7)	-12.3(5)	2.0(6)	1.1(6)
F3A	49.0(8)	27.9(7)	28.2(6)	9.3(5)	0.3(6)	-11.4(6)
O1A	17.9(8)	30.8(8)	17.5(7)	6.9(6)	2.2(5)	5.6(6)
C1A	18.1(10)	19.7(10)	12.9(9)	2.8(8)	2.5(7)	2.1(8)
C2A	16.3(10)	21.6(10)	22.2(10)	-0.2(8)	0.7(8)	5.8(8)
C3A	20.3(10)	23.6(10)	16.9(9)	-3.8(8)	4.2(8)	4.4(8)
C4A	16.8(10)	17.6(10)	17.5(9)	1.2(7)	3.8(8)	1.5(7)
C5A	18(1)	26.5(11)	16.6(9)	0.2(8)	2.1(8)	6.8(8)
C6A	17.5(10)	23.6(10)	17.3(9)	0.1(8)	5.4(7)	4.3(8)
C7A	25.9(12)	26.3(11)	18.3(10)	-0.2(8)	1.6(8)	0.7(9)
C8A	21.1(10)	22.6(10)	16.1(9)	1.0(8)	0.0(8)	1.5(8)
C9A	24.0(12)	43.5(13)	22.5(11)	-3.4(10)	-1.9(9)	6.6(10)
C10A	32.1(12)	36.2(12)	19.7(10)	-6.2(9)	-1.4(9)	7.8(10)
C11A	42.4(14)	33.8(12)	22.5(11)	9.2(9)	0.2(9)	-0.2(10)
O1W	26.1(9)	21.6(8)	65.1(11)	-8.2(8)	-20.0(8)	4.4(6)

Atom	Atom	Length/Å		Atom	Atom	Length/Å
F1	C7	1.341(2)		F1A	C7A	1.339(2)
F2	C7	1.342(2)		F2A	C7A	1.335(2)
F3	C7	1.340(2)		F3A	C7A	1.345(2)
O1	C1	1.432(2)		O1A	C1A	1.424(2)
C1	C2	1.520(2)		C1A	C2A	1.526(2)
C1	C6	1.527(2)		C1A	C6A	1.523(2)
C1	C7	1.526(3)		C1A	C7A	1.524(3)
C2	C3	1.529(2)		C2A	C3A	1.530(2)
C3	C4	1.534(2)		C3A	C4A	1.527(2)
C4	C5	1.528(2)		C4A	C5A	1.532(2)
C4	C8	1.556(2)		C4A	C8A	1.557(2)
C5	C6	1.533(2)		C5A	C6A	1.531(2)
C8	C9	1.532(3)		C8A	C9A	1.527(3)
C8	C10	1.527(3)		C8A	C10A	1.530(3)
C8	C11	1.531(3)		C8A	C11A	1.530(3)

Atom	Atom	Atom	Angle/°		Atom	Atom	Atom	Angle/°
O1	C1	C2	110.54(14)		O1A	C1A	C2A	110.29(14)
O1	C1	C6	106.57(14)		O1A	C1A	C6A	106.60(14)
O1	C1	C7	104.15(14)		O1A	C1A	C7A	104.61(14)
C2	C1	C6	111.00(15)		C6A	C1A	C2A	110.61(15)
C2	C1	C7	112.36(15)		C6A	C1A	C7A	112.06(15)
C7	C1	C6	111.85(15)		C7A	C1A	C2A	112.34(15)
C1	C2	C3	114.41(14)		C1A	C2A	C3A	114.55(15)
C2	C3	C4	111.77(15)		C4A	C3A	C2A	112.81(15)
C3	C4	C8	113.82(14)		C3A	C4A	C5A	109.07(15)
C5	C4	C3	108.85(14)		C3A	C4A	C8A	113.48(14)
C5	C4	C8	113.83(14)		C5A	C4A	C8A	113.89(14)
C4	C5	C6	112.14(14)		C6A	C5A	C4A	111.91(15)
C1	C6	C5	114.23(15)		C1A	C6A	C5A	114.07(15)
F1	C7	F2	106.32(15)		F1A	C7A	F3A	106.20(15)
F1	C7	C1	111.77(15)		F1A	C7A	C1A	111.60(16)
F2	C7	C1	111.85(16)		F2A	C7A	F1A	106.58(15)
F3	C7	F1	106.48(15)		F2A	C7A	F3A	106.28(16)
F3	C7	F2	106.30(15)		F2A	C7A	C1A	112.16(15)
F3	C7	C1	113.63(15)		F3A	C7A	C1A	113.54(15)
C9	C8	C4	109.82(15)		C9A	C8A	C4A	109.48(15)
C10	C8	C4	109.37(14)		C9A	C8A	C10A	107.62(16)
C10	C8	C9	107.68(16)		C9A	C8A	C11A	109.04(16)
C10	C8	C11	109.03(16)		C10A	C8A	C4A	109.51(15)
C11	C8	C4	112.14(15)		C10A	C8A	C11A	108.95(16)
C11	C8	C9	108.69(15)		C11A	C8A	C4A	112.13(15)

D	H	A	d(D-H)/Å	d(H-A)/Å	d(D-A)/Å	D-H-A/°
O1	H1	O1A ¹	0.84	1.81	2.6299(17)	166.2
O1A	H1A	O1W	0.84	1.80	2.6368(19)	174.7
O1W	H1WA	O1 ²	0.85	2.00	2.8478(19)	171.9
O1W	H1WB	O1 ³	0.85	2.01	2.8248(18)	160.1

¹-1/2+X,1/2-Y,1/2+Z; ²1/2-X,1/2+Y,1/2-Z; ³-1/2+X,1/2-Y,-1/2+Z

A	B	C	D	Angle/°	A	B	C	D	Angle/°
O1	C1	C2	C3	-166.25(15)	O1A	C1A	C2A	C3A	-165.44(15)
O1	C1	C6	C5	168.02(15)	O1A	C1A	C6A	C5A	169.20(15)
O1	C1	C7	F1	-62.02(18)	O1A	C1A	C7A	F1A	-58.56(18)
O1	C1	C7	F2	57.07(18)	O1A	C1A	C7A	F2A	60.96(19)
O1	C1	C7	F3	177.43(14)	O1A	C1A	C7A	F3A	-178.54(14)
C1	C2	C3	C4	54.3(2)	C1A	C2A	C3A	C4A	52.3(2)
C2	C1	C6	C5	47.6(2)	C2A	C1A	C6A	C5A	49.3(2)
C2	C1	C7	F1	57.6(2)	C2A	C1A	C7A	F1A	61.09(19)
C2	C1	C7	F2	176.74(14)	C2A	C1A	C7A	F2A	-179.40(15)
C2	C1	C7	F3	-62.9(2)	C2A	C1A	C7A	F3A	-58.9(2)
C2	C3	C4	C5	-56.69(19)	C2A	C3A	C4A	C5A	-54.7(2)
C2	C3	C4	C8	175.18(15)	C2A	C3A	C4A	C8A	177.16(15)
C3	C4	C5	C6	56.4(2)	C3A	C4A	C5A	C6A	56.0(2)
C3	C4	C8	C9	-175.11(16)	C3A	C4A	C8A	C9A	-177.97(16)
C3	C4	C8	C10	-57.1(2)	C3A	C4A	C8A	C10A	-60.2(2)
C3	C4	C8	C11	63.9(2)	C3A	C4A	C8A	C11A	60.9(2)
C4	C5	C6	C1	-53.4(2)	C4A	C5A	C6A	C1A	-55.2(2)
C5	C4	C8	C9	59.4(2)	C5A	C4A	C8A	C9A	56.4(2)
C5	C4	C8	C10	177.32(16)	C5A	C4A	C8A	C10A	174.22(16)
C5	C4	C8	C11	-61.6(2)	C5A	C4A	C8A	C11A	-64.7(2)
C6	C1	C2	C3	-48.2(2)	C6A	C1A	C2A	C3A	-47.8(2)
C6	C1	C7	F1	-176.73(14)	C6A	C1A	C7A	F1A	-173.66(14)
C6	C1	C7	F2	-57.64(19)	C6A	C1A	C7A	F2A	-54.1(2)
C6	C1	C7	F3	62.7(2)	C6A	C1A	C7A	F3A	66.4(2)
C7	C1	C2	C3	77.88(19)	C7A	C1A	C2A	C3A	78.3(2)
C7	C1	C6	C5	-78.8(2)	C7A	C1A	C6A	C5A	-76.9(2)
C8	C4	C5	C6	-175.50(15)	C8A	C4A	C5A	C6A	-176.11(15)

Table 8 Hydrogen Atom Coordinates ($\text{\AA}\times 10^4$) and Isotropic Displacement Parameters ($\text{\AA}^2\times 10^3$) for 17srv190.

Atom	<i>x</i>	<i>y</i>	<i>z</i>	U(eq)
H1	2873	946	4840	28
H2A	626	1623	3997	22
H2B	234	886	3772	22
H3A	913	1898	2722	24
H3B	-1183	1518	2754	24
H4	362	561	2378	19
H5A	3949	1307	2266	24
H5B	3707	566	2028	24
H6A	3508	258	3294	24
H6B	5502	690	3275	24
H9A	2224	579	869	41
H9B	74	650	362	41
H9C	304	173	1081	41
H10A	-2710	784	1538	44
H10B	-2675	1214	785	44
H10C	-2566	1549	1609	44
H11A	672	2114	1451	44
H11B	444	1843	593	44
H11C	2509	1728	1140	44
H1A	4974	4142	507	38(7)
H2AA	4308	4169	1861	24
H2AB	6284	4600	1798	24
H3AA	6216	4340	3080	24
H3AB	5926	3593	2884	24
H4A	9523	4314	2713	21
H5AA	11010	3350	2341	24
H5AB	8920	2975	2405	24
H6AA	9513	3967	1318	23
H6AB	9135	3225	1114	23
H9AA	12420	3310	3494	45
H9AB	12593	3668	4305	45
H9AC	12628	4076	3533	45
H10D	9692	4725	3992	44
H10E	9918	4264	4726	44
H10F	7755	4342	4229	44
H11D	7360	3188	3987	50
H11E	9425	3070	4534	50
H11F	9165	2780	3684	50
H1WA	2286	4915	347	59
H1WB	1535	4343	23	59

Refinement model description

Number of restraints - 0, number of constraints - unknown.

Details:

1. Fixed Uiso

At 1.2 times of:

All C(H) groups, All C(H,H) groups

At 1.5 times of:

All C(H,H,H) groups, All O(H) groups, All O(H,H) groups

2.a Free rotating group:

O1W(H1WA,H1WB)

2.b Ternary CH refined with riding coordinates:

C4(H4), C4A(H4A)

2.c Secondary CH2 refined with riding coordinates:

C2(H2A,H2B), C3(H3A,H3B), C5(H5A,H5B), C6(H6A,H6B), C2A(H2AA,H2AB), C3A(H3AA,H3AB), C5A(H5AA,H5AB), C6A(H6AA,H6AB)

2.d Idealised Me refined as rotating group:

C9(H9A,H9B,H9C), C10(H10A,H10B,H10C), C11(H11A,H11B,H11C), C9A(H9AA,H9AB,H9AC), C10A(H10D,H10E,H10F), C11A(H11D,H11E,H11F)

2.e Idealised tetrahedral OH refined as rotating group:

O1(H1), O1A(H1A)